ЖУРНАЛ
ПРИКЛАДНОЙ ХИМИИ

Volume 31 No. 12

December 1958

JOURNAL OF
APPLIED CHEMISTRY
OF THE USSR

(ZHURNAL PRIKLADNOI KHIMII)

IN ENGLISH TRANSLATION

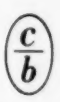

CONSULTANTS BUREAU, INC.

Volume 31 No. 12

December 1958

JOURNAL OF
APPLIED CHEMISTRY
OF THE USSR

(ZHURNAL PRIKLADNOI KHIMII)

A publication of the Academy of Sciences of the USSR

IN ENGLISH TRANSLATION

Year and issue of first translation:
Vol. 23, No. 1 January 1950

	U. S. and Canada	*Foreign*
Annual subscription	*$60.00*	*$65.00*
Annual subscription for libraries of non-profit academic institutions	*20.00*	*25.00*
Single issue	*7.50*	*7.50*

Copyright 1959
CONSULTANTS BUREAU INC.
227 W. 17th ST., NEW YORK 11, N. Y.

Editorial Board
(ZHURNAL PRIKLADNOI KHIMII)

P. B. Budnikov, S. I. Vol'fkovich, A. F. Dobrianskii,
O. E. Zviagintsev, N. I. Nikitin (Editor in Chief),
G. V. Pigulevskii, M. E. Pozin, L. K. Simonova
(Secretary), S. N. Ushakov, N. P. Fedot'ev

Note: The sale of photostatic copies of any portion of this copyright translation is expressly prohibited by the copyright owners.

Printed in the United States of America

JOURNAL OF APPLIED CHEMISTRY OF THE USSR

Volume 31, Number 12 December 1958

CONTENTS

	PAGE	RUSS. PAGE
Great New Expansion of Industrial Chemistry. V. S. Sominskii	1761	1769
Georgii Vasil'evich Pigulevskii (on his 70th birthday)	1771	1780
Interaction of Sulfur Dioxide with Calcium Oxide and Carbonate. A. N. Ketov and V. V. Pechkovskii	1774	1783
Dependence of the Carbonation Process on the Partial Pressure of Carbon Dioxide in the Incoming Gas and on the Temperature. G. N. Gasiuk, P. Ia. Krainii, A. G. Bol'shakov, and A. V. Kortnev	1778	1787
Effect of Ferric Oxide on the Properties of Borate and Boron-Free Ground Coat Enamels. G. I. Beliaev and N. F. Smakota	1783	1792
Interaction of Calcium Zirconate with B_2O_3 Mineralizer. A. K. Kuznetsov	1790	1799
Role of the Phase Transition NH_4NO_3 (IV) $\rightleftharpoons NH_4NO_3$ (III) in the Caking of Ammonium Nitrate. B. V. Erofeev and N. I. Mitskevich	1796	1805
Analysis of Diffusional Processes on the Basis of Developed Free Turbulence. V. V. Kafarov and V. I. Trofimov	1800	1809
Investigation of Steam Distillation. E. K. Siirde and P. G. Romankov	1807	1817
Anodic Behavior of Alloys of the Copper – Zinc System in 0.1 N Potassium Chloride Solution. V. V. Skorcheletti, I. A. Stepanov, and E. P. Kuksenko	1813	1823
Chemical and Mechanical Destruction of Graphite Anodes under Various conditions of Hydroxyl Ion (Water) Discharge. B. M. Bulygin	1821	1832
Desulfurization of Steel in an Induction Furnace by Means of Direct Current. O. A. Esin, S. I. Popel', S. G. Bratchikov, V. N. Razumov, and I. M. Plotnikov	1826	1837
Effect of Dilution of Chlorine with Nitrogen on the Corrosion of Metals at High Temperatures. Kh. L. Tseitlin and V. A. Strunkin	1832	1843
Corrosion of Iron and Zinc in 1 N H_2SO_4. L. I. Antropov and A. T. Petrenko	1839	1849
Electrochemical Method for Production of Sodium Formate from Carbon Dioxide and Sodium Amalgam. P. S. Chechel' and L. I. Antropov	1846	1856
Properties of Low-Substituted Cellulose Nitrate Esters. G. A. Petropavlovskii and N. I. Nikitin	1851	1862
Oxidation of Dimethylacetylenyl Carbinol by Cupric Chloride in Ammonia Solution. A. L. Klebanskii, I. V. Grachev, and O. M. Kuznetsova	1858	1869
Demethylation of Methylphenols. D. Tishchenko and S. Sheina	1864	1876

CONTENTS (continued)

	PAGE	RUSS. PAGE
Synthesis of β-Chloro Ethers from Unsaturated Hydrocarbons by the Vapor-Phase Method. A. K. Seleznev	1868	1880
Effect of Caustic Soda and Manganese and Cobalt Salts on the Oxidation of Isopropylbenzene to the Hydroperoxide. B. L. Moldavskii and L. L. Belostotskaia	1875	1885
Brief Communications		
Investigationof the Decarburization rate of 30 KhMA Steel Pipes in a Hydrogen Medium. V. V. Ipat'ev, O. P. Merkulova, and V. P. Teodorovich	1880	1891
Decarburization of Carbon Steels by Hydrogen at High Temperatures and Pressures. S. L. Skop, V. P. Teodorovich, and V. V. Ipat'ev	1884	1894
Soluble Poly-p-Xylylene. A. A. Vansheidt, E. P. Mel'nikova, L. V. Kukhareva, and M. G. Krakoviak	1888	1898
Some Reactions of Acid Dextrin Sulfates. G. Ia. Liandzberg	1891	1900
Preparation of Furfuryl Alcohol. A. P. Salchinkin and L. B. Lapkova	1894	1902
Author Index for Vol. 31, 1958	1897	
Tables of Contents for Vol. 31, 1958	1913	

GREAT NEW EXPANSION OF INDUSTRIAL CHEMISTRY

V. S. Sominskii

In the economic competition between socialistic construction and capitalism, a special and honorable position belongs by right to the chemical industry and the introduction of chemistry into the national economy.

The attainments of chemical science and technology ensure a high rate of growth of labor output and satisfaction of the needs of the population and the demands of industry in a shorter time than those of any other branch of industrial production.

Nearly 100 years ago Karl Marx stated that as mankind masters chemical methods of production so mechanical operations will increasingly give way to chemical processes. This prediction is now being fulfilled on an ever-increasing scale.

The outstanding feature of chemical methods of production is that they yield products needed by man, more rapidly, more cheaply, and with less expenditure of work.

Calculations show that the production of articles and goods from plastics involves only 1/3 to 1/4 of the cost and 1/5 to 1/10 of the labor required for the production of similar goods from metal.

The high costs of the new materials, which not long ago prevented their extensive adoption, were merely the consequence of the small scale of production or uneconomic methods. The well-known universal plastic material, polyethylene, which at present costs about 57,000 rubles per ton, will in the very near future fall in price (with its density taken into account) to not more than 2/3 of the price of steel.

The production of electrical cables and leads with synthetic insulation and sheathing will make the use of overhead wires and cables on poles unnecessary in all the regions of our country where timber is not available. This alone would effect savings amounting to a billion rubles in capital outlay in the course of five years, together with a great saving of labor [1]. Further, it should be take into account that the labor requirements in the cable industry are reduced by a factor of about 2.5 by the use of plastic sheaths, the production areas required for cable manufacture are only 1/3 of those needed formerly, the weight of the cables is reduced by 30%, and labor for wiring is reduced by 1/5. This is a by no means complete list of the advantages of chemical materials, and many similar examples could be cited.

In economic competition with capitalism, a vital part is played by the time in which the production of goods needed by the Soviet people can be sharply increased. The limitation of capital resources must not be ignored. Chemical industries have a great advantage over many others in that they require relatively less time for their organization, and the expenditure in new construction and reconstruction of existing undertakings is recovered in a shorter time than in any other branch of production.

A distinctive feature of chemical industries, known for a long time but fully realized only at the present day, is the great scope and variety of raw materials, the resources being virtually inexhaustible and readily accessible.

Finally, the fact cannot be ignored that the national economy as a whole simply cannot make technical progress without the use of chemical resources and methods. The older materials cannot satisfy the demands of designers of supersonic aircraft or builders of cosmic rockets. A decrease in the weight of machines with increase of specific power can be effected only with the aid of synthetic materials not found in nature.

In his address to the May (1958) Plenary Session of the Central Committee of the CPSU, Comrade N. S. Khrushchev [2a] stated: "We are now faced with one of the most important and urgent tasks — to ensure in a short time the accelerated development of the chemical industry and to create a powerful industry for polymer production. This question is of enormous national and political importance under modern conditions."

The decisions adopted by the May Plenary Session of the Central Committee of the CPSU , and the subsequent decrees of the Central Committee of the CPSU and the Council of Ministers USSR, were further reflected in the provisional figures of the state plan for the development of the national economy of the USSR during 1958-1965, presented for discussion at the extraordinary 21st Session of the CPSU. They outline a program of unprecedented rates and scales of development of the Soviet chemical industry, which was placed by the Communist party in the forefront of socialist industry.

The high rates of development of the chemical industry are directly related to changes in the fuel balance of the country. This is because most of the raw materials in the growing organic-synthesis industries are obtained by the conversion of combustible materials: coal, petroleum, and natural gas.

Until recently coal occupied the leading position in the fuel economy. It comprised 63.6% of the total fuel balance in 1955. However, it is known that petroleum and natural gases not only require much lower capital outlay for the production of an equivalent capacity (calculated as standard comparison fuel) and incomparably lower costs in winning and transport, but are also invaluable raw materials for chemical conversion.

During the past decade the petrochemical industry has developed on an enormous scale in the capitalist countries of Western Europe, and especially in the U.S.A. For example, it is expected that the total output of chemical products (including synthetic commercial products) from petroleum and natural gas in the U.S.A. will increase 1.8-fold in 1960 over the 1956 figure, i.e., from 15,000,000 tons to 27,000,000 tons [3a].

On Comrade N. S. Khrushchev's initiative the State Planning Commission of the USSR took steps to bring about radical changes in the fuel balance in the near future. These changes provide for an increase in the rate of oil production and a steep rise in the production of natural gas. By 1965 the production of natural gas will reach 150,000,000,000 m^3 [4]; this is equivalent as fuel to the present production of coal at the Donets, Moscow, and Pechora coalfields put together.

Because of the more rapid development of petroleum and natural-gas production, the structure of the fuel balance will change [5] as shown in the table.

The level of the petrochemical industry and of the production of intermediates from natural gas planned for the end of 1965 should satisfy the most important demands of the organic-synthesis industry.

Forms of fuel and power	Prop. of diff. types of fuel in total fuel balance of country (% calc. as stand. comparison fuel)				
	1940	1955	1957	1960	1972
Coal	59.2	63.6	60.8	55.6	32.2
Oil	18.5	21.0	23.4	25.2	34.4
Natural gas	1.6	2.3	4.0	8.9	23.3
Peat	5.6	4.7	3.8	3.7	2.4
Shale	0.3	0.7	0.7	0.6	0.6
Wood	13.5	5.7	4.4	3.2	1.3
Hydroelectric power	1.3	2.4	2.9	2.8	2.6
Atomic power	—	—	—	—	3.2

Among the great advantages of oil and natural gas is the possibility of conveying them over long distances by pipeline. Such regions as Omsk, Krasnoiarsk, and Irkutsk, which lie at great distances from oilfields, will become important suppliers of petrochemical products for the chemical industry of Western and Eastern Siberia in the near future. The supply of natural gas from Stavropol' to Leningrad will make it possible to use this raw material for large-scale production of organic intermediates in immediate proximity to facilities for the conversion of plastics.

The production of chemicals from oil and natural gas is considerably cheaper than from coal and food materials, and involves lower capital outlay. Considerable amounts of ethane, propane, butane pentane, isopentane, etc. can be produced by the gas-gasoline plants at relatively low cost.

The considerable increases of ethylene and propylene production planned for the near future are based on the conversion of by-product gases and gasoline from natural gas.

By 1965 petroleum by-product gases will provide a complete solution to the problem of synthetic-alcohol production; this will result in a saving of 4 tons of grain per ton of ethyl alcohol.

Substantial changes are planned in relation to one of the most important raw materials for organic synthesis – acetylene.

Until now acetylene was produced from calcium carbide. However, it can be obtained much more cheaply from natural gas and from refinery by-product gases. Thus, the cost of production of acetylene from the latter sources is on the average 50% lower, the capital outlay is 2/3, and the productivity of labor is nearly 4 times as great.

Natural gas must be the main source of ammonia in the future. The cost of ammonia from natural gas is almost halved in comparison with the cost of ammonia made by conversion of solid fuel.

However, in concentrating on petroleum and gas products, it would be wrong to disregard the possible development of other sources of raw materials for the chemical industry; foremost among these are coal and wood chemicals.

Extensive scientific research in the field of fuel gasification has made the use of many products of this branch of industry profitable.

The cost of the products has been lowered appreciably by the introduction of new methods of gasification (in fluidized beds, under pressure), the use of coal fines and low-grade coal instead of costly coke, and further progress in synthesis methods [6]. Attempts were being made only recently, and on a large scale, to produce synthetic fuel from coal. This proved to be uneconomic in our country, as such fuel cannot compete in any way with fuel from oil or natural gas. However, there is no doubt that the use of fuel-gasification products for complex organic synthesis is quite rational.

The utilization of such valuable raw materials as coke and semicoke tars and coke-oven gas directed toward the needs of metallurgy should be increased. While the relative proportion of coal in the fuel balance decreases, the absolute amount mined will increase, and the use of strip mining and hydraulic winning will lower its cost severalfold. Many years of research work by the Institute of Combustible Minerals of the Academy of Sciences USSR, the Department of Organic Chemistry of Irkutsk University, and the All-Union Scientific Research Institute of Petroleum and Gas Processing [7-9] have shown that coal, processed in various ways, remains one of the most important sources of raw materials for the chemical industries.

The use of chemicals from wood, a source of raw materials which is being used very little at present, should assist extension of the available sources of raw materials for the chemical industry. The by-products of the wood pulp industry could satisfy most of the expected demand for acetic and formic acids, polyhydric alcohols, and many other products. It is known that in the conversion of wood into cellulose almost 50% of the original material appears in the form of waste products, containing a high proportion of lignin. Much attention is now being devoted in a number of countries to searches for methods of rational utilization of lignin and its derivatives. Such work is being carried on in the USSR [10].

From the products obtained by processing of annual plants (cane, straw, etc) it is possible to isolate pentosans, which are the source of a whole range of intermediates for plastics production (such as furfural and its derivatives). Finally, pyrolysis of wood wastes yields a considerable amount of tar, rich in phenols [11]. It is true that these phenols cannot be regarded at the present time as an economic raw material, because of the lack of suitable methods for their separation. The same was true only recently for coal-tar phenols. However, the progress of chemical science and technology has already demonstrated the possibility of effective separation of coal-tar phenols [12], with subsequent production of complex insecticides, fungicides, and other products, and there is no doubt that equally good results will be achieved with phenols from wood pyrolysis.

The most attractive features of wood chemicals as sources of raw materials are their inexhaustibility, and the possibility of rapid natural replenishment. It may be predicted with confidence that in the not very distant future they will occupy one of the leading positions among the raw materials for organic synthesis.

The Soviet Union has very large oilfields, sources of natural gas, coalfields, and 1/3 of the world's wood supplies. We have everything necessary for rapid growth of the chemical industry and especially of organic synthesis.

Among the provisions for the development of the national economy of the USSR in 1959-1965 a leading place in the field of chemical industry is assigned to products of organic synthesis: plastics, man-made and synthetic fibers, synthetic rubber, synthetic fat substitutes and detergents, and numerous processes for the conversion of synthetic materials.

At the May Plenary Session of the Central Committee of the CPSU it was decided that the output of plastics is to be increased 8-fold during the next 7 years. The most extensive development will take place in the production of general-purpose polymerization plastics (polyethylene, polyvinyl chloride, polystyrene); this reflects recent changes in the range of plastics being produced. Thus, in the U.S.A., where the production of plastics has now exceeded 2,000,000 tons per year and continues to grow rapidly, plastics of this type have become predominant. Polyvinyl resins comprise about 18-20% of the total production, polystyrene accounts for 17-18%, and polyethylene 16-17%, so that these three groups together represent over 50% of the total production [13].

This significant growth of the production of polymerization plastics is due to the possibilities of highly economical application of these products for a great variety of industrial purposes and consumer goods, from pipes and machine parts, bodies and structural parts, to packaging of foods and the production of household goods and clothing. Most economical methods can be used for the conversion of plastics into goods: casting, vacuum molding, extrusion, etc.

Among the tasks confronting the USSR is the industrial production of polyethylene at high, low, and moderate pressures, and the organization of the production of polypropylene – superior to polyethylene in heat stability – obtained from a material abundantly available in petroleum gases.

In polystyrene production, new polymerization methods are to be operated industrially: suspension polymerization, by heterogeneous catalysis, etc.; hydrochlorination of acetylene is to be adopted in the production of vinyl chloride, and polyvinyl chloride is to be made by latex method, which yields emulsions for impregnation and surface treatment of leather, fabrics, paper, etc.

Our industry is most experienced in the production of resins of the phenolic and urea types, i.e., condensation plastics. The considerable growth in the production of these resins is determined by demands of the building industry,* electrical engineering, and machine construction. For example, the production of wood-shaving and wood-fiber blocks from wood wastes will require not less than 1,000,000 tons of resins of this type [13].

Polyester resins and materials made from them will play an important part in the range of plastics. Polyester resins reinforced by glass fibers can be used for the production of large articles, considerably lighter than steel but not inferior to it in strength. Car and bus bodies made from this material are 25-30% lighter than steel bodies, stronger, and do not require painting. In the U.S.A. 45,000 boats and launches, and hulls of river and marine vessels, were made from polyester resins in 1956.

A very large increase is planned in the production of organosilicon materials, which are unequalled in their retention of working properties both at high and at low temperatures. The weight and dimensions of electrical machinery are decreased by 25% with the use of these materials, while the service life is increased 5 to 6-fold.

Among the other plastics the production of which is to be increased are amino-resin adhesives, which can

*According to preliminary estimates of the Office of State Construction, the use of condensation resins and other types of plastics in building will lower building costs during the 1958-1965 period by about 15,000,000,000 rubles and will save almost 2,000,000,000 bricks, about 180,000 tons of cement, and 12,000,000 m^3 of lumber [14].

be used for producing strong bonds between steel parts, expanded plastics weighing 20-40 kg or less per cubic meter, etc.

The plastics industry is developing at an exceptionally high rate. According to the estimates of American economists, the plastics production of the U.S.A. should reach about 10,000,000 tons or 50 kg per capita of its population by 1975. To reach the same level, the plastics production of the USSR must rise to not less than 12,000,000 tons in the same year.

Scientists must work very hard in order to develop, in good time, new and more effective methods of polymerization for use in industry, to extend the range of plastics, and to discover new sources of raw materials.

Extension of the range of plastics and other organic materials will raise considerably the technical level of the varnish and paint industry, which is confronted with important tasks in supplying the demands of machine construction, the building industry, and many other branches of industry and the national economy. Rough estimates show that losses due to corrosion of ferrous metals, largely attributable to lack of progress in the varnish and paint industry, cost about 20,000,000,000 to 25,000,000,000 rubles annually. The main trend in the development of the varnish and paint industry will be the adoption of synthetic resins and coatings based on them; these have high resistance and are quick-drying.

For a long time, attempts were made in the surface-coatings industry to develop substitutes for vegetable oils. Although there were some successes, no important results were achieved, and the consumption of edible oils remains very high. It is now obvious that another solution must be sought: the introduction of coatings and paints for which oils are not required at all (products of organic origin), rather than replacement of vegetable oils by substitutes.

The surface-coatings industry must produce high-quality paints based on titanium, greatly improve the process for the production of zinc white, and extend the range of enamels, especially of the type resistant in moist hot climates.

The Party and Government have set the industry important tasks in relation to increase of the capacity for man-made fiber production. By the end of 1965 the total capacity for synthetic and man-made fibers must increase 4.6-fold [3b]; this includes an 18-fold increase for synthetic fibers, 22.6-fold for acetate, and 5-fold for man-made tire cord. By 1965 the total production of man-made fibers in the USSR will exceed 600,000 tons [3b]. The USSR will occupy one of the leading positions in the world, both in volume of production and in its range.*

The relatively greater rate of increase in the production of synthetic fibers is due to their high strength, resistance to chemicals and corrosive attack, good electrical properties, and resistance to moisture. These properties make synthetic fibers applicable over a very wide range of end uses, among which, in addition to the production of fabrics, footwear, etc., mention must be made of the production of nets and filters, ropes, fishing nets, high-pressure hose for use over great lengths, flexible storage vessels for storage and transport of fuels, lubricants, and chemicals.

The production of special paper with added nylon is of special interest. Addition of this material to paper stock increases the tensile strength of the paper 3.5-fold, and the flex strength 42-fold. This opens up real possibilities for the production of clothing fabrics on paper-making machines, which would result in a real revolution in light industry.

In the world consumption of fibers, man-made fibers have firmly occupied the second place, after cotton, and their consumption is double that of wool. During the past 30 years the relative proportion of man-made fibers has almost tripled, and in 1956 it was 22.3% (2,694,000 tons) of the total [15].

Over 20 different brands of synthetic fibers are now in commercial production, and there are reasons to expect a considerable extension of their range.

The largest proportion of the man-made fiber output consists of cellulose-based fibers; this is attribut-

*In 1956 the man-made fiber output of the USA was broken down as follows (% of total): viscose fibers 58%, acetate fibers 16.2%, synthetic fibers 25.8%.

able both to their relatively low cost and to the extensive sources of raw materials. Soviet scientists are confronted with the task of developing industrial methods for the production of high-grade pulp of high α-cellulose content and reactivity. It must be remembered that cellulose is a most important raw material for the production of numerous plastics as well as fibers. Research in this field is of great importance for the development and organization of many industrial processes.

Synthetic dyes occupy a special place in the development of man-made fiber production. Experience shows that there are no consumers for even the best fabrics if they are dyed in dull colors which fade rapidly in sunlight. Until recently, although the volume of dye production in the USSR was large, a considerable proportion (over 50%) consisted of sulfur dyes, which have low coloring power, dull shades, and in some instances cause weakening of the fabric.

During 1959-1965 the production of sulfur dyes will be greatly decreased with an increase of the relative output of vat, high-quality acid, and direct dyes, and new classes of dyes for synthetic fibers. The number of different dyes will be almost doubled (880-850, as against 439 in 1957). Of course, the production of intermediates for this branch of chemical industry will be appropriately developed also, as these intermediates are also used in many large-scale processes for the production of plastics and synthetic fibers.

One of the most important positions among large-scale industrial products is occupied by synthetic rubber and goods made from it. The production capacity for synthetic rubber will be increased 3.4-fold, in 1959-1965, over the 1957 level.

The Soviet Union was the first country in the world to produce synthetic rubber on the industrial scale, and only the U.S.A.• is ahead in total production and range.

One of the important reasons why the USSR is behind both in the volume of production and in the quality of the products is that the industry was based on the production of the less strong sodium butadiene rubber (SKB), with the use of alcohol as a starting material. At the May Plenary Session of the Central Committee of the CPSU, N. S. Khrushchev severely critized the earlier management by the former Ministry of Chemical Industry which utilized available resources for the improvement of this type of rubber and took no steps to develop new, more valuable and promising products which do not require alcohol as a raw material.

During the next 7 years the structure of the synthetic rubber industry of the USSR will change sharply. Butadiene-styrene and chloroprene rubbers will comprise over $\frac{1}{2}$ of the total production, and isoprene rubber, which is similar in properties to natural rubber, will comprise about $\frac{1}{4}$. The discovery of a method for the production of isoprene rubber by Soviet scientists was a most important contribution to this branch of industry and it is especially significant because the USSR lacks its own sources of natural rubber.

In all the synthetic-rubber plants now under construction, butadiene-styrene and butadiene-methylstyrene rubbers will be produced from butane and from butane-butylene fractions; this will lower production costs appreciably and reduce capital outlay by 35%. Research and development work on these types of rubber, produced in the greatest quantitites, will be extended in order to produce new types.

The new types of rubber will form the basis for development of long-life tires, which can withstand prolonged use and can carry heavier loads, and for production of a wide range of technical rubber goods. Theoretical investigations relating to formulation of rubber stocks, studies of the applications of ultrasonics, radioactive radiations, high-frequency current, infrared radiation, etc., are very important for the rubber industry. Of course, such investigations are equally important for many other branches of the chemical industry in which synthetic materials are processed.

One of the leading positions, if not the first place, in the problem of finding substitutes for industrial raw materials which are valuable as foodstuffs is held by the production of fat substitutes detergents and other surface-active substances.

•The present production of synthetic rubber (1957 data) is 1,100,000 tons in the U.S.A., 134,000 tons in Canada, and 70,000 tons in Eastern Germany.

Of the total U.S.A. production of synthetic rubber, 79% is butadiene-styrene rubber, 9% is chloroprene, 7% is butyl rubber and polyisobutylene, 3% is nitrile rubber, and 2% is special rubbers.

In 1957, 315,000 tons of vegetable oils, or about 1/3 of the total production of the USSR, was expended in the manufacture of detergents and soaps. However, a large proportion of edible oils used for such purposes can be successfully replaced by synthetic products. The conversion to synthetic materials is due not only to the need to save edible raw materials, but also to their relative cheapness and advantages over soaps made from fat. For example, it is known that up to 30% of soap is wasted in softening water; this leads in the USSR to losses of about 100,000 tons of fats per year [16]. Synthetic detergents are free from this defect, and are effective in hard and even in sea water.

The advantages of synthetic detergents have stimulated a rapid growth of their production. During the period from 1945 to 1957 their output in the U.S.A. rose from 68,000 to 1,282,000 tons, and they now comprise 63.7% of the total output, whereas the production of soap during the same period fell from 1,622,000 to 691,000 tons [17]. About 50% of the products is used in industry for technical purposes.

Measures are now being taken to allow the USSR to catch up in this field as soon as possible. The production of various types and kinds of alkyl sulfonates, alkyl aryl sulfonates, and other synthetic materials will be organized. One method for the production of a material of this type is by conversion of soft paraffin waxes, yielding detergent powders of the "Novost'" type [18].

Synthetic products will find extensive uses in agriculture as well as in industry and in the home. In particular, the production of chemical means for plant protection is to be greatly increased.

Losses of crops due to inadequate use of plant-protection methods are very detrimental to the national economy. The cost is measured in many billions of rubles annually. The labor requirements for weed control are unjustifiably high, and they could be minimized by the use of herbicides.

It has been shown that one ruble expended on chemical means of plant protection yields an average saving of 11 rubles' worth of crops, and up to 100 rubles and more for certain crops.

The production of organophosphorus and organic chlorine compounds – derivatives of carbamic acid and others – will be organized on the large scale in the USSR in 1958-1965. Preparations based on the vinyl ethers of phenols from coal are of considerable interest, from our point of view.

The development of the chemical industry in relation to the production of synthetic materials is unthinkable without further expansion of the most important inorganic industries, including the nitrogen and phosphorus industries.

One of the most important problems of the nitrogen industry is conversion to more economic methods of ammonia production; this, as was noted earlier, is directly associated with the utilization of natural gas. At the same time it must be taken into account that with the conversion of a number of metallurgical plants to the use of natural gas, large amounts of coke-oven gas become available, and in such cases the production of ammonia from coke-oven gas becomes economic. In addition to extensive changes in the production structure of the nitrogen industry, it is intended to introduce the use of liquid fertilizers – ammoniates and aqueous ammonia – in agriculture for direct introduction into the soil. This will lower capital investment and fertilizer costs.

The nitrogen industry is to organize large-scale production of urea, which is not only a high-grade fertilizer but also an intermediate for plastics production.

In the phosphorus industry, an electrothermal method of phosphorus production will be developed on a large scale, and the production of pyro- and polyphosphates, necessary in the manufacture of synthetic detergents, will be developed.

As the result of changes in the technical level and scales of production in these branches of industry, agriculture will be supplied with concentrated and mixed fertilizers, and this will effect considerable savings of transportation costs over long distances.

The production of trace-element fertilizers, containing boron, copper, manganese, and other elements, will be developed.

The production of animal fodder must be greatly increased.

In conjunction with large-scale construction of electric power stations, electrochemical, electrothermal and similar industries will be developed in their vicinity.

Of course, the heavy chemical industry will be considerably expanded with regard to volume of production and the range of products: acids, alkalies, and salts.

The experience gained in the development of the chemical industry shows that scientific research on a broad front is required for its successful progress. This requirement, long known, has become especially vital in relation to the rapid advance of chemical industry in the second half of the 20th century, i.e., during the past 7-8 years. We cannot overtake the foreign countries by developing their achievements; new and rapid advances of our own must be made [19].

Soviet chemical sciences is in the lead in many branches. Nevertheless, it is important to note N. S. Khrushchev's comment [2b] that ". . . despite the general high level of development of chemical science in the USSR, we are still considerably behind in certain aspects. This is primarily the case in the field of man-made and synthetic fibers and plastics".

In order to close this gap and to attain a general advance in research in the field of chemistry and especially polymer chemistry, the Central Committee of the CPSU and the Council of Ministers USSR have adopted a number of important measures in fulfillment of the decisions of the May Plenary Session of the Central Committee of the CPSU.

A number of new institutes and divisions will be organized during 1958-1960 in the Academy of Sciences USSR and the academies of sciences of the Union republics. These include the Institute of Petrochemical Synthesis, institutes of organic chemistry, the Institute of Natural Compounds, and a number of others.

In addition, it is intended to establish new industrial scientific research institutes, institute branches, and experimental stations.

Much attention in the development of chemical science is devoted to establishments of higher education. The Ministry of Higher Education must expand the existing research laboratories and establish a large number of new scientific laboratories in the universities and colleges during 1958-1960.

Among the new scientific laboratories is the multiple laboratory of the Lensoviet Technological Institute, Leningrad, which will be concerned with scientific research on the synthesis of polyester resins, paints and varnishes, the design of chemical equipment, enamels, physicochemical characteristics of polymers etc.

To eliminate duplication of research, a list has been established of the leading scientific research institutes which are called upon to coordinate polymer research in their respective branches of science. These institutes will derive much help from the industrial central laboratories, the most important of which will become the main supporting points of the institutes.

The Councils of National Economy have the task of strengthening the role of industrial laboratories, of equipping them, and of providing their personnel.

In the expansion of scientific research an important part is played by economic investigations. Such investigations have not received due attention in the past, and they must be considerably intensified.

The neglect of economic analysis of technological processes, which is found in a number of fields, is often very costly to the national economy and to science itself; instead of research in economically advantageous and promising directions, efforts and resources are wasted in investigations which cannot benefit science or industry. As examples, we can cite certain work on the improvement of rubber synthesis from alcohol, on synthesis of liquid fuel, on the production of acetic acid by dry distillation of wood, etc. For economic research it is necessary to recruit specialists who are well trained in chemical science and who have a deep understanding of scientific research and the industrial application of its results.

Broadening of the front of scientific research in all directions requires the availability of extensive scientific information. The number of scientific journals in the fields of polymer chemistry and industry is being accordingly increased, and the existing journals are being expanded.

The new institutes and the extended central industrial laboratories require well-trained personnel. The undertakings of the chemical industry are also in great need of specialists. The Ministry of Higher Education USSR has taken steps to increase considerably the number of students being trained for research in organic synthesis, graduates, and scientific workers. A number of changes will be made in the university courses, directed toward deeper studies of the latest advances of science and technology in the synthesis and uses of polymers, practical training in laboratories will be intensified, and practical work in industrial organizationswill be improved.

With the creation of the most favorable conditions for extensive scientific research,the efforts of Soviet scientists can be directed toward the most complex and difficult scientific problems. These problems are so diverse that even a mere list would occupy more space than this article permits. It is important to note that they are mainly concerned with the establishment of the theoretical principles and mechanism of formation of high polymers, studies of their properties, and extension of the number of starting materials for synthesis. Much attention must also be devoted to the development of more efficient methods for the production of already-known substances and to extension of their applications in industry, both in pure form and in conjunction with other products and materials.

There is an enormous program for the construction of new, and reconstruction of existing, plants. This requires large amounts of various equipment. It is known that many highly efficient industrial processes could not be introduced mainly because of lack of suitable equipment and of the necessary machine-building resources.

The building of chemical plants will be accompanied by the building of a number of new factories for the construction of chemical equipment. In addition, in order to fulfill the building program of the chemical industry, many machine-building factories will work on orders for the chemical industry.

For the most efficient development of the chemical equipment industry, it is very important to study the operating conditions in the conversion of chemical products, and,in particular, to obtain strict specifications with regard to corrosion resistance in presence of aggressive media, and at high temperatures and pressures. Equipment designers must work in conjunction with chemists right from the first stages in the industrial realization of the results of scientific research.

New undertakings and industries will use automatically-controlled equipment, continuous processes, with maximum use of automation for the regulation and control of production. Preliminary calculations show that productivity of labor will increase by at least 29% as the result of automation.

The entire history of the development of socialist industry served to prepare the chemical industry of the USSR, and especially the polymer industry, for its vigorous growth. This growth became possible as the result of outstanding achievements in machine building, power engineering, development of fuel and material resources, the diverse and fruitful activity of the army of Soviet scientists, engineers, and technicians, and the unselfish labor of the industrial workers.

The great program of work prescribed in the plan for the development of the national economy of the USSR during 1959-1965 inspires Soviet scientists and workers of the chemical industry to further progress so that our land may flourish, so that the standard of living of the Soviet people shall continue to rise. The provisional figures for the development of the national economy of the USSR during 1959-1965 presented for discussion at the 21st extraordinary Congress of the CPSU embody the confidence of the Soviet people that the most difficult tasks set by the Communist Party for the good of the people shall be fulfilled.

LITERATURE CITED

[1] V. Bushuev, Planning Economy 6, 17 (1958).

[2] N. Khrushchev, Acceleration of the Growth of the Chemical Industry and in Particular of the Production of Synthetic Materials and Goods Made from them for Satisfying the Needs of the Population and of the National Economy [in Russian] (State Political Press, 1958), a) p. 38, b) p. 52.

[3] N. Fedorenko, Questions of Economics 7, a) 41, b) 33 (1958).

[4] N. Lavrov, Pravda, September 5, 1958.

[5] E. Sokolova, Questions of Economics 5 (1958).

[6] N. Lavrov and I. Bogdanov, in the book: Chemical Processing of Fuels of Eastern Siberia [in Russian] (Moscow, Izd. AN SSSR, 1958).

[7] A. Blonskaia, A. Krichko, A. Kozovoi, and D. Muselevich, in the book: Chemical Processing of Fuels of Eastern Siberia [in Russian] (Moscow, Izd. AN SSSR, 1958).

[8] V. Larina, in the book: Chemical Processing of Fuels of Eastern Siberia [in Russian] (Moscow, Izd. AN SSSR, 1958).

[9] I. Rappoport, V. Kruglikov, and E. Kheifets, in the book: Prospects for the Development of Industrial Synthesis of Organic Chemical and High Polymers in Eastern Siberia [in Russian] (Moscow, Izd. AN SSSR, 1958).

[10] M. Zarubin and D. Tishchenko, Proceedings of Scientific and Technical Conference on the Theory and Practice of the Paper and Wood-Processing Industries [In Russian] (Moscow-Leningrad, 1958).

[11] D. Tishchenko, Proceedings of Scientific and Technical Conference on the Theory and Practice of the Paper and Wood-Processing Industries [in Russian] (Moscow-Leningrad, 1958).

[12] A. V. Kalabina, in the book: Chemical Processing of Fuels of Eastern Siberia [in Russian] (Moscow, Izd. AN SSR, 1958).

[13] L. Losev and D. Dankin, in the book: Prospects for the Development of Industrial Synthesis of Organic Chemicals and High Polymers in Eastern Siberia [in Russian] (Moscow, Izd. AN SSSR, 1958).

[14] V. Bushuev, Planning Economy 6, 21 (1958).

[15] G. E. Birger and Z. A. Rogovin, in the book: Prospects for the Development of Industrial Synthesis of Organic Chemicals and High Polymers in Eastern Siberia [in Russian] (Moscow, Izd. An SSSR, 1958).

[16] G. Torshchov and V. Popov, Industrial Economic Gazette 140 (1957).

[17] A. Feigin, The Petrochemical Industry of the Capitalist Countries [in Russian] (TsNIITENEFT', 1957).

[18] D. Orechkin and V. Veselov, in the book: Prospects for the Development of Industrial Synthesis of Organic Chemicals and High Polymers in Eastern Siberia [in Russian] (Moscow, Izd. AN SSR, 1958).

[19] A. Topchiev, Communist, 9 (1958).

GEORGII VASIL'EVICH PIGULEVSKII

(on his 70th birthday)

December 11, 1958 was the 70th birthday, and marked thecompletion of 48 years of scientific and teaching activity of Doctor of Chemical Sciences Prof. Georgii Vasil'evich Pigulevskii.

He was born in 1888 in the city of Kovno (Kaunas). He received his higher education in the University of Leningrad (formerly Petersburg), and has worked there continuously from 1920 to the present day. In 1934 he was appointed Professor of Organic Chemistry in the University. Since 1943 he has also been in charge of the Chemical Laboratory of the Division of Plant Resources of the Botanical Institute, Academy of Sciences USSR.

G. V. Pigulevskii is an eminent worker in the field of chemistry of natural compounds of vegetable origin. Over 160 of his publications deal with studies of essential oils, terpenes and fats. He is known by his work to a wide circle of chemists and botanists.

Pigulevskii's work on the essential oils embraces a wide range of problems. He is primarily interested in the composition of Russian essential oils and in possibilities of their practical utilization. He has studied the composition of oils from a large number of oil-bearing plants, especially conifers, and also from the Umbelliferae. One of the plants studied by him (Libanotis transcaucasica), which yields a valuable essential oil is now being cultivated. The essential oil of another plant of this family the wild carrot (Daucus carota), which contains up to 70% of geraniol, was found to be of great potential significance as a raw material for the perfume industry. This work (carried out by G. V. Pigulevskii jointly with V. I. Kovaleva) was recognized by the award of the prize and diploma of the D. I. Mendeleev All-Union Chemical Society. Recent work by Pigulevskii and his associates (M. V. Nazarenko, G. A. Kuznetsova, and others) on sesquiterpene compounds and furocoumarins from umbelliferous plants is also of great interest.

Pigulevskii has done much work on the problem of formation of essential oils in plants on the relationship between terpenes and resin acids, and on the origin of resins. He is interested in the influence of climatic conditions on the composition of essential oils, in changes in the composition of essential oils at different stages of plant growth, and similar problems. His studies of the formation of essential oils and resins in coniferous needles led him to advance a general hypothesis of the biosynthesis of essential oils and resins. The results of all these researches were published by Pigulevskii in a whole series of articles, and in a monograph entitled "Formation of Conversions of Essential Oils in Conifers" (1939). This research formed the foundation for the development of a theory of conifer tapping. In 1938, the book "Essential Oils" was published under editorship and with his direct participation.

Here we should also mention G. V. Pigulevskii's studies of the optical activity of terpene compounds isolated from various essential oils. As the result of this work he was able to establish for the first time the definite laws which govern the occurrence of optically-active forms of terpenes in plants of different families. These results are summarized by him in the paper entitled "The biogenesis of terpenes."

In addition to his direct studies of essential oils, Pigulevskii is conducting research on the chemistry of terpene hydrocarbons and their derivatives. Foremost in this work are his studies of the α-oxides of the terpene series. Pigulevskii and his associates have studied the oxides of myrcene linalool, limonene, Δ^1-, Δ^2-, and Δ^3-menthenes, pulegone, sabinene, etc. These studies, which cover various transformations of terpene oxides, are correlated with investigations of the stereochemistry of compounds of the terpene series.

Another direction of Pigulevskii's research work is the chemistry of fats. A series of his earlier papers deals with studies of fats and oils of vegetable origin, and with the influence of climatic conditions on their composition. Simultaneously with this he carried out extensive investigations into the chemistry of the higher fatty acids. He and his associates were the first to study the oxides of a series of unsaturated acids (oleic, linoleic, linolenic) and oxides of mixed triglycerides of unsaturated acids, and worked out convenient methods for their preparation. G. V. Pigulevskii (jointly with Z. Ia. Rubashko) proposed a new method for the preparation of hydroxy acids by catalytic hydrogenation of the oxides of unsaturated acids. Recently Pigulevskii (jointly with I. L. Kuranova) has been engaged in work on the Preparation of hydroxyamino derivatives of higher fatty acids.

G. V. Pigulevskii

During the whole of his scientific carrer Pigulevskii has been interested in new research techniques and has applied them with success. A vivid example of this is his highly successful use of Raman spectroscopy in studies of the composition of essential oils and the structure of terpene compounds. He started applying this method in his laboratory in the University of Leningrad in 1937, and was thus a pioneer among organic chemists in this field. Later he organized extensive training of the university studients in this branch of molecular spectroscopy. In 1955, he published jointly with A. T. Ryskal'chuk, an extensive summary of Raman spectra of compounds present in essential oils. This publication is of primary importance for chemists working in this field.

A prominent position in Pigulevskii's activities is occupied by his teaching work. He is an excellent teacher. His attitude to students and young specialists is one of great affection; he devoted and still devotes

much effort and energy to the creation of scientific cadres with a mastery of all the most modern research techniques in the field of organic chemistry. He has given a course on terpene chemistry for many years in the Leningrad University. In 1952, he published the book "Terpene Chemistry," which deals with all the latest advances in the subject.

Pigulevskii is associated with many scientific research institutions of the Soviet Union in his work. From Kishinev to Vladivostok and from Tashkent to Arkhangel'sk, specialists working on the chemistry of natural compounds are constantly turning to him for advice.

Apart from his scientific and teaching work, Pigulevskii takes a direct active part in building up our national fat, perfume, and food industries. For many years he acted as consultant to a number of organizations and branch institutes (the factory of synthetic aromatic substances, the 4th perfumery factory, the All-Union Scientific Research Institute of Fats, etc.).

During the Leningrad blockade in the Great Patriotic War,* Pigulevskii, with his characteristic energy, organized a group of chemists who prepared medicinal substances (streptocide, phenamine, etc.) needed by besieged Leningrad.

For many years he has been an active member of the D. I. Mendeleev All-Union Chemical Society; since 1940 he has been a member of the Scientific Council of the Leningrad Section of the All-Union Chemical Society.

Special mention must be made of his many years of work with the Journal of Applied Chemistry; he has been a member of the Editorial Board since 1937.

Georgii Vasil'evich Pigulevskii is one of the outstanding representatives of progressive Soviet science who devote all their energies and efforts to the service of our country. His scientific work has been recognized by the award of a number of prizes: that of the Russian Physicochemical Society (the A. M. Butlerov Prize, 1955), the Main Administration of Scientific Institutions (1927), the Committee for Chemical Industrialization of the Country (1930), and the D. I. Mendeleev All-Union Chemical Society (1954). For his many years of fruitful activity he was awarded the Order of Lenin in 1953.

On his 70th birthday, we wish Georgii Vasil'evich Pigulevskii many years of life, health, and successful creative work for the good of our country.

*World War II.

INTERACTION OF SULFUR DIOXIDE WITH CALCIUM OXIDE AND CARBONATE

A. N. Ketov and V. V. Pechkovskii

The A. M. Gor'kii State University, Perm'

Interaction of sulfur dioxide with calcium oxide and carbonate occurs in many processes of the heavy chemical industry and ferrous and nonferrous metallurgy. Thus, when sulfur ores from Razdol'e, containing over 70% limestone, are used in sulfuric acid production, there are considerable losses of sulfur in the form of calcium sulfate in the cinders.

In the solution of the problem of sulfur recovery from sulfurous waste gases liberated in enormous quantities in the smelting of nonferrous metals from sulfide ores, calcium oxide and carbonate have become important as absorbents [1].

Limestone is used in the blast-furnace process of iron production for binding the sulfur which enters with the charge. It has been reported [2] that one possible route by which sulfur can pass from the gaseous to the solid phase is by interaction of elemental sulfur with calcium oxide to form calcium sulfate and sulfide. However, it is also known [3] that part of the sulfur in the charge passes into the gas phase in the form of sulfur dioxide. It is therefore possible that the liberated sulfur dioxide may be subsequently bound by limestone.

All this prompted us to study the interaction of sulfur dioxide with calcium oxide and carbonate, in order to determine the mechanism of the process and to find the conditions in which sulfur-containing calcium compounds are formed.

The experimental procedure was as follows. A weighed sample of the substance, 1 g in each experiment, was placed in a porcelain boat for 30 minutes in the cold end of a quartz reaction tube, the other end of which was in a laboratory electric furnace, in order to remove atmospheric oxygen from the charge; it was then pushed through to the hot zone of the furnace and held for definite time intervals at a fixed temperature in a stream of oxygen-free, dry, sulfur dioxide.

Finely powdered calcium oxide and analytical-grade calcium carbonate were used for the experiments. To conform to the experimental requirements, the sulfur dioxide must not contain oxygen, sulfur trioxide, sulfuric acid vapor, or water. Among the methods tested by us for the preparation of sulfur dioxide, the most suitable was the method based on the reaction of concentrated sulfuric acid on sulfur [4]. The liberated sulfur dioxide was purified and dried. The flow rate of the gas through the system was measured by means of a rheometer, and was 4 liters/hour in all the experiments. The furnace temperature was measured by means of a thermocouple and galvanometer, and regulated by a laboratory autotransformer.

The solid products formed in the interaction of sulfur dioxide with calcium oxide and carbonate were analyzed for sulfite, sulfide, and sulfate sulfur, and the gaseous products, for elemental sulfur [6].

All the calculations consisted of determinations of the amounts of calcium carbonate or oxide converted into the corresponding sulfur compounds of calcium, as percentages of the initial amounts taken.

The principal experimental results are given in Tables 1-4.

Data on the influence of temperature on the degree of sulfation of calcium oxide by sulfur dioxide are presented in Table 1.

TABLE 1

Effect of Temperature on the Sulfurization of Calcium Oxide by Sulfur Dioxide (τ = 30 minutes)

Temperature (°C)	% Conversion of CaO into			
	$CaSO_3$	CaS	$CaSO_4$	total
400	6.2	0.0	1.7	7.9
500	4.2	0.3	10.8	15.3
600	4.0	3.1	22.0	29.1
700	2.9	5.2	28.4	36.5
800	1.7	4.9	37.1	43.7
900	1.6	5.7	45.0	52.3
1000	0.8	2.8	51.5	54.7

These data show that sulfur dioxide reacts with calcium oxide at an appreciable rate even at 400°. In the temperature range studied (400-1000°), the solid reaction products were found to contain calcium sulfite, which is the main reaction product at 400°.

It follows that when sulfur dioxide acts on calcium oxide, calcium sulfite is formed according to the equation

$$CaO + SO_2 = CaSO_3. \quad (1)$$

The solid reaction products formed from calcium oxide at 400-1000° also contain calcium sulfate, in amounts which increase considerably with increase of temperature. Calcium sulfate is formed by the oxidation of calcium sulfite by sulfur dioxide according to the equation

$$CaSO_3 + SO_2 = 2CaSO_4 + 0.5S_2. \quad (2)$$

Further confirmation is provided by the fact that, as Table 2 shows, the molar ratio of calcium sulfate to elemental sulfur formed is close to four in all the experiments, i.e., equals ratio of calcium sulfate to elemental sulfur corresponding to Equation (2).

TABLE 2

Molar Ratio of Calcium Sulfate to Elemental Sulfur Formed in the Reactions of Calcium Oxide and Carbonate with Sulfur Dioxide (τ = 30 minutes)

	Reaction products of						
	CaO				$CaCO_3$		
Temperature (°C)	400	600	800	1000	600	800	1000
$\frac{CaSO_4 \text{ molar}}{S_2 \text{ molar}}$	3.99	4.07	4.06	4.02	4.01	4.10	4.03

It should be noted that the calcium sulfite content decreases with increase of temperature. The explanation is that as the temperature increases the oxidation rate of calcium sulfite exceeds the rate of its formation by Reaction (1).

Examination of the data in Table 2 shows that the ratio of calcium sulfate to elemental sulfur in the reaction products of calcium oxide increases somewhat at 500-1000°. This effect may be attributed to the following reactions [2] at these temperatures:

$$2CaO + 1.5S_2 = 2CaS + SO_2, \quad (3)$$

$$CaSO_4 + S_2 = CaS + 2SO_2. \quad (4)$$

The presence of calcium sulfide in the reaction products indicates that under certain conditions Reactions (3, 4) do take place.

It follows from the data in Table 1 that the content of calcium sulfide in the reaction products of sulfur dioxide with calcium oxide and carbonate decreases above 800°. This is consistent with literature data which indicate [7] that at 600-1100° calcium sulfide is oxidized by sulfur dioxide according to the equation

$$CaS + 2SO_2 = CaSO_4 + S_2. \quad (5)$$

At temperatures above 800° the rate of Reaction (5) exceeds the formation rate of calcium sulfide by Reactions (3, 4), with a consequent decrease of the calcium sulfide content of the solid reaction products of calcium oxide and sulfur dioxide.

Therefore the interaction of calcium oxide with sulfur dioxide, when the latter is free from oxygen and the calcium oxide does not contain impurities which catalyze the oxidation of sulfur dioxide to sulfur trioxide, can be represented by Equations (1-5).

Data on the sulfurization of calcium carbonate by sulfur dioxide are presented in Table 3. These data lead to the conclusion that the sulfurization rate of calcium carbonate depends to a considerable extent on the temperature; a reaction between calcium carbonate and sulfur dioxide can be detected even at 500°.

TABLE 3

Effect of Temperature on the Rate of Sulfurization of Calcium Carbonate by Sulfur Dioxide (τ = 30 minutes)

Temperature (°C)	%Conversion of $CaCO_3$ into			
	$CaSO_3$	CaS	$CaSO_4$	total
500	3.2	0.0	0.7	3.9
600	15.7	0.0	3.5	19.2
700	37.1	0.8	16.6	54.5
800	9.5	11.2	60.2	80.9
900	3.2	6.1	82.5	91.8
1000	0.2	1.2	96.5	97.9

TABLE 4

Effect of Time and Temperature on the Sulfurization of Calcium Oxide by Sulfur Dioxide

τ (min)	%Conversion of CaO at temperature (°C) into						
	400			900			
	$CaSO_3$	$CaSO_4$	total	$CaSO_3$	CaS	$CaSO_4$	total
15	6.7	0.6	7.3	2.7	5.9	38.8	47.4
30	6.2	1.7	7.9	1.6	5.7	45.0	52.3
45	6.2	1.9	8.1	1.5	4.3	49.7	55.5
76	6.1	2.5	8.6	0.6	3.1	51.4	55.1

It is interesting to note that in the sulfurization of calcium carbonate by sulfur dioxide the rate of the process increases rapidly at temperatures above 600°. The explanation for this dependence of the sulfurization rate of calcium carbonate on the temperature is that up to 600° the sulfurization of calcium carbonate is limited by the rate of its dissociation according to the equation

$$CaCO_3 \rightleftharpoons CaO + CaO_2. \quad (6)$$

The fact that no interaction between calcium carbonate and sulfur dioxide was detected at temperatures below 500°, and also that the rate of sulfurization of calcium carbonate depends on its dissociation rate, shows that sulfur dioxide does not react directly with calcium carbonate, and that it reacts only with calcium oxide, formed by the decomposition of the latter.

Therefore, the sulfurization of pure calcium carbonate by means of oxygen-free sulfur dioxide proceeds in two stages: dissociation of calcium carbonate, and sulfurization of calcium oxide formed in the process by sulfur dioxide in accordance with Equations (1-5).

The results on Table 4 show that the degree of sulfurization of calcium oxide remains almost unchanged with increase of the reaction time over 15 minutes. The explanation is that in sulfurization of calcium oxide, the particles of the latter become coated with the reaction products, which prevent diffusion of sulfur dioxide into the calcium oxide grains and thereby retard the entire sulfurization process.

Comparison of Table 1 and Table 3 shows that at temperatures above 600° the sulfurization rate of calcium carbonate is higher than that of calcium oxide. Evidently in the case of calcium carbonate the liberated carbon dioxide prevents the formation of a dense coating of reaction products and thereby accelerates the process.

The data of Tables 1-3 lead to the conclusion that the only stable product formed in the sulfurization both of calcium oxide and of calcium carbonate is calcium sulfate. The formation of calcium sulfate proceeds mainly by way of the intermediate stage of sulfite formation from calcium oxide and carbonate by sulfur dioxide.

The suggested mechanism for the interaction of sulfur dioxide with calcium oxide and carbonate is valid only if the calcium oxide and carbonate do not contain impurities and the sulfur dioxide contains no free oxygen. If the sulfur dioxide contains oxygen, while the solid phase contains impurities which are catalytically active in the oxidation of sulfur dioxide to the trioxide, then the sulfurization of calcium oxide and carbonate by sulfur dioxide with formation of calcium sulfate proceeds also through an intermediate stage in which sulfur dioxide is oxidized to the trioxide [8].

SUMMARY

1. Oxygen-free, dry, sulfur dioxide begins to react at an appreciable rate with pure calcium oxide at 400°, and with analytical-grade calcium carbonate at 500°.

2. The final stable product of the reaction between calcium oxide and sulfur dioxide at 400-1000° is calcium sulfate, which is formed mainly by way of the intermediate stage of sulfite formation from calcium oxide.

3. The sulfurization of calcium carbonate by sulfur dioxide proceeds in two stages: dissociation of calcium carbonate, and sulfurization of the calcium oxide so formed by sulfur dioxide.

LITERATURE CITED

[1] Z. P. Rozenknop, Extraction of Sulfur Dioxide from Gases [in Russian] (Goskhimizdat, 1952).

[2] V. L Lukashin, Bull. Acad. Sci. USSR, OTN, No. 1 (1949).

[3] A. M. Pavlov, Metallurgy of Pig Iron, II [in Russian] (Metallurgy Press, 1949).

[4] Iu. V. Kariakin and L I. Angelov, Pure Chemical Reagents [in Russian] (Goskhimizdat, 1955).

[5] F. Foerster and K. Kubel, Z. anorg. Ch., 139, 261 (1924).

[6] A. V. Avdeeva, Gas Sulfur [in Russian] (Goskhimizdat, 1950).

[7] L. Wohler, F. Martin, and E. Schmidt, Z. anorg. Ch., 127, 273 (1923).

[8] S. L Vol'fkovich and F. G. Margolis, Bull. Acad. Sci. USSR No. 5 (1942).

Received March 15, 1957

DEPENDENCE OF THE CARBONATION PROCESS ON THE PARTIAL PRESSURE OF CARBON DIOXIDE IN THE INCOMING GAS AND ON THE TEMPERATURE•

G. N. Gasiuk, P. Ia. Krainii, A. G. Bol'shakov, and A. V. Kortnev

The Odessa Polytechnic Institute

There have been relative few theoretical and experimental studies.of the rate of absorption of carbon dioxide by ammoniated brines in relation to the effects of various factors. Most of these studies were performed by the static method, an important defect of which is that similarity is not maintained between the course of the experiment and the actual course of the process under industrial conditions.

Because of the specific characteristics of the static method, the region which has been studied least is the initial stage of the carbonation process (from 0.to 40-60%); the reason is that the rate of absorption of carbon dioxide is relatively high in this region, and determinations of the amount of absorbed carbon dioxide by the method used involve considerable errors.

Gol'dshtein [1] used a semidynamic method (the gas enters and leaves the apparatus during the experiment but the liquid is not renewed in the course of the experiment) which has the same disadvantages as the static methods. In the experimental part of this work there was a whole series of procedural errors which made the investigation valueless.

The results of kinetic studies of the carbonation process are still in the stage of approximate qualitative generalizations.

Knowledge of the quantitative laws governing the rate of absorption of carbon dioxide by ammoniated brines would be very useful for the design of new equipment, determination of the possibility of accelerating the process, automation, etc.

Adoption of the so-called deep preliminary carbonation regime [2] in the soda-ash industry, and the form of equipment used for this purpose, are of great significance in relation to acceleration of the carbonation process and increase of the conversion of sodium, ammonia, carbon dioxide, etc.

It is therefore desirable to investigate the possibilities of the use of gas lifts, which are widely used in technology for raising liquids, especially those containing solids in suspension, as absorption equipment for deep preliminary carbonation and simultaneously as equipment for raising the liquid.

Lopatto [3] and Grigorian [4] have shown that gas lifts can be used as high-speed absorbers, and that they can be utilized as process equipment in the production of sulfuric acid by the chamber process.

The purpose of the present investigation was to study the influence of various factors on the rate of absorption of carbon dioxide by ammoniated brines, and hence to elucidate the possibility of using gas lifts in the soda-ash industry as absorbers for deep preliminary carbonation.

In contrast to other workers [1, 5, 6] who used static methods for studying the rate of absorption of carbon dioxide by ammoniated brines, we used a dynamic method in an experimental laboratory gas-lift unit specially

•Communication I in a series on the initial stage of carbonation of ammoniated brines in gas-lift equipment.

developed and designed for the purpose [7].

The solutions were prepared from sodium chloride of "pure" grade, "chemically pure" ammonium bicarbonate, gaseous ammonia, and distilled water. The compositions of the ammoniated brines used in the experiments are given in the table.

Composition of Ammoniated Brines

Brine No.	NaCl		Direct titer	NH_3		CO_2		Carbonation	Density
	n.d.	g/l	n.d.	n.d.	g/l	n.d.	g/l	%	g/cc
1	87.0	254.0	115.0	115.0	97.8	—	—	—	1.118
2	88.0	257.0	73.0	73.0	62.0	—	—	—	1.135
3	88.2	257.5	42.9	42.9	36.4	—	—	—	1.148
4	87.6	256.0	13.9	13.9	11.8	—	—	—	1.165
5	88.2	257.5	89.9	89.9	76.4	11.62	12.8	12.9	1.151
6	87.6	256.0	90.0	90.9	76.5	24.9	27.4	27.6	1.164
7	87.6	256.0	90.1	90.1	77.55	38.0	41.8	42.9	1.173
8	87.0	254.0	90.1	90.1	76.55	54.5	60.0	60.6	1.189

The contents of the components in the brine varied relatively little during each experiment.

The results are expressed in the form of relationships representing the influence of various factors on the over-all absorption coefficients and conversion rates.

Analysis of the Experimental Data

The over-all absorption coefficients were calculated by means of the formula

$$K_G \cdot a = \frac{G}{V_1 \Delta p_{av}}, \qquad (1)$$

where V_1 is the effective volume of the apparatus (in m^3); $G = \frac{6\gamma_t (c_1 - c_2) V_0}{(100 - c_1)(100 - c_2)}$ is the amount of gas absorbed (in kg/hour); V_0 is the volumetric rate of the inert gas (in liters/minute) entering the apparatus at the experimental temperature and 760 mm; c_1 and c_2 are the concentrations of the absorbed gas at the entry and exit (in vol. % calculated as the dry ammonia-free gas); γ_t is the density of the absorbed gas at the experimental temperature and 760 mm (g/liter); $\Delta p = \frac{p_1 - p_2}{2.303 \log \frac{p_1}{p_2}}$ is the log mean difference of the partial pressures of the absorbed gas at entry and exit (atmos); $p_1 = \frac{p_3 + p_4 - p_5 - p_6}{760} \cdot \frac{c_1}{100}$ is the partial pressure of the absorbed gas at entry into the apparatus (atmos); $p_2 = \frac{p_3 - p_5 - p_6}{760} \cdot \frac{c_2}{100}$ is its partial pressure at the exit (atmos); p_3 is the barometric pressure (mm Hg); p_5 and p_6 are the vapor pressures of ammonia and water respectively over the ammoniated brines (mm Hg); p_4 is the gas pressure at the entry to the apparatus (mm Hg).

The total gas pressure at the exit was assumed to be equal to atmospheric, as the excess gas pressure was low and did not exceed 10 mm H_2O at the highest gas rates.

It must be pointed out that in calculations of the log mean difference of the partial pressure of carbon dioxide the equilibrium presence of carbon dioxide over the ammoniated brines was not taken into account, as it does not exceed 2 mm Hg even at 110% carbonation and 30° [6].

The conversion rate (absorption rate per unit working volume of the apparatus) was determined from the equation

$$U = K_G \cdot a \cdot \Delta p_{av} \qquad (2)$$

The effect of the partial pressure of carbon dioxide in the incoming gas on the over-all absorption coefficient and conversion rate was studied at 30°, immersion depth* 15%, gas rate 6000 $m^3/m^2 \cdot$ hour, and liquid rate 110 $m^3/m^2 \cdot$ hour. To eliminate the influence of hydrodynamic factors, measures were taken to reduce fluctuations in the gas and liquid rates and immersion depth to a mimimum.

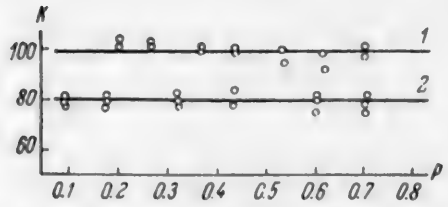

Fig. 1. Effect of partial pressure of carbon dioxide in the incoming gas on the over-all coefficient of adsorption in ammoniated brines: K) over-all absorption coefficient ($K \cdot 10^{-2}$ kg/$m^3 \cdot$ atmos $\cdot$ hr), p) partial pressure of carbon dioxide (atmos). 1) Brine No. 2, 2) brine No. 6.

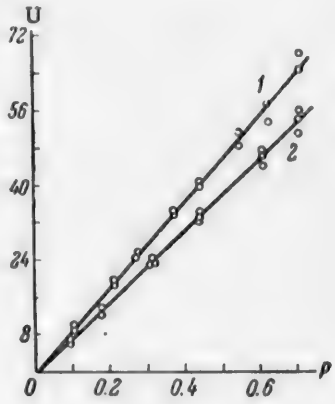

Fig. 2. Effect of partial pressure of carbon dioxide in the incoming gas on its rate of conversion by ammoniated brines: U) conversion rate ($U \cdot 10^{-2}$ kg/$m^3 \cdot$ hour), p) partial pressure (atmos). 1) Brine No. 2, 2) brine No. 6.

The experiments were performed with two ammoniated chloride brines, No. 2 and No. 6 (see table). The partial pressure of carbon dioxide in the incoming gas was varied from 0.1 to 0.7 atmos in experiments with brine No. 2, and from 0.035 to 0.7 atmos in experiments with brine No. 6. The over-all absorption coefficients are plotted against the partial pressure of carbon dioxide in the incoming gas in Fig. 1.

Figure 1 shows that the over-all absorption coefficients are constant, within the limits of experimental error, over a wide range of partial pressures of carbon dioxide in the incoming gas, and fit satisfactorily on straight lines parallel to the abscissa axis. The experimental data for two brines therefore show that in the absorption of carbon dioxide by ammoniated brines of different degrees of carbonation, the over-all absorption coefficient is independent of the partial pressure of carbon dioxide in the gas. The conversion rate is plotted against the partial pressure of carbon dioxide in the incoming gas in Fig. 2. It is seen that the conversion rate increases with increase of partial pressure of carbon dioxide in the gas. The values of the conversion rate fit satisfactorily on straight lines passing through the coordinate origin. Thus the conversion rate is directly proportional to the partial pressure of carbon dioxide in the incoming gas.

The straight lines in Fig. 2, representing the variations of the conversion rate with the partial pressure of carbon dioxide in the incoming gas, can be expressed in the form of the equation

$$U = Ap. \qquad (3)$$

where p is the partial pressure of carbon dioxide in the gas at the entry into the apparatus (atmos).

The value of the constant A depends on the immersion depth, the composition of the ammoniated brine, temperature, liquid and gas rates, etc. For the present instance at 30°, immersion depth 15%, gas rate 6000 $m^3/m^2 \cdot$ hour, and liquid rate 110 $m^3/m^2 \cdot$ hour, A = 9200 for brine No. 2 and 7700 for brine No. 6.

The relationships found to exist between the partial pressure of carbon dioxide in the incoming gas on the one hand, and the over-all absorption coefficient and the conversion rate (absorption rate) on the other, can be explained in the light of the two-film theory of diffusion on the hypothesis that in the carbonation

*The immersion depth is the ratio of the height of the liquid level above the gas inlet to the total height of the gas-lift pipe.

process (at least within the limits studied in our experiments) the liquid phase is decisive in the total resistance to absorption. As is known, the liquid-phase mass-transfer coefficient is independent of the partial pressure of the absorbed gas.

The dependence of the absorption rate on the partial pressure of carbon dioxide is consistent with the findings of Belopol'skii [6], who studied the carbonation kinetics of ammoniated brines (chloride and sulfate) by a static method. Belopol'skii showed that within the carbonation range of 100 to 130% the rate of absorption of carbon dioxide is proportional to its partial pressure in the carbonation gas. His values of the absorption coefficients, calculated for a given degree of carbonation, are also independent of the partial pressure of carbon dioxide.

Effect of temperature on the over-all absorption coefficient and conversion rate. Two series of experiments were carried out with brines No. 2 and 6, in order to determine the effect of temperature on the over-all mass-transfer coefficient and the rate of conversion of carbon dioxide by ammoniated chloride brines.

In each series of experiments the temperature was varied, with constant liquid and gas rates, carbon dioxide concentration in the incoming gas, and immersion depth. The process temperature was varied in 5-degree steps from 20 to 40° in the absorption of carbon dioxide by brine No. 2, and from 20 to 45° in experiments with brine No. 6.

Variations of the over-all absorption coefficient with temperature are plotted in semilogarithmic coordinates in Fig. 3.

Figure 3 shows that the plots of the over-all absorption coefficients against the temperature are linear (Line 1 for brine No. 2, and Line 2 for brine No. 6), and may be represented by the following expression:

$$K_G \cdot a = B \cdot e^{0.0238t}, \quad (4)$$

where t is the temperature (in °C).

The value of the constant B depends on the experimental conditions (immersion depth gas and liquid rates, brine composition). For the conditions used B = 4390 for brine No. 2.

In Fig. 4 the conversion rates of carbon dioxide by ammoniated brines are plotted against the temperature in logarithmic coordinates.

The plots of the conversion rate against the temperature are linear (Line 1 for brine No. 2, and Line 2 for brine No. 6), represented by a power relationship of the form

$$U = B' \cdot t^{0.49}, \quad (5)$$

where t is the temperature (in °C).

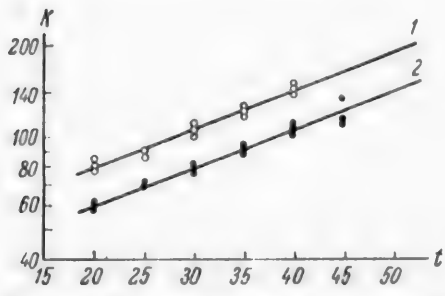

Fig. 3. Effect of temperature on the over-all coefficient of absorption of carbon dioxide by ammoniacal brines: K) over-all absorption coefficient (K · $\cdot 10^{-2}$ kg/m³ · atmos · hr), t) temperature (°C).

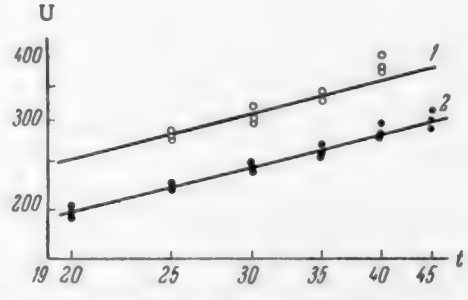

Fig. 4. Effect of temperature on the rate of conversion of carbon dioxide by ammoniacal brines: U) conversion rate (U · 10^{-2} kg/m³ · hr), t) temperature (°C).

For our experimental conditions (immersion depth 15%, gas rate 6000 m³/m² · hour, liquid rate 115 m³/m² · hour, carbon dioxide concentration of incoming gas 37-38%) the constant B = 614.

The relationships between the temperature on the one hand, and the over-all absorption coefficient and the conversion rate respectively on the other, are different. The reason is that the experiments were performed with constant concentration of carbon dioxide in the incoming gas. The partial pressure of ammonia and water vapor over the ammoniated brines increase with temperature, and therefore at constant gas concentration the partial pressure of carbon dioxide over the brine falls with rise of temperature. As was shown earlier, the over-all absorption coefficient is independent of the partial pressure of carbon dioxide, while the conversion rate is directly proportional to the partial pressure of carbon dioxide in the incoming gas. Therefore, our relationship between the conversion rate and the temperature is valid only if the gas concentration and not the partial pressure remains constant with change of temperature.

The relationships for the over-all absorption coefficient and the conversion rate of carbon dioxide by ammoniated chloride brines in the 20-45° temperature range are valid both for brines of zero degree of carbonation (brine No. 2) and for carbonated brines (brine No. 6). It may be assumed that they also hold for the whole initial stage of the carbonation process until crystals of sodium bicarbonate begin to form in the brine.

SUMMARY

1. The carbonation process was studied at different concentrations of carbon dioxide in the incoming gas and at different temperatures, in an improved experimental laboratory unit, by the dynamic method in a gas-lift apparatus; it was found that the over-all absorption coefficient at the initial stage of the carbonation process is independent of the partial pressure of carbon dioxide in the incoming gas, and the conversion rate is directly proportional to the concentration of carbon dioxide in the incoming gas.

2. The over-all absorption coefficient is an exponential function of the temperature, while the conversion rate is a power function.

LITERATURE CITED

[1] Ia. R. Gol'dshtein, J. Appl. Chem. 21, 1 (1948).*

[2] N. E. Kirichenko and L. N. Shokin, J. Chem. Ind. 4, 6 (1951). *

[3] E. K. Lopatto and L. I. Aleksandrova, Coll. Chem. Faculty Mechnikov State Univ., Odessa, 1 (1952).*

[4] G. O. Grigorian and A. G. Bol'shakov, Sci. Mem.OPI 2 (6), 1, 27, 51, 97 (1955).*

[5] A. P. Belopol'skii et al., J. Appl. Chem. 10, No. 3, 1 (1957; 10, No. 10, 717 (1937).*

[6] A. P. Belopol'skii et al., J. Appl. Chem. 19, No. 10-11, 1181 (1946); 20, No. 11 1154 (1947).*

[7] G. N. Gasiuk, A. G. Bol'shakov, A. V. Kortnev, and P. Ia. Krainii, J. Appl. Chem. 31, No. 7, 1019 (1958).*

Received May 3, 1957

*In Russian.

EFFECT OF FERRIC OXIDE ON THE PROPERTIES OF BORATE AND BORON-FREE GROUND COAT ENAMELS

G. I. Beliaev and N. F. Smakota

The Dnepropetrovsk Institute of Chemical Technology

During the firing of ground coats, action of atmospheric oxygen [1-4] and of the silicate melt [5] results in oxidation of steel and interaction of the iron oxides formed with the ground enamel. For example, Dietzel and Meures [1] consider that up to 30% of iron oxides dissolves in ground-coat enamels during firing. Petzold [6] states that a normally-fired ground coat contains 10-20% of iron oxides. K. P. Azarov reports that ground coats should dissolve up to 30-50% of iron oxides without supersaturation. He also showed that silicate melts react very vigorously with ferrous oxide, satisfactorily with magnetic oxide of iron, and badly with ferric oxide [7, 8].

One of the present authors [3, 2] has found that the oxidation of steel depends to a considerable extent on the composition of the ground-coat enamel and on the properties and state of the steel surface.

It is shown in the present paper that enrichment of the enamel layer with iron oxides during firing leads to changes of viscosity, surface tension, crystallizability, and other properties of the silicate melt, and also has a considerable influence on the quality of the ground coat and on the process of its formation.

The available literature on this subject contains mainly data on the influence of added iron oxides on enamel viscosity; moreover, the experiments were performed with borate enamels containing about 20% B_2O_3 [1, 4, 6, 9], although low-boron and boron-free ground-coat enamels are now widely used in the USSR.

We have therefore studied the effects of ferric oxide on such important physicochemical properties of borate and boron-free enamels as the viscosity, surface tension, wetting, crystallizability, oxidizability, and other properties which characterize fairly fully the behavior of ground-coat enamels during firing. Ferric oxide, Fe_2O_3, was added to the ground coat. Vargin has shown that in the melting of enamels with added iron oxides the equilibrium $FeO \rightleftharpoons Fe_2O_3$, is established; this equilibrium is greatly influenced by the composition of the melt and the melting conditions [10, 11].

EXPERIMENTAL

The experimental ground-coat enamels were made from frits No. 215 (borate) and No. 27 (boron-free), of factory production.

The chemical composition of the ground-coat frits (%) is given below:

Oxides	215	27
SiO_2	46.0	60.5
Al_2O_3	8.0	2.6
Na_2O	19.9	23.0
B_2O_3	18.3	—
CaF_2	5.6	13.3
Co_2O_3	0.6	0.6
Ni_2O_3	0.6	—
MnO_2	1.0	—

For preparation of the samples, the frits were ground to pass through a sieve with 144 holes/cm^2, and then mixed with ferric oxide. The ferric oxide was added in the form of Fe_2O_3 of "pure" grade, in amounts of 3, 6, 10, 15, 20, 25 and 30 g per 100 g of frit. The mixtures were melted in fireclay crucibles in a laboratory electric furnace at 1100-1150° and then granulated in water. The granules were ground in a ball mill, and the powder was pressed into cylindrical specimens 15 mm in diameter and 10 mm high, used for determinations of fluidity and contact angle.

The fluidity of the enamel was estimated from the length of a drop formed in 8 minutes on a steel plate set at an angle of 45° in a muffle furnace heated to 850°. The contact angle was determined by the "sessile drop" method.

The viscosity near the softening point was determined by the usual method of extension of a thread drawn from the melt [12]. The surface tension was determined by a simplified drop-weight method [13].

Data on the influence of Fe_2O_3 on the spreading of borate and boron-free enamels are presented in the table.

Effect of Added Ferric Oxide on Enamel Fluidity (mm)

Enamel	Fe_2O_3 added (g/100 g of frit)							
	0	3	6	10	15	20	25	30
Borate	53.5	57.5	58.0	61.5	60.0	55.5	39.0	35.0
Boron-Free	40.5	46.0	44.0	44.0	43.0	39.5	36.5	25.0

Viscosity curves are plotted in Fig. 1, while Figs. 2 and 3 show variations of contact angle and surface tension of ground-coat enamels with ferric oxide content.

The results presented in the graphs and table show that the borate enamel spreads much better than the boron-free over steel surfaces. The viscosity falls and the fluidity improves with increase of the ferric oxide content up to 10% in the borate enamel, but only up to 3% in the boron-free enamel.

Further increases of the ferric oxide content worsen the fluidity and increase the viscosity both of borate and boron-free melts. These results show that the viscosity of the melt changes continuously during the firing of a ground coat: it decreases at first to a certain minimum, but toward the end of the firing period it increases considerably as the enamel becomes enriched with iron oxides. This conclusion was confirmed by the following additional experiments: the enamel was removed mechanically from normally-fired coated steel plates, and specimens for determinations of fluidity and viscosity were prepared from the powders. It was found that

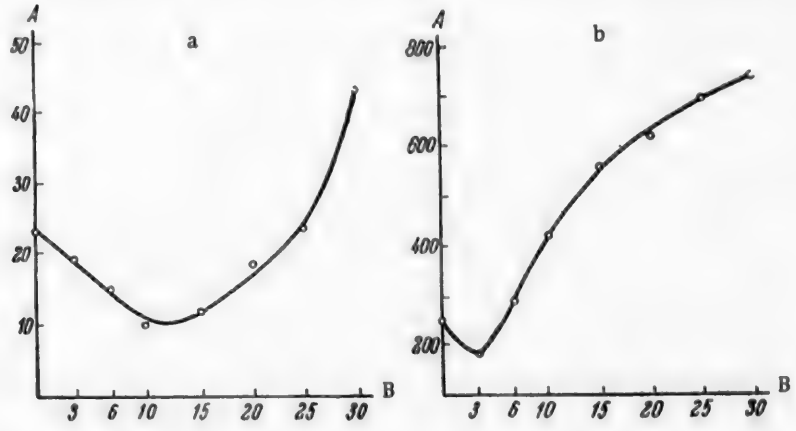

Fig. 1. Viscosity of borate (a) and boron-free (b) ground-coat enamels as a function of the ferric oxide content: A) viscosity $\eta \cdot 10^6$ (poises), B) amount of Fe_2O_3 per 100 g of frit (g).

the fluidity of the borate enamel fell from 53.5 to 40.5 mm, and of the boron-free from 44.0 to 26.0 mm after firing. The viscosity rose from $22.9 \cdot 10^6$ to $34.0 \cdot 10^6$ poises for the borate enamel, and from $258 \cdot 10^6$ to $655.7 \cdot 10^6$ poises for the boron-free. These results show that the fluidity of the boron-free enamel decreases during firing and enrichment of the melt with iron oxides, and its viscosity increases much more than that of a borate enamel. The viscosity increase is an indirect indication that a part of the iron oxides remained undissolved and was present in the enamel in a suspended state.

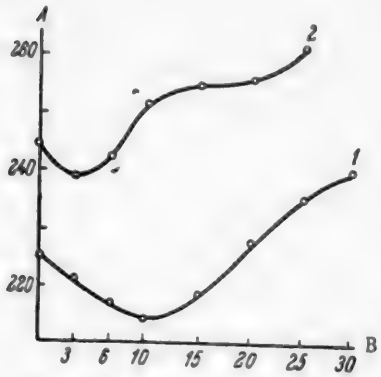

Fig. 2. Effect of ferric oxide on the surface tension of borate (1) and boron-free (2) ground-coat enamel: A) surface tension (dynes/cm), B) amounts of Fe_2O_3 per 100 g of frit (g).

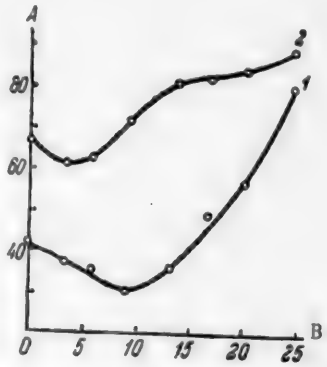

Fig. 3. Effect of ferric oxide on the wetting of steel by a borate (1) and boron-free (2) ground-coat: A) contact angle (degrees), B) amount of ferric oxide (%).

Figures 2 and 3 show that the borate enamel has lower surface tension and wets oxidized steel much better than the boron-free. Additions of up to 10% of Fe_2O_3 to the borate enamel, and up to 3% to the boron-free decrease surface tension and improve wetting of steel by the silicate melt. Further increases of the ferric oxide content in the enamels worsen wetting considerably and increase the surface tension of the enamel melts, especially the boron-free.

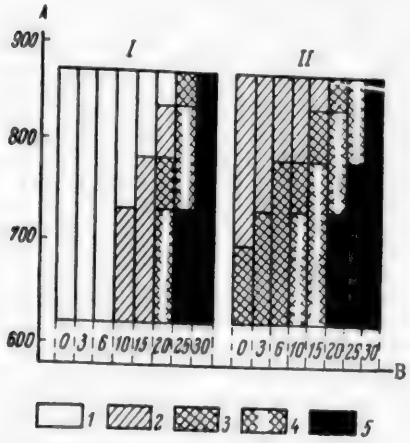

Fig. 4. Crystallizability of ground-coat enamels in relation to their Fe_2O_3 contents: A) temperature (°C), B) amount of Fe_2O_3 per 100 g of frit (g); 1) no crystals, 2) crystalline film, 3) crystalline crust, 4) crust and separate crystals, 5) complete crystallization; ground coats: I) borate, II) boron-free.

Crystallizability of the enamels was studied by the polythermal method [12] in a horizontal tubular temperature-gradient furnace with a maximum temperature of 870° and a temperature gradient of about 15° per cm. The boat with the melt was held in the furnace for 3 hours, extracted, and cooled rapidly in air. Qualitative extimates of the crystallizability [12] of the enamel melts were made visually and augmented by means of a binocular microscope. The results are shown schematically in Fig. 4. The experimental results indicate that the boron-free enamel has a greater tendency to crystallization than the borate, and that the crystallization tendency of ground-coat enamels increases with increasing content of ferric oxide in the melt. An appreciable increase of the crystallization tendency is observed on addition of 15% Fe_2O_3 to the frit in the case of the borate enamel, and of 6% in the case of the boron-free. These experiments convincingly confirm the earlier [2] view that excessive oxidizability of steel during firing of ground coats increases the tendency of the enamel coating to crystallization and flaw formation.

The following experiments were performed in order to elucidate the significance of enamel crystallization and the role of iron oxides in the formation of good ground coats.

Ground-coated steel specimens, 50 x 100 x 0.5 mm in size, were fired in a muffle furnace under the optimum conditions (870°, 4 mm). The ground coat after firing was bright, without blisters or flaws. The specimens were then put into the temperature-gradient furnace with maximum temperature 700°, and held there for 4 hours.

Examination of the cooled specimens showed that abundant flaws and surface bumps were produced in the ground coat as the result of prolonged exposure in the furance. The coating lost its luster and became uneven and rough. Photographs of specimens of borate and boron-free ground-coats before heat treatment (left) and after (right) are shown in Fig. 5.

These results indicate that flaws are formed as the result of saturation of the ground coat with iron oxides and secondary crystallization of the melt during firing.

Very interesting data, shedding light on the influence of enamel crystallization on ground-coat quality, were obtained by the following method. A production boron-free frit No. 27, was subjected to enforced crystallization by exposure in a muffle furnace at 700° for 5 hours. The fluidity and contact angle of the ground-coat frit, and the oxidizability of the steel during firing of the ground coats were then determined. The results of these experiments showed that the fusibility (fluidity) of a crystallized frit is 35.0 mm, and that of an ordinary frit, 40.5 mm. The wetting of oxidized steel by the ground-coat melt also deteriorated, as the contact angle θ increased from 67° for the ordinary frit to 110° for the crystallized frit. The oxidation rates of the steel during the firing of the ground coats were also different: the rate for the normal frit was 74 mg/dm^2, and for the crystallized frit, 93.5 mg/dm^2.

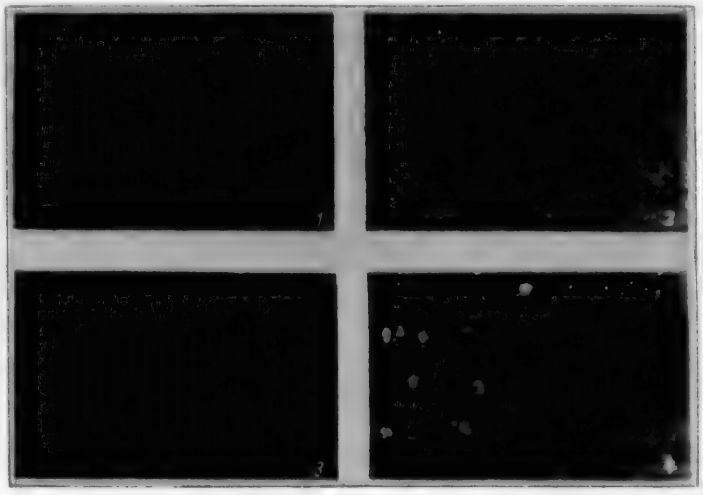

Fig. 5. Effect of heat treatment on flaw formation in ground coats. 1, 2) borate enamel; 3, 4) boron-free enamel; 1, 3) before heat treatment; 2, 4) after heat treatment.

To test the effect of a crystallized frit on the quality of the ground coat, enameling tests were performed with steel specimens. Slips with addition of 45% water, 3.0% Glukhovo clay, and 1.0% borax were made from the crystallized and normal frits. Steel plates coated with these slips were fired in a muffle furnace at 820, 860, and 900° for 2, 4, and 6 minutes. Visual examination of the specimens showed that the ground coat obtained from the crystallized frit was considerably inferior in quality to the coat formed from normal frit — it contained numerous flaws and bumps rich in crystalline iron compounds. In Fig. 6 specimens of the ground coats formed from crystallized frit are shown on the right, and similar specimens, but from normal frit, are shown on the left.

These results indicate that the intensity of interaction during firing between the enamel coating and the scale formed on the steel surface depends not only on the chemical composition of the enamel and, in particular, on the presence of B_2O_3 in it, but also on the relative proportions of the glassy and crystalline phases. The glassy component of the frit probably dissolves the scale more effectively, and reacts much more vigorously

with iron oxides than the crystalline component of the same composition. The course of oxidation of the steel during firing of ground coats was studied by means of periodic weighing of specimens without extraction from the tubular furnace [2]. Figure 7 shows the weight increases of the specimens during firing of ground coats at 850° for 8 minutes. This graph indicates that steel is oxidized much more rapidly during the firing of

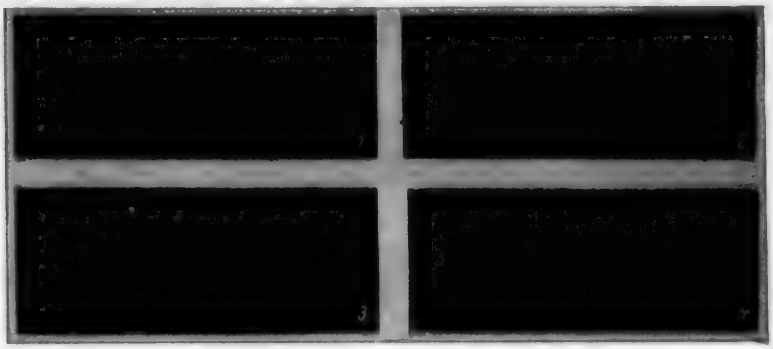

Fig. 6. Appearance of ground-coat enamels obtained from ordinary (1, 3) and crystallized (2, 4) frits; the specimens were fired at 900° for two (1, 2) and four (3, 4) minutes.

a boron-free than of a borate enamel. Additions of 6% Fe_2O_3 to the borate and 3% to the boron-free frit have virtually no effect on the oxidation rate of the steel. Further increase of the amount of ferric oxide in the frit increases the oxidizability of the steel during firing of the ground coat.

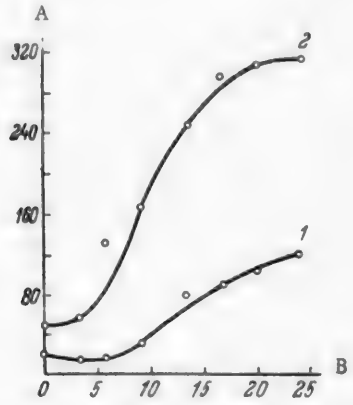

Fig. 7. Effect of additions of Fe_2O_3 to the frit on the oxidizability of steel during firing of ground coats: A) weight increase (mg/dm^2), B) amount of ferric oxide (%) Ground coats; 1) borate, 2) boron-free.

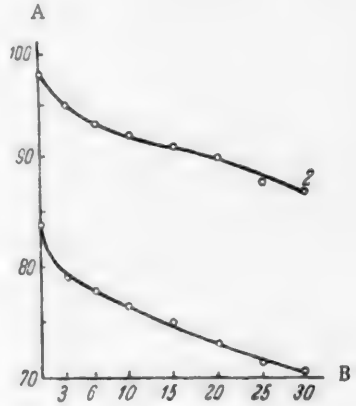

Fig. 8. Effect of ferric oxide on the coefficient of thermal expansion of ground-coat enamels: A) coefficient of thermal expansion $\alpha \cdot 10^{-7}$, B) amounts of Fe_2O_3 per 100 g of frit (in g) Enamels: 1) borate, 2) boron-free.

Dietzel, Meures, Petzold [9] and other workers consider that the coefficient of thermal expansion of the ground-coat enamel increases during firing owing to dissolution of iron oxides in it. However, doubt has recently been cast on these views [14].

We determined the coefficients of thermal expansion of borate and boron-free ground-coat enamels containing the amounts of ferric oxide indicated above. The coefficient of thermal expansion was determined in the 30-350° range by means of a dilatometer with an optical indicator. The results (Fig. 8) show clearly that the coefficient of thermal expansion of the ground coat decreases with increase of the amount of ferric oxide in the frit.

Finally, trial enamelings of steel specimens were carried out. Estimates of the surface quality lead to the conclusion that additions of up to 10% of ferric oxide to borate ground-coat enamels, and up to 3% to boron-

free, have no significant adverse effects on the coating quality. Further increase of the ferric oxide content leads to a sharp increase of ground-coat defects such as flaws, "copperheads", and blisters. The color of the coatings changes from black to brown, and the enamel becomes dull and rough. The adherence of the ground coat to the steel is worsened considerably.

SUMMARY

1. Additions of ferric oxide produce continuous variations in the physicochemical properties both of borate and of boron-free ground-coat enamels.

2. The viscosity of the ground-coat enamels decreases and the fluidity improves with increase of the ferric oxide content, up to 10% for borate and up to 3% for boron-free enamel. Further increases of the ferric oxide content in the frits worsen the fluidity and raise the viscosity of enamel melts.

3. Borate melts have lower surface tension and wet oxidized steel much better than boron-free. Additions of up to 10% of ferric oxide to borate enamels, and up to 3% to boron-free decrease the surface tension and improve wetting, but further increases of the ferric oxide content have an adverse effect on these properties.

4. Boron-free ground-coat enamels have a greater tendency to crystallization than borate enamels. Additions of ferric oxide increase the crystallization tendency of enamels, especially ground-coat enamels without boric anhydride.

5. Previous crystallization of the frit results in considerable worsening of the coating quality and increases the number of flaws and blisters.

6. Flaws and "copperheads" in ground coats are caused by supersaturation of the enamel layer with iron oxides, and by crystallization of the enamel melt. Boron-free ground-coat enamels have a greater tendency to form flaws because they crystallize readily on saturation with iron oxides.

7. The coefficients of thermal expansion of borate and boron-free ground-coat enamels decrease with increasing ferric oxide content.

8. Additions of up to 10% of ferric oxide to the borate frit, and up to 3% to the boron-free have no significant influence on the quality of the coating. Further increases of Fe_2O_3 content in the frits result in a considerable worsening of the external appearance of the coatings, increase flaws, and have an adverse effect on the adherence of the enamel to steel.

LITERATURE CITED

[1] A. Dietzel and K. Meures, Sprechsaal, 66, 751 (1933).

[2] G. I. Beliaev, Trans. Novocherkassk Polytech. Inst. 24 (38) (Industrial Construction Press, 1953).

[3] G. I. Beliaev, in the book; Production and Technical Conference on Enameling [in Russian] (Metallurgy Press, 1956).

[4] H. Hadwiger, Aus der Praxis der Blechgrundemaillierung, Silikattechnik, 7 (1956).

[5] G. I. Beliaev, J. Appl. Chem. 30, No. 7, 1077 (1957).*

[6] A. Petzold, Der Einfluss von Eisenoxyden auf die Viskositat von Grundemails. Mitteilung aus dem Institut fur angewandte Silikatforschung, Berlin (1953).

[7] K. P. Azarov, Refractories 9 (1950). [In Russian].

[8] K. P. Azarov, " Structure and properties of enamels," in the book: Structure of Glass [in Russian] (Izd. AN SSSR, 1955), No. 13.

[9] A. Petzold, Email. Berlin (1955).

[10] V. V. Vargin, Production of Colored Glass [in Russian] (State Light Industry Press, 1940).

*Original Russian pagination. See C.B. Translation.

[11] V. V. Vargin and A. A. Kefeli, Papers Dedicated to the Memory of Academician I.V. Grebenshchikov [in Russian] (State Defense Press, 1956).

[12] K. S. Evstrop'ev and N. A. Toropov, Chemistry of Silicon and Physical Chemistry of Silicates [In Russian] (Industrial Construction Press, 1956).

[13] K. P. Azarov, Zavod. Lab. 3 (1954).

[14] A. A. Appen, R. L. Bresker, and L. A. Kuznetsova, J. Appl. Chem. 29, No. 11, 1753 (1956).*

Received July 18, 1957

*Original Russian pagination. See C.B. Translation.

INTERACTION OF CALCIUM ZIRCONATE WITH B_2O_3 MINERALIZER

A. K. Kuznetsov

Institute of Silicate Chemistry, Academy of Sciences USSR

It is known [1-3] that additions of small amounts of boric anhydride to calcium zirconate lower its sintering temperature considerably and improve the ceramic properties of the fired body.

The present paper deals with a study of the phase composition of the products formed by the interaction of calcium zirconate with B_2O_3 mineralizer, and with the influence of this additive on the sintering of calcium zirconate. Data on the refractory properties of ceramics based on calcium zirconate were also checked.

Calcium zirconate was prepared by twofold firing of an equimolecular $CaCO_3$ – ZrO_2 mixture ("pure" grade reagents) at 1400°, the material being ground between the firings. The exposure time during each firing was 2 hours

The product [4] had the following phase composition (%): $CaZrO_3$ – 99.06, ZrO_2 (as solid solution) –0.934, CaO (free) – absent.

Individual portions of the finely ground $CaZrO_3$ were mixed either with 3.6 or 12 molar % of B_2O_3*, or with previously-synthesized calcium borates. The additions of the latter were equivalent to 6 molar % of B_2O_3. The samples were mixed thoroughly and molded into specimens under a pressure of 460 kg/cm².

Three different firing temperatures were used: 1400, 1500, and 1600°, the heating rate being 3° per minute. The exposure time at each final temperature was 2 hours.

Complex thermal analysis [5] of a mixture of $CaZrO_3$ with 6 molar % B_2O_3 shows (Fig. 1,a) that boric acid reacts very vigorously with calcium zirconate. The differential thermal curve shows three exothermic effects at 730, 770, and 970°, and two endothermic effects at 180 and 1250° (the first endothermic effect is due to the removal of water combined with the boric acid). The endothermic effect at about 1250° is accompanied by abrupt shrinkage of the specimen.

Comparison of the x-ray patterns (Fig. 2) of specimens quenched at temperatures corresponding to the start and end of each heat effect shows that from 650° intensity maxima appear on the ionization curve, corresponding to a solid solution of CaO in ZrO_2.

The amount of solid solution increases with the firing temperature. The results of chemical phase analysis [5] (Table 1) confirm the x-ray data.

In the 650-1050° range, corresponding to the three exothermic effects on the thermogram (Fig. 1), the $CaZrO_3$ content decreases sharply and the amount of solid solution increases. The amount of the latter also increases with increase of the B_2O_3 content in the specimen (Table 2).

It was found in the x-ray investigation that increase of the B_2O_3 content to 24 molar % has the result that the specimen consists of the solid solution only after being fired at 900°; maxima corresponding to calcium zirconate are not found on the ionization curve.

*B_2O_3 was added to $CaZrO_3$ in the form of an equivalent amount of H_3BO_3 (in aqueous solution).

The formation of a solid solution from calcium zirconate in presence of B_2O_3 may be represented as follows. Boric anhydride, being a more ractive oxide than ZrO_2, binds a part of the calcium oxide present in the calcium zirconate lattice. Defects therefore arise in the cationic portion of the lattice, which is reconstructed into a lattice corresponding to the solid solution.

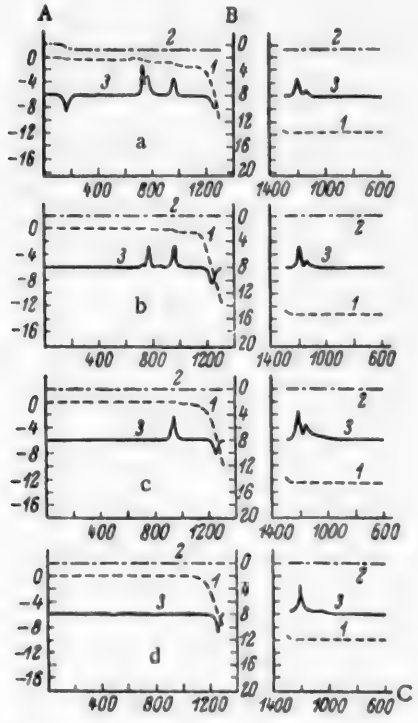

Fig. 1. Multiple thermograms for calcium zirconate with additions of B_2O_3 and calcium borates: a) $CaZrO_3 + B_2O_3$, b) $CaZrO_3 + CaO \cdot 2B_2O_3$ (equivalent to 6 molar % B_2O_3), c) $CaZrO_3 + CaO \cdot B_2O_3$ (equivalent to 6 molar % B_2O_3), d) $CaZrO_3 + 2CaO \cdot B_2O_3$ (equivalent to 6 molar % B_2O_3). A) length change of Specimen 1 (%), B) weight loss of Specimen 2 (wt. %), C) differential thermal effects.

The formation of a solid solution by removal of CaO ions from $CaZrO_3$ lattice confirms the hypothesis of Avgustinik and Antselevich [6] that a solid solution of CaO in ZrO_2 is a type II solid solution

TABLE 1

Chemical Phase Analysis of Specimens of $CaZrO_3$ with 6 Molar % of B_2O_3, Fired at Different Temperatures.

Firing temperature (°C)	Amount of $CaZrO_3$ (%)	Amount of solid solution (%)
650	99.06	0.93
850	85.90	7.42
1050	75.25	18.09
1200	15.15	18.01
1300	75.28	18.09

of the vacancy type. According to their data, the number of atoms in the unit cell of a solid solution of ZrO_2 with 10molar % CaO is 11, rather than the 12 required for the unit cell of a cubic lattice of the CaF_2 type.

It is known from the literature [7] that boric anhydride forms four different compounds with calcium oxide: calcium diborate ($CaO \cdot 2B_2O_3$), monocalcium borate ($CaO \cdot B_2O_3$), dicalcium borate ($2CaO \cdot B_2O_3$), and tricalcium borate ($3CaO \cdot B_2O_3$). It seemed likely that the exothermic effects on the thermogram (Fig. 1) are due to the formation of calcium borates and their conversion from acidic to basic salts during subsequent heating To test this hypothesis, complex thermal analysis was performed on mixtures of $CaZrO_3$ with previously-synthesized calcium borates. For example, if $CaO \cdot 2B_2O_3$ rather than boric acid is added to $CaZrO_3$, then the first exothermic effect, corresponding to the formation of calcium diborate (730°), disappears) from the thermogram (Fig. 1,b). The only heat effects remaining are those corresponding to the conversion of $CaO \cdot 2B_2O_3$ first $CaO \cdot B_2O_3$ (exothermic effect at 770°), and then into $2CaO \cdot B_2O_3$ (exothermic effect at 1000°).

When $CaO \cdot B_2O_3$ is added to calcium zirconate (Fig. 1,c), only the last exothermic effect (at 1000°) remains on the differential curve, corresponding to conversion of $CaO \cdot B_2O_3$ into $2CaO \cdot B_2O_3$. This last exothermic effect vanishes from the thermogram on addition of $2CaO \cdot B_2O_3$ to calcium zirconate (Fig. 1, d).

Chemical phase analysis of specimens with additions of boric acid and calcium borates (equivalent to 6 molar % B_2O_3) shows (Table 3) that the calcium zirconate content decreases on addition of boric acid or of any of the borates except $3CaO \cdot B_2O_3$.

For elucidation of the causes of the lowering of the sintering temperature of $CaZrO_3$ in presence of B_2O_3 or calcium borates, we studied the processes taking place in the 1150-1300° range, accompanied by an

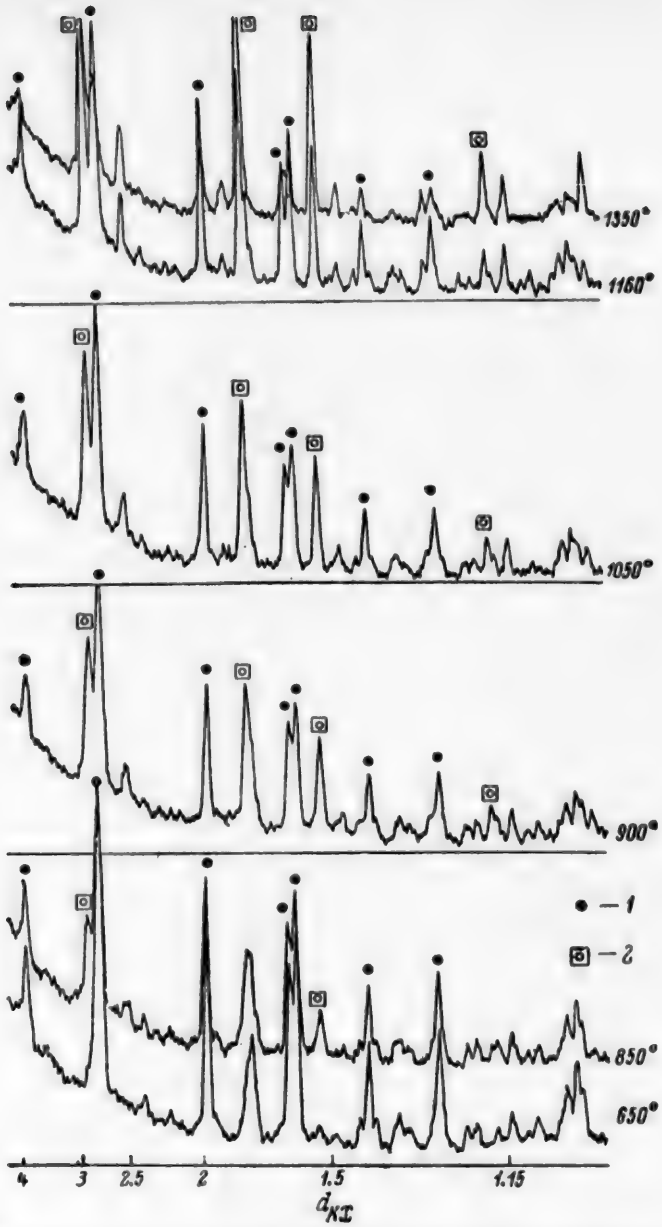

Fig. 2. X-ray patterns obtained during the heating of a mixture of $CaZrO_3$ with 6 molar % B_2O_3: 1) $CaZrO_3$, 2) solid solution of CaO in ZrO_2.

endothermic effect on the thermogram, and by abrupt shrinkage of the specimen.

The endothermic effect (1250°) is reversible. It is reproduced on repeated heating. It cannot be attributed to polymorphous transition of any particular phase, as the x-ray pattern taken at temperatures of 1160-1350°, corresponding to the beginning and end of the endothermic effect (Fig. 2), do not reveal any structural changes.

The endothermic effect increases with increasing B_2O_3 content and, finally, with 10 wt % of B_2O_3 the specimen melts completely at 1250°.

All this indicates that the endothermic effect at 1250° is associated with fusion of the substance. The substance which melts is evidently the eutectic mixture of $2CaO \cdot B_2O_3$ and $CaO \cdot B_2O_3$ (m. p. of $2CaO \cdot B_2O_3$

is 1298°, m.p. of $CaO \cdot B_2O_3$ is 1154° [7]). The cooling curve (Fig. 1,a,b,c) has two exothermic effects, corresponding to crystallization of these compounds.

TABLE 2

Effect of B_2O_3 Content in the Specimen on the Amount of Solid Solution Formed

Starting material	Amount of B_2O_3 (molar %)	Firing temp. (°C)	Exposure (hours)	$CaZrO_3$ content (%)	Am't of solid solution (%)	Chem. anal. of solid sol'n (%)		
						ZrO_2	CaO	B_2O_3
$CaZrO_3$	3	1300	2	93.90	4.25	90.42	9.54	Her
	6	1300	2	75.20	18.08	90.16	9.83	Her
	12	1300	2	50.30	37.30	90.15	9.86	Her

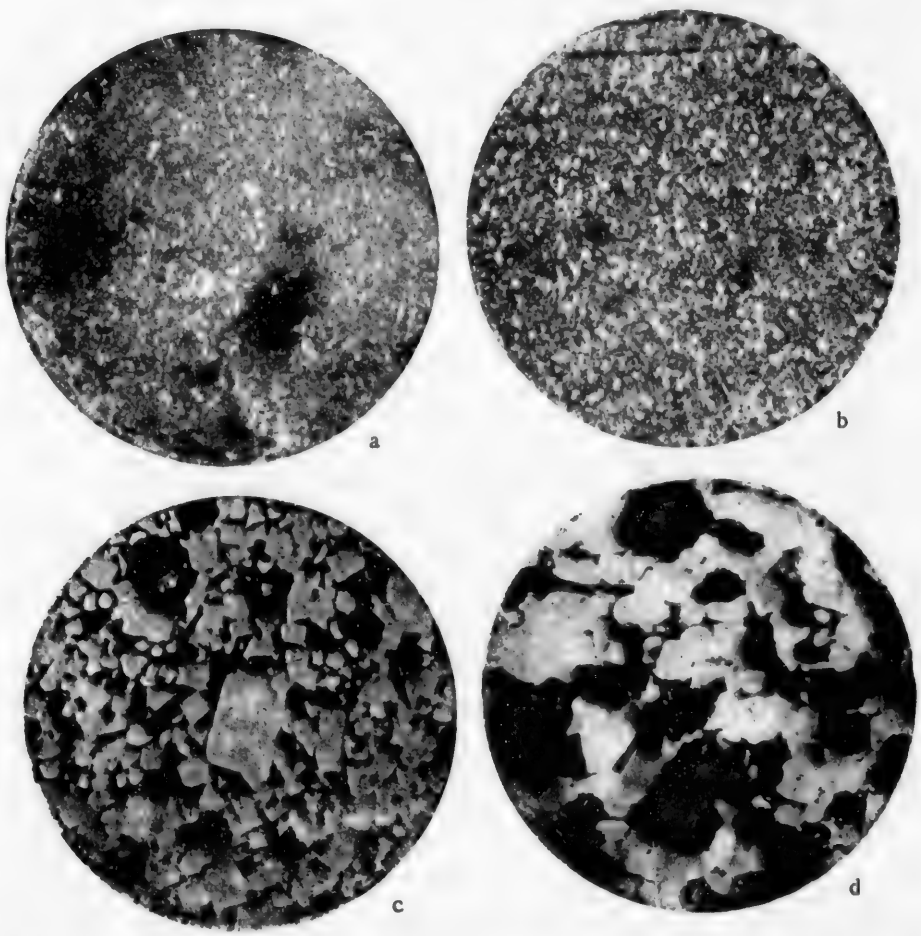

Fig. 3. Photomicrographs of specimens of calcium zirconate with additions of 6 molar % B_2O_3; exposure 2 hours; firing temperature (°C): a) 1150, b) 1300, c) 1600, d) 1600 (without mineralizer); magnification 300.

Microscopic examination of specimens fired at temperatures corresponding to the beginning and end of the endothermic effect (1150 and 1300°) shows that intensive growth of $CaZrO_3$ crystals takes place in this region. The crystals are difficult to distinguish (they are 1-2 μ in size) on the surface of a polished section of the first specimen (Fig. 3,a; temperature 1150°), whereas the second photomicrograph (Fig. 3,b; temperature 1300°)

TABLE 3

Chemical Phase Analysis of the Specimens (Fired at 1300° for 2 hours)

Addition to $CaZrO_3$, equivalent to 6 molar % B_2O_3	Theoretical $CaZrO_3$ content (%)	% of $CaZrO_3$* (calculated on 100%)	Actual $CaZrO_3$ content of specimen (%)
Without mineralizer	—	—	99.06
B_2O_3	78.8	81.70	75.20
$CaO \cdot 2B_2O_3$	81.1	84.70	83.00
$CaO \cdot B_2O_3$	83.5	87.10	84.32
$2CaO \cdot B_2O_3$	87.9	93.2	92.72
$3CaO \cdot B_2O_3$	92.2	100.0	99.08

*The $CaZrO_3$ content in the specimen with mineralizer is taken as 100%.

reveals fairly well-defined crystals. On further increase of the firing temperature (to 1600°) the crystals increase so much in size to ~15 μ) that large crystals with sharp faces can be distinguished under the microscope even at a low magnification (Fig. 3,c).

Table 4

Refractory Properties of the Specimens

Addition to $CaZrO_3$	Amount added (% by wt)	Firing temperature (°C)	Exposure (hours)	Shrinkage (%)	Porosity (%)	Aver. coef. of lin. expansion, 20-1300° range	Compres. strength (kg/cm^2)	Thermal conductivity $\left(\frac{kcal}{m \cdot degree \cdot hr}\right) \cdot 400$	Refractoriness* (°C)	Deformation under load of 2 mg/cm^2			Heat endurance***
										start of softening	4% compression	40% compression	
No addition	—	1600	2	15.75	21.34	$9.4 \cdot 10^{-6}$	982	0.80 ; 0.70	2300	1670°	1830°	1830°	3
$2CaO \cdot B_2O_3$	0.5	1600	2	20.50	0.01	$9.8 \cdot 10^{-6}$	2650	0.85 ; 0.75	2300	1840°	1840°	1840°	2

*The refractoriness was taken as the temperature of visible surface fusion.

**The load-deformation tests were stopped at 1840°.

***The heat endurance was estimated as the number of cycles of heating to 1300° and cooling in air before appearance of cracks in the specimens (30 × 30 mm cubes).

Well-defined crystals of calcium zirconate cannot be distinguished in specimens without added B_2O_3, even at high firing temperature (1600° and over; Fig. 3,d).

It follows that the considerable lowering of the sintering temperature of calcium zirconate in presence of B_2O_3 is due to the formation of a liquid phase at 1150-1300°; this liquid phase assists agglomerative crystallization of $CaZrO_3$, with an approximately 15-fold increase of crystal size.

The ceramic and refractory properties of calcium zirconate were studied with specimens containing added $2CaO \cdot B_2O_3$. Dicalcium borate produced the same lowering of the sintering temperature of calcium zirconate as B_2O_3, but it does not result in the formation of considerable amounts of solid solution.

Investigation of the ceramic properties of calcium zirconate body with additions of 0.5, 1, and 2 wt. % of $2CaO \cdot B_2O_3$ fired at different temperatures showed that specimens containing 0.5 wt. % $2CaO \cdot B_2O_3$ and fired at 1600° have slight porosity and high mechanical strength. These specimens were used for more detailed tests of refractory properties. Parallel tests were performed on specimens without mineralizer and containing added $2CaO \cdot B_2O_3$, fired simultaneously. The results are presented in Table 4.

The results in this table show that addition of $2CaO \cdot B_2O_3$ improves most of the technical properties of the material.

Our experiments did not confirm the findings of Nadler and Fitzsimmons [8] concerning the good thermal endurance of ceramics based on calcium zirconate. Because of the high coefficient of linear expansion and poor thermal conductivity, specimens of calcium zirconate either with or without mineralizer have poor thermal endurance. Therefore calcium zirconate can be used only for refractory wares used without abrupt changes of temperature.

LITERATURE CITED

[1] E. K. Keler, N. A. Godina, A. K. Kuznetsov, and A. B. Andreev, J. Appl. Chem. 30, No. 5, 682 (1957). •

[2] K. E. Lisker, Candidate's Dissertation (Leningrad, 1954).

[3] E. K. Keler and A. K. Kuznetsov, J. Inorg. Chem. 1, No. 6, 1292-1295 (1956) [USSR].

[4] E. K. Keler and N. A. Godina, Refractories 9, 416 (1953).

[5] E. K. Keler and A. K. Kuznetsov, Proc. Acad. Sci. USSR 88, No. 6, 1031-1034 (1953).

[6] A. I. Avgustinik and N. S. Antselevich, J. Phys. Chem. 27, 973 (1953) [USSR].

[7] E. T. Carlson, J. Res. Nat. Bur. Stand., 9, 825 (1932).

[8] M. R. Nadler and E. S. Fitzsimmons, J. Am. Cer. Soc., 38, 6, 5-8 (1955).

Received July 20, 1957

•Original Russian pagination. See C.B. Translation.

ROLE OF THE PHASE TRANSITION NH_4NO_3 (IV) ⇌ NH_4NO_3 (III) IN THE CAKING OF AMMONIUM NITRATE

B. V. Erofeev and N. I. Mitskevich

Institute of Chemistry, Academy of Sciences Belorussian SSR

The question of the caking of ammonium nitrate has been the subject of a large number of investigations, some of which are listed at the end of this paper [1-10]. Among the possible factors causing or assisting the caking of ammonium nitrate, a number of authors name phase transitions between the NH_4NO_3 (IV) and NH_4NO_3 (III) modifications; the transition point here is 32.3°. Thus, Bostanzhoglo and Rossi [2] consider that the recrystallization which takes place in the transition from one phase to the other favors caking of the salt. Dubovitskii and Margolis [3] also note the significance of phase transitions of ammonium nitrate in relation to its caking. Zabolotskii and Shvetsova [4] consider that phase transitions of ammonium nitrate, in conjunction with its hydroscopicity, constitute one of the main causes of caking of this salt. In contrast to the opinions of the above-named authors, Klevke and Tselym [8] state that the caking of ammonium nitrate cannot be regarded as the result of phase transitions. A similar view is advanced by Kurin [9]. In a later investigation by Shneerson, Klevke, and Miniovich [10] it was confirmed experimentally that phase transitions favor caking of the salt. However, the ammonium nitrate samples used by these authors contained moisture. The curve for the caking against the moisture content (Fig. 2) [10] shows that phase transitions should not result in caking of the dry salt.

In the investigations cited the question of changes, during phase transitions, of such physicochemical properties of ammonium nitrate as density and dispersion, which should have an influence on caking, was not studied.

The present paper, therefore, contains the results of experiments on the specific volume of modifications III and IV of ammonium nitrate, on the heat of solution, and on x-ray structural analysis of modification IV, in relation to the number of phase transitions undergone by the salt.

In distinction from earlier investigations, we studied the changes in the properties of ammonium nitrate (modifications IV and III) resulting from a large number of phase transitions (mostly up to 30-40 transitions).

EXPERIMENTAL

Variations of specific volume with the number of NH_4NO_3 (IV) ⇌ NH_4NO_3 (III) phase transitions were studied by two methods: dilatometric and pycnometric. We used the dilatometric method in earlier studies of the kinetics of phase transition in NH_4NO_3 [11-14]. The final values for the densities of the (IV) and (III) modifications of NH_4NO_3 found in these experiments are given below as the "dilatometric" densities. In these experiments repeated NH_4NO_3 (IV) ⇌ NH_4NO_3 (III) transitions were effected directly in dilatometers, mercury being the dilatometric liquid.

In studies of the effect of the number of NH_4NO_3 (IV) ⇌ NH_4NO_3 (III) transitions on the heat of solution, the experiments were performed with the salt placed in a Petri dish contained in a drying oven at a temperature above (modification IV) or below (modification III) the transition point. The density was determined pycnometrically in these experiments, benzene being the pycnometric liquid.

Separate conglomerates of the crystals, covered with a collodion film, were used for the x-ray studies. The prepared samples were studied by means of a Laue camera. The heats of solution of ammonium nitrate samples after different numbers of IV ⇌ III, transitions were studied with the aid of a colorimeter of the Cohen type, with an isothermal jacket.

Results of the Investigation

The variations of the specific volume of modification IV of ammonium nitrate with the number of NH_4NO_3 (IV) ⇌ NH_4NO_3 (III) transitions are plotted in Fig. 1. Curve 1 (sample 3) and 2 (sample 5) represent specific-volume variations determined dilatometrically, while Curve 3 represents pycnometric results. Curve 4 shows variations of the specific volume of modification III (sample 3). Figure 1 shows that the changes of specific volume of modification IV virtually coincide for duplicate experiments. Variations of the specific volume of modification III, also determined dilatometrically, do not differ appreciably from those of modification IV. However the dilatometric values for changes of specific volume of modification IV are 2-3 times the pycnometric values. This difference between the dilatometric and pycnometric data must be attributed to the effect of atmospheric moisture while the samples were being heated and cooled in the drying oven. The influence of moisture was excluded in the dilatometric determination. Sample 3 was dried for 5 days at 45-48° before being put into the dilatometer, while sample 5 was held for 30 days over sulfuric acid at room temperature under vacuum. The salt reached constant weight in both cases.

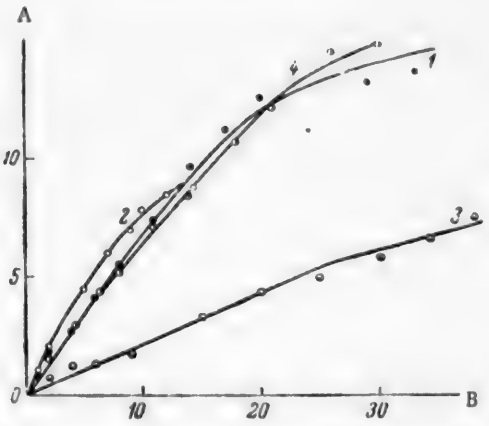

Fig. 1. Specific-volume variations of NH_4NO_3 modifications in relation to the number of NH_4NO_3 (IV) ⇌ ⇌ NH_4NO_3 (III): A) change of specific volume (%) B) number of transitions; explanation in text.

Figure 1 shows that the specific volume increases continuously even after 30-35 transitions. The sole exception is the point corresponding to the 24th transition on Curve 1; this lies too low. The explanation of the position of this point is that between the 23rd and 24th transitions, the dilatometer with the sample remained at room temperature for 18 days, whereas the intervals between the other transitions did not exceed 18-20 hours.

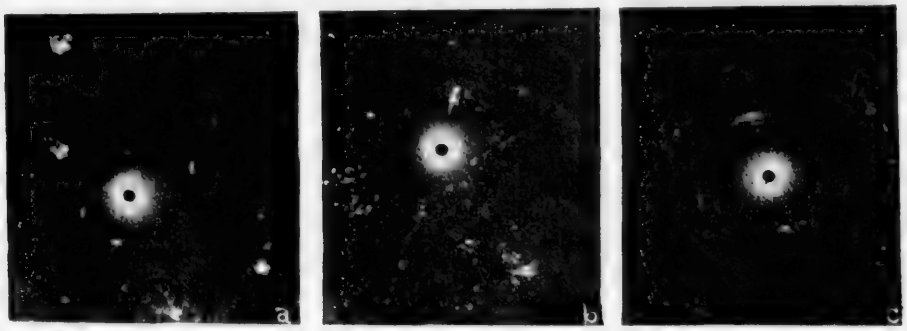

Fig. 2. Laue diffraction patterns of ammonium nitrate: a) before NH_4NO_3 (IV) ⇌ ⇌ NH_4NO_3 (III), b) after 6 transitions; c) after 16 NH_4NO_3 (IV) ⇌ NH_4NO_3 (III) transitions.

It was found by x-ray structural investigation of ammonium nitrate samples, after different numbers of NH_4NO_3 (IV) ⇌ NH_4NO_3 (III) transitions, that the salt crystallites decrease in size as the result of the transitions. Figure 2 shows Laue diffraction patterns of a sample of the salt before the transition (a) and after 6 (b) and 16 (c) transitions. The pattern for the sample before the transition contains several random spots, indicating the

presence of large crystals. The pattern after 6 transitions contains many more spots, but smaller in size. This pattern also reveals the incipient appearance of diffraction rings, which are clearly seen in the pattern of the same sample after 16 transitions. The changes of the diffraction pattern seen in Fig. 2 indicate that large crystals are converted into fine, randomly oriented ones. It follows from the x-ray investigation that NH_4NO_3 (IV) $\rightleftharpoons$ $\rightleftharpoons NH_4NO_3$ (III) transitions result in comminution of the salt crystals. This result is consistent with the earlier data on the changes of specific volume of ammonium nitrate with the number of transitions. It is known that the density of finely-divided substances is lower, and the specific volume correspondingly higher, than those of macrocrystalline substances.

Determinations of the heat of solution of ammonium nitrate in water after different numbers of NH_4NO_3 (IV) $\rightleftharpoons NH_4NO_3$ (III) transitions gave the following results.

Number of IV $\rightleftharpoons$ III transition	Specific volume	Final concentration of solution (g/liter)	Heat of solution (cal per g of salt)
0	0.5834	5.96	87.62
1	0.5834	4.96	86.78
5	0.5908	7.50	85.56
10	0.5939	9.52	85.57
20	0.6087	7.86	83.78
20	0.6087	7.37	83.71

Variations of the heat of solution of NH_4NO_3 (IV) are plotted against the number of transitions in Fig. 3. Figure 3 shows that the heat of solution decreases with increase of the number of IV $\rightleftharpoons$ III transitions.

Density determinations (pycnometric) were also performed on the ammonium nitrate samples (modification IV) the heats of solution of which are given above and plotted in Fig. 3. The heats of solution are plotted against the specific volume of these samples in Fig. 4. Figure 4 indicates that there is a definite relationship between the heat of solution and the specific volume of ammonium nitrate, namely: the lower the specific volume, the higher is the absolute value of the heat of solution.

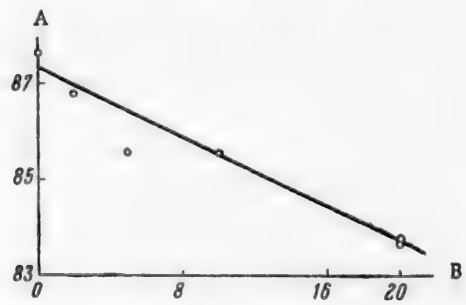

Fig. 3. Variation of the heat of solution of NH_4NO_3 (IV) in water with the number of NH_4NO_3 (IV) $\rightleftharpoons$ $\rightleftharpoons NH_4NO_3$ (III) transitions: A) heat of solution (cal/g), B) number of transitions.

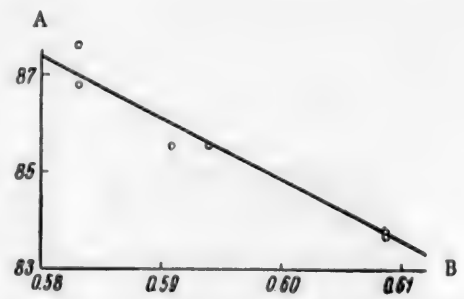

Fig. 4. Variation of the heat of solution of NH_4NO_3 (IV) in water with the specific volume of NH_4NO_3 (IV): A) heat of solution (cal/g), B) specific volume of NH_4NO_3 (IV) (cc/g).

The data on the dependence of the heat of solution on the number of transitions and on the specific volume are consistent with the results for the dependence of the specific volume on the number of transitions, and with x-ray data on samples of ammonium nitrate subjected to different numbers of NH_4NO_3 (IV) $\rightleftharpoons$ $\rightleftharpoons NH_4NO_3$ (III) transitions. The specific volume and dispersion increase, and the heat of solution decreases, with the number of transitions undergone by the sample.

DISCUSSION OF RESULTS

It follows from the results of specific-volume determinations, x-ray studies, and variations of the heat of solution of ammonium nitrate with the number of NH_4NO_3 (IV) $\rightleftharpoons NH_4NO_3$ (III) transitions undergone by the

samples that this transition in itself cannot be the cause of caking of ammonium nitrate. The experimental results indicate that the reverse is true, namely, that the NH_4NO_3 (IV) $\rightleftharpoons NH_4NO_3$ (III) transition results in loosening of the salt structure; this is confirmed by the results of all three methods used in the investigation. However, at the same time the loosening of the structure, which results from subdivision of the crystallites and the enthalpy increase must undoubtedly increase the ability of the ammonium nitrate to take part in various interactions, with an increase in the rates of solution and recrystallization. The reported effects [1, 7, 9, 10] of moisture on the caking of ammonium nitrate must therefore be interpreted as follows: the salt which has undergone the NH_4NO_3 (IV) $\rightleftharpoons NH_4NO_3$ (III) transition recrystallizes more rapidly in presence of moisture; this process includes recrystallization leading to formation of intercrystallite bridges.

SUMMARY

1. The specific volume and heat of solution of NH_4NO_3 (IV) subjected to different numbers (up to 30-40) of NH_4NO_3 (IV) $\rightleftharpoons NH_4NO_3$ (III) transitions were determined, and it is shown that the specific volume increases and the heat of solution and crystallite size decrease with increasing number of transitions.

2. The NH_4NO_3 (IV) $\rightleftharpoons NH_4NO_3$ (III) transition loosens the structure of ammonium nitrate and therefore cannot in itself be the cause of caking of this salt.

LITERATURE CITED

[1] M Lowry and F. Hemmings, J. Soc. Chem. Ind., 39, 1011 (1929).

[2] K. F. Bostanzhoglo and B. D. Rossi, Ammonium Nitrate Explosive Substances [in Russian] (1940).

[3] A. M. Dubovitskii and F. G. Margolis, J. Chem. Ind. 5, 136 (1947) [USSR].

[4] T. V. Zabolotskii and K. I. Shvetsova, J. Chem. Ind. 6, 171 (1954) [USSR].

[5] F. G. Margolis, A. M. Dubovitskii, and T. V. Glazova, J. Chem. Ind. 5, 838 (1951).

[6] J. Whetstone, Ind. Eng. Ch., 44, 2663 (1952).

[7] A. M. Dubovitskii, F. G. Margolis, and T. V. Glazova, J. Appl. Chem. 27, No. 4, 368 (1954).*

[8] V. A. Klevke and N. K. Teslym, J. Chem. Ind. 5, 139 (1947) [USSR].

[9] N. P. Kurin, J. Chem. Ind. 7, 1 (1953) [USSR].

[10] A. L. Shneerson, A. V. Klevke, and M. A. Miniovich, J. Appl. Chem. 29, No. 5, 682 (1956).*

[11] B. V. Erofeev and N. I. Mitskevich, J. Phys. Chem. 24, 1235 (1950) [USSR].

[12] B. V. Erofeev and N. I. Mitskevich, J. Phys. Chem. 26, 848 (1952) [USSR].

[13] B. V. Erofeev and N. I. Mitskevich, J. Phys. Chem. 26, 1631 (1952) [USSR].

[14] B. V. Erofeev and N. I. Mitskevich, J. Phys. Chem. 27, 118 (1953).

Received May 3, 1957

*Original Russian pagination. See C.B. Translation.

ANALYSIS OF DIFFUSIONAL PROCESSES ON THE BASIS OF DEVELOPED FREE TURBULENCE

V. V. Kafarov and V. I. Trofimov

Recent experience on the operation of diffusion equipment has led to considerable intensification of the processes. Development of the theory of such intensified regimes is urgently required in relation to these new operational conditions.

The principal problem in the theory of diffusional processes is the influence of the molecular mass-transfer mechanism on the amount of substance transferred from one phase to another.

According to the film theory, the amount of substance transferred is proportional to $D^{0.5-0.6}$ where D is the coefficient of molecular diffusion.

According to the surface-renewal theory of Higbie [1] and Danckwerts [2], the amount of substance transferred in proportional to $D^{0.5}$.

Unlike Danckwerts, Kishinevskii [3] took turbulent mass-transfer into account and found that the mass-transfer coefficient is proportional to D raised to a power less than 0.5.

According to the theory of developed free turbulence [4], the influence of molecular transfer becomes vanishingly small at the point of phase inversion (in the emulsification regime), the amount of energy transferred is proportional to $\mu^{0.038-0.045}$, and the amount of substance transferred is proportional to $D^{0.038-0.045}$.

The distinctive feature of developed free turbulence is a continuously changing dynamic state of the interphase boundary.

The amounts of energy and mass transferred in conditions of developed free turbulence are determined only by the hydrodynamic characteristics of the process.

A number of recent publications [5,6] provide evidence is favor of the concept of developed free turbulence.

Proof of the predominance of either molecular or turbulent transfer and, accordingly, of the validity of one or the other theoretical concept, may be provided by experiments conducted in such a manner that the phase-contact area remains fixed, and therefore molecular transfer is measured directly.

This method was used in the above-mentioned investigation by Lewis [5], and also by Johnson and Huang [7].

The results of preliminary experiments [8] confirmed that it is possible to determine the phase-contact area* in packed columns under a reduced regime – at the point of phase inversion. Phase inversion is a critical state of the system in a packed column, and is maintained for all packings and systems irrespectively of their physical properties. The following are strictly and uniquely determined: the linear gas velocity, the pressure difference, the amount of liquid held up in the packing, and the virtual phase-contact area.

*More accurately, the value obtained earlier for the "phase-contact area" should be described as the virtual area of phase contact, i.e., a quantity which represents the dynamic variation of the phase-contact area (including its renewal) relative to the surface area of the packing.

For confirmation of the present theory of mass transfer based on developed free turbulence, it was necessary to prove, in addition to the previously established concepts of the influence of molecular mass-transfer coefficients on total energy and mass transfer [4, 8-11], that the mass-transfer coefficients in conditions of developed free turbulence at the critical state vary in the same manner for different systems, are determined only by the solubility of a given gas in the liquid, and are almost independent of the coefficient of molecular diffusion.

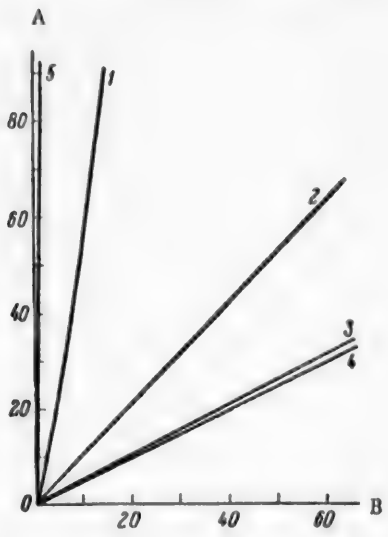

Fig. 1. Equilibrium curves of the systems studied: A) concentration of gas in air (kg/1000 kg of air), B) concentration of gas in water (kg/1000 kg of water); curves: 1) sulfur dioxide–water (t = 15°), 2) acetone–water (t = 15°), 3) ammonia–water (t = = 20°), 4) ethanol–water (t = 18°), 5) carbon dioxide–water (t = 10°).

Accordingly, experiments were performed on the absorption of ammonia, sulfur dioxide, acetone, and ethanol, and on the desorption of carbon dioxide from a air by water, in absorbers 54 and 103 mm in diameter, packed with porcelain rings 6 × 6, 8 × 8, 10 × 10 and 15 × 15 mm in size. Descriptions of the absorbers, experimental procedure, packing characteristics, and methods for determination of ammonia in the liquid and gas are given in an earlier paper [8]. Equilibrium curves for the systems studied are given in Fig. 1.

Values of the Henry constant expressed in concentration units for the two phases were determined from the equilibrium lines for the respective substances, plotted in x–y coordinates (x and y expressed in kg/kg). The slopes of the equilibrium lines in the range of working concentrations remain virtually constant for ammonia, acetone, ethanol, and carbon dioxide. The average slope of the equilibrium curve for sulfur dioxide in the concentration range in question was determined by the Gauss method.

The concentration of sulfur dioxide in the gas at the column entry and exit was determined by absorption in aqueous iodine solution and titration with thiosulfate in presence of starch until the color disappeared. The concentration of sulfur dioxide in the liquid was determined by titration of excess iodine by standard thiosulfate solution in presence of the same indicator.

The content of ethanol vapor in air was determined by absorption in a measured volume of oxidizing misture (100 cc of 0.5 N dichromate solution, 100 cc of concentrated sulfuric acid, and 50 cc of water). After oxidation of the ethanol to acetic acid the excess dichromate was determined iodometrically. Free iodine was titrated by standard thiosulfate solution in presence of starch. For determination of ethanol in the liquid, a measured volume was treated with double the volumes of 0.5 N dichromate solution and concentrated sulfuric acid. The subsequent analysis was performed as in the determination of ethanol in air.

Acetone vapor in air was determined by absorption in a mixture of measured volumes of alkali and hydroxylamine hydrochloride solutions. Excess alkali after the absorption was titrated by hydrochloric acid solution in presence of methyl orange. Acetone in the liquid was determined by treatment of a sample with measured volumes of alkali and hydroxylamine hydrochloride solutions, followed by titration of excess alkali by hydrochloric acid in presence of the same indicator.

Carbon dioxide in air was determined by measurement of the volume of carbon dioxide absorbed by concentrated alkali in the apparatus described by Sherwood et al. [12], with a measuring tube with scale divisions equivalent to 0.25 cc per cm.

Concentration of carbon dioxide in water was determined by titration of a measured volume of the liquid by 0.1 N alkali solution in presence of phenolphthalein.

In the experiments, the L/G ratio* in the absorbers was varied from 1 to 8 (in 8 steps); the absolute quantity of gas fed into the absorbers was varied from 2.3 to 31 m^3/hour (a 13.5-fold increase), the amount of liquid

*Liquid-gas ratio.

from 5 to 160 liters/hour (over 30-fold), and the volume of the packing from 0.25 to 5.15 liters (more than 20-fold).

The experimental results were presented in the form of volume coefficients of absorption for L/G ratios from 1 to 8. The volume coefficient of absorption was calculated from the equation

$$K_V = \frac{G_a}{\Delta Y_{av} \cdot V}, \quad (1)$$

where K_V is the volume coefficient of absorption $\frac{\text{kg}}{\text{m}^3 \cdot \text{hr} \cdot \frac{\text{kg}}{\text{kg}}}$, G_a is the weight of substance absorbed (kg/hour), ΔY_{av} is the mean logarithmic difference of the concentrations of the absorbed substance (kg/kg), and V is the volume of packing in the absorber (m^3).

The results were plotted in logarithmic coordinates (Fig. 2).

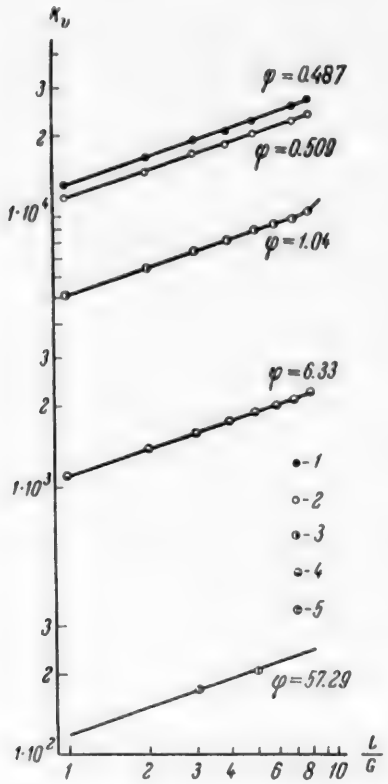

Fig. 2. Variation of the volume coefficient of absorption (K_V) at the inversion point with the L/G ratio for an absorber 54 mm in diameter packed with 8 × 8 mm rings: systems: 1) ethanol–water, 2) ammonia–water, 3) acetone–water, 4) sulfur dioxide–water, 5) carbon dioxide–water.

Figure 2 shows that the volume coefficients of absorption for ammonia, sulfur dioxide, acetone ethanol, and carbon dioxide for the same packing increase with increase of the L/G ratio, and their values conform to linear equations of the same slope; this shows that the nature of the variations of the mass-transfer coefficient is the same for different substances.

The straight lines are represented by equations of the type:

$$K_V = A\left(\frac{L}{G}\right)^{0.337} \frac{\text{kg}}{\text{m}^3 \cdot \text{hr} \cdot \text{kg/kg}}. \quad (2)$$

Values of the constant A for different systems are given in the table.

If the experimental data for different systems and sizes of packing are presented as the ratios of the volume coefficient of mass transfer (K_V) at the given L/G ratio to the volume coefficient (K_V) for the same system for L/G = 1, then under conditions corresponding to the inversion point the experimental data for different systems at different L/G ratios are grouped around a single straight line with a slope of 0.337 (Fig. 3), in complete agreement with Equation (2).

Unfortunately, the literature does not contain any experimental results, obtained by other workers, for maximum L/G ratios at the inversion point. Only Molstad and Parsley [13] reached ratios close to the inversion point in the absorption of ethanol in water in a packed column containing 25 × 25 mm rings. Their experimental results, also plotted in our graph, likewise conform to the same law.

The influence of the packing dimensions on the coefficient of mass transfer at the inversion point was determined by analysis of experimental data on the absorption of ammonia and acetone from air by water in an absorber 103 mm in diameter, packed with 6 × 6, 8 × 8, 10 × 10 and 15 × 15 mm rings.

Values of the Constant A and the Henry Coefficient for Different Systems

System	Constant A of Equation (2)	Henry coefficient φ	$\varphi' = \frac{1}{\varphi}$	$\frac{A}{A_{NH_3}}$	$\frac{\varphi'}{\varphi'_{NH_3}}$	Diffusion coefficient at 20° (m^2/hour)		$\frac{D_G}{D_{NH_3}}$	$\frac{D_L}{D_{NH_3}}$
						in gas, D_G	in liquid, D_L		
Ammonia – water	11.8000	0.509	1.970	1.000	1.000	$0.680 \cdot 10^{-1}$	$0.660 \cdot 10^{-5}$	1.000	1.000
Sulfur dioxide – water	1.110	6.330	0.158	0.094	0.081	$0.410 \cdot 10^{-1}$	$0.455 \cdot 10^{-5}$	0.604	0.690
Acetone – water	5.120	1.035	0.966	0.434	0.492	$0.334 \cdot 10^{-1}$	$0.315 \cdot 10^{-5}$	0.493	0.477
Ethanol – water	13.000	0.487	2.050	1.100	1.040	$0.406 \cdot 10^{-1}$	$0.203 \cdot 10^{-5}$	0.598	0.308
Carbon dioxide – water	120	57.29	0.0174	0.010	0.0089	$0.550 \cdot 10^{-1}$	$0.64 \cdot 10^{-5}$	0.809	0.974

The experimental data in this case were presented in the form of relationships between the equivalent packing diameter and the coefficient of absorption per unit virtual phase-contact area, determined by means of the equation derived earlier [8].

The equivalent packing diameter is given by the expression $d_e = \frac{4F_0}{\sigma}$ where F_0 is the open section of the packing (in m^2/m^3), and σ is the specific surface of the packing (in m^2/m^3).

The results of the experiments are plotted in logarithmic coordinates in Fig. 4. It follows from Fig. 4 that the coefficients of absorption of acetone and ammonia for different packing dimensions are grouped around straight lines represented by the general equation

$$K_{gen} = Bd_e^{1.51} \frac{kg}{m^2 \cdot hr \cdot kg/kg}. \qquad (3)$$

The values of the constant B are: for the system ammonia–water B = 48,400, and for the system acetone–water, B = 22,500.

The ratio of the constant B for the system acetone–water to the constant B for the system ammonia–water is close to the inverse ratio of the Henry coefficients φ' for the same systems: $\frac{B_{NH_3}}{B_{ac}} = \frac{48400}{22500} = 2.15$; $\frac{\varphi'_{NH_3}}{\varphi'_{ac}} = \frac{1.970}{0.966} = 2.04$.

On the basis of Equation (3) and the equation derived earlier for the phase-contact area [8] the volume coefficient of absorption at the inversion point can be represented by the equation

$$K_V = 5.9B\sigma d_e^{1.51}\left(\frac{L}{G}\right)^{0.337}\left(\frac{\gamma_G}{\gamma_L}\right)^{0.187} \times \left(\frac{\mu_L}{\mu_G}\right)^{0.0375} \frac{kg}{m^3 \cdot hr \cdot kg/kg}, \qquad (4)$$

where γ_G, γ_L are the densities and μ_G, μ_L the viscosities of the gas and liquid respectively.

The values of the constants A and B in Equations (2) and (4) are determined by the solubility of the gas in the liquid, i.e., they are proportional to the Henry coefficient (both A and B are in inverse ratio to the slope of the equilibrium curve). This is easily shown by comparison of the ratios of the constants A for different systems (relative to ammonia) with the ratios of the corresponding cotangents of

φ', proportional to the Henry coefficient (see table).

The table shows that in every case of ratio of the constants A corresponds to the inverse ratio of the Henry coefficients for the same systems.

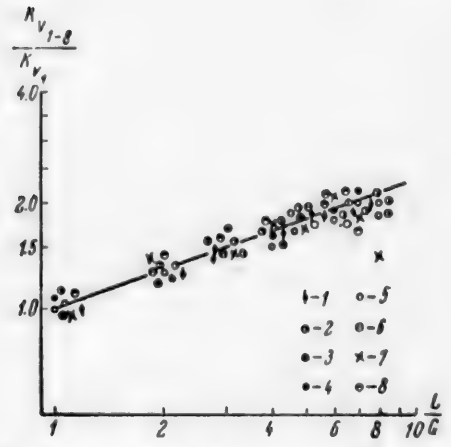

Fig. 3. Variations of the experimental and calculated values of $\frac{K_{V_{1-8}}}{K_{V_1}}$ at the inversion point with the L/G ratio for different packing dimensions and systems: Systems and packing-ring sizes respectively: 1) sulfur dioxide–water, 8 × 8 mm; 2) acetone–water, 8 × 8 mm; 3) ethanol–water, 8 × 8 mm; 4) ammonia–water, 6 × 6 mm; 7) ammonia–water, 15 × × 15 mm; 8) ethanol–water, 25 × 25 mm (data of Molstad and Parsley [13]).

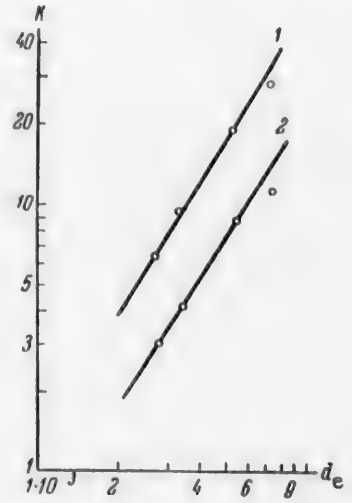

Fig. 4. Variations of the absorption coefficients (K'_G) of ammonia and acetone per unit virtual phase-contact area with different equivalent packing heights (d_e): systems: 1) ammonia–water, 2) acetone–water.

At the same time, the ratios of both the gas-phase and the liquid-phase coefficients of molecular diffusion differ considerably from the ratios of the constants A for the same systems, and the variation of the diffusion coefficients themselves is relatively small and remains of the same order of magnitude.

The mass-transfer coefficients for the different systems differ considerably (to the same extent as the constants A), so that it is evident that under these conditions the amount of substance transferred is determined not by the coefficients of molecular diffusion but only by the hydrodynamic conditions and the solubilities of the gases.

Therefore, taking Equation (4) into account and expressing the equivalent diameter as $d_e = \frac{4F_0}{\sigma_G}$, we can calculate the absorption coefficients for any systems in the reduced state (at the inversion point) from the expression

$$\frac{K_{V_2}}{K_{V_1}} = \frac{\varphi_1}{\varphi_2}\left(\frac{\sigma_1}{\sigma_2}\right)^{0.51}\left(\frac{F_{0_2}}{F_{0_1}}\right)^{1.51}\left[\frac{\left(\frac{L}{G}\right)_2}{\left(\frac{L}{G}\right)_1}\right]^{0.337}\left[\frac{\left(\frac{\gamma_G}{\gamma_L}\right)_2}{\left(\frac{\gamma_G}{\gamma_L}\right)_1}\right]^{0.187}\left[\frac{\left(\frac{\mu_L}{\mu_G}\right)_2}{\left(\frac{\mu_L}{\mu_G}\right)_1}\right]^{0.0375} \quad (5)$$

where φ_2 and φ_1 are the Henry coefficients.

The volume coefficient of absorption for ammonia at $\varphi = 0.509$ can be found from the equation

$$K_V = 2.3 \cdot 10^6 \cdot \sigma^{-0.51} \cdot F_0^{1.51}\left(\frac{L}{G}\right)^{0.337}\left(\frac{\gamma_G}{\gamma_L}\right)^{0.187}\left(\frac{\mu_L}{\mu_G}\right)^{0.0375} \frac{\text{kg}}{\text{m}^3 \cdot \text{hr} \cdot \text{kg/kg}}, \quad (6)$$

and Equations (5) and (6) can be used to calculate the volume coefficient of absorption for any gas.

If follows from Equations (5) and (6) that the indexes of the coefficients of molecular viscosity are very small, and therefore under these conditions molecular transfer frictional energy, like molecular mass transfer, has a very low value.

In this case, as in a one-phase stream, the Peclet turbulent transfer criterion $Pe_T = \frac{Wl}{\epsilon_d}$, where W is the linear velocity of the stream (m/second), l is the geometrical dimension of the system (m), and ϵ_d is the coefficient of turbulent diffusion (m^2/second), should be constant [14, 15].

For a two-phase stream constancy of the Pe_T criterion may be represented in terms of a constant ratio of the gas velocity W, which is the determining hydrodynamic characteristic of the gas flow, to the determining diffusional parameter under these hydrodynamic conditions, as the coefficient of turbulent diffusion in a two-phase stream cannot be determined directly. Such a parameter for packed columns may be the height of packing equivalent to one contact step, and, in particular, the equivalent packing height h.

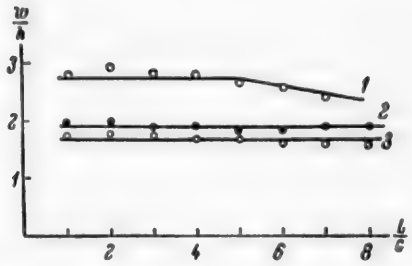

Fig. 5. Variation of W/h with L/G for the system ammonia–water: packing rings (mm): 1) 15 × 15, 2) 8 × 8, 3) 6 × 6.

Then, if W/h is constant at different L/G ratios at the inversion point, turbulent transfer will take place under the given hydrodynamic conditions, i.e., conditions of developed free turbulence will be present.

We accordingly analyzed the experimental data at the inversion point for the system ammonia–water, for packing rings 6 × 6, 8 × 8, and 15 × 15 mm in size, at different L/G ratios.

The equivalent packing height was determined from the equations

$$h = \frac{H}{n} \text{ meters} \tag{7}$$

$$n = \frac{\lg\left[\left(1 - m\frac{G}{L}\right)\frac{y_i}{y_f} + m\frac{G}{L}\right]}{\lg\frac{L}{mG}}, \tag{8}$$

where h is the packing height equivalent to one theoretical plate (m); H is the height of the packing in the column (m); n is number of theoretical plates: m is the slope of the equilibrium line, in the same units as the concentration of the absorbed gas; y_i and y_f are the contents of the absorbed gas in air before and after passing through the packing (kg/kg).

The linear gas velocity in the full section of the column at L/G ratios from 1 to 8 for the different packing dimensions were determined by means of the equation derived earlier [8].

The values found for W and h are plotted in the form W/h as a function of L/G in Fig. 5.

Figure 5 shows that W/h remains constant with variations of L/G for a given size of packing rings; this shows that only turbulent transfer occurs in the two-phase stream. It has been shown previously [15] that only turbulent transfer occurs in a one-phase stream.

The explanation for the decrease of W/h with 15 × 15 mm rings at L/G > 6 is that in the absorption of a gas at high L/G ratios the fraction of the gas absorbed relative to the inert gas is considerable, and therefore the total amounts of gas in the upper and lower sections of the column are different; accordingly, the upper layers of the packing are operating somewhat below the inversion point. As has already been noted [8], this effect is most prominent with large rings.

SUMMARY

1. It is shown that in conditions of developed free turbulence at the inversion point the absorption coefficients are determined by the hydrodynamics of the process and the solubility of the gas, which are independent of the molecular diffusion coefficients.

2. It is shown that in packed columns at the inversion point, in a two-phase stream as in a one-phase stream, conditions arise for turbulent mass and energy transfer, determined by the predominant influence of turbulent viscosity and turbulent diffusion.

3. An equation is derived for calculation of absorption coefficients in packed columns at the inversion point.

LITERATURE CITED

[1] R. Higbie, Trans. Am. Inst. Chem. Engrs., 31, 365 (1935).

[2] P. V. Danckwerts, Trans. Farad. Soc., 46, 300, 701 (1950); 47, 1914 (1951).

[3] M. Kh. Kishinevskii, J. Appl. Chem. 24, 542 (1951) [USSR].*

[4] V. V. Kafarov, Collected Papers on Processes and Equipment [in Russian] (1953); J. Appl. Chem. 29, No. 1, 40 (1956) [USSR].*

[5] I. B. Lewis, Chem. Eng. Sci., 3, 248 (1954).

[6] K. Sigwart and H. Nassenstein, Umschau, 56, 10, 299 (1956).

[7] A. I. Johnson and C. J. Huang, Am. Ind. Eng. J., 2, 412 (1956).

[8] V. Kafarov and V. I. Trofimov, J. Appl. Chem 30, No. 2, 211 (1957) [USSR].*

[9] V. V. Kafarov and Iu. I. Dytnerskii, Trans. MKhTI, 22 (1956).

[10] V. V. Kafarov, Chem. Ind. 5 (1953) [USSR].

[11] V. V. Kafarov, Trans. MKhTI, 23 (1956).

[12] T. Sherwood, F. C. Draemel, and N. E. Rukman, Ind. Eng. Ch. 27, 3, 283 (1937).

[13] M. G. Molstad and L. F. Parsley, Chem. Eng. Progr., 46, 20 (1950).

[14] V. V. Kafarov, J. Appl. Chem. 28, 1234 (1955) [USSR].*

[15] R. H. Wilhelm, Chem. Eng. Progr., 49, 152 (1953).

Received June 21, 1957

*Original Russian pagination. See C.B. Translation.

INVESTIGATION OF STEAM DISTILLATION•

E. K. Siirde and P. G. Romankov

The Tallinn Polytechnic Institute

Steam distillation is a type of distillation which has been known for a long time and which is used in many operations in the chemical and oil industries. Steam distillation makes it possible to lower the boiling points of substances to be separated. Lowering of the boiling point eliminates the risk of thermal decomposition of organic substances. In general, steam distillation can be used only if the distilled substance is insoluble or slightly soluble in water.

Despite the fact that steam distillation and its potentialities have long been known, the mechanism of the process has not been studied sufficiently. This is confirmed by the limited amount of literature data available on the subject of steam distillation. In published researches on steam distillation most attention is devoted to thermodynamic equilibrium and possibilities of attaining it, and some data are available on the heat of steam distillation [1-6], etc., but there is hardly any information in the literature concerning mass transfer in relation to the hydrodynamics of the process.

Steam distillation is a process which must be considered as a whole, with all its peculiarities taken into account. This was the principle upon which the present investigation was based.

The Hydrodynamics of Bubbling

In steam distillation a current of steam is introduced into a layer of the liquid to be distilled. The steam may pass through the liquid layer in the form of large separate bubbles, it may form a disperse system (foam) with the liquid, or it may pass through it as a steam. When steam passes through the liquid layer, the distilled substance evaporates into the current of steam, and this is accompanied by cooling of the steam and, in the case of three-phase steam distillation;•• by its partial condensation. All these factors causes changes in the volume of the steam passing through the liquid layer, which in turn influence the physical nature of the bubbling process and cause differences in its hydrodynamics.

The hydrodynamics of steam distillation was studied by means of photography and by direct observations of the process.

Glass apparatus was used for the steam distillation. Photographs of the process were taken with different dimensions of the apparatus, different heights of the liquid layer, different diameters of the inlet tube for steam or air, and with the use of a distribution grid.

The liquids used were benzene, toluene, acetone, and water. Steam and air were bubbled through them. The hydrodynamic conditions were varied by variations of the injection rates of the steam and air into the liquid, and by variations of the temperature conditions. Analysis of the photographs taken in the course of steam distillation leads to the following conclusions.

•Communication I.

••This term refers to distillation accompanied by partial condensation of steam, so that both the distilled liquid and water are present simultaneously in the still.

Differences in the bubbling process depend primarily on the velocity of the injected steam – as the steam velocity increases, the dispersed layer becomes larger and the layer of homogeneous liquid smaller.

Differences of bubbling hydrodynamics are also caused by the vapor of the distilled liquid entering the gaseous phase during the process. The vapor of the liquid, entering the gaseous phase, increases the volume of the passing steam and thereby also the velocity of the whole gaseous phase, calculated for the cross-sectional area of the apparatus. The volume ratio of the vapor of the distilled liquid passing into the gaseous phase to the volume of steam is given in the expression:

$$\frac{V_1}{V_0} = \frac{P_1}{P_0} \tag{1}$$

where V_1 and V_0 are the volumes and P_1 and P_0 the partial pressures of the vapor and steam.

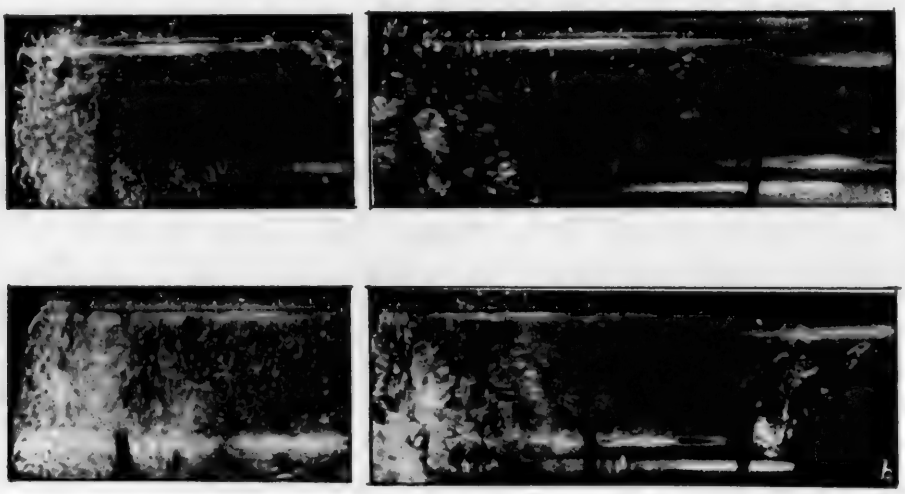

Fig. 1. Bubbling in different liquids in relation to the volume of liquid evaporated in an air stream; a) water, b) toluene.

Figure 1 represents the bubbling of air at 20° through a layer of water (a) and of toluene (b), 400 mm high. In both cases the air was introduced into the liquid layer at 6 liters/minute, and the relative humidity of the air was 0.7. The volume of water vapor formed from the water when air was blown through it, calculated by means of Equation (1), was 0.042 liter/minute, and the volume of toluene vapor was 0.198 liter/minute, on the assumption that the air stream was fully saturated with the respective vapors.

Either individual bubbles or a continuous stream of steam arise at the end of the steam nozzle, dependent on the rate at which the steam is introduced into the liquid.

A large steam bubble, on becoming detached from the end of the steam nozzle, disintegrates into individual smaller bubbles as it moves through the liquid layer. The individual steam bubbles so formed separate further into yet smaller bubbles as they move through the liquid, and leave the liquid layer in that form. With increase of the rate at which steam is injected into the liquid, the disintegration of large bubbles into very small ones occurs simultaneously with disintegration into bubbles of intermediate size.

A continuous stream of steam also separates into individual bubbles and simultaneously into very small bubbles. The formation of such small bubbles can also be observed directly at the edges of the stream of steam.

When steam is introduced into a liquid at a moderate rate through a grid, bubbles are formed which disintegrate into smaller ones as they move through the liquid layer. If the steam is introduced through the grid at a high rate, bubbles are formed which do not disintegrate further on passing through the liquid layer.

It is difficult to see any differences in the structure of the upper layers of liquid when steam is bubbled through a liquid by means of a grid and nozzle respectively. The thicker the liquid layer traversed by the steam, and the higher the steam velocity, the less difference is there in the bubbling conditions at different heights in the liquid layer.

The diameter of the apparatus and the number of nozzles in it influence bubbling hydrodynamics. The smaller the diameter of the apparatus, or the less the cross-sectional area per nozzle, the nearer to the nozzle orifice do the streams or steam bubbles break up into small bubbles, with an increase in the height of the dispersed or foam layer in the apparatus.

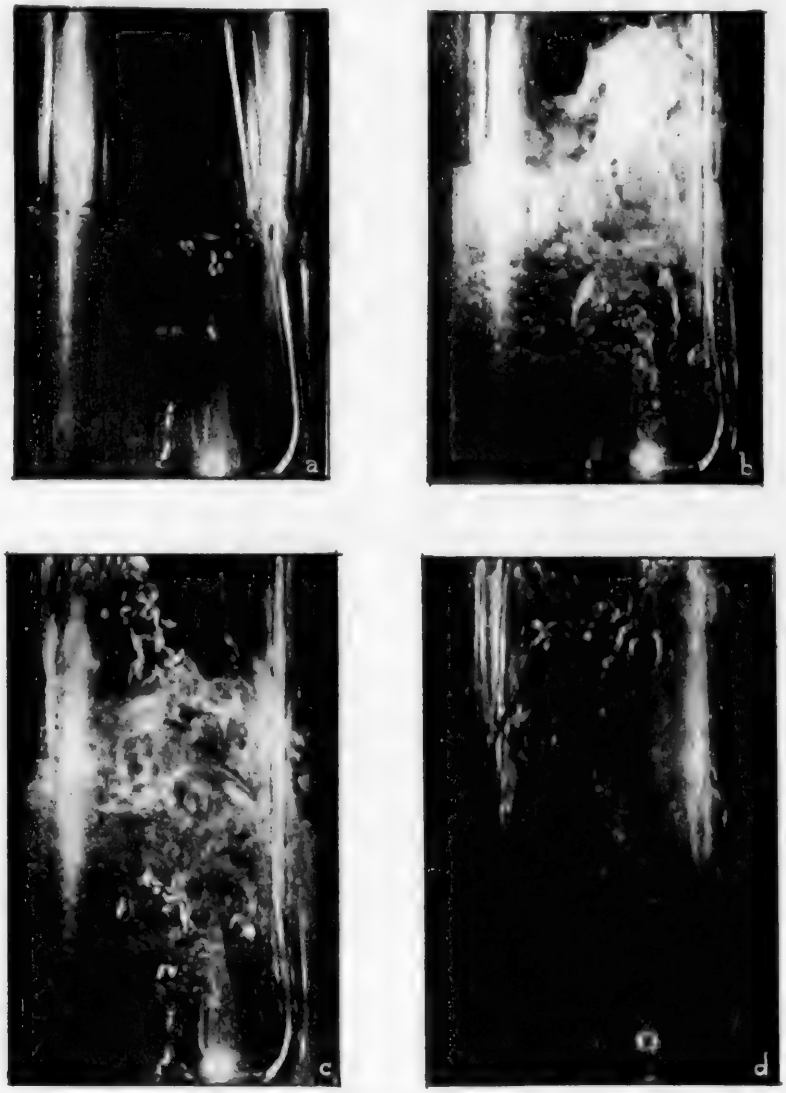

Fig. 2. Different regimes in the bubbling process: a) bubbling regime, b) and d) streaming regime, c) foam regime.

As the result of studies of bubbling by photography of the motion of the steam (or gas) passing through the liquid layer, the whole process may be divided into four stages:

1) formation of a bubble or stream of steam (or gas), 2) motion of the bubble or stream of steam (or gas) through the liquid – the compact stage, 3) separation of the bubble or stream, moving in the liquid, into

smaller bubbles, and extension of this process – the division stage, and 4) disintegration of the separate bubbles into fine bubbles – the dispersion stage.

According to photographic data and direct observations, the following are the principal factors determining the origin and changes of a given hydrodynamic regime at different stages of the bubbling stage: 1) at the stage of bubble formation – the entry velocity of the steam and the nozzle diameter; 2) at the compact stage – Archimedes forces and resistance forces; 3) at the division stage – turbulence stresses, which in turn depend on the velocity of the gaseous phase through the liquid, i.e., on the entry velocity of the steam and the amount of evaporating liquid, the diameter of the apparatus or the extent of the region of influence of the introduced steam, and the height of the liquid layer; 4) at the dispersion stage – turbulence stresses and forces of surface tension.

The bubbling process may be subdivided into three regimes according to the time of passage of the steam or gas through the liquid layer: 1) the bubbling regime, 2) the foam regime, and 3) the steam regime.

Photographs illustrating the different regimes are shown in Fig. 1. Photograph (a) corresponds to the bubbling regime,(b) and (d) to the streaming regime, and (c) to the foam regime. The hydrodynamic characteristics are greatly influenced by the stages of motion of the gas and by the role played by one or another of these stages in the bubbling process as a whole; for example, the start of the foam regime may be considered to be the moment when all the gas bubbles, having already subdivided into minute bubbles, collect in the upper layer.

In view of the fact that mass transfer depends on the hydrodynamic conditions, the latter must be arranged appropriately for successful mass transfer. For example, in the bubbling regime a relatively high liquid layer should be used, so that the path of the bubble through the liquid should be longer and there should be enough time for diffusion of the vapor from the liquid into the gass for complete saturation of the latter. Conversely, relatively thin layers may be used in the foam regime, because the high turbulence ensures more effective mass transfer. However, there ia limiting height of the liquid layer; below this, the steam passes through the liquid in the form of a stream, as shown in Fig. 2, b. The limiting height of the liquid layer depends on the velocity of the incoming steam, the nozzle diameter, the volume ratio fo the vapor formed from the distilled liquid to the steam blown through, and other factors.

Entrainment of the Distilled Liquid in Droplet Form

Entrainment of the distilled liquid and its transfer in drop form into the distillate is favored, on the one hand, by certain properties of the vapor phase, such as its velocity in the apparatus, density, etc., and on the other by hydrodynamic conditions favoring formation of droplets and mist. When gas bubbles pass through the liquid layer, and especially when they break up at the liquid surface as the result of rupture of the liquid film, numerous droplets ~60 μ in diameter are formed together with a small number of drops about 1 mm in diameter [7]. Therefore emergence of the vapor from the liquid may be regarded as the start of mechanical transfer of the liquid into the distillate. It may be assumed that the vapor does not carry over the large drops, but only the minute droplets, the dimensions of which are determined by the physical properties of the liquid, primarily its surface tension. The shape of the apparatus apparently also has an influence on the process; under equal conditions entrainment of liquid droplets is less in cylindrical apparatus than in apparatus of any other shape [8].

In passing to a description of the experiments carried out in order to study liquid entrainment, we may note that these results also confirm the existence of the above-named hydrodynamic regimes which influence the bubbling process.

The following method was used for determination of the amounts of liquid carried over in droplet form. A solution of sodium chloride, of known concentration, was put into the still and steam was bubbled through it at various rates. The amount of liquid carried over in droplet form into the distillate was determined by titration with silver nitrate. In experiments on the distillation of technical,very impure,aniline,the presence of aniline which entered the distillate in droplet form was estimated by color. The steam velocity was calculated from the cross-sectional area of the apparatus, the density of the steam being assumed to be that of saturated steam at 100°.

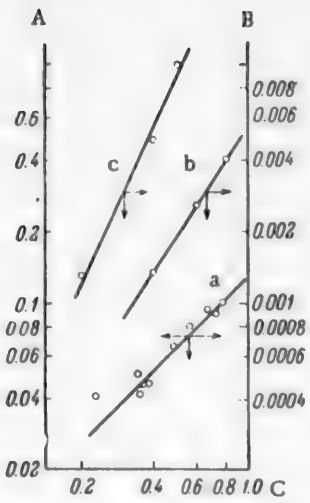

Fig. 3. Amounts of solution entrained in droplet form with the steam: A) amount of liquid carried over with the vapor (%); B) molar ratio of water to steam; C) linear velocity of the steam per unit cross section of the apparatus (m/second): a) sodium chloride solution, height of apparatus above the liquid layer 1250 mm; b) ethyl alcohol solution, distance between plates 460 mm; c) ethyl alcohol solution, distance between plates 300 mm.

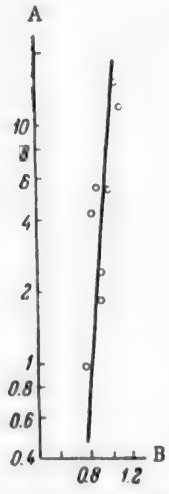

Fig. 4. Amounts of sodium chloride solution entrained in droplet form in steam under "throw-over"conditions: A) amount of liquid carried over with the vapor (%); B) linear velocity of the steam per unit cross section of the apparatus (m/second).

The amount of liquid carried over with the steam was expressed as a percentage of the volume of condensate obtained from the steam passed through the liquid, or as the molar ratio of the amount of water carried over in droplet form with the steam to the amount of steam. The experimental results, expressed in this form, are represented by the Line a in Fig. 3. For comparison, Fig. 3 (Lines b and c) also shows certain literature data on liquid entrainment in rectification [9]. The results refer to an aqueous solution of ethyl alcohol of 35% molar concentration.

If the steam passes through the liquid in the form of streams or large individual bubbles which do not have time to disintegrate in the liquid layer, entrainment often reaches "throw-over" dimensions. This may occur in the streaming regime if the steam is injected at high or very high velocities. Experiments analogous to those described above were performed for investigation of this effect.

Steam was bubbled through sodium chloride solution. The difference between these and the preceding experiments was that the temperature of the injected steam was 250° and the sodium chloride solution boiled violently in the still (the temperature was 108-110°). It may be assumed that the hydrodynamics of the bubbling process under these conditions corresponded to the photograph in Fig. 2, d. The results of this experiment are plotted in Fig. 4. Comparison of the experimental data presented in Figs. 3 and 4 reveals a quantitative difference in the entrainment due to the difference of the regimes. The results of experiments on the steam distillation of aniline are presented in Fig. 5 in the form of data on the saturation coefficient.•

The results of these experiments confirm our views of the role of hydrodynamic conditions in the bubbling process, and clarify the characteristics of the different regimes. They also indicate that from the point of view of entrainment the most suitable bubbling regime for industrial operation is the foam regime, as in this regime the amount of liquid carried over with the steam into the distillate is very much less than in the steam regime.

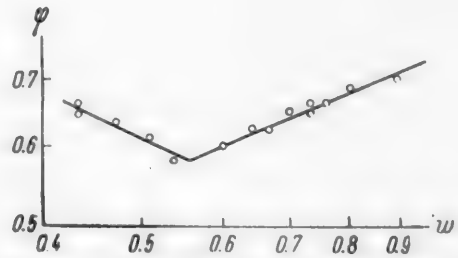

Fig. 5. Variation of the saturation coefficient φ with the linear velocity W of the injected steam in the steam distillation of aniline.

•The saturation coefficient represents the degree of saturation of the current of steam with the vapor of the substance being distilled.

SUMMARY

1. In addition to generally known factors, the hydrodynamics of the bubbling process in steam distillation is also influenced by the volume of the vapor of the distilled liquid which is added to the injected steam.

2. The following hydrodynamic regimes arise in steam distillation by the bubbling method: a) bubbling, b) foam, and c) streaming.

3. Entrainment of the distilled liquid in the form of droplets during bubbling depends on the hydrodynamic regime as well as on the design of the distillation equipment. It is greatest in the steaming regime.

LITERATURE CITED

[1] S. L. Libinson and A. B. Pakschwer, Chemische Apparatur, 15, 277, (1928); 16, 25, 47, 71 (1929).

[2] J. Perry, Chemical Engineer's Handbook, 1 (Moscow, 1937) [Russian translation].

[3] E. M. Baker, and E.E. Pettibane, Ing. Eng. Ch., 21, 6, 562 (1929).

[4] N. I. Gel'perin and E. N. Gel'perin, Oil and Fat Ind. 4, 12 (1954) [USSR].

[5] K. Thorman, Die chemische Fabrik, 13, 1, 2 (1940).

[6] V. A. Gurvich, Scientific Principles of Petroleum Process [In Russian] (State Technical Press, 1940).

[7] F. Knelman, N. Dambrowski, and D. M. Newitt, Nature, 4397, 261 (1954).

[8] A. I. Kaiser, Handbuch der chemisch-technischen Apparate maschinellen Hilfmittel und Werkstoffe. I. Leipzig (1934).

[9] E. Kirschbaum, Destillier-und Rektifiziertechnik. Verl. Springer (1940).

Received June 5, 1958

ANODIC BEHAVIOR OF ALLOYS OF THE COPPER—ZINC SYSTEM IN 0.1 N POTASSIUM CHLORIDE SOLUTION

V. V. Skorchelettl, I. A. Stepanov, and E. P. Kuksenko

The use of chemically-resistant alloys was and still is the most reliable means of corrosion prevention, if it is impossible to avoid the use of metallic materials. Copious data are available on the corrosion resistance of various alloys in media of industrial importance. However, there have been relatively few investigations of the relationship between the oxidation kinetics of alloys and their composition.

After the publication of Tammann's expensive investigations [1] of the laws governing the chemical resistance of solid solutions, several papers were published in the 1920's and 1930's [2],* which largely confirm the validity of the "n/8 law". These investigations did not make any fundamental additions to the concepts formulated by Tammann. However, these concepts did not gain full acceptance because of their sketchy nature. Recently Gratsianskii [3] has published the results of a number of investigations of corrosion resistance of certain systems of solid solutions.

Most of the paper cited above are concerned with the connection between the composition of alloys and their chemical resistance or equilibrium potentials; however, the effects of alloy composition on the oxidation kinetics are also of considerable interest.

The copper–zinc alloy system is a convenient object for study of certain aspects of oxidation kinetics. In a number of cases, corrosion of these alloys is accompanied by dezincing, i.e., deposition of the more noble component, in the form of a separate phase, on the alloy surface. Similar effects are observed in the corrosion of other alloys the components of which differ considerably in chemical activity. The problem of selective-component corrosion is therefore one of general significance. Further, copper–zinc alloys can be used for investigations of the influence of composition on the form of the polarization curve, as the oxidation conditions may be selected in such a way that the oxidation proceeds with formation of ions differing in valence ($Cu^{\cdot}$ and $Zn^{\cdot\cdot}$). This makes it possible to study variations of the slope of the potential–log current density plots with changes of composition. The present investigation is concerned with these two problems.

Finally, attention must be drawn to the practical importance of corrosion of copper–zinc alloys (various brasses).

EXPERIMENTAL

The alloys were made from the pure components, partly by fusion in a high-frequency furnace in an argon atmosphere, and partly by fusion in evacuated sealed quartz tubes. The ingots were subjected to homogenizing annealing for 24 hours at 800° with slow cooling in the furnace. They were then rolled cold into plates ~0.5 mm. thick, and to eliminate the effects of cold hardening, they were annealed at 450° in low-capacity evacuated glass bulbs and cooled in water, in order to avoid sublimation of zinc onto the walls of the cooling bulbs. The losses of zinc did not exceed 0.3% in this treatment. Fusion in quartz tubes, for a few minutes did not result in any appreciable reduction of silica (the Si content of the alloys did not exceed 0.01%). The compositions of the alloys studied are given in the table.

*The paper by Landau and Oldach [2] contains a detailed summary of numerous investigations.

The electrodes, in the form of circular plates ~1 cm in diameter, were fixed horizontally in the lower part of the cell. The lower surface was attached by means of polystyrene to the horizontal end of a glass stopper. The upper electrode surface was polarized with the aid of an auxiliary platinum electrode separated

Compositions of the Alloys Studied

Alloy No.	Zinc content (atomic %)	Notes
	Fusion in argon. Series I	
1	0.0 (pure copper)	
2	4.22	
3	2.80	
4	13.60	α solid solutions
5	24.20	
6	26.20	
7	37.12	
	Fusion in quartz tubes. Series II	
8	35.9	α solid solution
9	38.15	α + β solid solutions
10	39.42	
11	44.0	β solid solutions
12	47.2	

from the working part of the cell by a tube with a porous glass filter. The potentials were determined relative to a 0.1 N calomel electrode (all the results were recalculated to the hydrogen scale). The electrolyte was 0.1 N KCl solution. After the electrode had been fixed, dissolved oxygen was removed from the electrolyte by a stream of oxygen-free nitrogen.

Anodic behavior of alloys comprising α solid solutions (alloys of Series I). Figure 1 shows polarization curves for pure copper and for the alloy containing 4.22% Zn. It is seen that the potential of copper increases linearly with log current density. At $\varphi \simeq +0.2$ v there is a horizontal plateau. At $i \simeq 10^{-3}$ amp/cm² the potential rises steeply (the line is almost vertical), and continues to increase rapidly with increase of i. The reverse polarization curve, determined for the same electrode immediately after the direct, takes a different course. The potential decreases slowly, reaches about +0.2 v, and then remains almost constant. The anodic curve plotted for 0.1 N KCl solution previously saturated with CuCl (with excess of the solid phase) is similar in form to the reverse curve for the solution which did not previously contain CuCl.

The curves in Fig. 1 have slope factor b = 0.056. This is indicative of concentration polarization. The concentration of Cu^+ ions at the electrode surface C = const i, if it is assumed that C = 0 within the volume of the solution. In this case the equilibrium electrode potential may be represented as a function of the current density i:

$$\varphi = \varphi_0 + \frac{RT}{zF} \ln \text{const} \cdot i \quad \text{or} \quad \varphi = a + b \lg i, \qquad (1)$$

$$\text{where } b = \frac{2.3RT}{zF}.$$

In chloride solutions copper undergoes anodic dissolution, forming Cu^+ ions (z = 1); this is associated with the low concentration of Cu^+ due to complex formation with Cl^- ions. In the present instance Equation (1) gives b = 0.058 (at 20°), which is close to the value found. If anodic dissolution of copper proceeded at an appreciable overvoltage under our conditions, the factor b should be greater, because in that case $b = \frac{2.3RT}{\beta zF}$, where $\beta < 1$.

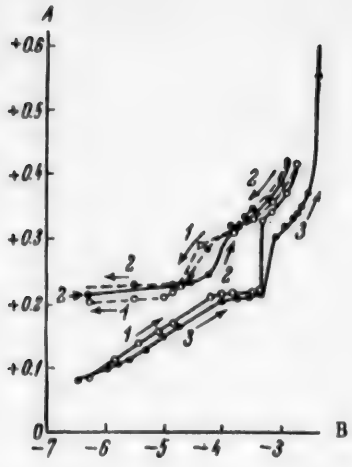

Fig. 1. Anodic polarization curves determined for 0.1 N KCl solution: A) potential (v) on the hydrogen scale, B) log current density (in amps / cm^2); curves; 1) pure copper; 2) the same, but in solution previously saturated with CuCl; 3) alloy with 4.22% Zn; continuous line — direct curves; dash lines — return curves.

Concentration polarization in the anodic dissolution of copper in chlorides has been observed before [4]. Gorbachev and Gusev have also shown that in neutral solutions copper is oxidized anodically with concentration polarization [5].

At sufficiently high current densities, the layer near the electrode becomes supersaturated with respect to CuCl, and the latter begins to crystallize. The potential then ceases to increase (horizontal plateau). The equilibrium standard potential of the process

$$Cu_s + Cl'_{soln} \rightarrow CuCl_s$$

is $\varphi_0 = +0.137$V [6]. Since, $a_{Cu(s)} = a_{CuCl(s)} = 1$, we have

$$\varphi = +0.137 + 0.059 \lg \frac{1}{a_{Cl'}} .$$

Taking the activities of K^+ and Cl^- ions only into account (for 0.1 N KCl $\gamma_{\pm} = 0.77$ [7]), we have $\varphi = +0.202$V, which is very close to the experimental value for the potential of the horizontal plateau.

Thus, for pure copper, the straight line of slope factor 0.056 corresponds to increase of Cu^+ concentration at the electrode surface. This is followed by crystallization of CuCl, not necessarily in immediate close contact with the electrode surface (the plateau). Further increase of current strength results in passivation of the electrode. The role of CuCl formation is also confirmed by the return course of the polarization curve. The potential falls with decrease of i and remains almost constant when it has reached about +0.2 v. Naturally, if the electrode is held long enough at a current density less than the value corresponding to the CuCl crystallization plateau, the potential also increases and the electrode becomes passive.

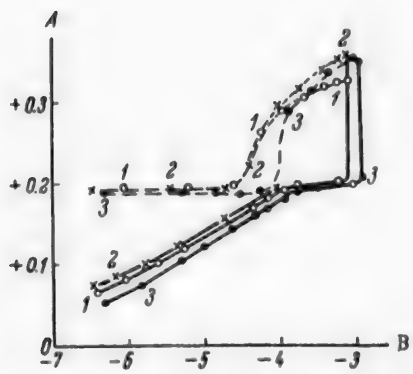

Fig. 2. Anodic polarization curves determined for 0.1 N KCl solution: A) potential (v) on the hydrogen scale, B) log current density (in amps/cm^2); curves; 1) alloy with 12.8% Zn, 2) with 13.6% Zn, 3) with 24.2% Zn; continuous lines — direct curves; dash lines — return curves.

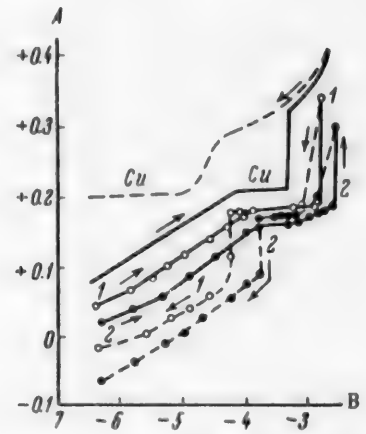

Fig. 3. Anodic polarization curves determined for 0.1 N KCl solution: A) potential (v) on the hydrogen scale, B) log current density (in amps/cm^2); curves: 1) alloy with 26.2% Zn, 2) with 37.12% Zn; the curve for pure copper (Fig. 1) is included for comparison; continuous lines — direct curves; dash lines — return curves.

The anodic behavior of alloys containing less than 25% Zn is similar to that of pure copper, but the curves lie somewhat further in the negative direction (Curve 3 in Fig. 1, and curves in Fig. 2). These alloys do not undergo dezincing, at least during the determination of polarization curves. Alloys richer in zinc are dezinced rapidly, as shown by the form of the polarization curves (Fig. 3). The CuCl crystallization plateaus are found at higher negative potentials than the plateaus for copper and alloys containing less than 25% Zn. The return curves show a sharp drop of potential with decrease of current density. Both these characteristics are associated with dezincing.

In experiments performed in a cell with a window of plane-parallel glass, through which the state of the electrode surface could be observed with the aid of a microscope, it was found that at the current density corresponding to the plateau, spots of CuCl were formed on alloys with 26.20 and 37.12% Zn; it is under these spots that metallic copper is mainly deposited upon increase of current density. Prolonged exposure at the current density corresponding to the plateau results in a fall of potential; this is associated with increase of the electrode surface as the result of deposition of copper and decrease of the true current density. At lower polarizations, corresponding to the sloping curve, the potential becomes increasingly possitive in the course of time owing to increased concentration of $Cu^{\cdot}$ ions.

The return curves in Fig. 3 indicate rapid depassivation of the electrodes, after which the layer near the electrode becomes poorer in cuprous chloride owing to its decomposition. The potential drops sharply because of the increased electrode surface.

The rate of disappearance of the CuCl precipitate, accompanied by liberation of metallic copper, can be studied by means of potential determinations at intervals, with the polarizing current switched off.

The results of one such experiment are presented in Fig. 4.

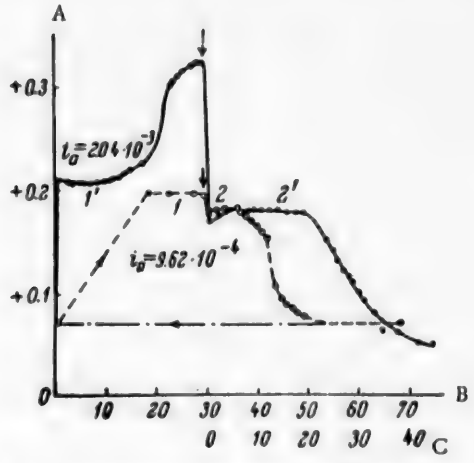

Fig. 4. Variations of the potential of an alloy containing 26.2% Zn during passivation with the polarizing current switched off: A) potential (v) on the hydrogen scale, B) time from start of experiment (minutes); current densities are indicated on the curves; explanation in text.

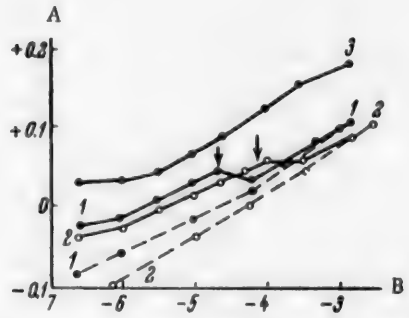

Fig. 5. Anodic polarization curves determined for 0.1 N KCl solution: A) potential (v) on the hydrogen scale, B) log current density (in amps/cm^2); curves: 1) alloy with 44% Zn, 2) with 47.2% Zn, 3) with 44% Zn and rapid determination of the polarization curve; continuous line – direct curves; dash lines – return curves.

The electrode (26.2% Zn) was first polarized at $i = 9.62 \cdot 10^{-4}$ A/cm^2 (dash line). After the plateau 1 corresponding to CuCl crystallization the current was switched off (this is indicated by an arrow); the potential then shifted somewhat in the negative direction, remained constant over a short plateau 2 (decomposition of CuCl), and then fell to almost the initial value. The electrode was then polarized again (indicated by the horizontal arrow pointing to the left) at $i = 2.04 \cdot 10^{-3}$ A/cm^2, i.e., at roughly double the previous current density. After the plateau 1' of CuCl formation (continuous line) and passivation, the current was switched off; the potential fell to the plateau 2' and dropped again when decomposition of CuCl was complete. The check at plateau 2 lasted about 9 minutes, and at plateau 2' about 20 minutes. The amount of CuCl formed is determined by the quantity of electricity passed; this also determines the time of its decomposition if the rates of the processes are equal.

Anodic behavior of alloys consisting of $\alpha + \beta$ and pure β solid solutions (alloys of Series II). Alloys of Series II include one alloy (No. 8, 35.9% Zn) of the α type of solid solution. Its polarization curve is similar to those described above. Polarization curves of alloys with 38.15 and 39.14% Zn, corresponding to $\alpha + \beta$ solid solutions, are characterized by a gradual shortening of the plateau of CuCl crystallization with increase of the zinc content. As in the case of alloys consisting of α solid solutions, deposition of metallic copper becomes visible at the start of the plateau.

In determination of the polarization curves for these alloys, longer exposures were needed for stabilization of the potential at a given current density; this resulted in a larger increase of the electrode surface and fall of true current density. Because of this the ascending portions of the polarization curves deviate somewhat from linearity ("sag").

Figure 5 shows curves for β solid solutions (44.0 and 47.2% Zn). In this case neither a CuCl crystallization plateau nor passivation are observed in the polarization range studied. Copper is deposited at a relatively low current density, at potentials far from the potential of solid CuCl formation. The start of dezincing, associated with a sharp increase of the electrode surface, usually precedes the break on the potential curve which is characterized by a fall of potential.

When the curves are determined by the slow method, the slope decreases somewhat with increase of zinc content, which might be attributed to the increased concentration of zinc in the alloys (formation of $Zn^{\cdot\cdot}$). However, rapid determination of the curve (ig. 5) shows that under such conditions the surface does not have time to increase considerably, as the result of dissolution and dezincing of the alloy, and therefore the slope factor remains close to 0.056.

Dezincing of copper–zinc alloys. This process is usually regarded as the consequence of entry of copper and zinc ions into solution followed by reduction of copper at the electrode surface (see literature citations in [8]). Indeed, when an alloy consisting of a solid solution is oxidized, ions of both components should enter the layer of liquid near the electrode. However, whereas both components pass into solution under certain polarization conditions, there is no reason to assume that one of them will be reduced again under the same conditions. The surface of the solid solution constitutes a "foreign" electrode for ions of the more noble component. Only if the more noble component were already present on the electrode surface as a separate phase would the conditions be favorable for the start of its reduction with a small deviation of the equilibrium potential. Oxidation of the alloy can then continue at a more negative potential than the equilibrium potential of the noble component (for the given concentration of this component in solution), and the metallic phase present on the surface at the same potential will then be the site of reduction.

The fact that the potential of the alloy undergoing oxidation is on the negative side of the equilibrium potential of the nobler component does not yet mean that its reduction can begin at the alloy surface. The potential difference must be sufficient for the formation of a nucleus of the new phase in a short time; this process always involves the overcoming of certain obstacles.

The formation of a new phase may be caused by the action of different factors. In particular, in the anodic polarization of Cu–Zn alloys in the range of α solid solutions, and with zinc contents above 25%, copper is formed by way of crystalline CuCl. For these alloys the equilibrium potential of CuCl crystallization may be expressed as

$$\varphi = \varphi_0 + \frac{RT}{zF} \ln \frac{a_{CuCl_s}}{a_{Cl^-} a_{Cu}}, \qquad (2)$$

where a_{Cu} is the activity of copper in the alloy.

It is seen that the potential should shift in the positive direction with decrease of a_{Cu}. However, in anodic polarization of the alloys, a CuCl precipitate is formed, not because the electrode potential reaches a definite value corresponding to the equilibrium $Cu_{alloy} \rightleftharpoons CuCl_s$, but because of supersaturation of the layer near the electrode with cuprous chloride. Figure 6 shows a plot of the observed crystallization potentials of CuCl against the alloy composition, and a curve calculated from Equation (2). Beyond 25% Zn the curves diverge sharply; this corresponds to a deviation from the equilibrium $Cu_{phase} \rightleftharpoons CuCl_s$ sufficient for formation

of nuclei of metallic copper. The presence of CuCl crystals probably facilitates this process. Therefore, alloys which give polarization curves with horizontal plateaus are dezinced by way of formation of solid CuCl.

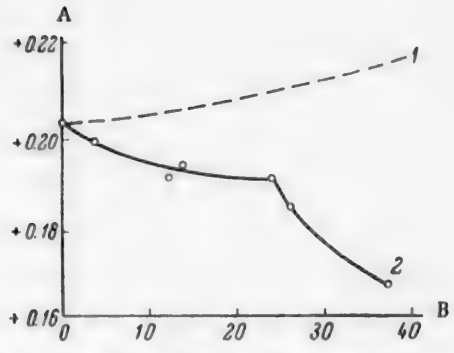

Fig. 6. Calculated potentials of solid CuCl formation in relation to alloy composition (1), and potentials at which CuCl crystallizes from supersaturated solutions at the electrode surface (2): A) potential (y) in the hydrogen scale, B) Zn content (atomic %).

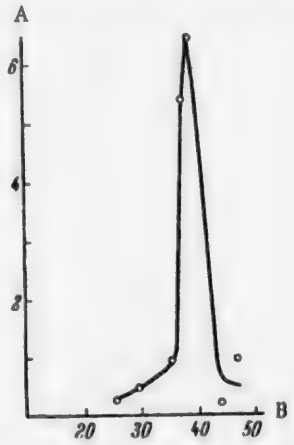

Fig. 7. Effect of alloy composition on the current density at which metallic copper is formed on the electrode surface: A) current density (amp/cm$^2 \cdot 10^{-4}$), B) Zn content of alloy (atomic %).

No plateau is observed for alloys belonging to β solid solution. Their polarization curves lie at considerably higher negative potentials, so that copper can be reduced directly from solutions at lower current densities than is the case with alloys of type α. Current densities at which formation of metallic copper can be observed visually are plotted in Fig. 7. The left-hand branch corresponds to α and α + β, and the right-hand branch to β solid solutions. Figure 7 confirms what has been said concerning the mechanism of dezincing.

Potential–alloy-composition curves for different current densities (Fig. 8) show distinct breaks at 25% Zn; this is also associated with the tendency to dezincing found in alloys containing over 25% Zn. It should be noted that this concentration corresponds to one of Tammann's possible boundaries of chemical action [1].

Slope of log current density–potential plots as a function of alloy composition. For copper and alloys of low copper content, the slope factor $b \simeq 0.056$. Alloys with 44 and 47% Zn show a tendency to a decrease of b. However, this seems to be only an apparent tendency because when the polarization curves are determined more rapidly the slope factor remains consistently close to that for pure copper. Evidently, as was indicated earlier, when the curves are determined slowly the surface relief develops and the current density decreases as a result.

If the reactions of copper and zinc oxidation proceeded in parallel, the slope should decrease with increase of the zinc content of the alloy. To account for the constancy of b we must assume that the surface composition of the alloy undergoing oxidation deviates considerably from the composition within the alloy (it is richer in copper), and that the course of dissolution of the alloy is determined mainly by the oxidation of copper, which is the slower process. With the aid of certain assumptions which simplify the problem considerably, it is possible to derive a relationship between the composition of the surface at which oxidation takes place, the volume composition of the alloy, and the specific oxidation rates of its components.

Assume that the alloy is homogenous throughout and that its surface is uniform from the energy aspect. This means that any atom of a given component requires the same energy activation for transfer into solution. This, of course, is not true and this assumption introduces a small error into the result.

Suppose that v_1 and v_2 represent the specific oxidation rates of components I and II of a certain binary solid solution at a given polarization. N_0 and $1 - N_0$ are their respective mole fractions within the alloy, and N and $1 - N$ are their mole fractions in the surface layer. Then $-dN/d\tau$, where τ is time, represents the rate of decrease of the concentration of component I on the surface of the alloy during oxidation. As atoms of component I pass into solution from the surface of the alloy at rate v_1N, either atoms of the same component

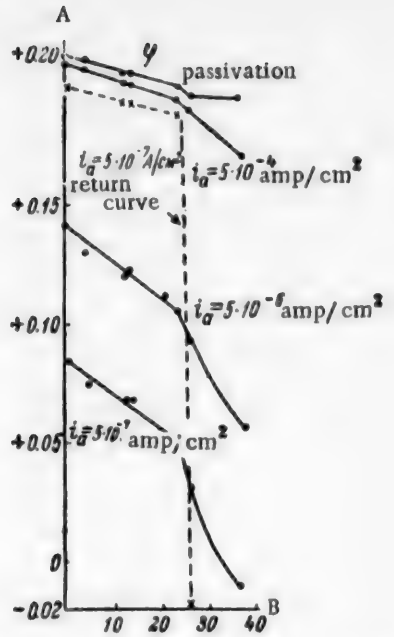

Fig. 8. Effect of alloy composition on the potential of α solid solutions at different constant current densities in 0.1 N KCl solution: continuous lines represent the direct, and the dash line the return course of the polarization curve at $i = 5 \cdot 10^{-7}$ A/cm². A) potential (v) on the hydrogen scale, B) Zn content of alloy (atomic %).

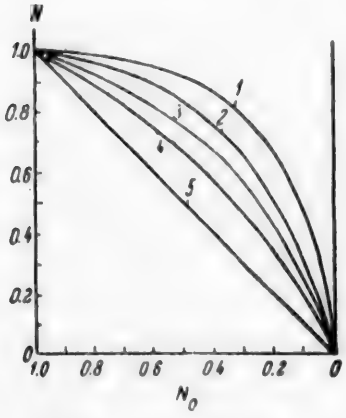

Fig. 9. Plot of the function $N = \frac{v_2 N_0}{v_1 + (v_2 - v_1) N_0}$ for different $\frac{v_2}{v_1}$ ratios: N) mole fraction of component 1 in the surface layer, N_0) the same in the body of the alloy; ratio v_2/v_1: 1) 10, 2) 5, 3) 3, 4) 2, 5) 1.

(probability N_0) or atoms of component II (probability $1 - N_0$) become exposed. As atoms of component II pass into solution at rate $v_2(1 - N)$, atoms of component I may become exposed; the probability of this is N_0. Then in the steady state

$$-\frac{dN}{d\tau} = v_1 N - v_2 N N_0 - v_2 (1 - N) N_0 = 0,$$

and hence

$$N = \frac{v_2 N_0}{v_1 + (v_2 - v_1) N_0} = \text{const}. \qquad (3)$$

If component I is more noble than component II, then $v_1 < v_2$. If there is a great difference between the oxidation rates, i. e. $v_1 \ll v_2$, then v_1 can be neglected and (3) gives $N \simeq 1$, so that the whole surface is covered by atoms of the more noble component.

If component II is more noble than component I, then $v_1 > v_2$ or $v_1 \gg v_2$. In the latter case

$$N = \frac{v_2 N_0}{v_1 (1 - N_0)} \cong 0.$$

The alloy surface becomes enriched with the more noble component, to an extent which depends on the difference between the oxidation rates v_1 and v_2.

The Function (3) is plotted in Fig. 9 for various values of v_2/v_1. It is seen that, for example when $v_2/v_1 = 10$, the surface of the alloy is greatly enriched with the more noble component. Thus, when $N_0 = 0.75$, which corresponds to 25% Zn in this instance, $N = 0.967$, or 3.5% Zn. Even higher values of v_2/v_1 may be expected for Cu–Zn alloys.

The constancy of the slope of the polarization curve can be attributed qualitatively, with the aid of Equation (3), to considerable enrichment with copper of the alloy surface undergoing oxidation under steady-state conditions.

SUMMARY

1. Investigations of the anodic behavior of copper–zinc alloys, in the range of α, α + β, and β solid solutions, in 0.1 N potassium chloride solution at current densities between $0.5 \cdot 10^{-6}$ and $0.5 \cdot 10^{-2}$ amp/cm² showed that under these conditions alloys containing over 25% Zn tend to undergo dezincing.

2. Consideration of the dezincing mechanism revealed differences in the course of the process for alloy consisting of α and β solid solutions respectively.

LITERATURE CITED

[1] G. Tammann, Z. anorg. allg. Ch., 107, 188 (1919).

[2] V. V. Skorcheletti and B. M. Idel'chik, Metallurgists 2, 30 (1934); 3, 27; Comm. Central Inst. Metals Metals 17, 185 (1935); R. Landau and C. Oldach, Trans. Electroch. Soc., 81 521 (1942).

[3] N. N. Gratsianskii et al. J. Phys. Chem. 30, 651 (1956); 30, 1267 (1956); 31, 418 (1957); 31, 887 (1957); 31, 1740 (1957); 31, 2458 (1957) [USSR].

[4] Lal and Thirsk, J. Chem. Soc., 2638 (1953).

[5] S. V. Gorbachev and N. I. Gusev, J. Phys. Chem. 32, 188 (1958) [USSR].

[6] W. Latimer, Oxidation States of the Elements and Their Potentials in Aqueous Solutions (IL, 1954) p. 190 [Russian translation].

[7] Chemist's Handbook [in Russian] (Chem. Press, 1952), 3, p. 481.

[8] Lombardi, La metallurgia ital., 45, 449 (1953); 46, 91 (1954)

Received March 28, 1958

CHEMICAL AND MECHANICAL DESTRUCTION OF GRAPHITE ANODES UNDER VARIOUS CONDITIONS OF HYDROXYL ION (WATER) DISCHARGE*

B. M. Bulygin

The Ivanovo Institute of Chemical Technology

Artificial graphite used in anodes in a number of electrochemical processes undergoes gradual destruction. The destruction rate depends on the electrolysis conditions and on the properties of the graphite used. The cause of destruction of anodic graphite in aqueous solution is oxidation of its surface by atomic (adsorbed) oxygen before the latter recombines into O_2 molecules. Because of the porous structure of the graphite, the electrolyte penetrates to some depth into the anode, so that the structure of the surface layer is weakened and graphite particles crumble off mechanically. The total losses of graphite during electrolysis are therefore made up of two components: chemical and mechanical losses.

Most previous investigations of the anodic corrosion of graphite have been carried out in electrolytes in which simultaneous discharge of chloride and hydroxyl (water)ions is possible – in solutions of sodium chloride or hydrochloric acid. These investigations include the work of Sprosser [1], Katsen and Sokolov [2], Sirak [3], Korshunov [4], Filippov [5], Johnson [6], Janes [7], etc. Because of the large fluctuations of current efficiencies for chlorine and oxygen under different experimental conditions, it is not possible to determine precisely the effects of current density, temperature, pH, and other electrolysis conditions on the destruction of graphite. Graphite is virtually unattacked by chlorine, and therefore the destruction of graphite anodes should be studied in solutions in which oxygen only is liberated, i.e., in solution of alkalies and oxyacids.

Such investigations have been performed by Sirak [3], Filippov and Nechporenko [8], and Thiele [9]. They obtained data on the destruction mechanism, noted a parallelism between chemical and mechanical destruction under various conditions of electrolysis in alkali solutions, and found that these types of attack conform to opposing laws in acid media. Sirak and Thiele noted the "swelling" of graphite in acids and the possible formation of solid oxides on variable composition on the graphite surface at high anode polarizations.

We carried out an extensive series of experiments on the destruction of graphite in electrolytes for different conditions of oxygen evolution over wide ranges of temperature and current density. The influence of these factors on chemical attack and mechanical breakdown respectively was studied separately.

EXPERIMENTAL

1) The electrolysis experiments were performed without the use of diaphragms, with circulating electrolytes, in 100 ml beakers kept at constant temperature to within $\pm 1^\circ$. The specimens were made from Acheson electrodes. They were thin (1-2 mm) graphite plates pressed against each side of a graphite contact by means of a rubber tube and ring (Fig. 1). Before the start of each experiment, the specimens were boiled in water for 30 minutes and dried at 120° to constant weight. After the experiments the specimens were washed in running water for 3-4 hours and again dried to constant weight.

The anode sludge was allowed to settle, washed with water, transfered into a porcelain crucible, and

*Communication I in the series on certain aspects of the destruction of graphite anodes in aqueous electrolyte solutions.

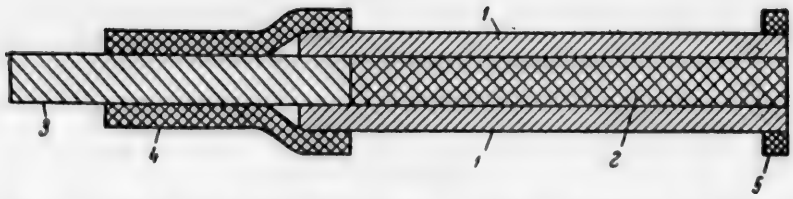

Fig. 1. Fixing of the graphite specimens: 1) graphite specimen, 2) rubber lining, 3) graphite contact, 4) rubber tube, 5) rubber ring.

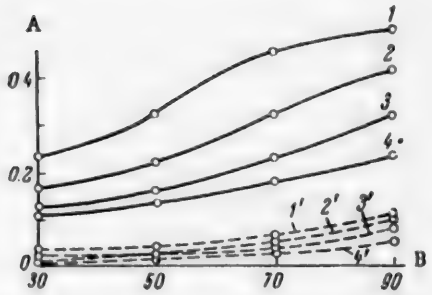

Fig. 2. Chemical and mechanical destruction of a graphite anode in a solution containing 10 g NaOH per liter: A) chemical (continuous line) and mechanical (dash line) destruction ΔG (in g/5 amp-hrs), B) temperature (°C); current density (amps/m²): 1) 1' – 200; 2) 2' – 1000; 3) 3' – 1500; 4) 4' – 3000.

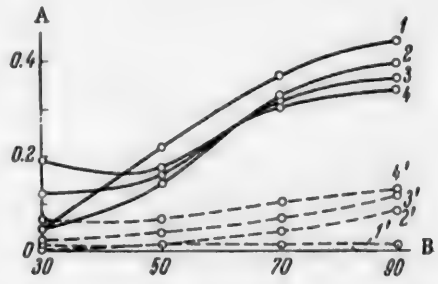

Fig. 3. Chemical and mechanical destruction of a graphite anode in a solution containing 5 g HCl per liter. (designations as in Fig. 2).

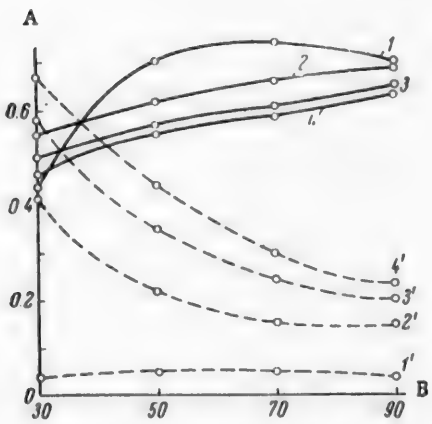

Fig. 4. Chemical and mechanical destruction of a graphite anode in a solution containing 5 g H_2SO_4 per liter. (designations as in Fig. 2).

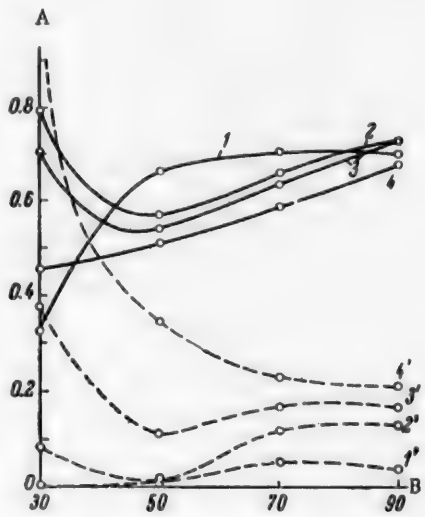

Fig. 5. Chemical and mechanical destruction of a graphite anode in a solution containing 5 g HNO_3 per liter. (designations as in Fig. 2).

dried to constant weight. Chemical attack was calculated as the difference between the total and the mechanical destruction.

2) The experiments were performed at 30, 40, 70, and 90°, at current densities of 200, 1000, 1500, and 3000 amps/m² in different solutions. The destruction data are plotted in Figs. 2-8.

In these graphs the chemical (continuous lines) and mechanical (dash line) destruction (ΔG), expressed in grams per 5 amp-hrs of electricity passed, is plotted as a function of temperature at different current densities. The results in the graph represent average data for several parallel experiments. The mean relative error of the method used is 2.5%.

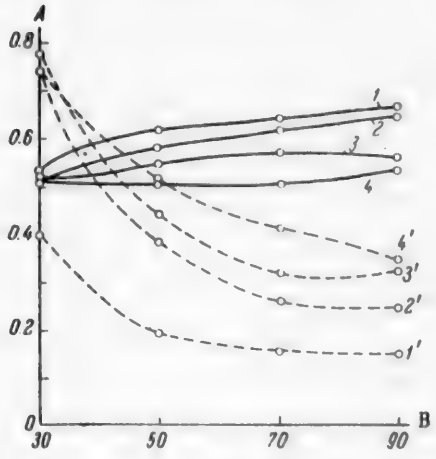

Fig. 6. Chemical and mechanical destruction of a graphite anode in a solution containing 5 g H_3PO_4 per liter. (designations as in Fig. 2).

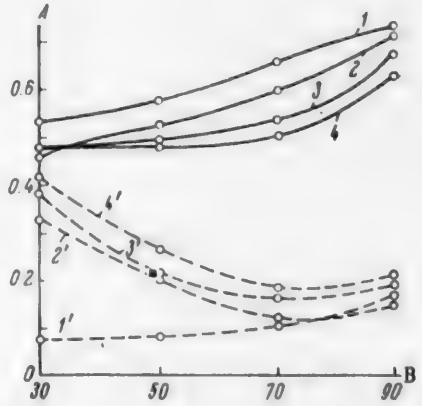

Fig. 7. Chemical and mechanical destruction of a graphite anode in a solution containing 5 g Na_2SO_4 per liter. (designations as in Fig. 2).

DISCUSSION OF RESULTS

The results show that the electrolysis conditions have an important influence on the nature of the destruction of graphite anodes. The mechanism of the oxidizing action of oxygen may be represented as follows.

Fig. 8. Chemical and mechanical destruction of a graphite anode in a solution containing 33 g NaClO and 10 g NaOH per liter: current density (amps/m^2): 1, 4) 3000 2) 1500, 3) 1000.

The atomic oxygen formed during discharge is adsorbed on the graphite surface, distorting its structure somewhat. Some of the oxygen at the active centers of the surface interacts with the electrode material, forming molecules of gaseous oxides (CO and CO_2). The latter may be formed either directly (in an alkaline medium, at low polarization), or through formation and decomposition of intermediate surface oxides (in an acid medium, at high polarization). At a high enough potential (above the desorption potential) the gaseous oxides together with recombined O_2 molecules begin to escape into the atmosphere at a definite rate, leaving behind a fresh unoxidized layer of graphite. The adsorption layer is renewed continuously by oxygen atoms entering it as the result of discharge. Evidently, the rate of combustion of the graphite must depend on the renewal rate of the adsorption layer. It is from this aspect that the influence of various external electrolysis factors on the chemical attack must be considered.

Rise of temperature increases chemical losses owing to increase of the rate of the chemical oxidation reaction and decrease of the desorption potential. As the anode gas contains free oxygen in addition to CO_2 the slow stage in CO_2 formation must be the oxidation reaction itself rather than discharge of OH^- (H_2O).

The lag of the oxidation rate behind the discharge rate also accounts for the decrease of specific chemical loss at high current densities in all electrolytes. However, if the current density is too low (200 amps/m^2), and at low temperatures, the discharge process becomes determining; the number of oxygen atoms formed in unit time becomes insufficient for oxidation of all the active centers of the surface. As a result, the chemical attack curves converge, and the curve for 200 amps/m^2 may even drop below the curves for 1000, 15000 and, 3000 amps/m^2 (in acid solutions).

The absolute chemical losses in electrolysis of acid and neutral solutions are 1.5-2 times the losses in alkaline solutions under the same conditions. This is due to differences in the mechanism of oxide formation at different pH. On the one hand, oxygen liberated from acid solutions is a more active oxidizing agent than oxygen liberated from discharging OH^- ions. On the other hand, in acid solutions oxidation of graphite proceeds by formation of intermediate surface oxides and of certain soluble compounds, such as pyromellitic acid [10], which evidently require a lower activation energy than the final oxidation product, CO_2. A significant fact is that chemical losses in acid and neutral media are almost independent of the specific character of the anion. This confirms earlier conclusions [11] that water molecules are decomposed during the electrolysis of aqueous solutions of oxyacids and their salts. However, as Figs. 3 and 8 show, simultaneous discharge of two ions (in particular, Cl^- and OH^-) or depolarization of the anode by some reducing agent (such as hypochlorite) reduces chemical losses considerably. The very small chemical (and total) losses in NaClO solution show that the possibility of oxidation of graphite by ClO^- ions is negligible.

Mechanical losses are most intimately associated with the structure of the graphite surface. In an alkaline solution (Fig. 2) electrolysis does not cause structural changes in the surface, and, therefore, mechanical destruction in it is very low, is of a surface character, and is proportional to chemical oxidation. In solutions of oxyacids (Figs. 4-6), however, the relationships are the reverse of those found for chemical oxidation. Here increase of temperature decreases mechanical destruction appreciably (especially in the 30-50° range), while increase of current density increases it.

The process of mechanical breakdown in acid solutions may be represented as follows.

Adsorption of polar water molecules on the electrode surface deforms the graphite crystal lattice somewhat. Solid oxides of graphite are formed on the deformed surface during discharge. They are more stable at low temperatures. Acid anions, also adsorbed on the anode, enter into oxygen exchange with these oxides (this has been confirmed in the case of platanium by the experiments of Gerovich and Kaganovich [12]). The crystal structure of the graphite is thereby disturbed and "swelling" (in Thiele's terminology) begins, leading to mechanical crumbling. Factors favoring the formation of surface oxides and stable adsorption of anions increase mechanical losses. Low temperature and high current density are such factors.

Mechanical destruction is especially great at low temperatures in nitric acid solution in which, as was reported by Sirak [3], the amount of solid oxides of graphite formed is the greatest.

It must be emphasized that only oxyacid anions have this destructive effect. In hydrochloric acid (Fig. 3), in which oxygen exchange is impossible, mechanical losses do not increase at low temperatures. In hypochlorite solution mechanical losses are virtually zero.

SUMMARY

1. It was shown in a study of the anodic corrosion of graphite in aqueous electrolyte solutions under conditions of exclusive discharge of hydroxyl (H_2O) ions that destruction in acid and alkaline media proceeds by different mechanisms.

In an alkaline medium, if the polarization is low, the surface structure of the graphite is not changed and gaseous oxides (CO and CO_2) are formed by direct interaction between adsorbed atomic oxygen and the electrode material. The rate of the oxidation reaction is determined by the renewal rate of the adsorption layer, and increases with the temperature. Mechanical losses are proportional to chemical oxidation.

In an acid medium, with high polarization, the final gaseous oxidation products are formed by way of formation and decomposition of solid surface oxides which distort the graphite structure. Low temperatures and high current densities favor adsorption of oxyacid anions, oxygen exchange between these anions and the solid graphite oxides, loosening of the structure, and ultimately large mechanical losses.

2. Introduction of anions lowering anode polarization (Cl^-, ClO^-), into the solution decreases destruction.

3. In conditions of industrial electrolysis of saturated NaCl solutions, admixtures of oxyacid anions (such as SO_4^{2-}) have a greater destructive action than additions of alkali at the same current efficiency for chlorine.

LITERATURE CITED

[1] Sprosser, Z. Elektroch., 7, 971 (1901).

[2] I. S. Katsen and P. I. Sokolov, J. Appl. Chem. 5, 916 (1932) [USSR].

[3] L. Ia. Siriak, J. Appl. Chem. 6, 808 (1933) [USSR].

[4] L. A. Korshunov, J. Chem. Ind. 12, 384 (1935) [USSR].

[5] T. S. Filippov, Trans. Ukrainian State Inst. Appl. Chem. 1 (1936).

[6] N. J. Johnson, Trans. Electroch. Soc., 86, 127 (1944).

[7] M. Janes, Trans. Electroch. Soc., 92, 22 (1947).

[8] T. S. Filippov and N. I. Nechiporenko, Trans. Ukrainian State Inst. Appl. Chem. 3, No. 1, 104 (1937).

[9] H. Thiele, Z. Elektroch. 55, 193 (1951).

[10] M. Janes, N. J. Johnson, and F. B. Pilcher, Trans. Electroch. Soc., 102, 474 (1955).

[11] T. S. Filippov, D. P. Semchenko, and B. G. Gribanovskii, Bull. Ordzhonikidze Industrial Inst. Novocherkassk, Che. Ser. 3 (1938).

[12] M. A. Gerovich and R. I. Kaganovich, Summaries of Papers at the 4th Conference on Electrochemistry [in Russian] 48 (1956).

Received April 26, 1957.

DESULFURIZATION OF STEEL IN AN INDUCTION FURNACE BY MEANS OF DIRECT CURRENT

O. A. Esin, S. I. Popel', S. G. Bratchikov, V. N. Razumov, and I. M. Plotnikov

It was shown earlier that when direct current passes through a system in which the cathode is liquid steel or pig iron, and the electrolyte is slag, desulfurization of the metal is more rapid and more complete [1, 2]. The experiments were performed either in ladles or in a Steinberg–Gramolin furnace with metal the sulfur content of which was usually in appreciable excess of the equilibrium value relative to the slag.

In the present investigation electrochemical desulfurization of steel in an induction furnace was studied. In contrast to the earlier work, the sulfur concentration in the metal usually did not exceed the equilibrium value relative to the slag [3, 4]. Therefore, exposure of the steel without passage of current resulted in its enrichment with sulfur.

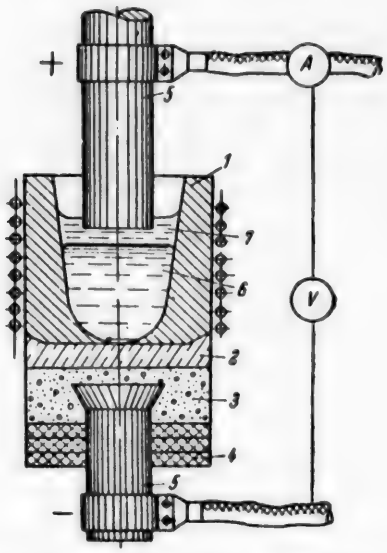

Apparatus for electrochemical desulfurization of steel: 1) magnesite lining of crucible, 2) conduction layer of magnesia and pitch, 3) packing layer of graphite and pitch, 4) asbestos cement plates, 5) carbon electrodes, 6) steel, 7) slag.

EXPERIMENTAL

The experiments were performed in a crucible 60 kg in capacity. The direct-current source was a welding machine, variable between 0 and 1200 amps. The voltage at the electrode clamps was 25-50 v.

The apparatus is shown schematically in the diagram. The current was passed by means of graphite electrodes (100 mm in diameter), one of which (the anode) was immersed in the slag and the other was in contact with the conducting packing at the bottom of the crucible. This packing consisted of two layers. A mixture of graphite and pitch was in direct contact with the electrode. This was covered with a mixture of magnesite powder and pitch. This layer protected the metal against carburization. The crucible walls were packed with a mixture of magnesite powder and water glass, as electrochemical desulfurization is less effective in presence of acid slags [1].

The carbon concentration was varied by additions of graphite or cast iron to mild steel. If cast iron was added, manganese (up to 0.5%) and silicon (up to 0.7%) was introduced into the metal with it. The contents of other impurities remained slight (0.02-0.07% P, and not over 0.1% Cr and 0.2% Ni), and varied little during the course of the experiments. The slag was made from ground calcite, clay, and quartz sand. In some cases fluorspar was added as a flux.

After the metal (50-60 kg) had been melted, the slag (5-6 kg) was put in and samples were taken for analysis. The anode was then inserted and a direct current was passed with the inductor switched off. Samples

were taken again after a definite time (3-10 minutes). During the electrolysis the slag was generally heated at the anode and hardened at the walls. The temperature of the metal did not change appreciably. Only in a few instances, if the current density was too low, it solidified in a layer on the bottom of the crucible.

The area of the metal surface was about 400 cm^2. The area of contact between the anode and the slag varied with the immersion depth, and was 200 cm^2 on the average. Accordingly, the anodic current density was approximately double the cathodic. Duplicate determinations of sulfur in the metal generally agreed to within 0.002%. The analytical error for the slag phase was greater.

RESULTS AND DISCUSSION

Preliminary experiments showed that the concentration of sulfur in the metal and slag falls appreciably at current densities close to 1.5 amp/cm^2. This is probably due to an increase of the sulfur concentration in the slag. If the process is controlled by diffusion, then equilibrium becomes established at the interphase; this equilibrium is represented by the expression for the distribution coefficient (L_{FeS}):

$$L_{FeS} = \frac{a_{S^{2-}} \cdot a_{Fe^{2+}}}{a_S \cdot a_{Fe}} \quad (1)$$

As the diffusion rate is not sufficient to equalize the concentrations, in absence of current the activities $a_{S^{2-}}$ and $a_{Fe^{2+}}$ are lower near the metal than within the bulk of the slag.

When the current is passed, metallic iron is deposited on the cathode:

$$Fe^{2+}_{sl} + 2e = Fe_{met}. \quad (2)$$

Accordingly, the content and activity ($a_{S^{2-}}$) of sulfur, may increase to some extent without disturbance of the equilibrium distribution (1). Therefore, only a part of the sulfur ions supplied by diffusion can pass from the slag into the metal.

As the current density (i) increases, the cathodic deposition of iron is accelerated and beyond a certain value of i the decrease of $a_{Fe^{2+}}$ becomes so great that it is not compensated by increase of $a_{S^{2-}}$ as the result of diffusion from the volume of the slag. In this case equilibrium distribution is maintained by transfer of sulfur from the metal into the slag; the value of a_S then decreases and $a_{S^{2-}}$ increases. In other words, electrochemical desulfurization of steel can be effected only at a certain critical current density i_{cr}, which depends on the rate of access of sulfur ions from within the slag to the steel surface.

The decrease of a_S and increase of $a_{S^{2-}}$ at $i > i_{cr}$ changes the direction of sulfur diffusion. The sulfur concentration now decreases in the metal and increases in the slag. This might retard the cathodic dissolution of sulfur. However, removal of sulfur from the slag at the anode could accelerate its diffusion from the cathode, i.e., electrochemical desulfurization of steel.

It follows from the data in Table 1 that in the first two experiments, in which the cathodic current density was 1.5-1.8 amps/cm^2, and the carbon content of the steel was low, the total desulfurization effect was small (0.003-0.004%), and the rate of the process reached 0.001% S/minute.

With carbon contents of 0.4% and over, the desulfurization was more effective, as the activity of sulfur in the metal (a_S) increased [4], and the equilibrium distribution (1) was shifted in the direction of higher $a_{S^{2-}}$. The rate of sulfur diffusion to the interface fell, and cathodic reduction of sulfur became possible at lower current densities.

In these experiments the total decrease of the sulfur content of the metal reached 0.011% in 6 minutes (Fusion 6) and 0.018% in 12 minutes (Fusion 5), while the average rate rose to 0.002% S/ minute.

With regard to the slag phase, the decrease of S concentration observed at the start of the experiment was replaced by an increase in a number of cases (Fusions 2, 3, 5).

Decrease of the S content of the slag with a simultaneous decrease of its concentration in the metal indicates that sulfur is oxidized at the anode and passes from metal onto the slag at a lower rate.

TABLE 1

Variations of Sulfur Contents of Metal and Slag at Cathodic Current Densities of 1.5-1.8 amps/cm²

Expt. (fusion) No.	Time from start (min.)	Cathodic current density, (amp/cm²)	Concentrations in metal (%)		Composition of slag (%)								Decrease of sulfur content of metal (%)	Mean desulfurization rate (%S per min · 10⁴)
			C	S	CaO	SiO_2	Al_2O_3	FeO	Fe_2O_3	MgO	CaF_2	S		
1	0	0	0.02	0.027	33.7	26.0	11.3	15.6	—	7.2	4.1	—	0.003	7
	4	1.5—1.8	0.03	0.024	32.6	25.4	6.7	15.0	5.5	8.3	2.5	—		
2	0	0	0.08	0.025	39.5	29.5	7.6	4.3	None	12.0	6.4	0.20	0.004	2
	3	1.5—1.6	—	0.024	Not determined							0.10		
	9	1.8	—	0.022	Not determined							0.15		
	19	1.8	0.11	0.021	36.1	27.1	6.7	6.5	None	18.7	5.8	0.20		
3	0	0	0.40	0.027	42.9	34.1	7.7	1.8	2.6	11.4	—	0.46	0.006	4
	5	1.6—1.8	—	0.025	Not determined							0.07		6
	12	1.6—1.7	0.40	0.021	39.7	34.2	6.7	0.7	1.1	18.0	—	0.10		
4	0	0	0.86	0.032	48.8	37.9	7.5	0.8	0.01	4.5	10.6	0.26	0.006	8
	5	1.6—1.7	—	0.028	Not determined							0.20		3
	11	1.7—1.8	0.84	0.026	47.3	38.7	7.3	0.7	0.08	5.6	10.3	0.16		
5	0	0	1.33	0.042	48.4	32.5	5.5	3.4	0.03	3.1	5.9	0.24	0.018	13
	3	1.7—1.8	—	0.038								0.18		23
	6	1.4—1.6	—	0.031										23
	9	1.3—1.6	1.38	0.024								0.26		
6	0	0	1.50	0.041	49.8	33.4	6.1	2.4	0.2	2.3	6.7	0.42	0.011	18
	6	1.6—1.7	1.66	0.030	48.5	33.8	6.4	2.4	0.08	3.6	6.7	0.32		
7	0	0	3.3	0.028	37.1	33.6	4.9	2.3	—	9.1	12.0	—	0.011	15
	6	1.5—1.6	—	0.019										10
	8	1.8	—	0.017										

TABLE 2

Electrochemical Desulfurization of Steel at Current Densities Near to 2 amps/cm^2 and Over

Expt. (fusion) No.	Time from start (min)	Cathodic current density amp/cm^2	Concentration in metal (%)		Composition of slag (%)								Decrease of sulfur content of metal (%)	Mean desulfurization rate (%S per min · 10^4)
			C	S	CaO	SiO_2	Al_2O_3	FeO	Fe_2O_3	MgO	CaF_2	S		
8	0	—	0.65	0.026	32.1	28.5	4.9	4.8	0.08	13.4	11.0	0.15		
	6	2.0	—	0.024	Not determined							0.17	0.008	6.5
	12	2.0		0.022								0.10		
		1.9—2	0.48	0.018	34.5	28.5	5.0	4.0	None	17.7	6.1	0.14		
9	0	—	1.42	0.030	34.2	39.4	8.1	2.0	0.08	8.6	9.4	0.58		
	4	1.9—2.0	1.42	0.030								0.24	0.013	12
	11	1.9—2.0	1.45	0.017	32.4	39.6	6.6	0.9	0.3	13.5	8.1	0.28		
10	0	—	1.38	0.041	49.4	33.8	5.2	2.5	0.7	2.2	7.2	0.18		
	9	1.9	1.14	0.026	44.0	34.6	5.0	3.0	0.3	3.4	11.8	0.14	0.015	17
11	0	—	1.56	0.040	41.3	36.6	8.6	1.3	None	3.8	12.5	0.25		
	6	1.9—2	—	0.025	Not determined							0.26	0.015	25
12	0	—	0.92	0.033	43.3	38.3	7.4	3.2	0.08	2.6	6.6	0.28		
	3	1.9	1.02	0.023	37.4	34.2	9.6	3.0	0.08	10.0	6.4	0.06	0.010	30
13	0	—	0.03	0.031	35.7	26.3	9.4	11.3	3.7	3.2	10.2	0.11		
	2	3.0	0.03	0.026	35.1	25.5	9.3	12.8	5.6	4.2	7.4	0.12		
	12	2.0	0.09	0.019	31.2	26.0	8.1	10.5	4.6	13.1	6.3	0.12	0.012	75

Gradually the rate of the cathode process approaches the rate of the anode process, and then exceeds it in a number of experiments, so that the sulfur content of the slag increases. Despite this, the rate of anodic oxidation of sulfur becomes too low by the end of the experiment, and when the ratio $\frac{[\%\,S_{sl}]}{[\%\,S_{met}]}$ approaches the equilibrium value, the sulfur content of the metal does not decrease.

Further increase of current density imporved the process characteristics. This is illustrated by the data in Table 2.

At current densities close to 2 amps/cm^2 (Fusions -12) the average rate and exent of sulfurization exceed the preceding values only slightly. It is interesting to note that in the ninth experiment, with a higher content of sulfur than usual in the slag, during the first four minutes of electrolysis the concentration of S in the slag fell without desulfurization of the metal. When the sulfur content of the slag fell to 0.24% further electrolysis at the same current density resulted in desulfurization of the steel at a rate close to 0.002% S/minutes.

Increase of current density of 3 amps/cm^2 in Experiment 13 increased the desulfurization effectiveness appreciably. In this case the degree of desulfurization of the soft iron (C = 0.03%) was close to the best results in the preceding experiments with high-carbon steel, and the maximum rate of the process was considerably higher, reaching 0.0075% S/minute. It is true that the lower sulfur content of the slag in this experiment may have favored better results.

These results therefore show that electrochemical desulfurization of steel occurs at definite current densities. The effectiveness of the process increases with current density and carbon content of the metal. The desulfurization rate is limited by development of the anode process, which gradually slows down. The causes of the retardation are not clear. It may be due to increase of the S concentration in the surface layer of graphite or to retarded transfer of sulfur to the anode. In fact, after the experiment the sulfur content in the upper part of the graphite rod was 0.01%, while at the region of contact with the slag it was 0.02%, or twice as high. Moreover, in a number of cases the slag became enriched with magnesia during the experiment (Tables 1 and 2) and became more viscous; this may have retarded diffusion of sulfur toward the anode.

Since the desulfurization rate is determined by the anode process, it was considered desirable to carry out the electrolysis with both electrodes immersed in the slag.

TABLE 3

Desulfurization of Steel by Electrolysis of Slag

Expt. (fusion) No.	Time from start (min)	Current density for metal surface (amp/cm^2)	Content in metal (%)		Composition of slag (wt. %)								Decrease of sulfur content of metal (%)	Steel desulfurization rate (%S per min · 10^4)
			C	S	CaO	SiO_2	Al_2O_3	FeO + Fe_2O_3	MnO	MgO	CaF_2	P_2O_5	S	
14	0	—	1.17	0.030	42.8	31.2	4.3	5.0	2.0	5.5	8.0	0.25	0.21	6
	60	2.2	0.91	0.027	34.0	26.3	2.8	7.1	2.1	19.0	7.6	0.14	0.25	
	12.0	2.2	0.92	0.023	31.9	25.7	3.8	9.7	1.2	27.6	9.3	0.084	0.47	
													} 0.007	
15	0	—	0.50	0.028	35.4	35.8	7.8	4.9	1.3	6.5	8.1	0.10	0.12	10
	5	1.8	—	0.023	32.2	34.4	7.0	4.4	1.3	10.5	9.9	0.10	0.16	
	8.5	1.9	0.47	0.018	32.9	32.9	6.4	2.6	1.1	14.7	9.1	0.10	0.14	16
													} 0.010	
16	0	—	0.27	0.030	39.7	33.0	6.6	4.2	1.9	5.1	9.4	0.08	0.10	10
	5.5	2.2	0.23	0.025	31.0	30.0	6.0	4.2	2.8	15.4	10.4	0.11	0.09	
	11	2.2	—	0.024	32.3	30.1	5.0	2.9	2.5	18.5	8.5	0.10	0.12	1
													} 0.006	

The results of experiments in which a current lead was not connected from below are presented in Table 3. They are similar to the results discussed earlier. In particular, in Experiment 15, where the current density (per unit area of the metal surface, as before) was 1.8-1.9 amps/cm^2, the sulfur content fell from 0.028% to 0.018% in 8.5 minutes. This method is much simpler from the design aspect, and would not involve any great difficulties in industrial adoption.

The current efficiencies for sulfur were low in all the experiments. The best values were 10-20%; this indicates that other processes develop to a considerable extent. The most probable of such process are oxidation of ferrous to ferric ions and liberation of oxygen with formation of CO and CO_2 at the anode, and reduction of iron at the cathode.

SUMMARY

1. In the case of sulfur-rich slags desulfurization of steel by the electrolytic method commences at current densities close to 1.5 amp/cm^2 at the cathode and about 3 amps/cm^2 at the anode. The rate of the process increases with the current density.

2. Soft iron is desulfurized less rapidly and completely than high-carbon steel at a given current density.

3. Electrolysis of slag may be used as a method for desulfurization of metal under it.

4. Current efficiencies for sulfur were estimated. They do not exceed 10-20%.

The authors are grateful to V. M. Shestakov for assistance in this work.

LITERATURE CITED

[1] O. E. Esin, A. I. Kholodov, P. V. Gel'd, and S. L. Popel', collected papers "The Steel Smelting Industry" [in Russian], supplement to the journal Steel (Metallurgy Press, 1958), p. 151.

[2] I. L. Korkin, O. A. Esin, and V. V. Mikhailov, Bull. Acad. Sci. USSR, OTN 12, 71 (1957).

[3] K. G. Trubin and G. N. Oiks, Metallurgy of Steel [in Russian] (Metallurgy Press, 1951).

[4] O. A. Esin and P. V. Gel'd, Physical Chemistry of Pyrometallurgical Processes, 2 [in Russian] (Metallurgy Press, 1954).

Received June 1, 1957

EFFECT OF DILUTION OF CHLORINE WITH NITROGEN ON THE CORROSION OF METALS AT HIGH TEMPERATURES

Kh. L. Tseitlin and V. A. Strunkin

The K. E. Voroshilov Institute of Organic Intermediates and Dyes

The preceding papers [1-4] contain data on the high corrosiveness of chlorine and on conditions for retardation of its reactions with metals by additions of air or steam, or by variations of the gas rate. However, other methods for decreasing corrosion must be used in many instances. It is known that at low pressures the addition of an inert gas to an active substance retards diffusion of the latter to the walls of the vessel [5], and this may also retard corrosion.

It was desired to investigate the possibility of varying the corrosion rate by variations of chlorine concentration in a medium of inert gas. It was first decided to study the influence of dilution of chlorine with technical nitrogen, supplied in steel cylinders to the consumer.

EXPERIMENTAL

The procedure did not differ, in general, from that described earlier [1]. Technical chlorine and nitrogen from cylinders were dried separately in Drechsel flasks filled with concentrated sulfuric acid, passed through

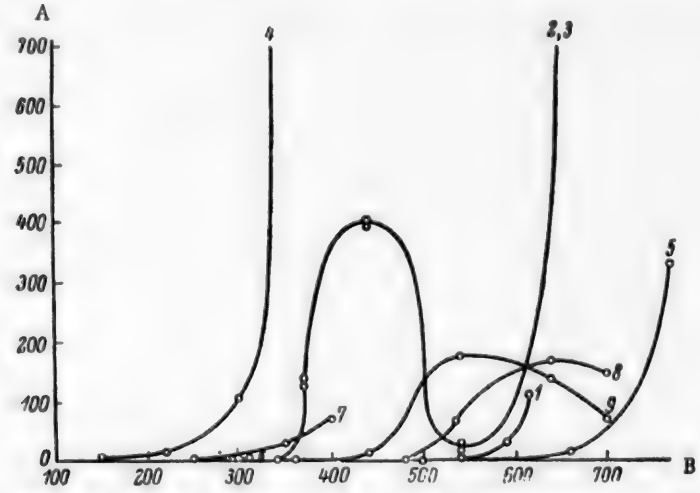

Corrosion of metals by chlorine diluted with technical nitrogen: A) corrosion (g/m² · hour), B) temperature (°C); curves: 1) Al, 2) Fe, 3) St. 3, 4) Cu, 5) Ni, 6) Pb, 7) Ta, 8) 1Kh18N9T steel, 9) Kh17 steel.

rheometers, mixed in a flask containing glass wool, entered a preheater tube, and then passed into the quartz apparatus for corrosion testing, heated in an electric crucible furnace. The exit gases passed through a condenser, were neutralized by means of alkali solution, and escaped into the air.

TABLE 1

Effect of Dilution of Chlorine with Nitrogen on the Corrosion of Metals at High Temperatures

Duration of Tests 6 Hours

Metal	Temperature (°C)	Corrosion (g / m² · hour)		Resistance in a current of chlorine diluted with nitrogen
		by chlorine	by chlorine diluted with nitrogen in 1 : 10 ratio	
Aluminum	130	0.0		Up to 500° – specimens bright, no pitting in region of contact with quartz. The water used for washing the specimens contained chlorine
	160	524.3•		
	170	1112.7•	0.1	
	450		0.1	
	500		0.1	Above 560° – vigorous reaction with formation of volatile chloride, soluble in water with effervescence; specimens coated with white film containing chlorine. No pitting in contact region.
	590		28.8	
	616		111.3	
Armco iron	285	0.2		310° – specimens bright, covered with thin iridescent film.
	310	1859.5•	0.1	
	370		135.5	370-440° – vigorous formation of ferric chloride began after 1.5 hours.
	440		394.4••	
	540		14.6	540° – specimens coated with dark gray deposit insoluble in water; small amounts of volatile ferric chloride formed.
	660		1371.0••	660° – vigorous formation of ferric chloride.
Carbon steel	260	0.1		Up to 340° corrosion slight, specimens coated with dark film containing chlorine. Volatile ferric chloride formed at higher temperatures; specimens after experiment coated with a dark film slowly soluble in water and containing chlorine.
	285	10195.0•		
	304		0.1	
	340		0.6	
	370		123.8	
	440		403.2••	
	540		28.0	540° – pitting in region of contact with quartz. Small amounts of volatile corrosion products.
	660		1302.0••	660° – violent formation of ferric chloride, specimens covered with swollen films of corrosion products containing chlorine.
Copper	150	1.0	4.0	150-300° – specimens coated with film containing chlorine. Film flakes off on impact. Film Thickness 0.5 mm at 300°. Corrosion products of low volatility, remain almost entirely on specimen surface.
	220	16.0	13.5	
	300	26154.0•	103.8	

•Tests up to 60 minutes.

••Tests lasting 1.5-4 hours.

TABLE 1 (continued)

Metal	Corrosion ($g/m^2 \cdot hour$)	Corrosion ($g/m^2 \cdot hour$)		Resistance in a current of chlorine diluted with nitrogen
		by chlorine	by chlorine diluted with nitrogen in 1 : 10 ratio	
Copper	350		2512.0••	350° – violent reaction, melted dark corrosion products containing about 61% Cu and 48% Cl on bottom of apparatus.
1Kh18N9T steel	418	0.5	0.3	Up to 480° specimens bright, coated with iridescent films.
	450	20.2		
	480	63.7	0.3	
	535	223.5••	65.6	Above 500° – corrosion begins rapidly, accompanied by volatilization of ferric chloride into the cooling system, with partial entrainment of chromium compounds. Dark corrosion products remaining on the specimens have relatively higher contents of chromium and nickel, are not completely soluble in sulfuric or hydrochloric acids, and contain almost no chlorine. Attack irregular (bright patches remain on strongly corroded steel surface).
	640	21620.0•	165.1	
	700		144.2	
Kh17 steel	300	0.2		360° – specimens bright, coated with iridescent film.
	360	1.8	0.6	
	440	31.5	11.6	Above 420° – corrosion accompanied by volatilization of ferric chloride without chromium.
	540	639.4••	175.9	
	640		138.2••	540° – dark gray corrosion products remaining on the specimens have a higher chromium content, are insoluble in sulfuric and hydrochloric acids, contain no chlorine.
	700		73.2	700° – especially strong attack at the region of contact with quartz and upper corners of the specimens. Corrosion products remain on the specimens contain chlorine and are incompletely soluble in water
Nickel	500	0.5	0.5	500° – specimens bright, coated with a thin dark film.
	540	2.1		
	570		6.7	570-660° – specimens coated with thin deposit of greenish corrosion products. Yellowish nickel chloride in condenser.
	660	40.9	15.1	
	740	121.8•		
	770	2191.0•	352.4••	770° – specimens coated with yellowish-green layer which flakes off.

TABLE 1 (continued)

Metal	Corrosion ($g/m^2 \cdot hour$)	Corrosion ($g/m^2 \cdot hour$)		Resistance in a current of chlorine diluted with nitrogen
		by chlorine	by chlorine diluted with nitrogen in 1 : 10 ratio	
Lead	250	1.7	1.9	250° – some dulling of the specimens. Above 270° – specimens coated with dark gray deposit.
	275	1.8		
	296	19.3	4.5	
	309	32.2	5.0	
Tantalum	250	0.0	0.0	250° – specimens bright
	300	3.3	4.1	300-350° – specimens bright; white powder in condenser.
	350	595.6••	27.6	
	400	2358.0•	67.6••	400° – specimens bright, coated with dark violet iridescent film. White powder in condenser.

TABLE 2

Effect of Dilution of Chlorine with Purified Nitrogen on the Corrosion of Metals at High Temperatures

Duration of Tests 6 Hours

Metal	Temperature (°C)	Corrosion ($g/m^2 \cdot hour$)		Resistance in a current of chlorine diluted with purified nitrogen
		chlorine diluted with technical nitrogen	chlorine diluted with purified	
Aluminum	450	0.1	129.9	450° – formation of volatile chloride began after 2 hours. Specimens coated with pale corrosion products, attack irregular. Periodic rise of temperature due to heat of reaction
	500	0.1	2.0	500° – formation of volatile chloride began after 5 hours. Specimens coated with gray deposit free from chlorine, incompletely soluble in water. Local corrosion, reaching 600 mm/year in some regions of the metal.
Armco iron	540	14.6	311.2••	540° – condenser filled rapidly with volatile ferric chloride. Specimens covered with dark corrosion products free from chlorine and incompletely soluble in water.
Carbon steel	540	28.0	75.6••	540° – volatile ferric chloride formed rapidly. Corrosion products remaining on the specimen contain chlorine and are incompletely soluble in water. Deep attack (about 1000 mm/year) in region of contact with quartz.

•, ••Same as Table 1.

TABLE 2 (continued)

Metal	Temperature (°C)	Corrosion ($g/m^2 \cdot$ hour)		Resistance in a current of chlorine diluted with purified nitrogen
		chlorine diluted with technical nitrogen	chlorine diluted with purified nitrogen	
1Kh18N9T steel	700	167.0	397.3	700° – chlorination begins rapidly. Brown fumes given off on removal of specimens from apparatus. Corrosion products, removed in flake form contained chlorine and were found to be incompletely soluble in water. Specimens do not emit metallic sound after experiment.
Kh17 steel	700	73.2	220.7	700° – as in experiment with 1Kh18N9T. Corrosion rates of two specimens 69 and 371.6 $g/m^2 \cdot$ hour respectively.

The chlorine and nitrogen rates were 16 and 404 ml/minute, respectively, (weight ratio 1 : 10). The chlorine conformed to GOST 6718-53, and the nitrogen contained about 0.5% oxygen.

The results of the experiments are given in Tables 1 and 2 and in the diagram. It was found that considerable dilution of chlorine with nitrogen greatly reduces corrosion of all the metal tested, under certain conditions (Table 1).

In one experiment mercury from a cracked thermometer fell into the apparatus heated to about 550°. An instantaneous reaction, accompanied by an explosion, took place in a current of greatly diluted chlorine.

In some of the experiments (Table 2) technical nitrogen was freed from oxygen ("purified" nitrogen) by passage through freshly prepared pyrogallol solution continuously circulated through a system of columns packed with glass rings [6] before beind dried.

The gaseous stream became more corrosive in all cases as the result of purification of the nitrogen.

In the temperature ranges in which corrosion of iron and its alloys is slow, the induction period was shortened and the rate of reaction with formation of volatile chlorides rose. However, even if purified nitrogen is used, the metal surfaces are partially coated with layers of nonvolatile and insoluble corrosion products of complex composition, which may retard the corrosion process.

DISCUSSION OF RESULTS

In a heterogeneous exothermic reaction, dilution of the active substance by an inert gas decreases the rates of diffusion and heat evolution and assists removal of heat of reaction; corrosion therefore decreases. This is demonstrated by numerous examples of reactions between metals and chlorine diluted with nitrogen. The usual sharp and considerable rise of temperature in the apparatus due to the heat of the corrosion reaction was observed in only 3 experiments out of 50 when the chlorine was diluted with nitrogen. The temperature of the experiment had to be raised considerably in every instance in order to bring about a violent reaction between the metal and chlorine.

It has already been reported [2] that the corrosion of many metals by chlorine, like the vapor pressures of corresponding chlorides, increases with temperature. The same is generally true if the chlorine is greatly diluted with technical nitrogen containing oxygen. However, there was a decrease of corrosion and deviation from this general behavior in the case of iron and steel at 520-560°, and to a smaller extent in the case of stainless steels at 640-700°; this may be attributed to predominant oxidation of the metal surface by oxygen

with formation of oxide layers which retard the process, and to a decrease of the rate of formation of volatile ferric chloride.

An oxide does not react more vigorously with the chlorinating gas if the chloride formed volatilizes at a low temperature [7]. On the contrary, according to our results and literature data, there is a correlation between the corrosion of metals in chlorine and the volatilities of the corresponding chlorides. In particular, we believe that metals whose chlorides are volatile below 350° [8] should be strongly attacked in a current of chlorine even below 350°. This has been established for Al, Fe, and Ta and, in our opinion, also for Ti, Nb, Mo, Hg, W and other metals.

The results of an increasing number of investigations dealing with high-temperature chlorination are being published in the literature. In particular, many recent investigations are concerned with high-temperature chlorination of organic substances; if such processes are carried out industrially without due consideration, considerable difficulties may arise owing to excessive corrosion of the equipment and risk of fire. For normal operation of chlorination equipment, even for exothermic chlorination processes which occur at relatively low temperatures (50-200°) (such as the chlorination of benzene, acetylene, etc.) in presence of metallic catalysts (shavings, rings, spheres, or lumps of steel, cast iron, aluminum, or copper), the rates, compositions, and proportions of the reagents, temperature, and other factors must be strictly regulated. Even slight deviations from the process conditions may result in a violent exothermic reaction (combustion) between the metal and dry chlorine, accompanied by heating of the catalyst and metal equipment to incandescence or even to fusion. The difficulties are naturally greater with reactions which proceed above 200°.

It is therefore very important to formulate, at least in general terms, certain considerations concerning the retardation of corrosion of metals by chlorine at high temperatures. Our work has shown that metal corrosion can be decreased by: 1) decrease of the chlorine rate; 2) in a number of cases, by additions of steam, oxygen, or air to the chlorine; 3) considerable dilution of the chlorine by an inert gas, and in particular by nitrogen.

In the temperature range studied dilution of chlorine with nitrogen decreases particularly sharply the corrosion of metals which burn readily in chlorine and the chlorides of which have high vapor pressures (aluminum, iron and its alloys, tantalum). Dilution of the chlorine has less effect on those metals whose chlorides have low vapor pressures (lead and, to a certain temperature, nickel). The same may be said of copper, the chlorides of which melt at relatively low temperatures; in this case dilution of the chlorine is effective only at about 300°, which may be attributed to a considerable decrease of the temperature rise of the surface due to heat of reaction.

It is reported in the literature that, in order to avoid excessive evolution of heat, strongly exothermic processes should in practice be carried out in very dilute mixtures [9], and that the resistance of metals to such agents as hydrogen sulfide may be increased by dilution of the gas with an inert gas [10, 11]. Our experiments have shown that the corrosion of equipment by chlorine can likewise be decreased if the chlorine is diluted with an inert gas. However, dilution of chlorine with technical nitrogen has relatively little effect in raising the maximum temperature at which the metals are satisfactorily resistant. The exception is aluminum, the temperature limit of resistance of which rises sharply because of the unusual ease with which it forms a complete protective film by oxidation of the surface by oxygen present in the gas stream.

It should be pointed out in conclusion that technical nitrogen as supplied in cylinders often cannot be regarded as an inert gas, as the oxygen present in it (about 0.5%) is highly reactive under certain conditions; this has been demonstrated particularly clearly in the case of aluminum.

SUMMARY

1. Strong dilution of chorine with technical nitrogen sharply lowers the corrosion rates of aluminum, iron and its alloys, tantalum, and (to a smaller extent) of copper (above 230°), nickel (above 600°). amd lead (above 250°); the maximum temperature of satisfactory stability is raised relatively little by such dilution, except in the case of aluminum.

2. Removal of oxygen from technical nitrogen makes the gas stream containing chlorine more corrosive toward the metals studied.

3. The causes of retardation of metal corrosion when chlorine is diluted with nitrogen are discussed, and methods for decreasing corrosiveness of the medium are considered.

LITERATURE CITED

[1] Kh. L. Tseitlin, J. Appl. Chem. 27, No. 9, 953 (1954).*

[2] Kh. L. Tseitlin, J. Appl. Chem. 28, No. 5, 490 (1955).*

[3] Kh. L. Tseitlin, J. Appl. Chem. 29, No. 2, 299 (1956).*

[4] Kh. L. Tseitlin and V. A. Strunkin, J. Appl. Chem. 29, No. 11, 1664 (1956). *

[5] K. Bailey, Retardation of Chemical Reactions (Chemistry Press, 1940), p. 68 [Russian translation].

[6] E. V. Alekseevskii, R. K. Gol'ts, and A. P. Musakin, Quantitative Analysis [in Russian] (Goskhimizdat, 1955), p. 530.

[7] V. I. Spitsyn, Chlorination of Oxides and Their Mixtures with Carbon [in Russian] (Moscow, Inst. Appl. Mineralogy, 1931), p. 24.

[8] A. B. McIntosh, Ind. Ch., 32, 376, 195 (1956).

[9] D. A. Frank-Kamenetskii, Diffusion and Heat Transfer in Chemical Kinetics [in Russian] (Izd. AN. SSSR, 1947), p. 330.

[10] E. B. Backensto, R. D. Drew, and C. C. Stapleford, Corrosion, 12, 1, 22 (1956).

[11] Kh. L. Tseitlin, L. V. Merzloukhova, and V. A. Strunkin, J. Appl. Chem. 30, No. 10, 1553 (1957).*

Received May 3, 1957

*Original Russian pagination. See C. B. Translation.

CORRESPONDENCE OF IRON AND ZINC IN 1 N H_2SO_4•

L. I. Antropov and A. T. Petrenko

The S. Ordzhonikidze Polytechnic Institute, Novocherkassk

There is as yet no agreed opinion concerning the mechanism of interaction of inhibitors with protected metals. However, it may be assumed that, irrespectively of whether the interaction is confined to ordinary electrostatic adsorption, or if the bond is strengthened to specific adsorption, or even if a chemical compound is formed between the metal and the inhibitor, in all such cases adsorption of the inhibitor of the metal surface is a necessary condition for it to have an influence on the corrosion rate. Additives introduced into a corrosive medium can influence the corrosion rate only if they can be adsorbed on the metal surface. Consideration of the conditions for such adsorption is special significance in relation to inhibitors of the adsorption type, the surface activity and therefore the inhibiting effect of which depends primarily on the electrochemical nature and the sign of the surface charge on the protected metal.

It is known that the charge of a corroding metal is determined by the relationship between the zero-charge potential ($E_{q=0}$) and the equilibrium potential of the metal (E_{eq}) or, in other words, by the value of the latter on the zero-point scale.

$$\varphi_{eq} = E_{eq} - E_{q=0}.$$

When $\varphi_{eq} < 0$, the surface of the corroding metal is negatively charged and additives of the cationic type are the most likely inhibitors. When $\varphi_{eq} > 0$, the metal surface under corrosion conditions is positively charged, and adsorption inhibitors must be sought primarily among anionic additives. If φ_{eq} is close to zero, substances of all these electrochemical types may serve as inhibitors.

The equilibrium potentials of iron and zinc undergoing corrosion in acid media are only a little on the negative side of the corresponding zero points •• [1-5], i.e., under these conditions they may absorb any surface-active substances, whatever their electrochemical nature.

Numerous inhibitors of the acid corrosion of iron have now been studied••• [6]. Experimental results obtained by different workers indicate that inhibitors for iron include chemical compounds of all three electrochemical types: they include cation-active, molecularly active, and anion-active substances. Iron is much easier to protect by means of inhibitors than is zinc [7]. Only a few organic inhbitiors are known for zinc [7-10], and they are substances of the cationic and molecular types.

The present paper deals with a study of the influence of surface-active substances of different electrochemical types on the corrosion of iron and zinc in 1 N H_2SO_4 solution.

•Communication III in the series on the theory of metal corrosion and the inhibiting action of organic substances.

••Under these conditions $E_{eq\,Zn} = -0.77$ [1], and $E_{q=0\,Zn} = -0.63$ v [2]. The equilibrium potential of iron in acid media varies from -0.23 to -0.26 v [3-5], while $E_{q=0\,Fe}$, calculated from the electronic exit work function, is zero volts. Hence, $\varphi_{eq\,Zn} = -0.14$ v,)and $\varphi_{eq\,Fe} = -0.26$ v.

•••About 200 inhibitors for iron and steel are listed in a review article by Beskov and Balezin [6].

EXPERIMENTAL

The experiments were performed with technical iron containing the following impurities (%):

Mn	Ni	Si	Cr	C	S	P
0.45	0.20	0.17	0.15	0.12	0.045	0.035

and Ts-1 electrolytic zinc, containing not more than 0.06% impurities, including (%):

Pb	Fe	Cd	Cu	Sn
0.025	0.015	0.014	0.002	0.001

The sulfuric acid and surface-active agents used were of chemically pure grade.

The corrosion rates were determined from the weight loss of the specimens. The experiments were performed in an air thermostat at 20 ± 0.5°. The duration of each experiment was 24 hours for iron and 1 hour for zinc. The test specimens were spade-shaped, with surface areas of 5 cm^2 (Fe) and 6 cm^2 (Zn), and were freely suspended in the solutions by their stems. To prevent intensified water-line corrosion, the stems of the specimens were coated with KhSL-1 chemically resistant lacquer [11].

The zinc specimens were cleaned by means of a file and then treated with No. 1 emery paper before the experiments. The iron specimens were first cleaned mechanically on a grinding machine, and then polished with emery paper. All the specimens were polished lengthwise, in order that the surfaces should be reproducible. After the mechanical treatment the specimens were kept for 24 hours at room temperature to allow the surface to return to the steady state from the state of activation induced by distrubance of the crystal lattice; this gave more consistent results. Before the experiments the specimens were degreased (zinc chemically, iron electrochemically), washed with hot and with cold distilled water, etched, again washed, dried with filter paper, and weighed. Directly before the experiments the specimens were pickled in order to remove the thin oxide film formed by the action of atmospheric oxygen.

After each experiment the corrosion products were removed from the specimen surface by a powerful jet of water, with simultaneous rubbing of the surface with a glass rod fitted with a rubber tip. The specimens were dried with filter paper and weighed.

Each experiment was performed at least in triplicate. The variations between parallel experiments were 3-4% for iron, and 7-10% for zinc.

In addition to the usual organic substances, organosilicon compounds were also tested as inhibitors.

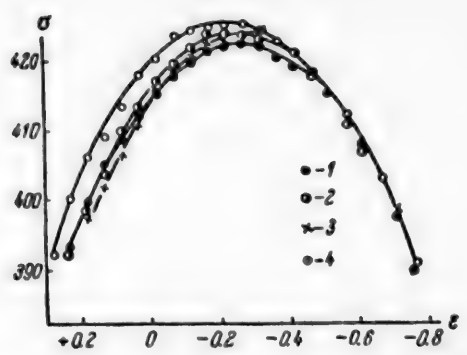

Fig. 1. Electrocapillary curves of mercury in 1 N sulfuric acid containing additives at saturation concentrations: additives: $C_9H_{19}SiON$, 2) $(CH_3)_3Si-(CH_2)_3S_2P(i-C_3H_7)_2$, 3) $(C_3H_7)_3SiC_2P(OCH_3)_2$, 4) without additive.

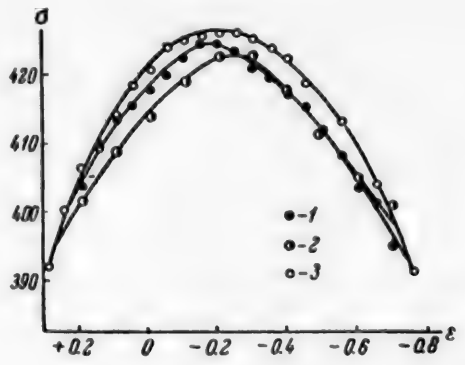

Fig. 2. Electrocapillary curves of mercury in 1 N sulfuric acid containing additives: additives (in g/liter): 1) 0.01 p-tolylurea 2) 0.75 anthranilic acid, 3) without additive.

The surface activity and electrochemical nature of the particles of the substances used as inhibitors were investigated by means of electrocapillary measurements.

A capillary electrometer with a mercury column 77.6 cm high and capillary radius $7.6 \cdot 10^{-4}$ cm was used for the electrocapillary determinations. The pressure on the mercury meniscus was varied by means of compressed air and measured with a mercury manometer. All the electrocapillary curves were determined for 1 N H_2SO_4 solution at 20 ± 0.5°.

The results of the electrocapillary determinations, presented in Figs. 1-6, show that the surface-active substances studied include all three electrochemical types.

The results of the corrosion tests are given in the table, where K is the retardation coefficient, i.e., the ratio of the corrosion rate in pure acid to the corrosion rate in the acid with the additive.

It follows from the data in the table that most of the substances added inhibit the corrosion of iron to some extent. The retardation coefficient increases with the inhibitor concentration in all cases except thiourea. In the case of thiourea, as reported in the literature [12], the retardation coefficient decreases with increase of concentration.

The strongest inhibiting effect on the corrosion of iron in 1 N H_2SO_4 solution is exerted by additives containing organosilicon cations and iodide ions, at concentrations of 1 g/liter. The retardation coefficients are all roughly the same in these cases (K = 17-20).

Only a few of the additives tested have an appreciable inhibiting effect on the corrosion of zinc. Most of the additives studied either have no effect on the rate of solution of zinc in 1 N H_2SO_4 (anthranilic acid, tetrabutylammonium sulfate, ethyldimethylsilylmethanol, etc.), or even increase it (p-tolylthiourea, trimethylsilylmethyl thiocyanate, etc.). Tribenzylamine, (trimethylsilylmethyl) diethylamylammonium iodide and trimethylbenzylammonium chloride slightly retard the corrosion of zinc; the retardation coefficient in their presence does not exceed 1.8, and the last two additives exert an inhibiting effect only at concentrations not less than 1.0. g/liter.

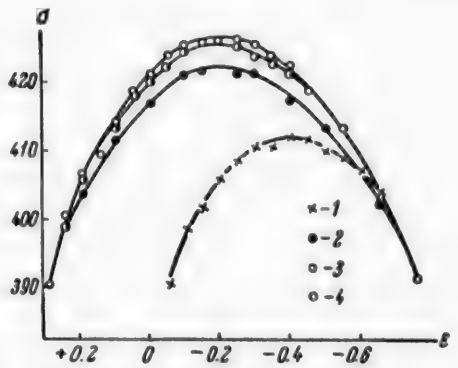

Fig. 3. Electrocapillary curves of mercury in 1 N sulfuric acid containing additives at saturation concentrations: additives: 1) 5 g/liter of thiourea, 2) $C_{16}H_{38}P_2S_4SiO_4$, 3) $(CH_3)_3Si(CH_2)_3S_2P(OC_2H_5)_2$, 4) no additive.

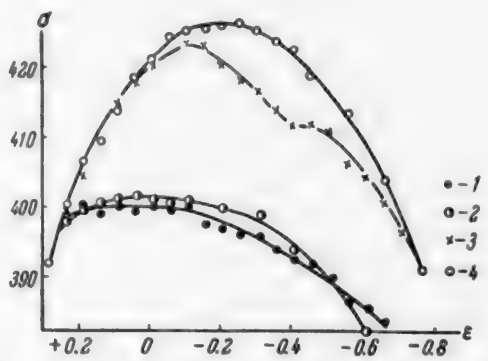

Fig. 4. Electrocapillary curves of mercury in 1 N sulfuric acid containing additives at saturation concentrations: additives: 1) $C_7H_{15}SiON$, 2) trimethylsilylmethyl thiocyanate, 3) ethylmethylsilylmethanol, 4) no additive.

Additives containing organosilicon cations have a stronger inhibiting effect on the corrosion of zinc; these include the iodides of (trimethylsilylmethyl)diethylmethylammonium, (trimethylsilylmethyl)ethylmethylcyanoethylammonium, (trimethylsilylmethyl)diethylamylammonium, bis(trimethylsilylmethyl)ethylmethylammonium, and (trimethylsilylpropyl)triethylammonium. The retardation coefficient with 2 g of these additives per liter varies from 3 to 8.

Results of Corrosion Measurements

Type of additive	Additive	Concentration (g/liter)	K	
			Fe	Zn
Molecular	Anthranilic acid	0.1	1.1	1.2
	The same	1.0	3.0	—
	p-Tolylurea	0.01	4.1	0.7
	Trimethylsilylmethyl thiocyanate	Saturated solution	13.5	0.8
	Ethyldimethylsilylmethanol	The same	1.5	1.0
	$C_{10}H_{38}P_2S_4SiO_4$	»	1.0	0.8
	$C_7H_{15}SiON$ *	»	1.6	1.0
	$(CH_3)_3Si(CH_2)_3S_2P(OC_2H_5)_2$ *	»	1.1	0.8
Anionic	Thiourea	0.1	10.2	—
	The same	1.0	6.9	—
	»	5.0	1.7	—
	$C_9H_{19}SiON$ *	Saturated solution	1.8	1.1
	$(CH_3)_3Si(CH_2)_3S_2P(i-C_3H_7)_2$ *	The same	1.4	0.7
	$(C_3H_7)_3SiC_2S_2P(OCH_3)_2$ *	»	1.4	0.6
Cationic	Tribenzylamine	0.1	2.1	1.9
	Tetrabutylammonium sulfate	1.0	1.3	1.0
	Pyramidon	0.5	2.3	—
	The same	2.0	—	1.2
	Trimethylbenzylammonium chloride	0.1	1.2	1.0
	The same	1.0	2.8	1.2
	(Trimethylsilylmethyl)diethylmethylammonium iodide	0.1	2.4	—
	The same	1.0	17.6	—
	»	2.0	—	2.9
	(Trimethylsilylmethyl)ethylmethylcyanoethylammonium iodide	0.1	6.2	—
	The same	1.0	19.0	—
	»	2.0	—	6.8
Cationic	(Trimethylsilylmethyl)ethylamylammonium iodide	0.1	2.6	—
	The same	1.0	17.0	—
	»	2.0	—	4.3
	Bis(trimethylsilylmethyl)ethylmethylammonium iodide	0.1	2.1	—
	The same	1.0	16.2	3.0
	»	5.0	—	19.0
	(Trimethylsilylpropyl)triethylammonium iodide	2.0	—	8.1

*Names of these additives are not given, as their composition is not known with certainty.

DISCUSSION OF RESULTS

Of the substances studied, organosilicon compounds have the greatest inhibiting effects on the corrosion of iron and zinc. Organosilicon polymers have practical applications in various branches of industry [13-18], especially because of the their ability to form dense insulating films of high heat resistance on metallic surfaces [15, 16]. A method has been developed for applying polymerized protective films from vapors of organosilicon compounds onto metal surfaces for prevention of corrosion [17, 18]. Studies of nonpolymerizing organosilicon compounds as inhibitors have been commenced only very recently [19]. It is to be expected that further studies of compounds in this class may reveal other effective organosilicon inhibitors of acid corrosion of iron and zinc.

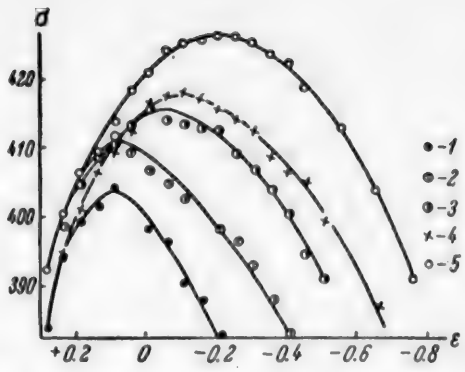

Fig. 5. Electrocapillary curves of mercury in 1 N sulfuric acid containing additives: additives (in g/liter): 1) 0.1 tribenzylamine, 2) 1.0 tetrabutylammonium sulfate, 3) 2.0 pyramidon, 4) 1.0 trimethylbenzylammonium chloride, 5) no additives.

Comparison of the results of electrocapillary (Figs. 1-6) and corrosion determinations (table) shows that substances of any of the three electrochemical types may act as inhibitors of acid corrosion of iron, but the protective effect is greatest with cation-active substances.

Although, as already noted, the adsorption conditions on the surfaces of iron and zinc corroding in acid media are approximately the same, only cation-active substances (tribenzylamine, pyramidon, and compounds containing organosilicon cations) have an inhibiting effect in the case of zinc. Additions of the anionic and molecular types either accelerate the corrosion of zinc (for example, p-tolylthiourea), or have no appreciable effect on it (ethyldimethylsilylmethanol).

Results of polarization determinations show that most of the additives studied influence the rates of both electrode processes — passage of metal ions into solution and liberation of hydrogen. The different effects of adsorbed surface-active substances on the corrosion of iron and zinc respectively can be ascribed to the fact that these metals belong to different groups with regard to their hydrogen overvoltage [20].

The over-all rate of a process can be influenced most easily by action on its slow step. In the case of hydrogen evolution on iron during acid corrosion, the slow step is combination of atoms into molecules, and therefore substances which retard this combination are inhibitors of acid corrosion of iron. Since interaction of uncharged particles (atoms) is involved in this process, the charge of the inhibitor should not have an appreciable effect on its rate. Irrespectively of the sign of the charge on the additive, adsorption of it on the electrode surface may retard the recombination process, as incorporation of the additive particles between the hydrogen atoms hinders collisions of the latter. This accounts for the experimental fact that inhibitors of iron corrosion belong to different electrochemical types. The higher effectiveness of cation-active inhibitors may be due to the fact that the nature of the slow step in the liberation of hydrogen on iron may be changed in their presence [21].

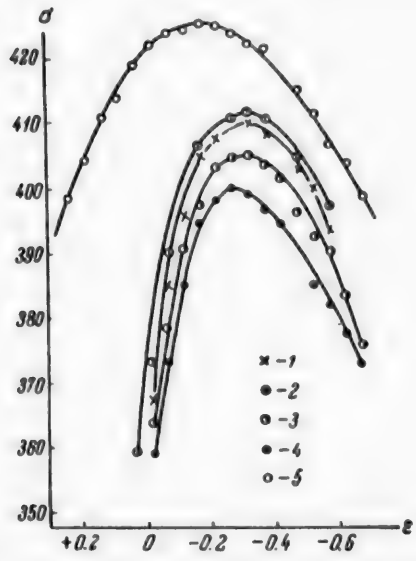

Fig. 6. Electrocapillary curves of mercury in 1 N sulfuric acid containing additives: additives (in g/liter): 1) 1.0 (trimethylsilylmethyl)diethylmethylammonium iodide, 2) 1.0 (trimethylsilylmethyl)-ethylmethylcyanoethylammonium iodide, 3) 1.0 (trimethylsilylmethyl)diethylamylammonium iodide, 4) 1.0. bis(trimethylsilylmethyl)ethylmethylammonium iodide, 5) no additive.

In the case of zinc the slow step is discharge of hydrogen ions. In this case the inhibiting action of cation-active substances and the stimulating effect of anionic additives may be attributed to the corresponding effects of the charge of the adsorbed particles on the discharge of hydrogen ions and transfer of metal ions into solution. It has already been noted in the literature that the influence of additives on hydrogen overvoltage on the lead and mercury — metals on which the discharge of hydrogen ions is slow — varies according to their charge. Iofa, Kabanov, Kuchinskii, and Chistiakov [22] found that additives of the cationic type increase hydrogen overvoltage on mercury while anionic additives decrease it. Vaniukova and Kabanov [23] found that hydrogen overvoltage on lead is increased more in presence of cationic than of molecular additives.

Adsorption of cation-active substances, in consequence of a shift of the potential of the metal in the positive direction at a distance of one ionic radius from the metal surface (ψ_1), leads to retarded discharge of hydrogen ions and slows down transfer of metal ions into solution. Adsorption of anionic additives shifts the ψ_1 potential in the negative direction; this facilitates the above-named reactions and thereby accelerates corrosion. Additives of the anionic type can have an inhibiting effect only if the influence of the sign of the charge of the additive on discharge of hydrogen ions and transfer of metal ions into solution is weaker then the influence of the other factors. Such factors may include, for example, mechanical insulation of the metal from the action of the corrosive medium, if the surface concentration of the additive is high enough or if a protective layer of adsorption compounds of metal and additive is formed. Molecular additives may have different effects on the ψ_1 potential, according to dipole orientation, and therefore may influence the rates of the electrode processes differently. If a molecule is adsorbed so that its positive end is directed toward the metal, its influence on the ψ_1 potential and the electrode processes is analogous to that of a surface-active cation. However, it is weaker. If the position of the charges is reversed, the action of molecules is analogous to the action of anionic additives. If a molecular additive does not give rise to additional charge, but merely increases the thickness of the double layer, their adsorption decreases the field intensity and retards discharge of hydrogen ions and ionization of the metal. This explains why some molecular additives (n-heptylic acid [10]) have an inhibiting effect on zinc corrosion while others (p-tolylthiourea, etc.) stimulate it.

Thus, in the choice of adsorption inhibitor of acid corrosion, it is necessary to take into account the hydrogen overvoltage on the protected metal as well as the adsorption conditions. Corrosion of metals on which the recombination of hydrogen atoms is slow may be inhibited by most surface-active substances which can be adsorbed under the given conditions. In the case of metals for which discharge is the slow step in the liberation of hydrogen, cationic additives are the most likely corrosion inhibitors.

This is true only if the additives are not susceptible to reduction. Substances which are reduced under these conditions may stimulate corrosion owing to their depolarizing action.

SUMMARY

1. In selection of acid-corrosion inhibitors the range of substances from which adsorption inhibitors should be sought may be restricted if the nature of hydrogen overvoltage on the protected metal is taken into account in addition to the adsorption conditions.

2. In the case of zinc, on which discharge of hydrogen ions is retarded, cation-active substances are effective as adsorption inhibitors. Conversely, anion-active substances accelerate zinc corrosion. This may be due to the respective effects of the sign of the charge of the adsorbed particles on discharge of hydrogen ions and transfer of metal ions into solution.

3. In the case of iron, on which recombination of hydrogen atoms is retarded, any substances absorbed on its surface have an inhibiting effect, regardless of the sign of the charge on their particles. The explanation is that the slow step in this case is interaction of uncharged particles.

4. Surface-active substances of the cationic type are the most universal inhibitors, as they exert a protective effect in all cases when they can be absorbed on the metal surface, irrespectively of the nature of the hydrogen overvoltage on the protected metal.

5. The corrosion of iron and zinc in 1 N H_2SO_4 is effectively inhibited by organosilicon compounds, which retard the dissolution of iron approximately 20-fold at 0.1% concentration, and of zinc 2.5 to 8-fold at 0.1-0.2% concentrations under these conditions.

LITERATURE CITED

[1] A. G. Pecherskaia and V. V. Stender, J. Appl. Chem. 23, 920 (1950).

[2] S. Glasstone, Introduction to Electrochemistry (Moscow, IL, 1951) [Russian translation].

[3] V. A. Kuznetsov and Z. A. Iofa, Zh. Fiz. Khim. 21, 201 (1947).

[4] Z. A Iofa and L. A. Medvedeva, Proc. Acad. Sci. USSR 69, 213 (1949).

[5] Z. A. Iofa, E. L. Klakhovetskaia, and K. Sharifov, Proc. Acad. Sci. USSR 84, 543 (1952).

[6] S. D. Beskov and S. A. Balezin, Sci. Mem. V. I. Lenin MGPI 44, 3 (1947).

[7] W. Wiederholt, Werkst. u. Korrosion, 6, 247 (1955).

[8] A. Sieverts and P. Lueg, Z. anorg. allg. Ch., 126, 193 (1923).

[9] Sh. Ch. Jao and Ch. A. Mann, Ind. Eng. Ch., 39, 910 (1947).

[10] P. A. Rebinder and K. P. Rebinder, Zh. Fiz. Khim., 1, 175 (1930).

[11] Departmental Technical Specification, Ministry of Chemical Industry 2256-50 [USSR].

[12] S. A. Balezin and S. K. Novikov, Sci. Mem. V. I. Lenin MGPI 44, 62 (1947).

[13] A. P. Kreshkov, Organosilicon Compounds in Technology [in Russian] (Industrial Construction Press, 1950).

[14] K. A. Androanov and A. A. Zhdanov, Progr. Chem. 21, 207 (1952) [USSR].

[15] Tonindustrie Ztg. Keram. Rdsch. 32 (1953).

[16] M. M. Koton, J. Appl. Chem. 12, 1435 (1939) [USSR].

[17] L. D. Iudin, Proc. Acad. Sci. USSR 25, 610 (1939).

[18] L. V. Krotov and L. D. Iudin, Scientific Research in the Chemical Institutes and Laboratories of Academy of Sciences USSR in 1939, Abstracts of Papers [in Russian] (Moscow–Leningrad, 1940).

[19] L. I. Antropov, V. P. Grigor'ev, and A. T. Petrenko, J. Appl. Chem. 31, No. 10, 1497 (1958).*

[20] L. I. Antropov, Zh. Fiz. Khim. 26, 1688 (1952).

[21] A. T. Petrenko and L. I. Antropov, J. Appl. Chem. 31, No. 6, 949 (1958). *

[22] Z. Iofa, B. Kabanov, E. Kuchinskii, and F. Chistiakov, Zh. Fiz. Khim. 13, 1105 (1949).

[23] L. Vaniukova and B. Kabanov, Zh. Fiz. Khim. 14, 1620 (1940).

Received May 8, 1957

*Original Russian pagination. See C.B. Translation.

ELECTROCHEMICAL METHOD FOR PRODUCTION OF SODIUM FORMATE FROM CARBON DIOXIDE AND SODIUM AMALGAM

P. S. Chechel' and L. I. Antropov

The S. Ordzhonikidze Polytechnic Institute, Novocherkassk

It is known that under certain conditions carbon dioxide can be reduced to formic acid at cathodes consisting of metals and amalgams on which the hydrogen overvoltage is high [1-5].

In earlier work on this problem the concentration of formate (neutralization product of the formic acid formed) never exceeded 1 g/liter.

Fischer and Prziza [6] found that the use of carbon dioxide at high pressures is important in the cathodic reduction of carbon dioxide: the higher the pressure, the greater is the permissible current density. However, the production of concentrated formate solutions is restricted by the fact that formic acid inevitably enters the anode space and is decomposed at the anode. Therefore, even at 50 atmos the formate concentration obtainable is relatively low (not over 96.6 g/liter calculated as formic acid).

Many workers have long been attracted by the possibility of preparing sodium formate by reduction of carbon dioxide by sodium amalgam. The high negative potential (−1.7 to −1.9 v) established on the amalgam surface during decomposition by aqueous solutions creates favorable conditions for reduction of many compounds; this includes the reduction of carbon dioxide to formic acid.

Rabinovich and Mashovets [7] showed that formic acid (or, rather, sodium formate) can be prepared by this method, and determined the synthesis conditions. The process can be represented as

$$2Na(Hg) + 2CO_2 + H_2O = HCOONa + NaHCO_3 + Hg.$$

With complete utilization of the amalgam, the formation of one molecule of formate is accompanied by formation of one molecule of bicarbonate.

However, the conditions found by Rabinovich and Mashovets, and by other workers, for the synthesis of formic acid did not satisfy economic production requirements.

This paper contains the results of work on the production of sodium formate from carbon dioxide and sodium amalgam in concentrations which may be of practical significance.

EXPERIMENTAL

The electrolytic cell shown in the diagram was used for the experiments. The distinguishing feature of the cell is the presence of a large and continuously renewed surface of sodium amalgam. It consists of two main parts connected by a ground-glass joint. The body of the lower part of the cell contains a perforated cylinder of somewhat smaller diameter than the body itself; it carries an outlet stopcock and a sealed-in wire for making contact during determinations of the potential of the amalgam. The area of the amalgam surface in the cell was 28 cm^2.

The top part of the cell consists of a main body, a liquid seal, an electrolytic bridge and a side tube with a stopcock for saturating the working solution with the gas. A screw stirrer, rotated by a special motor fixed on a stand, is inserted from above. The stirrer is so designed that in the assembled apparatus its blades are com-

pletely immersed in the amalgam, while a special hood fitted at the top forms a liquid seal. The rotation of the stirrer and the angle of its blades are so arranged that the amalgam circulates upward in the center and downward at the periphery. By the action of upward and centrifugal forces, the amalgam in the cell is ejected at a high velocity in the form of fine streams through the perforated cylinder into the outer part of the cell.

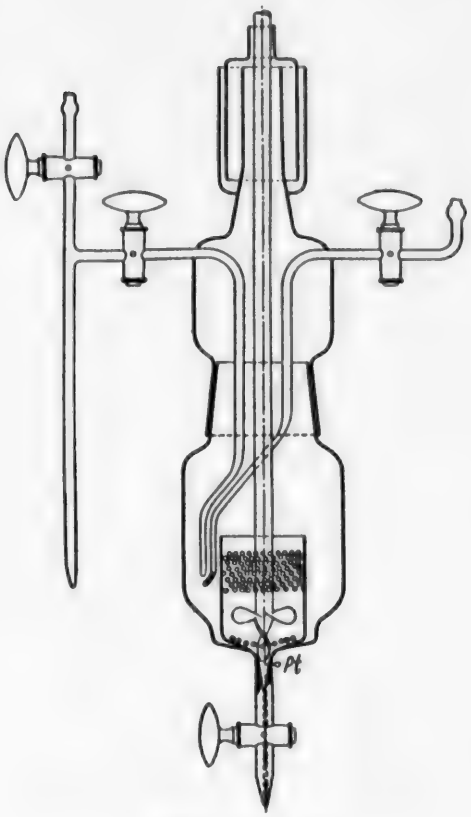

Electrolytic cell.

The experimental procedure was as follows. The cell was first charged with 20-25 ml of 0.245% sodium amalgam (composition by weight) and 50 ml of solution, and the stirrer was then set in motion. Carbon dioxide was bubbled through the solution during the experiment. When the amalgam had been completely decomposed, the mercury was let out through the stopcock and weighed on an analytical balance, and a new portion of amalgam was put in through the gas inlet tube. For this operation the gas was disconnected and a special funnel was inserted into the inlet tube.

The experiments were continued intermittently until the maximum concentrations of sodium formate attainable under the given conditions had been reached.

The end of decomposition of the amalgam was determined by the change of its potential: a rapid change of potential from −1.7 to −1.0 v corresponded to almost complete decomposition of the amalgam.

The concentration of the formate obtained was determined by the permanganate method [8]. The formate concentrations in all the tables are calculated as formic acid.

Chemically pure reagents were used for the experiments. The experiments were performed at 20°.

RESULTS

Several series of experiments were carried out.

In the first series, carbon dioxide was passed continuously through the cell at 1.5 liter/hour only until the solution was saturated with respect to sodium bicarbonate. The carbon dioxide was then turned off, sodium bicarbonate was partially converted into carbonate by decomposition of the amalgam, the carbon dioxide was then turned on again, etc. Under these conditions there was a continuous accumulation of sodium carbonate in a saturated solution of sodium bicarbonate. If positive results had been obtained it would have been possible to avoid filtration of sodium bicarbonate until concentrated solutions of sodium formate had been obtained.* However, it proved impossible to obtain concentrated sodium formate solution by this method. Analyses showed that the formic acid concentration reached before a saturated solution of sodium formate is obtained subsequently remains almost unchanged at about 44-45 g/liter (65-66.5 g/liter calculated as sodium formate).

The second series of experiments, summarized in Table 1, differed from the first in that carbon dioxide was passed continuously into the cell and the precipitated sodium carbonate was separated off at intervals. In this way it is fairly easy to raise the formic acid content to 184 g/liter, with an over-all yield of 34.6%. This is equivalent to 272 g of sodium formate per liter.

Solutions of higher concentrations cannot be obtained, as on further increase of the sodium formate content the yield of formic acid falls to zero and the liquid becomes so thick that rapid stirring in presence of pre-

*At 20° the solubility of $NaHCO_3$ is 96 g/liter, and that of HCOONa is 972 g/liter.

cipitated bicarbonate forms a suspension of mercury in the liquid.

It is desirable to continue the synthesis until the solution contains 230-250 g of formate per liter. This is also justified by the fact that the yield is then higher, about 40%.

TABLE 1

Results of Second Series of Experiments•

Cycle No.	Amount of amalgam (ml)	Decomposition time		Yield of HCOOH			
		in cycle	from start of experiment	during cycle		from start of experiment	
				g/liter	%	g/liter	%
1	92.5	5hr 35min	5 hr 35min	36.8	60.0	36.8	60.0
2	52.5	2 25	8 00	15.2	43.7	52.0	54.0
3	100.0	6 00	14 00	28.0	42.2	80.0	49.2
4	119.0	7 50	21 50	26.0	33.1	106.0	43.8
5	160.0	9 30	30 20	28.0	30.2	134.0	40.0
6	218.0	11 50	42 10	42.2	29.0	176.0	36.7
7	82.0	3 03	43 13	7.8	14.3	184.0	34.6

The third series of experiments was concerned with a study of the effect of the degree of saturation of the solution with carbon dioxide on the process efficiency. A saturated solution of sodium bicarbonate containing 157 g of sodium formate per liter (106 g/liter calculated as formic acid) was taken. The experimental conditions were chosen so that the results could be regarded as average in relation to the data in Table 1.

The results of the third series are presented in Table 2; it follows from these results that when the carbon dioxide is passed at a low rate through the cell, the amalgam is decomposed, but very little formic acid is formed. As the feed rate of carbon dioxide through the cell increases, the decomposition rate of the amalgam and the yield of formic acid both rise, approaching the limiting values which correspond to solutions saturated with respect to carbon dioxide.

TABLE 2

Results of Third Series of Experiments

CO_2 feed rate (l/hr)	Amount of amalgam (ml)	Decomposition time	Initial HCOOH conc. in saturated $NaHCO_3$ solution, g/liter	Final HCOOH conc. in saturated $NaHCO_3$ solution, (g/liter)	Gain of HCOOH (g per liter)	HCOOH yield (%)	Notes
0.5	64.5	4hr 28min	106.00	106.50	0.50	1.17	Solution remains clear to end of experiment
1.5	64.5	3 53	106.00	119.40	13.40	31.30	$NaHCO_3$ precipitated during experiment
3.0	64.5	2 13	106.00	120.75	14.75	34.50	$NaHCO_3$ precipitated during experiment
6.0	64.5	2 08	106.00	123.50	17.50	40.90	$NaHCO_3$ precipitated during experiment

•The precipitated $NaHCO_3$ was filtered off at intervals (5 times) and the filtrate, made up to its initial volume (50 ml) was returned to the cell each time.

After the experiments had been repeated many times, about 120 ml of sodium formate solution (in saturated sodium bicarbonate solution) was obtained; free formic acid was isolated from it by the usual method. The sodium formate solution was first evaporated down, sulfuric acid was added in some excess, the precipitated sodium sulfate was filtered off, and formic acid was obtained from the filtrate by distillation. 40 ml of solution containing 254 g of formic acid per liter was obtained.

DISCUSSION OF THE PRACTICAL APPLICABILITY OF THE RESULTS

Calculations show that, with a 34.6% yield of formic acid, the formation of 1 kg of sodium formate is accompanied by the formation of 5.82 kg of sodium bicarbonate. With a 40% yield the formation of 1 kg of sodium formate is accompanied by the formation of 4.88 kg of sodium bicarbonate. In the first case (Table 1) the decomposition rate of the amalgam, in current units, is 245 amps/m^2, and the formation rate of formic acid is 85 amps/m^2. In the second case the respective rates are 230 amps/m^2 and 92 amps/m^2.

Table 3 shows that the rates of amalgam decomposition and formic acid formation greatly depend on the degree of saturation of the solution with carbon dioxide. Table 3 is based on the data in Table 2.

TABLE 3

Decomposition Rate of Amalgam

Bubbling rate of CO_2 through cell (liters/hour)	Yield of HCOOH (%)	Decomposition rate of amalgam (amp/m^2)	Formation rate of HCOOH (amp/m^2)
0.5	1.17	200	2.34
1.5	31.30	230	72.00
3.0	34.50	406	140.00
6.0	40.90	416	170.00

A deficiency of dissolved carbon dioxide in a solution cannot be allowed to exist during the synthesis, as otherwise the hydrogenation process is partially or completely replaced by carbonation, with formation of Na_2CO_3.

In the production of concentrated sodium formate solutions a sufficiently high rate of amalgam decomposition is attained and economically acceptable yields of the reduction product are obtained if the following conditions are maintained: 1) good surface contact between the amalgam and the solution in which the amalgam is decomposed; 2) fairly high solubility of carbon dioxide in the solution; 3) intermittent or continuous filtration of the precipitated sodium bicarbonate.

The necessary surface contact can be ensured by vigorous stirring, accompanied by spraying of the amalgam in the solution. The problem can be successfully solved by the use of the design features of the stirring device used in the present investigation.

Adequate solubility of carbon dioxide can be ensured by means of an efficient bubbling device or, more simply, by the creation of carbon dioxide pressure over the solution in addition to ordinary agitation of the solution. Literature data [6] indicate that the effectiveness of the reduction process should increase at higher pressures, i.e., higher decomposition rates of the amalgam should be attained, with increased yields of formic acid.

The need for intermittent or continuous removal of sodium bicarbonate is dictated by a single requirement — the solution must not be allowed to thicken in the reaction space.

Calculations based on the results of this investigation enable preliminary estimates to be made with regard to the possible industrial adoption of the electrochemical process for the production of sodium formate (together with sodium bicarbonate).

If, under the conditions of chlorine production, the decomposition of sodium amalgam is combined with synthesis of formic acid from carbon dioxide, then (with 34.6% yield) 0.298 ton of HCOONa and 1.735 tons of $NaHCO_3$ can be obtained instead of 1 ton of NaOH normally produced. If the prices of NaOH, HCOONa, and $NaHCO_3$ are 925, 2100, and 350 rubles per ton respectively [9], the value of the product is increased by about 308 rubles.

Of course, these calculations do not provide a basis for a direct decision concerning the suitability of the industrial adoption of the proposed method for production of sodium formate and bicarbonate, as such a decision can be made only with consideration of all the economic factors which ultimately determine the value of the final product.

It may be advisable to build plants in which carbon dioxide is formed as a by-product in proximity to chlorine plants. In this case utilization of the carbon dioxide may prove to be economically advantageous.

SUMMARY

1. It has been shown in principle, under laboratory conditions, that concentrated solutions of sodium formate can be made by reduction of carbon dioxide by sodium amalgam, at relatively high rates of decomposition of the amalgam.

2. If sodium amalgam is decomposed in solutions through which carbon dioxide is bubbled at atmospheric pressure, it is easy to obtain 272 g of sodium formate per liter, which is equivalent to 184 g of formic acid per liter, with 34.6% yield, and at a decomposition rate of the amalgam of the order of 245 amps/m^2.

3. Preliminary calculations show the economic feasibility of adoption of the electrochemical process for sodium formate production (together with sodium carbonate) at chlorine plants, especially in regions where electric power is cheap.

LITERATURE CITED

[1] N. N. Beketov, J. Russ. Phys.-Chem. Soc. 1, 33 (1869).

[2] E. Royer, Comptes rendus 70, 731 (1870).

[3] A. Lieben, Monatsh., 16, 211 (1895); 8, 582 (1897).

[4] A. Coehn and St. Jahn, Berichte 37, 2836 (1904).

[5] R. Ehrenfeld, Ber., 38, 4138 (1905).

[6] F. Fischer and O. Prziza, Ber., 47, 256 (1914); Zentralblatt 641 (1914).

[7] M. A. Rabinovich and A. P. Mashovets, Ukrain. Chem. J. 6, No. 5-6 (1931).

[8] Berle and Lunge, Chemical and Technical Investigation Methods (State Sci.-Tech. Chem. Lit. Press, 1941) 3, 2 [Russian translation].

[9] Wholesale Prices of Chemical Products and Goods [in Russian] (Goskhimizdat, 1955).

Received April 24, 1957

PROPERTIES OF LOW-SUBSTITUTED CELLULOSE NITRATE ESTERS

G. A. Petropavlovskii and N. I. Nikitin

It was shown in our earlier investigations that cellulose ethers (methylcellulose, carboxymethylcellulose) of very low degrees of substitution are soluble in dilute caustic soda at low temperatures. This property is a consequence of changes in the cellulose structure [1, 2]. As these cellulose ethers are very similar in a number of properties at very low degrees of substitution, it follows that other low-substituted cellulose derivatives should have a number of properties in common.

For confirmation of this hypothesis we studied the properties of cellulose nitrates of very low degrees of substitution. In contrast to methyl- and carboxymethylcellulose, cellulose nitrates are esters, in which the ester bond is less stable and is readily broken down, for example by the action of alkalies.

Whereas in the case of cellulose ethers there are definite limiting degrees of substitution at which these substances become soluble in water or alkalies, in the case of cellulose nitrates such low-substituted products have not been studied as yet.

Preparation of Low-Substituted Cellulose Nitrates

It is known [3, 4] that the nitration of cellulose by the usual mixtures of sulfuric and nitric acid proceeds extremely rapidly.

The nitration rate may be decreased [3] by the use of mixtures containing large amounts of water. Thus, Crane and Joyce [5] prepared low-substituted products by nitration with mixtures containing 57 to 67% H_2SO_4, 16 to 6% HNO_3, and 25 to 27% H_2O. These nitration products were amorphous porous substances containing from 3.5 to 4.5% nitrogen. Nitration resulted in complete gelation of the cellulose to a transparent, soft, pasty mass. If follows that the nitration mixtures of the composition used have a strong hydrolyzing action on cellulose. We therefore carried out a search for nitration mixtures which would, under appropriate nitration conditions, result in low degrees of esterification without excessive hydrolysis of the cellulose.

The compositions of the nitration mixtures used and the degrees of esterification of the products obtained with the use of the these mixtures are given in Table 1.

The products of nitration by mixtures of the compositions given in Table 1 were white fibrous substances which did not differ in appearance from the original cellulose. Their nitrogen contents were determined by the Lunge nitrometer method.

For investigation of the nature of nitration by these mixtures, experiments were performed on the influence of temperature and time on the nitration rate. As was to be expected, temperature and time influence the nitrogen content of the product only until equilibrium is reached in a given acid mixture.

However, at about 40° the nitrogen content of the product decreases, and the yield is also reduced considerably. The low-substituted cellulose nitrate so formed loses its fibrous form and consists of a loose powder composed of small fragments of the original fibers. This indicates that the reaction product is strongly hydrolyzed and oxidized at this temperature.

For characterization of the physical structure of the products, we determined their average degree of polymerization and solubility in dilute caustic soda solutions. The degree of polymerization was determined from the viscosities of acetone solutions of high-substituted nitrates prepared from the low-substituted products.

TABLE 1

Compositions of Nitration Mixtures and Degrees of Esterification of the Products

Reaction time 2 hours, temperature 10°

Nitration mixture comp., %			Yield of product (% of weight taken)	Nitrogen content (%)	Degree of substitution γ
H_2SO_4	HNO_3	H_2O			
30	32	38	101.4%	0.40	4.7
31	32	37	—	0.77	9.1
32	32	36	107.0	1.33	16.0
33	32	35	108.0	1.90	23.4
35	32	33	108.0	2.85	36.3

Solubility in 6% NaOH* solution was determined by the method used for other low-substituted cellulose derivatives [1]. The results are presented in Table 2.

It follows from Table 2 that the solubility of low-substituted cellulose nitrates at room temperature is low. The solubility rises with decreased degree of polymerization. In contrast, at low temperatures the solubility is complete, starting from γ of approximately 6. At $\gamma = 16$ it is also 100%, but is halved at $\gamma = 36$. When the degree of esterification is 50 (N = 4%), the solubility at low temperatures is very slight.

This curious fact can be explained as follows. As reported by us earlier, the inital stages of esterification lead to a sharp increase in the swelling power of the fiber, and the result of the additional influence of low temperatures is that the fiber becomes soluble in dilute alkali. This effect was discussed by us previously in relation to low-substituted methyl- and carboxymethylcelluloses. The fact that low-substituted cellulose nitrate, which is an ester, also has this property puts it on a common basis with the above-named cellulose ethers and confirms the views advanced at the beginning of this paper.

TABLE 2

Degree of Polymerization and Solubility of Low-Substituted Cellulose Nitrates in 6% NaOH Solution

Sample No.	Solubility in 6% NaOH solution		Nitrogen content of product (%)	Degree of		Notes
	at 18°	on freezing		substitution γ	polymerization	
1	2.53	100	0.54	6.3	749	Samples No. 1, 3, and 6 prepared at 11.5, 21.5, and 31.5° respectively; samples No. 2, 4, 5, 7, and 8 were all prepared at 11.5°, but with different acid mixtures
2	4.90	100	0.84	10.0	—	
3	6.67	100	0.88	10.7	349	
4	—	100	1.10	13.5	488	
5	7.60	100	1.17	14.0	—	
6	10.71	100	1.32	16.0	219	
7	—	62.9	2.83	36.3	488	
8	—	6.0	3.90	51.6	698	

The fact that above a certain degree of substitution low-substituted cellulose nitrate loses the hydrophilic properties which it originally acquired can be attributed to the introduction of ONO_2 groups, which are highly hydrophobic radicals, in considerable amounts. The same effect is found in the case of methylcellulose, but there it is less pronounced and occurs at higher degrees of substitution.

*Concentration by weight.

The data in Table 2 also show that the degree of polymerization of products soluble in 6% NaOH solution at low temperatures reached 750, i.e., it was quite high.

Since the degree of polymerization of the original cellulose (bleached linters) was 1500, it follows that the nitration mixtures of the composition used had a considerable hydrolyzing effect. The hydrolysis was accelerated appreciably on increase of temperature; for example, at 31.5° the degree of polymerization fell to 200.

It is known [6] that ordinary cellulose nitrates are rapidly saponified when treated with alkaline solutions. It was therefore of interest to study the behavior of low-substituted products in this respect, as rapid saponification of the ester would cause, in addition to rapid degradation in solution, the removal of the groups (ONO_2) which determine the solubility of the low-substituted products. Table 3 contains the results of our experiments on the resistance of low-substituted nitrates to the action of NaOH solutions of various concentrations.

TABLE 3

Action of NaOH Solutions of Different Concentrations on Low-Substituted Cellulose Nitrates

NaOH concentration (wt. %)	Nitrogen content of product (%)		Nitrogen loss (% of initial)	Solubility at 18° (%)
	before treatment	after treatment		
4.3	0.10	0.12	—	0.0
	0.84	0.72	14.3	3.0
	1.17	0.90	23.0	5.0
6.6	0.10	0.12	—	0.0
	0.84	0.79	5.9	4.9
	1.17	1.01	13.6	7.6
12.0	0.10	0.08	20	5.4
	0.84	0.36	56.5	38.7
	1.17	0.52	55.5	43.2
18.5	0.10	0.02	80.0	12.3
	0.84	0.24	75.0	39.9
	1.17	0.49	58.1	45.8
35.0	0.10	0.00	100.0	23.6
	0.84	0.00	100.0	48.3
	1.17	0.00	100.0	50.4

In these experiments samples of about 1 g of low-substituted cellulose nitrate were treated for 24 hours at room temperature (between 18 and 20°) with 100 ml of NaOH solutions of known concentrations. At the end of this time the fibrous residue was transferred to a No. 1 glass filter, and washed with 50 ml of NaOH solution of the same concentration and then with distilled water to a neutral reaction. The weight of the bone-dry residue was determined and its nitrogen content was found by the Lunge method.

The data in Table 3 lead to the following conclusions:

1) Low-substituted cellulose nitrates dissolve only slightly when treated with weak solutions of NaOH at 18 to 20° for considerable periods. The nitrogen content of the residue d ecreases somewhat. Although this may be the result of partial fractionation of the original substance, it is quite clear that weak NaOH solutions have little saponifying action on it.

2) Increase of the alkali concentration results in progressive increases of solubility and nitrogen loss from the residue. The latter fact indicates that increase of solubility with the NaOH concentration up to 35% is the consequence of denitration, accompanied by oxidation and degradation. The degree of denitration increases with the NaOH concentration. When the NaOH concentration reaches 35%, low-substituted cellulose nitrates are broken down completely by the alkali, losing up to 50% in weight. Increase of temperature has an

effect analogous of increase of alkali concentration. For example, the results obtained at 98° are presented in Table 4.

It is also interesting to note that the dissolved cellulose nitrate is likewise decomposed at a low rate by alkali at room temperatures. Preliminary experiments showed that the denitration of cellulose in 4% NaOH solution in homogeneous conditions at 18° took the following course.

Nitrogen content of cellulose nitrate

Initial	After 24 hours	After 48 hours
1.71	1.48	1.21

It must be emphasized in conclusion that denitration of low-substituted cellulose nitrate by dilute NaOH solutions is slow either in homogeneous or in heterogenous conditions. Accordingly, it is possible both to prepare and to store solutions of low-substituted cellulose nitrate in 4-6% NaOH solutions at low-temperatures.

TABLE 4

Action of Dilute Alkali on Low-Substituted Cellulose Nitrate at High Temperatures

NaOH concentration (%)	Initial nitrogen content (%)	Solubility (%)	Nitrogen content of residues (%)
4.3	0.84	42.7	0.0
6.6	0.84	43.0	0.0

Our subsequent experiments were concerned with a study of the chemical structure of these low-substituted cellulose nitrates; in particular, with determinations of functional groups and studies of the distribution of primary and secondary hydroxyls substituted by ONO_2 radicals. The functional groups determined were carboxyl and aldehyde groups.

Carboxyl groups at the sixth carbon atoms were determined by the known calcium acetate method [7], which is not described here. The results of these determinations are presented in Table 5.

Table 5 shows that the carboxyl group contents of low-substituted cellulose nitrates are almost the same as the carboxyl group content of the original linters.

Aldehyde groups were determined by the iodine-number method, first proposed by Willstatter and Schudel, and subsequently modified by various workers [8].

TABLE 5

Carboxyl Group Contents of Low-Substituted Cellulose Nitrates

Sample No.	Nitrogen content of product (%)	Degree of substitution γ	COOH group content (%)
1 (linters)	——	——	0.04
2* 2*	0.77	9.1	0.05
3 3	1.30	16.0	0.04
4 4	1.90	23.4	0.08
5 5	2.40	30	0.04

TABLE 6

Iodine Numbers of Low-Substituted Cellulose Nitrate

Sample No.	Nitrogen content (%)	Degree of substitution γ	Iodine number
1 (linters)	——	——	0.50
2**	0.77	9.1	0.65
3	1.90	23.4	0.52
4	1.30	16.0	0.61
5	2.40	30.0	0.89
6	0.54	6.3	0.56
7	1.32	16.0	0.69

*Samples 2-5 obtained by nitration with mixtures of the following composition (%): H_2SO_4—31—35, HNO_3—32, H_2O—33—37, at 10°.

**Samples 2-7 obtained by nitration with mixtures of the following composition (%): H_2SO_4 — 31—35, HNO_3—32, H_2O — 33—37.

The iodine numbers of the low-substituted cellulose nitrates were determined by oxidation with iodine in 0.05 molar $Na_2B_2O_7 \cdot 10H_2O$ at 20° and pH = 9.2.

The results of these experiments are presented in Table 6.

It follows from Table 6 that the iodine numbers of low-substituted cellulose nitrates differ little from that of linters; this indicates that the nitrates were either unoxidized or oxidized very little.

The chemical heterogeneity of low-substituted cellulose nitrates was studied by the method first proposed by Irvine and Rutherford [9], and used for cellulose nitrate by Murray and Purves [10].

This method is based on the following principle: when cellulose nitrate is heated at 115-120° with a solution of anhydrous sodium iodide in acetone or some other ketone, the nitrate groups at the sixth carbon atom react with the iodine and are completely replaced by it. Nitrate groups at the secondary hydroxyls do not react with iodine. This makes it possible to estimate the chemical heterogeneity of cellulose nitrate in its glucose residues.

Our cellulose iodonitrates were fibrous substances, the color of which was almost white, or brown, according to the iodine content. The yields of iodonitrates from the original cellulose nitrates were about 100% of the theoretical. This shows that low-substituted cellulose nitrate does not undergo appreciable decomposition when iodinated under these conditions.

The nitrogen and iodine contents of the cellulose iodonitrates were determined. According to Murray and Purves [10] nitrogen determinations by the Lunge nitrometer method give high results; therefore, we used the Devarda method [11], which is not described here. The results of nitrogen determinations in the orginal cellulose nitrates by the Devarda method were compared with the nitrometer results.

The results of nitrogen determinations in cellulose iodonitrates by the Devarda method were satisfactorily consistent. The iodine contents of cellulose iodonitrates were determined by the method of Baubigny and Chavanne [12], which also gave consistent results. The results of iodine and nitrogen determinations in cellulose iodonitrates are given in Table 7.

TABLE 7

Relative Proportions of Primary and Secondary Nitro Groups in Low-Substituted Cellulose Nitrates.

Orig. cellulose nitrate		Cellulose iodonitrate				Molar % of ONO_2 in orig. cellulose nitrate		
nitrogen content (%)	No. of ONO_2 groups per glucose residue	iodine content (%)	iodine atoms per glucose residue	nitrogen content (%)	No. of ONO_2 groups per glucose residue	replaced by iodine	remaining	lost
0.36	0.0421	2.61	0.034	0.067	0.0078	80	18.5	1.5
0.84	0.0999	6.02	0.0827	0.095	0.0116	82.7	11.6	5.7
1.32	0.1595	7.58	0.1059	0.154	0.019	66.4	11.9	21.7
2.40	0.3009	14.20	0.2123	0.275	0.0367	70.5	12.1	17.4
4.30	0.5774	21.90	0.3603	0.660	0.0969	62.4	16.7	20.9

This table also contains calculations, performed by the method of Murray and Purves [10], showing the amounts of ONO_2 groups replaced by iodine and remaining in the product (the ratio of these represents the distribution of nitrate groups substituting primary and secondary hydroxyls).

The data in Table 7 show that more then 2/3 of the nitrate groups in the original low-substituted cellulose nitrates were replaced by iodine. The proportion of nitrate groups replaced by iodine decreases with increasing degree of substitution of the original cellulose nitrate, in the range studied. This indicates that in lower nitrates the primary hydroxyls are evidently more reactive. On further increase of the degree of esterification the secondary hydroxyls become more reactive, and the difference between the number of secondary and primary substituted hydroxyl groups decreases.

In a study of products containing from 2.5 to 9% nitrogen, Murray and Purves showed that in this range about half the nitrate groups replace hydroxyls in the 6 position. Our data, which largely relate to products of lower degree of substitution and which differ somewhat from the results of Murray and Purves, approach the latter results in the region studied by these authors.

Different acid mixtures were used for the preparation of our low-substituted esters; this suggests that the reactivity of the primary and secondary hydroxyl groups depended on the composition of the nitration mixtures.

Our studies of the chemical structure of low-substituted cellulose nitrates and their resistance to the action of dilute caustic soda solutions showed that the solubility of these substances at low temperatures can be utilized for the production of viscous concentrated alkaline solutions, suitable for further use.

We prepared solutions of low-substituted cellulose nitrate, at concentrations of up to 8%, in 6% NaOH solution. Cellulose nitrates of moderately low degrees of polymerization (200-300) dissolve in alkali without the need for freezing, but also at low temperatures. Concentrated solutions of low-substituted cellulose nitrates were used for preparation of films. The films were made by a method used previously for the preparation of films of other low-substituted cellulose derivatives [2]. Only the properties of films with the same nitrogen contents as the original fibers are described in this paper.

TABLE 8

Mechanical Strength of Unplasticized Films (film thickness 0.03 mm)

Nitrogen content of film (%)	Solution concentration (%)	Tensile strength (mg/mm^2)	Elongation at break (%)	Degree of polymerization (DP)	Moisture content of film (%)
0.60	4.0	9.20	9.6	749	11.7
1.20	4.0	9.40	4.8	349	11.5
1.29	8.0	8.38	2.6	219	11.4
0.25	4.0	7.53	4.2	—	11.2

Water was the precipitant mainly used for production of the films. Table 8 contains data on the mechanical strength of unplasticized films of low nitrogen contents.

TABLE 9

Hygroscopicity and Water Absorption of Films of Low-Nitrogen Content

Hygroscopicity (%)	Water absorption (%)	Nitrogen content (%)
18.2	99.0	0.36
18.1	100.0	0.54
18.1	96.0	0.88
16.7	100.5	1.32

The data in Table 8 show that the tensile strength of the films is considerable. It varies little with the degree of polymerization in the range in question. The elasticity (as indicated by elongation at rupture) is a function of degree of polymerization, increasing with the latter.

Table 9 contains data on hygroscopicity at 80% relative humidity and on water absorption during 48 hours in water. It follows from Table 9 that with regard to hygroscopocity and water absorption the films were similar to ordinary regenerated cellulose films of the Cellophane type.

SUMMARY

1. A study was made of the nitration of cellulose by mixtures of sulfuric and nitric acids for the production of nitrates having degree of substitution γ 5-20. Such products can be made by nitration with mixtures containing: H_2SO_4 31—38%, HNO_3 32%, H_2O 37—32% at temperatures up to 30°, and with different reaction times.

2. Low-substituted cellulose nitrates are white fibrous substances, similar to the original cellulose but partially hydrolyzed. Their degree of polymerization ranges from 300 to 750.

3. Cellulose nitrates having degree of substitution γ 5-20 are completely soluble at low temperatures in dilute caustic soda, giving viscous colorless solutions.

4. Low-substituted cellulose nitrates undergo little saponification when treated with dilute NaOH solutions at temperatures from 18 to 20°.

5. Concentrated NaOH solutions decompose low-substituted cellulose nitrate completely at room temperature.

6. These cellulose nitrates are not oxidized products, as their carboxyl and aldehyde group contents do not differ greatly from the contents of these groups in the original cellulose.

7. Iodination of low-substituted cellulose nitrates showed that they are chemically heterogeneous, as more than 2/3 of their nitrate groups replaced primary hydroxyls.

8. Viscous concentrated solutions of low-substituted cellulose nitrates were used for film preparation. These films, of low nitrogen content, have considerable mechanical strength, greater than that of ordinary Cellophane. The hygroscopicity and water absorption of the films are similar to the corresponding properties of films of regenerated cellulose of the Cellophane type.

LITERATURE CITED

[1] N. I. Nikitin and G. A. Petropavlovskii, J. Appl. Chem. 29, 1540 (1956).*

[2] G. A. Petropavlovskii and G. A. Nikitin, J. Appl. Chem. 29, 1707 (1956).*

[3] A. P. Zakoshchikov, Nitrocellulose [in Russian] (1950), p. 314.

[4] E. Ott, Cellulose and Cellulose Derivatives (1943) p. 630.

[5] S. N. Ushakov, Cellulose Esters and Plastics [in Russian] (1941), p. 121.

[6] Z. A. Rogovin, Nitrocellulose Silk [in Russian] (1934), p. 192.

[7] Paper Manufacturer's Handbook [in Russian] vol. 1 (1955), p. 757.

[8] V. I. Sharkov and O. A. Dobush, J. Appl. Chem. 28, 994 (1955).*

[9] J. Irvine and J. Rutherford, J. Am. Chem. Soc. 54, 1491 (1932).

[10] G. Murray and C. Purves. J. Am. Chem. Soc. 62, 3195 (1940).

[11] C. Doreé, Methods of Cellulose Chemistry (1935), p. 209 [Russian translation].

[12] H. Meyer, Analysis and Structure Determination of Organic Substances (1935), p. 141 [Russian translation].

Received July 3, 1958

*Original Russian pagination. See C.B. Translation.

OXIDATION OF DIMETHYLACETYLENYL CARBINOL BY CUPRIC CHLORIDE IN AMMONIA SOLUTION•

A. L. Klebanskii, I. V. Grachev, and O. M. Kuznetsova

This paper contains the result of an investigation of the influence of various factors on the oxidation of dimethylacetylenyl carbinol by cupric chloride in ammonia solution, carried out in order to confirm the views advanced earlier on the mechanism of this reaction [1].

The results show that oxygen is not essential for the reaction. In presence of cupric salts in ammonia solution, dimethylacetylenyl carbinol is converted into dimethyl-2,7-octadiyne-3,5-diol-2,7 regardless of whether the reaction was conducted in oxygen or nitrogen. The reaction rate is somewhat higher in oxygen than in nitrogen, but the difference is relatively small. However, if the experiments were conducted in an oxygen atmosphere with a deficiency of cupric salt, the amount of dimethylacetylenyl carbinol consumed was greater than in absence of oxygen. The reason for this acceleration is oxidation of the univalent copper formed in the reaction.

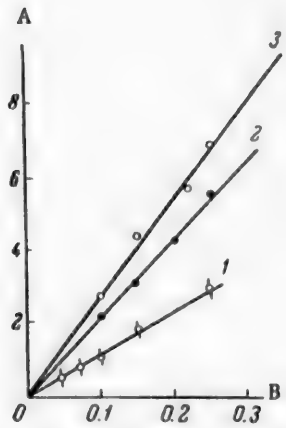

Fig. 1. Effect of cupric chloride concentration on the reaction rate: A) reaction rate v (× 100), B) $CuCl_2$ concentration (moles/liter); initial concentrations of dimethylacetylenyl carbinol (moles/liter): 1) 0.05, 2) 0.10, 3) 0.15.

Fig. 2. Effect of dimethylacetylenyl carbinol concentration on the reaction rate: A) reaction rate v (× 100); B) carbinol concentration (moles/liter); Molar ratio $(CH_3)_2C(OH)C \equiv CH : CuCl_2$: 1) 1 : 1.5, 2) 1 : 1.

As in any complex consecutive reaction, the rate of formation of the final product — dimethyl-2,7-octadiyne-3,5-diol-2,7 — is determined by the rate of the slowest intermediate reaction. According to our

•Communication II in the series on the formation of diacetylene compounds from monosubstituted acetylene derivatives.

data, the over-all reaction rate depends both on the concentration of dimethylacetylenyl carbinol and on the concentration of cupric chloride; this indicates that the reaction is bimolecular (Figs. 1, 2). Therefore, both the original compounds are involved in the stage which determines the reaction rate.

According to our views on the formation mechanism of diacetylene compounds, two intermediate reactions are possible. One consists of the formation of an intermediate unstable copper acetylene derivative, with simultaneous ionization of acetylene, and the other consists of oxidation of this compound by the cupric salt. This process was earlier represented by three consecutive reactions:

$$R{-}C{\equiv}CH \xrightleftharpoons{(Cu^{+}\ \text{or}\ Cu^{++})} R{-}C{\equiv}C{:} + H^{+}, \quad (1)$$

$$R{-}C{\equiv}C{:} + Cu^{++} \rightarrow R{-}C{\equiv}C{\cdot} + Cu^{+}, \quad (2)$$

$$R{-}C{\equiv}C{\cdot} + .C{\equiv}C{-}R \rightarrow R{-}C{\equiv}C{-}C{\equiv}C{-}R. \quad (3)$$

The rate of the over-all process is determined by either the first or the second of these reactions. The third stage must proceed at a very high rate, typical for reactions of that type. It was shown earlier [1] that the determining step is the first stage, i.e., ionization of the acetylene compound under the influence of copper salts. The second stage proceeds at higher rate than the first, and therefore the copper compound formed does not accumulate, but is oxidized to the diacetylene compound immediately after its formation.

In view of the fact that one of the final products of the reaction between cupric chloride and dimethylacetylenyl carbinol is a cuprous salt, it might be expected that it may have some influence on the process because of its greater tendency, as compared with cupric copper, to react with acetylene compounds. However, removal of cuprous copper from the reaction zone by precipitation during the reaction in the form of sparingly soluble salts did not greatly affect the reaction rate. Similarly, additions of cuprous copper had no influence on the oxidation rate of dimethylacetylenyl carbinol under the conditions studied; this is illustrated by the data in Table 1.

TABLE 1

Influence of CuCl on the Oxidation of Dimethylacetylenyl Carbinol by $CuCl_2$

Molar proportions of substance taken					pH of medium	Ions introduced (per molecule of dimethylacetylenyl carbinol)					Amount of dimethylacetylenyl carbinol converted in 60 min. (%) in atmos. of	
									OH^-			
$(CH_3)_2C(OH)C{\equiv}CH$	$CuCl_2$	CuCl	NH_4OH	NH_4Cl		sum: $Cu^{++} + Cu^{+}$	NH_4^+	Cl^-	in nitrogen	in oxygen	nitrogen	oxygen
1	1	0	4	0	9.8	1	4	2	4	4	32.17	36.17
1	1	0	0	4	3.0	1	4	6	0	0	0	0
1	0.9	0.1	3.9	0.1	9.7	1	4	2	3.9	4	28.01	34.75
1	0.5	0.5	3.5	0.5	9.7	1	4	2	3.5	4	18.73	35.42
1	0.5	0	2.0	0	9.8	0.5	2	1	2	2	17.37	
1	0	1	3.0	1.0	9.7	1	4	2	3	4	0	33.27

It should be noted that, in accordance with earlier data [1] on the influence of NH_4^+ and OH^- ions on the process, the amounts of ammonia and ammonium chloride added were varied so that the contents of ammonium and hydroxyl ions in the reaction mixture remained constant; account was taken of the formation of OH ions in the oxidation of cuprous to cupric copper when the process was carried out in oxygen

$$2Cu^{+} + 0.5O_2 + H_2O \rightarrow 2Cu^{++} + 2OH^{-}. \quad (4)$$

TABLE 2

Conversion of Dimethylacetylenyl Carbinol as a Function of the $\frac{CuCl_2}{(CH_3)_2C(OH)C \equiv CH}$ Molar Ratio

Initial molar concentrations: $CuCl_2$ 0.1, NH_3 0.4

Conc. of dimethylacetylenyl carbinol (moles per liter)	Experiments in nitrogen atmosphere							Experiments in oxygen atmosphere							
	0.025	0.05	0.075	0.10	0.15	0.20	0.025	0.05	0.075	0.1	0.15	0.20	0.25		
Molar ratio $\frac{CuCl_2}{(CH_3)_2C(OH)C \equiv CH}$	4.0	2.0	1.33	1.0	0.66	0.5	4.0	2.0	1.33	1.0	0.66	0.5	0.4		
Amount of dimethylacetylenyl carbinol converted (%)	21.75	48.35	57.75	63.31	60	49.51	22.75	48.57	58.27	66.75	74.0	70.71	68.2		
Reaction rate	0.00543	0.02417	0.4331	0.6351	0.090	0.095	—	0.02428	0.04370	0.06675	0.111	0.1414	0.1630		

EXPERIMENTAL

Influence of the molar ratio $\frac{CuCl_2}{(CH_3)_2C(OH)C \equiv CH}$ on the oxidation of dimethylacetylenyl carbinol. The oxidation of dimethylacetylenyl carbinol to dimethyl-2,7-octadiyne-3,5-diol-2,7 was studied in homogeneous conditions, at dimethylacetylenyl carbinol concentrations not higher than 0.4 M, at temperatures not above 40°, and in presence of excess ammonia (4 moles per mole of $CuCl_2$).

The experiments were performed in a flask with a tube reaching down to the bottom for the supply either of pure nitrogen or of oxygen.

Dimethylacetylenyl carbinol was prepared by the method of A. E. Favorskii [2]; b. p. 103-104°, $d_4^{20} = 0.8628$, $n_D^{20} = 1.4209$.

Cupric chloride was used in the hydrate form ($CuCl_2 \cdot 2H_2O$) of analytical-reagent grade, analyzed for its $CuCl_2$ content; ammonia was used in the form of 13% aqueous solution.

After addition of the cuprammonium solution, air was evacuated from the flask and oxygen-free nitrogen was passed throught the solution for 20 minutes. The nitrogen was first passed through a flask containing ammonia solution in order to compensate for loss of ammonia. Dimethylacetylenyl carbinol was added to the cuprammonium solution while nitrogen was passed through. The correct reaction temperature was maintained by means of Hoeppler ultrathermostat.

The oxidation rate of dimethylacetylenyl carbinol was estimated from the amount of the carbinol reacted.

The dimethylacetylenyl carbinol content was determined by titration of the nitric acid, liberated in the reaction between silver nitrate and the carbinol, by 0.1 N KOH solution [3].

The reaction rate is expressed in terms of the amount (in moles/liter) of dimethylacetylenyl carbinol converted in 120 minutes.

The results of the experiments are presented in Table 2.

For determination of the balance for the reaction

(more)

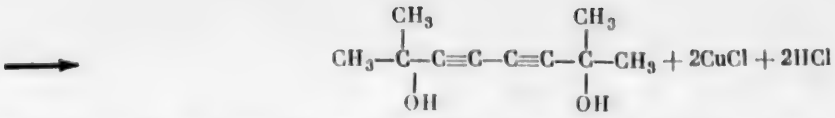

(5)

the cuprammonium solutions of dimethylacetylenyl carbinol were analyzed for the inital components and reaction products. The amount of dimethyl-2,7-octadiyne-3,5-diol-2,7 was determined by extraction of the glycol from the reaction mass by means of ether. The amount of hydrochloric acid formed according to Equation (5) was found by potentiometric titration (with a glass electrode), by 0.1 N hydrochloric acid, of the cuprammonium solution before and after addition of dimethylacetylenyl carbinol (Table 3).

TABLE 3

Determination of Starting Materials and Reaction Products in the Oxidation of Dimethylacetylenyl Carbinol (Initial concentrations (moles/liter): $CuCl_2$ 0.1490, NH_3 0.6, $(CH_3)_2C(OH)C{\equiv}CH$ 0.1495; reaction temperature 30°, volume of reaction mixture 250 ml

Reaction time (min)	Amounts converted (wt. %)		Found (% of theoretical)	
	$CuCl_2$	$(CH_3)_2C(OH)C{\equiv}CH$	glycol	CuCl
10	7.11	6.87		
30	15.45	16.99	14.66	17.11
60	29.80	30.75	26.66	31.07
120	45.87	46.17	44.00	46.19

The results of potentiometric titrations of the reaction mixture are given in Table 4.

These data indicate that the amounts of reaction products correspond to the amounts of dimethylacetylenyl carbinol and cupric chloride converted, for any degree of conversion.

Effect of the concentrations of dimethylacetylenyl carbinol and cuprous chloride on the reaction rate. The experimental conditions were: reaction temperature 30 ± 0.1°, duration of experiment 60 ± 0.5 minutes, nitrogen atmosphere; the molar proportions of the starting materials $(CH_3)_2C(OH)-CH$: $CuCl_2$: NH_3 were 1) 1:1:4, 2) 1:1.5:6; the volume of the reaction mixture was 250 ml, pH = 9.8. The reaction rate was expressed as moles/liter of dimethylacetylenyl carbinol converted in 60 minutes.

TABLE 4

Initial concentrations (moles/liter): $CuCl_2$ 0.2, $(CH_3)_2C(OH)C{\equiv}CH$ 0.2, NH_3 0.8; reaction temperature 20°, experiments in air

Reaction time (min)	Amount of $(CH_3)_2C(OH)C{\equiv}CH$ converted (wt. %)	HCl found (% of theoretical)
60	21.73	20.02
90	36.57	35.31
180	46.23	44.91

It was previously found that the reaction rate for dimethylacetylenyl carbinol concentrations of about 0.15 mole/liter is constant within the limits of experimental error, regardless of whether the mixture was stirred or not. The effects of the concentrations of dimethylacetylenyl carbinol and cupric chloride on the reaction rate are shown in Figs. 1 and 2.

Effect of degree of conversion on the reaction rate. The initial concentrations (in moles/liter) were: $(CH_3)_2C(OH)C{\equiv}OH$ 0.1426, $CuCl_2$ 0.1430, the reaction temperature was 30 ± 0.1°, and the experiments were performed in a nitrogen atmosphere.

The experimental results are plotted in Fig. 3.

Effect of temperature on the reaction rate. The experiments were performed at 40, 35, 30, and 25°. The temperature was kept constant by means of a Hoeppler ultrathermostat; the temperature fluctuations were ±0.05°. The experiments were carried out in a nitrogen atmosphere, with the components in stoichiometric

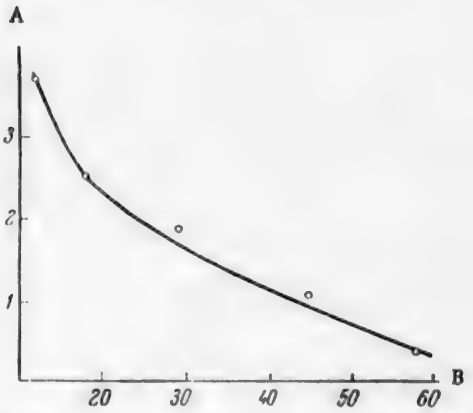

Fig. 3. Effect of the degree of conversion of dimethylacetylenyl carbinol on the reaction rate: A) reaction rate v (×100), B) degree of conversion of dimethylacetylenyl carbinol (%).

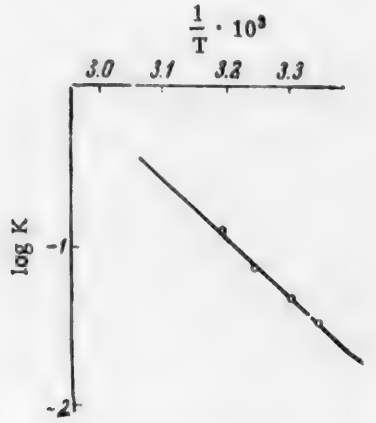

Fig. 4. Variation of log K with $\frac{1}{T}$.

proportions. The initial concentrations of dimethylacetylenyl carbinol and cupric chloride were 0.1426 and 0.1430 mole/liter, respectively. The duration of each experiment was 60 minutes.

The rate constants were calculated from the usual equation for bimolecular reactions.

The reaction rate—temperature relationship is plotted in Fig. 4. The activation energy calculated from these data is 18,423 cal/mole.

The Arrhenius equation for this reaction takes the form

$$\log k = 11.95 - \frac{4027}{T}.$$

Effect of cuprous chloride on the oxidation of dimethylacetylenyl carbinol by means of cupric chloride. The experiments were performed as described above, at 30°, both in nitrogen and in oxygen. Various amounts of cuprous chloride, prepared and purified by the method described in the literature [4], were added to the cuprammonium solution. Cupric chloride was replaced by cuprous chloride in such a way as to retain the stoichiometric ratio of the starting materials (dimethylacetylenyl carbinol and copper salt). Accordingly, ammonium chloride was added to the reaction mixture (before addition of the carbinol) in order to provide constant contents of NH_4^+ and Cl^- ions. The course of the reaction was followed by analysis of the reaction mixture for dimethylacetylenyl carbinol. Variations of the pH of the mixture were also followed by means of the glass electrode (Table 1).

To remove cuprous ions formed during oxidation of dimethylacetylenyl carbinol, potassium iodide was added to the cuprammonium solution in the ratio of 2 moles per mole of $CuCl_2$. A white precipitate of cuprous iodide formed 20 minutes after the start of the experiment. Analysis of the reaction mixture for dimethylacetylenyl carbinol showed that 40.37% of the carbinol reacted in 60 minutes (33.75% reacted in absence of KI).

Experiments on the oxidation of dimethylacetylenyl carbinol by other oxidizing agents. The oxidizing agents tried were stannic chloride, ferric chloride, potassium ferricyanide, sodium hypochlorite, mercuric bromide, and mercuric sulfate. The experiments were performed with the starting materials in stoichiometric proportions, in alkaline (7-10%) solutions with stirring, at 60 and 90°. The diacetylene glycol was not obtained from dimethylacetylenyl carbinol with the aid of these oxidizing agents. In a number of cases the reaction proceeded in a different direction, and products of a different character were formed; their structure was not investigated.

SUMMARY

1. Dimethylacetylenyl carbinol is oxidized by cupric chloride in ammonia solution to give dimethyl-2,7-octadiyne-3,5-diol-2,7 according to the equation

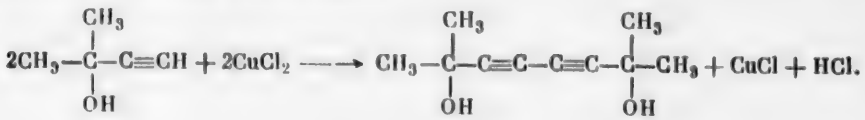

2. Kinetic studies of the oxidation of dimethylacetylenyl carbinol by cupric chloride in ammonia solution showed that oxidation of dimethylacetylenyl carbinol to the diacetylene glycol is a reaction of the second order, the rate constant of which is given by the equation

$$\log k = 11.95 - \frac{40.28}{T}$$

up to 50% oxidation in the 25-40° temperature range.

3. Addition of cuprous copper to the reaction mixture has no appreciable effect (in a nitrogen medium) on the rate of reaction between dimethylacetylenyl carbinol and cupric chloride.

4. If other oxidizing agents are used instead of cupric chloride for this reaction, the diacetylene compound is not formed.

LITERATURE CITED

[1] A. L. Klebanskii, L. V. Grachev, and O. M. Kuznetsova, J. Gen. Chem. 27, 2977 (1957).*

[2] A. E. Favorskii, Author's Certif. 31017 (1933).

[3] A. A. Korotkov and T. A. Parfenova, Trans. All-Union Sci. Res. Inst. Synthetic Rubber 3, 69 (1951).

[4] Iu. V. Kariakin, Pure Chemical Reagents [in Russian] (Goskhimizdat, 1947) p. 343.

Received April 11, 1957

*Original Russian pagination. See C.B. Translation.

DEMETHYLATION OF METHYLPHENOLS

D. Tishchenko and S. Sheina

The S. M. Kirov Academy of Wood Technology

There are at present no technically acceptable methods for conversion of methylphenols, and in particular cresols, into phenol. It is generally known that the phenols obtained by semicoking of coal consist mainly of homologs of phenol, whereas phenols from the coke-over process contain more ordinary phenol. It follows that pyrolysis of the homologs yields ordinary phenol. This hypothesis was tested experimentally by Jones and Neuworth [1], but they did not provide a solution of the problem of industrial conversion of phenol homologs into phenol. During the same period we studied the controlled thermal decomposition of individual cresols and certain xylenols.* Our results augment the data of the above-named authors but we do not consider them to be valuable from the technological standpoint. Only o- and p-cresol were decomposed, as m-cresol is a technically valuable substance, and also 2,4- and 2,6-xylenols. The gases were collected in a gas holder, and the condensate was distilled through a column of 10-12 theoretical plates and separated on heating into benzene–toluene, phenolic, and tail fractions. Naphthalene and anthracene were found in the last of these. The phenolic fraction was anlayzed as a binary mixture by the bromometric method, the amounts of bromine equivalent to phenol and the decomposed homolog being known; the method was previously verified for synthetic mixtures of known composition. Experiments showed that appreciable thermal decomposition of o- and p-cresol with formation of phenol commences at 700-720°, but the reaction only reaches an acceptable rate at 780-800°. The optimum conditions are not the same for the two isomers: for a contact time (c. t.) of one second; in the case of o-cresol the highest yield of phenol (51 molar %) on the o-cresol converted (58% of the amount passed) was obtained at 800°; in the case of p-cresol the corresponding values are 62 molar %, 51% of the amount passed, 780°. Decrease of the pyrolysis temperature rapidly lowers the % conversion at constant c.t. in both cases, while increase of temperature lowers the yield. For the above-named xylenols the yield of phenol (c.t. 1 second) at 800° does not exceed 23 molar %, the degree of conversion is over 80%, and the yields of gas, benzene and toluene, and high-boiling residue are double the corresponding yields from the cresols; this indicates that the temperature optimum for the conversion of these xylenols is far below 800°. These two xylenols are almost inseparable from m- and p-cresol by ordinary rectification. Therefore it is impossible to convert the cresol fraction into phenol by pyrolysis with high yields.

The cresol fraction from coke-oven tar contains not less than 40% m-cresol; it is therefore quite suitable for the production of thermosetting phenolic resins and its conversion into phenol is uneconomic because of the shortage of phenolic resins and their derivatives. However, there is still a persistent shortage of phenol. One cause is the shortage of benzene – the raw material for phenol synthesis. In a number of cases pyrolysis of hydrocarbon material yields at least as much toluene as benzene, while there is only a limited demand for toluene. Therefore there are two potential ways of increasing phenol production: 1) conversion of cresol fractions poor in m-cresol into phenol, and 2) synthesis of o- and p-cresol from toluene by the usual methods, with subsequent conversion of the cresols into phenol. Of course, such conversion should give high yields of phenol and should be simple to carry out.

A method is recommended in the patent literature [2] for demethylation of cresols, whereby cresol vapor is passed, mixed with hydrogen, over nickel chromite supported on silica gel, kieselguhr, or pumice at temperatures

*Experiments performed by K. M. Kissel' and L. V. Kromina.

above 420°. A test of this method showed that demethylation proceeds only under the above conditions, both in presence and in absence of catalyst and hydrogen. It was necessary to find some new method for demethylation.

It has long been known that o-cresol and other homologs of phenol may be converted into the corresponding phenolic acids by fusion with large excess of alkali at about 330° [3]. It has been reported more recently that the low yields of salicylic acid (about 30% in the case of o-cresol) can be increased by addition of oxidizing agents to the melt [4]. The mechanism of this reaction has never been explained. It is not known whether the reaction consists of oxidation of the methyl group by oxygen from the air, from the oxidizing agent, or whether it involves some other process.

Some kind of working hypothesis is needed for deliberate control of any variant of this technically unsuitable conversion (which involves the irrecoverable loss of 10 to 15 units of alkali and equivalent amounts of mineral acid with final product weight as unit). It has long been known that higher primary alcohols are converted into salts of the corresponding carboxylic acids, with evolution of hydrogen, when fused with alkali [5]

$$R{-}CH_2OH + 3HOK = H_2O + 2H_2 + R{-}C{\begin{matrix}OK\\OK\\OK\end{matrix}} = 2H_2 + 2KOH + R{-}C{\begin{matrix}O\\OK\end{matrix}}.$$

An analogous conversion may be postulated for the case under consideration:

$$HO{-}C_6H_4{-}C{\begin{matrix}H\\H\\H\end{matrix} + 4\,HONa = NaO{-}C_6H_4{-}C{\begin{matrix}ONa\\ONa\\ONa\end{matrix} + H_2O + 3H_2 =$$

$$= NaO{-}C_6H_4{-}C{\begin{matrix}O\\ONa\end{matrix} + 2NaOH + 3H_2.$$

If these considerations are justified, then the desired conversion of methylphenols into phenol may be effected when a mixture of their vapors with water vapor is blown through alkali (such as soda lime) at temperatures above the temperature at which the corresponding hydroxybenzoic acid decomposes into carbon dioxide and phenol:

$$NaO{-}C_6H_4{-}C{\begin{matrix}O\\ONa\end{matrix} + 2HOH \rightleftarrows 2NaOH + HO{-}C_6H_4{-}COOH,$$

$$HO{-}C_6H_4{-}COOH = C_6H_5OH + CO_2;$$

$$CO_2 + 2NaOH = Na_2CO_3 + H_2O.$$

The very first experiment showed that this conversion may be effected at temperatures 200-250° lower than demethylation by pyrolysis (550-580° instead of 780-800°); o- and p-cresols yielded phenol, carbon dioxide, and hydrogen in quantities roughly corresponding to the above equations. This revealed a new form of conversion of methylphenols — dehydrogenative oxidation to phenol.

Only the results of experiments on the dehydrogenative oxidation of methylphenols in presence of soda lime are reported in this paper.

The process is intermittent if soda lime is used: carbon dioxide combines with caustic soda and as the latter becomes consumed the % conversion of the cresol passed into phenol decreases; when steam is blown through the spent soda lime at 550-600° the activity of the latter is restored, probably by causticization of the carbonate by lime. It is not difficult to recover alkali from the finally-spent mixture ($CaCO_3 + Na_2CO_3$) by the usual procedure (dissolution, causticization, evaporation, and slaking of the quicklime by caustic soda solution). This process of dehydrogenative oxidation therefore involves consumption of heat, steam, and lime.

Experiments on the dehydrogenative oxidation of methylphenols were carried out in a flow system at 1 : 1.5 weight ratio of methylphenols to water, and c. t. 2 seconds. The analysis of the reaction products is

described above. The results of one series of experiments with o-cresol are presented in Table 1.

Determinations of carbon dioxide in the soda lime before after each experiment showed that the amount of carbon dioxide is very close to the amount calculated from the above equation (89-101%).

Experiments with p-cresol were performed under the same conditions, but the c.t. varied somewhat (Table 2).

As before, all the carbon dioxide formed in the conversion was found in the soda lime. Not less than 85% of the calculated amount of hydrogen was obtained in every experiment; therefore the suggested reaction mechanism is consistent with the facts.

These results show that under the same conditions o- and p-cresol undergo approximately 40% conversion into phenol per pass over soda lime, in yeilds of 70, 82, and 86% of the theoretical. In both cases crystalline phenol was isolated by rectification from the reaction products in yields corresponding to the analytical data.

TABLE 1

Dehydrogenative Oxidation of o-Cresol to Phenol

Expt. No.	Weight of o-cresol (g)	Temperature (°C)	Phenol yield (% of theoretical)	Conversion of o-cresol (% of weight taken)	Analysis of gas (%)		
					H_2	CO_2	CO
1	23.0	580	83.3	38.2	80	2.0	2.8
2	32.0	600	54.8	42.1	76	2.2	3.0
3	23.7	530	58.2	36.2	79	2.0	2.0
4	23.6	530—550	51.4	46.0	71	2.5	2.0
5	24.0	580	72.4	34.1	78	1.8	2.0
6	27.5	480	86.4	31.0	—	—	—
7	100.0	580	86.9	44.9	—	—	—

TABLE 2

Dehydrogenative Oxidation of p-Cresol to Phenol

Expt. No.	Weight of p-cresol (g)	Temperature (°C)	Contact time (sec)	Phenol yield (% of theoretical)	Conversion of p-cresol (% of weight taken)	H_2 content of gas (%)
1	26.9	580	1.6	67.2	48.3	82
2	20.7	570	1.4	82.1	40.0	73
3	35.9	560	2.1	72.3	39.2	80
4	30.8	570	1.6	69.4	43.0	81

An experiment was performed on the dehydrogenative oxidation of m-cresol (193 g) under the same conditions (at 580°). The exit gas contained 86% hydrogen. Distillation of the reaction products yielded considerable amounts of naphthalene, not found in the previous experiments. Bromometric analysis of phenol—m-cresol mixtures is less accurate than in the previous cases (both phenol and m-cresol react with 3 molecules of bromine per molecule), and in presence of naphthalene this method is inapplicable. Therefore the amount of m-cresol converted was calculated from the weight of carbon dioxide bound by the soda lime, 16.8 g, which corresponds to 41.2 g of m-cresol of 21% of the weight taken. In other experiment only 17% of the m-cresol reacted at 570°. It follows that m-cresol is more resistant than o- and p-cresol both to dehydrogenative oxidation and to pyrolysis [1], as the phenolic hydroxyl, being a substituent of the first type, activates only the o- and p-positions in the ring.

From this information certain conclusions can be drawn concerning the behavior of isomeric xylenols during dehydrogenative oxidation. The main components of the technical xylenol fraction from coal tar are 3,5-dimethylphenol (I), 3,4-dimethylphenol (II), 2,5-dimethylphenol (III), and 2,4-dimethylphenol (IV). In I, II, and III at least one methyl group is in the meta position relative to the hydroxyl, and therefore they should yield mainly m-cresol by dehydrogenative oxidation, while IV should yield a mixture of o- and p-cresols and phenol. Coal-tar xylenols containing up to 40% of I, which has three reactive positions, are suitable for the production of thermosetting phenolic resins, and therefore it is hardly advisable to use them for dehydrogenative oxidation. Shale phenols are almost devoid of I [6], and can be used as a raw material for the production of phenol and m-cresol by the method described.

EXPERIMENTAL

The unit for dehydrogenative oxidation of methylphenols consisted of a steam generator, a steam superheater, a buret with a stopcock for supply of methylphenol into the current of superheated steam, furnace-heated stainless steel tubes filled with soda lime, condenser and receiver for collection of the liquid reaction products, and a gas holder for collection of the gas. The temperature of the superheated steam inside the tubes containing soda lime was measured by means of thermocouples. The soda lime was dried at 200°, sieved to a grain size of 3-4 mm, and analyzed for carbon dioxide by the Lunge method. The heating elements of the steam generator, superheater, and furnace were connected in series with rheostats and ammeters. Methylphenols were melted by additions of small amounts of benzene, and the density of the mixture was determined. Before the start of each experiment the instruments were connected in the circuit, the superheated steam and soda lime were taken to the required temperature, the required amount of steam per minute was produced (this was checked by collection of the condensate in a graduated receiver), the required amount of liquefied methylphenol was fed in (as indicated by the buret readings), the temperatures were finally adjusted, and the experiment was commenced, the condensate being collected in another receiver (branched, with a ground-glass joint) and the gas being passed to the gas holder. The usual methods were used for analysis of the gas for carbon dioxide, carbon monoxide, and hydrogen. The liquid condensate was extracted with ether to separate water, the extract was dried by means of calcined sodium sulfate, the ether was evaporated off, and the extract was fractionated. The phenol fraction was analyzed as described above. In the case of o- and p-cresols there was no residue boiling at a higher temperature than the original methylphenols, but in the case of m-cresol there was such residue. In this case the column became clogged with crystals of naphthalene.

SUMMARY

1. Thermal decomposition of o- and p-cresols yields phenol in yields of about 50 and 60% respectively, calculated on converted cresol, with 58-60% conversion (contact time about 1 second), but the optimum decomposition conditions are different for the two cresols. The stability of m-cresol is considerably higher.

2. A method is proposed for converting methylphenols into phenol; the method consists of dehydrogenative oxidation by steam in presence of alkali, and yields phenol, and carbon dioxide in molar proportions of 1 : 3 : 1. The mechanism of this conversion is discussed; it proceeds at an adequate rate at temperatures 200-250° lower than the pyrolysis of the same methylphenols.

3. It is possible to obtain up to 82-86% of the theoretical yield of phenol from o- and p-cresol, with 35-45% conversion of the methylphenols per pass over the "catalyst" (soda lime), with a contact time of about 2 second.

LITERATURE CITED

[1] Jones and Neuworth, Ind. Eng. Ch. 44, 2872 (1952).

[2] German Patents 408,811 and 420,393.

[3] Kolbe, Lieb. Ann., 115, 201 (1860); Jacobson, Ber., 12, 434 (1879); Graebe, Ber., 39, 796 (1906).

[4] Lock, and Stitz, Ber., 72, 77, (1939).

[5] Dumas and Stas, Lieb. Ann., 36, 210 (1840).

[6] Raudsepp, Trans. Tallinn Polytech. Inst. A, 63, 90 (1955).

Received March 12, 1957

SYNTHESIS OF β-CHLORO ETHERS FROM UNSATURATED HYDROCARBONS BY THE VAPOR-PHASE METHOD

A. K. Seleznev

Organic Chemistry Laboratory, the Groznyi Petroleum Institute

Several methods for the preparation of β-chloro ethers are described in the literature. Gaspari [1] alkylated ethylene chlorhydrin by means of dimethyl and diethyl sulfate in heated sealed tubes, and obtained β-chloroethyl methyl and β-chloroethyl ethers in low yields. Dewael [2] used this method for the synthesis of ethers of isomeric propylene chlorhydrins. To prepare the propyl ether, Dewael treated propylene chlorhydrin with sulfuryl chloride. Karvonen [3] prepared the same β-chloro ethers by the action of phosphorus pentachloride on ethylene glycol monoethers. Likhosherstov and Skliarov [4] prepared β-chloroethyl methyl and β-chloroethers by passing ethylene into a solution of benzenesulfodichloramide in alcohol with vigorous shaking. Skliarov [5] prepared a series of β-chloro ethers from ethylene and propylene by means of benzenesulfodichloramide. The experiments were performed in a rotary autoclave, with the use of liquefied olefins, alcohols, and chloramide. Cooper and Partridge [6] used Bennett's method to prepare β-chloroethyl propyl ether by the action of thionyl chloride on ethylene glycol propyl ether. Palomaa and Kenetti [7] prepared β-chloroethyl butyl ether by the action of phosphorus trichloride on the butyl ether of ethylene chlorhydrin. Chalmers [8] prepared β-chloroethyl butyl ether by the action of thionyl chloride on ethylene glycol butyl ether. Petrov [9] described a method for vapor-phase chloroalkoxylation of olefins. In this method superheated alcohol vapor is mixed with gaseous chlorine and then with gaseous pseudobutylene in a reactor.

Our previous communications [10-12] describe vapor-phase syntheses of ethylene chlorhydrin ethyl ether, and propylene chlorhydrin ethyl and methyl ethers. The chloro ethers were tested as deparaffinization solvents for aviation oil.

The aim of the present investigation was to prepare certain β-chloro ethers by the vapor-phase method from synthetic ethylene and the propane—propylene cracking fraction.

EXPERIMENTAL

The experiments on the synthesis of β-chloro ethers were carried out by the method described previously (diagram of the apparatus is given in [10, 11]). The reactor was a Pyrex glass tube, 3.5 cm in diameter and 120 cm long, with an external heating coil. The reaction tube was filled with marble to neutralize HCl. At a definite temperature (measured by means of a thermometer in the upper part of the reactor) alcohol vapor entered the tube from below from a heated flask, and chlorine was fed in simultaneously from below through another tube from a metal cylinder, the rate being measured by a rheometer. At the same time, the gas (ethylene, or propane—propylene cracking fraction) was supplied from the top of the reactor through a tube reaching down to the middle of the reactor, at a definite rate from a gas container. At the end of the experiments the reaction products were washed with water, dried, and fractionated.

β-Chloroethyl methyl ether.*. Two experiments were performed on the synthesis of β-chloroethyl methyl ether (mixed with the dichloride), in order to determine the effect of the amount of alcohol taken for the reaction on the yield of chloro ether. 300 ml of methyl alcohol was used in the first experiment, and

*V. V. Balashova took part in the experimental work.

200 ml in the second. The temperature in the upper part of the reactor was maintained in the 75-80° range during the experiments.

Experiment 1. 42.1 liters of ethylene and 300 ml of methyl alcohol was used in the experiment; 55.7 liters of chlorine was passed. The experiment was continued for 6 hours. Ethylene was absorbed at an average rate of 7 liters/hour. At the end of the experiment the reaction product was treated with water to wash out the alcohol, dried over calcium chloride, and 77.2 g of it was distilled. The following fractions were obtained: 1) 64-87° 2.54 g, 2) 87-94° 55.73 g (d_4^{20} 1.1092, n_D^{20} 1.4167), 3) 94-101° 6.22 g (n_D^{20} 1.4165) and 4) residue 11.68 g.

Analysis of the 87-94° fraction, by Carius:

0.1146 g substance: 0.1976 g AgCl, chloro ether 0.0974 g (85%).
0.1214 g substance: 0.209 g AgCl, chloro ether 0.1034 g (85.2%).

The contents of chloro ether and dichloride were calculated from the weight of the 87-94° fraction taken for the Carius determination and the weight of silver chloride formed.

$$\underset{(0.1146-y)-x}{ClH_2—CH_2—O—CH_3} — AgCl \qquad \underset{y-(0.1976-x)}{C_2H_4Cl_2} — 2AgCl \ .$$

The analytical data show that the 87-94° fraction consisted of 85% chloro ether and 15% dichloride. The yield of chloro ether was therefore 47.4 g, or 26.7% of the theoretical calculated on the ethylene consumed. The 87-94° fraction is being tested as solvent for deparaffinization of aviation oil.

Experiment 2. 41.7 liters of ethylene and 200 ml of methyl alcohol was used in the experiment; 60.2 liters of chlorine was passed. The experiment was continued for 6 hours. Ethylene was absorbed at an average rate of 7 liters/hour. After treatment, 84.86 g of the reaction product was fractionated. The following fractions were obtained: 1) 64-87° 3.23 g, 2) 87-94° 59.73 g (d_4^{20} 1.1139, n_D^{20} 1.4204), 3) 94-102° (n_D^{20} 1.4167) and 4) residue 13.2 g.

Analysis of the 87-94° fraction, by Carius:

0.1832 g substance: 0.3664 g AgCl, chloro ether 0.1191 g (65%).
0.189 g substance: 0.376 g AgCl, chloro ether 0.1243 g (65.75%).

The analytical data show that the 87-94° fractionconsists of 65.3% chloro ether and 34.7% dichloride. The yield of chloroether was 39 g (22.15% of the theoretical on the ethylene consumed).

Comparison of the results of Experiments 1 and 2 shows that the yield of chloro ether increases with increase of the amount of alcohol used for chloroalkoxylation of ethylene.

The pure ether was isolated from the 87-94° fraction (Experiment 2), consisting of 65.4% chloroether and 34.7% dichloride. The dichloride was separated from the chloro ether by means of sulfuric acid [13].

30 ml of 87% sulfuric acid was added to 52 ml of the 87-94° fraction, cooled by means of ice. The dichloride which separated out in the top layer was removed. The dichloride was removed more completely from the layer containing the chloro ether by means of ligroin (b. p. 50°). The sulfuric acid was diluted with water and cooled, the chloro ether was extracted in ligroin , and the ligroin extract was washed and dried over calcium chloride. After evaporation of the ligroin the residue was treated with caustic soda to remove the dichloride. After the alkali treatment, the ether was washed, dried over calcium chloride, and distilled. The 91-92° fraction (29 g) was isolated; it had the following constants: d_4^{20} 1.0340, n_D^{20} 1.4110, MR_D* 22.46. C_3H_7OCl. Calculated 22.56.

Found %: C 38.18, 38.16; H 7.52, 7.54. C_3H_7OCl. Calculated %: C 38.11, H 7.46.

Analysis of 91-92° fraction, by Carius:

0.123 g substance: 0.1858 g AgCl.

Found %: Cl 37.58. C_3H_7OCl. Calculated %: Cl 37.50.

*Molar refraction.

The 91-92° fraction corresponds to pure β-chloroethyl methyl ether.

Literature data for b. p. of β-chloroethyl methyl ether: 90-91° [1], 89.4° [3], 92-93° (n_D^{20} 1.4110, d_4^{20} 1.0345) [5].

β-Chloroethyl propyl ether. 74 liters of ethylene and 300 ml of n-propyl alcohol (b. p. 95-97°, n_D^{20} 1.3867); was used in the experiment; 98 liters of chlorine was passed. The experiment was continued for 10 hours. Ethylene was absorbed at an average rate of 7.4 liters/hour. The temperature in the upper part of the reactor was maintained in the 100-107° range during the experiment. At the end of the experiment the reaction product was treated with water to wash out the alcohol, dried over calcium chloride, and 237.7 g of it was distilled. The following fractions were obtained: 1) 74-85°-26.7 g, 2) 85-135° 180 g (d_4^{20} 1.138, n_D^{20} 1.4320), 3) 135-140° 8.3 g (n_D^{20} 1.4178) and 4) residue 21.7 g.

Analysis of 85-135° fraction, by Carius:

0.1224 g substance: 0.2658 g AgCl, chloro ether 0.0514 g (42%).
0.1344 g substance: 0.292 g AgCl, chloro ether 0.0572 g (42.6%).

The analytical data show that the 85-135° fraction consisted of 42% chloro ether and 58% dichloride. The yield of chloro ether was 75.6 g, or 18.6% of the theoretical on the ethylene consumed. The ether was isolated in pure form by the method described for β-chloroethyl methyl ether.

After the appropriate treatment the product was distilled through a laboratory fractionating column. The 130-131° fraction (15.3 g) was isolated for analysis; it had the following constants: n_D^{20} 1.164, d_4^{20} 0.965, MR_D 31.9. $C_5H_{11}OCl$. Calculated 31.8.

0.143 g substance: 13.1073 g benzene, Δt 0.46.
0.1302 g substance: 13.7876 g benzene, Δt 0.396.

Found M. W 121.45, 122.32. $C_5H_{11}OCl$. Calculated M. W 122.6.

Found %: C 49.08, 49.05; H 9.09, 9.12. $C_5H_{11}OCl$. Calculated %: C 48.98, H 9.04.

Analysis of the 130-131° fraction, by Carius:

0.1228 g substance: 0.1435 g AgCl.
0.1228 g substance: 0.1435 g AgCl.
0.1436 g substance: 0.1647 g AgCl.

Found %: Cl 28.92, 28.83, $C_5H_{11}OCl$. Calculated %: Cl 28.92.

The 130-131° fraction corresponds to pure β-chloroethyl propyl ether. The ether is a colorless liquid with a pleasant odor.

Literature data for b. p. of β-chloroethyl propyl ether: 129-131° (760 mm), n_D^{20} 1.4163 [6]; 130° (756.3 mm), n_D^{20} 1.41756 [3]; 119-120°, n_D^{20} 1.4260, d_4^{20} 0.9931 [5].

The β-chloro ether mixed with the dichloride is being tested as a solvent for deparaffinization of aviation oil.

β-Chloroethyl isobutyl ether. 49 liters of ethylene and 300 ml of isobutyl alcohol (b.p. 106-108°) was used in the experiment; 62 liters of chlorine was passed. The experiment was continued for 6 hours 50 minutes. Ethylene was absorbed at an average rate of 7 liters/hour. The temperature in the upper part of the reactor was maintained in the 112-115° range during the experiment. At the end of the experiment the reaction product was diluted with water, and the upper layer was washed, dried over Na_2SO_4, and fractionated. The following fractions were obtained: 1) 55-109° 262.7 g, 2) 109-130° 40.8 g, 3) 130-145° 56.2 g (n_D^{20} 1.4148), 4)145-150° 27.3 g (n_D^{20} 1.4173) and 5) residue 17.3 g.

The β-chloroethyl isobutyl ether was isolated in pure form from the 130-145° and 145-150° fractions. Isobutyl alcohol does not distill off completely during fractionation; part of it is mixed with the fractions containing the chloro ether. Likhosherstov [4] separated residual higher alcohols from the distilled β-chloro ethers either by means of concentrated calcium chloride solution with prolonged shaking, or by washing the fractions with large amounts of water. We used sulfuric acid for separation of residual isobutyl alcohol from

the chloro ether. Sulfuric acid forms a compound of the oxonium type with the chloro ether. As is known, sulfuric acid reacts with alcohols to form acid esters which are isolated as salts on neutralization. Aschan [14] prepared sulfates from alcohols (menthol, borneol, etc.) by means of diethyloxonium sulfate. Sulfate esters of alcohols are formed much more easily from oxonium sulfates than by the direct action of sulfuric acid. Evidently, a significant role is played here by the dissociation of sulfuric acid which occurs in the formation of the oxonium compound:

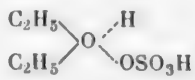

$$+ R \cdot OH \longrightarrow R \cdot O \cdot SO_3H + H_2O + (C_2H_5)_2O.$$

The 130-145° and 145-150° fractions (83 g) were cooled in ice and 30 ml of chemically pure sulfuric acid (sp. gr. 1.84) was added in small portions. After 24 hours the acid ester and excess sulfuric acid were neutralized with concentrated caustic soda solution with cooling, and water was then added to dissolve the salt formed. The chloro ether which separated out was extracted in ligroin (40-50°). The residue after distillation of the ligroin was treated with alkali, with gentle heating, to remove the chlorides present as impurities in the chloro ether. β-Chloro ethers are much more resistant than chlorides to the action of caustic alkali. After the alkali treatment the product was diluted with water to dissolve the precipitate and the chloro ether was extracted in ligroin . The residue after evaporation of the ligroin was distilled through a laboratory fractionating column. The 140.5-141.5° fraction (25.4 g) was isolated for analysis; it had the following characteristics: n_D^{20} 1.4170, d_4^{20} 0.9383, MR_D 36.61. $C_6H_{13}OCl$. Calculated 36.42.

Analysis of the 140.5-141.5° fraction, by Carius:

0.1212 g substance: 0.1268 g AgCl.
0.1226 g substance: 0.1287 g AgCl.

Found %: Cl 25.89, 25.97. $C_6H_{13}OCl$. Calculated %: Cl 25.95.

Elementary analysis

4.555 mg substance: 8.822 mg CO_2, 3.927 mg H_2O.
7.628 mg substance: 14.799 mg CO_2, 6.586 mg H_2O.

Found %: C 52.84, 52.92, H 9.64, 9.66. $C_6H_{13}OCl$. Calculated %: C 52.75; H 9.60.

The 140.5-141.5° fraction corresponds to pure β-chloroethyl isobutyl ether. The ether is a colorless liquid with a pleasant odor; it has not been described in the literature.

β-Chloroethyl butyl ether. 40 liters of ethylene and 300 ml of n-butyl alcohol (n_D^{20} 1.3994) was used in the experiment; 53 liters of chlorine was passed. The experiment was continued for 6 hours. Ethylene was absorbed at an average rate of 6.7 liters/hour. The temperature in the upper part of the reactor was maintained in the 112-118° range during the experiment. At the end of the experiment the reaction product was diluted with water; the upper layer was washed, dried over Na_2SO_4, and distilled. The following fractions were obtained: 1) up to 121°, 2) 121-141° 20.6 g (n_D^{20} 1.4154), 3) 141-152° 27.7 g (n_D^{20} 1.4195), 4) 152-161° 13.8 g (n_D^{20} 1.4217) and 5) residue 18.4 g.

The chloro ether was isolated in the pure state from the 141-152° and 152-161° fractions (41.5 g) by the method described for β-chloroethyl isobutyl ether. After treatment the product was distilled through a laboratory fractionationg column. The 151.2-151.5° fraction (14.5 g) was isolated for analysis; it had the following constants: n_D^{20} 1.4218, d_4^{20} 0.952, MR_D 36.45. $C_6H_{13}OCl$. Calculated 36.42

0.1248 g substance: 12.7011 g benzene, Δt 0.382.

Found: M. W. 136.72. $C_6H_{13}OCl$. Calculated: M. W. 136.63.

Found %: C 52.70, 52.79; H 9.63, 9.67. $C_6H_{13}OCl$. Calculated %: C 52.75, H 9.60.

Analysis of the 151.2-151.5° fraction, by Carius:

0.1418 g substance: 0.1485 g AgCl.
0.1321 g substance: 0.1390 g AgCl.

Found %: Cl 25.91, 26.02. $C_6H_{13}OCl$. Calculated %: Cl 25.95.

The 151.2-151.5° fraction corresponds to pure β-chloroethyl butyl ether. The ether is a colorless liquid with a pleasant odor.

Literature data for b. p. of β-chloroethyl butyl ether: 154.5° (750 mm), d_4^{20} 0.952 [7]; 153-154° (755 mm); n_D^{20} 1.4220 [8]; 139-141°, n_D^{20} 1.42260, d_4^{20} 0.9931 [5].

β-Chloroisopropyl isopropyl ether $CH_3-CH(O-CH(CH_3)_2)-CH_2Cl$. 200 ml of isopropyl alcohol (b. p. 81-82°, n_D^{20} 1.3773), 141 liters of a propane–propylene cracking fraction containing 41 liters (29%) of propylene, and 43 liters of chlorine was used in the experiment. The experiment was continued for 5 hours 50 minutes. The gas (141 liters) was passed three times through the reactor. 33.4 liter (23.6%) of propylene was absorbed. The temperature in the upper part of the reactor was maintained in the 97-112° range during the experiment. At the end of the experiment the reaction production was diluted with water to wash out the alcohol, dried over calcium chloride, and 112.5 g of it was distilled. The following fractions were obtained: 1) 39-97° 3.4 g, 2) 97-123° 88.85 g (d_4^{20} 1.110, n_D^{20} 1.4300), 3) 123-130.5° 5.50 g (d_4^{20} 1.026, n_D^{20} 1.4210), 4) 130.5-135° 7.50 g (d_4^{20} 0.9976, n_D^{20} 1.4162) and 5) residue 6.15 g.

Analysis of the 97-123° fraction, by Carius:

0.113 g substance: 0.216 g AgCl, chloro ether 0.0475 g (42%).
0.1214 g substance: 0.231 g AgCl, chloro ether 0.5176 g (42.6%).

The analytical data show that the 97-123° fraction consisted of 42% chloro ether and 58% dichloride. The yield of chloro ether was therefore 35.54 g, or 17.5% of the theoretically calculated on the absorbed propylene.

The chloro ether was isolated in the pure state from the 97-123° fraction by the method described for β-chloroethyl methyl ether. 20 ml of the 97-123° fraction was used for isolation of the ether. The product was fractionated after treatment. The following fractions were obtained: 1) up to 120° 0.8 g, 2) 120°-124° 2.4 g, 3) 124-125° 2.3 g and 4) residue 0.5 g.

The 124-125° fraction had the following constants: n_D^{20} 1.4120, d_4^{20} 0.9372, MR_D 36.27. $C_6H_{13}OCl$. Calculated 36.41.

Analysis of the 124-125° fraction, by Carius:

0.1342 g substance: 0.1412 g AgCl.

Found %: Cl 26.02. $C_6H_{13}OCl$. Calculated %: Cl 25.95.

Elementary analysis

4.562 mg substance: 8.835 mg CO_2, 3.933 mg H_2O.
7.634 mg substance: 14.810 mg CO_2, 6.591 mg H_2O.

Found %: C 52.85, 52.93; H 9.65, 9.66. $C_6H_{13}OCl$. Calculated %: C 52.75, H 9.59.

The 124-125° fraction corresponds to pure β-chloroisopropyl isopropyl ether. The ether is a colorless liquid with a pleasant odor; it has not been described in the literature.

The β-chloro ether mixed with the dichloride is being tested as a solvent for deparaffinization of aviation oil.

β-Chloroisopropyl butyl ether $CH_3-CH(O-C_4H_9)-CH_2Cl$. 300 ml of n-butyl alcohol (n_D^{20} 1.3994), 111.4 liters of a propane–propylene cracking fraction containing 34.7 liters (31.2%) of propylene, and 40 liters of chlorine was used in the experiment. The experiment was continued for 5 hours 40 minutes. The gas (111.4 liters) was passed through the reactor four times. 28.3 liters (25.4%) of propylene was absorbed. The temperature in the upper part of the reactor was maintained in the 115-120° range during the experiment. At the end

of the experiment the reaction product was treated with water, dried over Na_2SO_4, and distilled. The following fractions were obtained: 1) up to 120°, 2) 121-140° 27.2 g, 3) 140-145° 6.5 g (n_D^{20} 1.4173), 4) 145-155° 16.5 g (n_D^{20} 1.4252), 5) 155-165° 14.5 g (n_D^{20} 1.4237 and 6) residue 27.7 g.

The chloro ether wasisolated in the pure state from the 145-155° and 155-165° fraction (31 g) by the method described for β-chloroethyl isobutyl ether. The product was fractionated through a laboratory column after treatment. This yielded a fraction boiling at 161-162° (12 g) with the following constants: n_D^{20} 1.4225, d_4^{20} 0.933, MR_D 41.07. $C_7H_{15}OCl$. Calculated 41.04.

0.1928 g substance: 14.2932 g benzene, Δt 0.465.
0.1636 g substance: 14.5384 g benzene, Δt 0.390.

Found: M. W. 148.52, 147.73. $C_7H_{15}OCl$. Calculated: 150.65.

Analysis of the 161-162° fraction, by Carius:

0.1384 g substance: 0.1316 g AgCl.
0.1218 g substance: 0.1162 g AgCl.

Found %: Cl 23.53, 23.61. $C_7H_{15}OCl$. Calculated %: Cl 23.53.

Elementary analysis

4.888 mg substance: 10.013 mg CO_2, 4.411 mg H_2O
8.422 mg substance: 17.244 mg CO_2, 7.574 mg H_2O

Found %: C 55.90, 55.87; H 10.10, 10.06. $C_7H_{15}OCl$. Calculated %: C 55.81, H 10.04.

The 161-162° fraction corresponds to pure β-chloroisopropyl butyl ether. The ether is a colorless liquid with a pleasant odor; it has not been described in the literature.

SUMMARY

1. A study has been made of the conditions for the vapor-phase chloroalkoxylation of ethylene and propylene, produced by cracking, with various alcohols; the methyl, propyl, butyl, and isobutyl ethers of ethylene chlorhydrin and the isopropyl and butyl ethers of propylene chlorhydrin were prepared; the last three ethers are not described in the literature.

2. In the chloroalkoxylation of ethylene, the percentage content of the chloro ether in the reaction products (Experiment 1) increases with the amount of alcohol taken.

LITERATURE CITED

[1] DeGaspari, Gazz. 27, II, 293; Beil. vol. 1, 337, (1918).

[2] A. Dewael, Bl. Soc. Chim. Belg. 34 10, 343 (1925); 39, 10, 395 (1930).

[3] A. Karvonen, Zentr., II, 1270 (1912); III, 807 (1919).

[4] M. V. Likhosherstov and V. A. Skliarov, Trans. Voronezh State Univ. 8, 2 (1935).

[5] V. A. Skliarov, J. G. Chem. 9, 23, 2121 (1939). [USSR]

[6] F. C. Cooper and M. W. Partridge, J. Chem. Soc. 459 (1950).

[7] M. H. Palomaa and A. Kenetti, Ber., 64, 4, 797 (1931).

[8] W. Chalmers, Can. J. Research, 7, 464 (1932).

[9] A. A. Petrov, Trans. Voronezh State Univ. 8, 2 (1935).

[10] A. K. Seleznev, J. Appl. Chem. 28, No. 5, 560 (1955).*

[11] A. K. Seleznev, J. Appl. Chem. 27, No. 6, 650 (1954).*

*Original Russian pagination. See C.B. Translation.

[12] A. K. Seleznev, J. Appl. Chem. 29, No. 1, 158 (1956). *

[13] A. K. Seleznev, J. Appl. Chem. 27, No. 3, 327 (1954). *

[14] O. Aschan and A. Schwalbe, Finska Kem. Medd., 40, 133; 41, 98 (1932).

Received April 19, 1957

*Original Russian pagination. See C.B. Translation.

EFFECT OF CAUSTIC SODA AND MANGANESE AND COBALT SALTS ON THE OXIDATION OF ISOPROPYLBENZENE TO THE HYDROPEROXIDE

B. L. Moldavskii and I. L. Belostotskaia

The Leningrad Scientific Research Institute of Petroleum Processing and Production of Synthetic Liquid Fuel

The production of isopropylbenzene hydroperoxide is now an industrial process [1]. The hydroperoxide is prepared by oxidation of isopropylbenzene by atmospheric oxygen. The reaction proceeds by a radical chain mechanism [2], and is highly sensitive to the presence of various impurities in the original isopropylbenzene. The oxidation is usually performed in presence of previously added isopropylbenzene hydroperoxide, introduced to eliminate the induction period, and of catalysts. The catalysts used are manganese or cobalt salts soluble in hydrocarbons, etc.

The literature contains a number of references to the fact that addition of small amounts of alkali to isopropylbenzene accelerates the oxidation, both in emulsion and in a homogeneous medium [2, 3].* The favorable influence of alkali is attributed to the fact that the alkali neutralizes the acids formed during oxidation, which decompose the hydroperoxide. Our experiments have shown that another explanation is possible. Moreover, a series of new observations, not described in the literature, was made in a study of the joint influence of alkali and metal salts on the oxidation.

The apparatus used for the oxidation experiments is shown in the diagram.

The isopropylbenzene to be oxidized was put into a glass reactor 1 with a sealed-in No. 1 Schott glass filter. Air was fed into the reactor from the cylinder 2 through the manostat 3 and the column 4 packed with ascarite. After passing through the layer of isopropylbenzene, the air entered the rheometer 7 through the condenser 5 fitted with a trap 6. The reactor was contained in an oil thermostat 8 containing an electric coil 9 connected to the current supply through a relay. The relay was connected to a contact thermometer 10. The temperature in the thermostat was kept constant to within $\pm$ 0.2° throughout the experiment. The following experimental procedure was used: 30 ml of isopropylbenzene was put into the reactor while air was passed through, and the required amount of hydroperoxide was added from a pipet. In addition, in some cases powdered manganese resinate (manganese abietate) or cobalt stearate, 15% caustic soda solution, or both, were added. The technical product, containing about 70% of isopropylbenzene hydroperoxide, was used. The reactor was inserted into the thermostat heated to the experimental temperature, and the experiment was commenced. The amount of hydroperoxide formed in the reaction products was determined iodometrically in glacial acetic acid solution. The oxidation experiments were performed with two different samples of commercial isopropylbenzene, made by alkylation of benzene with propylene in presence of phosphoric acid catalyst.

Both samples were distilled through a laboratory column with efficiency of about 14 theoretical plates, and the 151-151.5° fraction was collected for the experiments. The fraction was treated three times with cold concentrated sulfuric acid (a total of 10% on the amount of fraction taken) in a separating funnel, washed

*Recently M. S. Nemtsov, L. L. Radchenko, and S. L. Fisher published a paper containing considerable data on the influence of alkali on the oxidation of isopropylbenzene [4].

with water, alkali, and water again, dried, and distilled in the same temperature range. The fraction obtained from isopropylbenzene Sample 1 had $n_D^{20} = 1.4911$ and bromine number 0.4, and the fraction from Sample 2 had $n_D^{20} = 1.4917$ and bromine number 0.6.

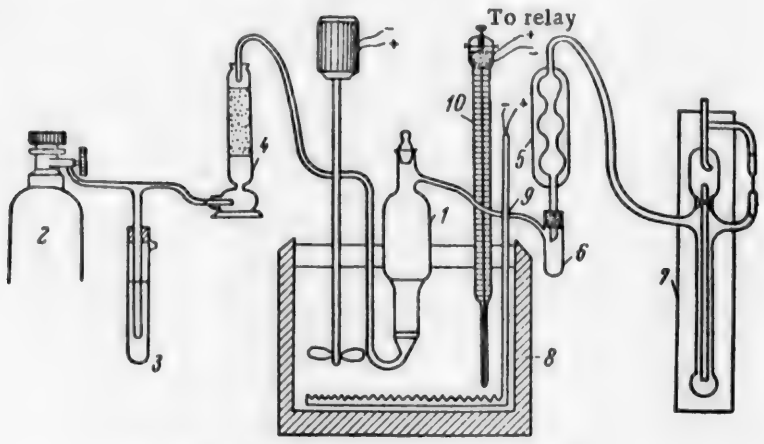

Apparatus for oxidation of isopropylbenzene.

The purpose in the first series of experiments was to determine the course of oxidation of isopropylbenzene in presence of manganese resinate and caustic soda, on addition of substances capable of inhibiting the oxidation process. Phenol and thiophene were used as inhibitors. The inhibiting effect of phenol on oxidation of isopropylbenzene has already been described in the literature [5, 6]. There is no information in the literature on the influence of thiophene on the oxidation of isopropylbenzene; the only reference is to its inhibiting effect on the oxidation of isopropylthiophene [5].

The results of the experiments are presented in Table 1.

TABLE 1

Effects of Phenol and Thiophene on the Oxidation Rate of Isopropylbenzene in Presence of Manganese Resinate and Caustic Soda (2.5% isopropylbenzene hydroperoxide added, temperature of experiment 110°, air rate 6 liter/hour, all additions in the cold)

Expt. No.	Amount (%) added to isopropylbenzene (Sample 1)				Hydroperoxide formed in 6 hours (%)	Decrease of degree of oxidation (%)
	manganese resinate	NaOH	phenol	thiophene		
1	—	—	—	—	9.8	0
2	—	—	0.025	—	8.5	13.3
3	—	—	—	0.2	8.1	17.3
4	0.01	—	—	—	18.6	0
5	0.01	—	0.025	—	13.3	28.5
6	0.01	—	—	0.2	10.0	46.2
7	—	0.1	—	—	28.0	0
8	—	0.1	0.025	—	28.2	0
9	—	0.1	—	0.2	26.7	4.6

It follows from the data in Table 1 that additions of phenol and thiophene decrease of rate of isopropylbenzene oxidation, especially in presence of manganese resinate. This is quite understandable, as catalysts — salts of variable-variable-metals — accelerate oxidation by favoring decomposition of the hydroperoxide with

formation of free radicals which initiate the oxidation reaction, while additives which inhibit oxidation bind the the active radicals, forming either inactive radicals, forming either inactive radicals or stable products, and thus prevent the development of the reaction chains [7]. Addition of 0.1% NaOH to isopropylbenzene protects it against the inhibiting effects of phenol and thiophene. Thus, the explanation of the favorable effect of alkali on the oxidation of isopropylbenzene is that NaOH may prevent the inhibiting action of traces of impurities, both those present in the original isopropylbenzene and those which may be formed as by-products during oxidation, such as phenol formic acid, etc. Further confirmation of this view is provided by the fact that, for example, in presence of manganese resinate the oxidation rate of unpurified isopropylbenzene greatly increases after treatment with sulfuric acid. The amount of hydroperoxide formed in 6 hours increases from 12% for the unpurified sample to 19% for a sample purified by means of sulfuric acid. If sufficient NaOH is taken instead of manganese resinate, preliminary treatment of the isopropylbenzene with sulfuric acid becomes superfluous. Thus, with addition of 0.2% NaOH, 36% hydroperoxide formed in 6 hours in untreated isopropylbenzene, and 34% in isopropylbenzene treated with sulfuric acid under the same conditions.

If our hypothesis on the influence of alkali on impurities which inhibit isopropylbenzene oxidation is correct, then a particularly strong effect should be produced by the simultaneous use of alkali and salts of variable-valence metals in the oxidation. However, positive results were not obtained in preliminary experiments, in which both substances were added to isopropylbenzene in the cold. Subsequent experiments showed that the sequence in which the two components are added has a decisive effect on the oxidation rate. In some of the experiments all the components were added in the cold, i.e., before the reactor was inserted in the oil bath heated to 110°, and in other experiments they were added after the reactor had been inserted in the bath and the temperature had reached 110° (start of the experiment). Finally, in some experiments one component was added to the cold and the other to the heated isopropylbenzene.

The results of these experiments are presented in Table 2.

The following conclusions may be drawn from Table 2; 1) additions of manganese resinate or caustic soda (separately) to cold isopropylbenzene increase the oxidation rate of isopropylbenzene much more than additions of the same reagents at the temperature of the experiment (compare Experiments Nos. 2 and 3, and 4 and 5); 2) addition of both reagents (together) in the cold produces less effect than addition of caustic soda alone (compare Experiments Nos 4 and 6); 3) additions, at the temperature of the experiment, of manganese resinate or cobalt stearate to isopropylbenzene containing caustic soda added in the cold greatly increase the rate of hydroperoxide formation (compare Experiments Nos. 6 and 7, 11 and 12, 17 and 18, 19 and 20); 4) oxidation may also be accelerated by addition of caustic soda to isopropylbenzene at the temperature of the experiment, provided that it is added before the metal salts (compare Experiments Nos. 13 and 14).

These experiments therefore showed that if metal salts and caustic soda are used in conjunction, it is possible to accelerate the oxidation of isopropylbenzene to a considerably greater extent than by addition of either component separately. The components must be introduced in a definite sequence into the reaction mixture to produce this effect.

Not enough experimental data are available at the present time to provide any detailed explanation of this effect. It is only possible to put forward certain hypotheses. Alkali, which opposes the inhibiting influence of impurities capable of reacting with the radicals, should be most effective in its action if introduced into the reaction mixture before free radicals have been formed in it, in appreciable quantity, by the action of variable-valence metals on the hydroperoxide. Therefore the greatest effect of the combined use of caustic soda and metal salts is to be expected if the alkali is introduced before the metal salts. Special experiments showed that the sequence in which alkali and metal salts are added in the cold is of no significance. The effect is observed only if the metal salts are added after the alkali, to heated isopropylbenzene. The probable explanation is that, when hydroperoxide is decomposed by metal salts at low temperatures, the free radicals formed are utilized less fully for the required purpose, as the temperature required for initiation of the oxidation of isopropylbenzene to the hydroperoxide is higher than the temperature required for decomposition of the hydroperoxide by metal salts. Our suggested explanation of the role of alkali in the oxidation of isopropylbenzene is incomplete. The high oxidation rate of isopropylbenzene in presence of alkali alone, higher than the oxidation rate in presence of metal salts alone, suggests that the alkali has other functions. The literature contains no data on the ability of alkali to cause decomposition of hydroperoxides with formation of free radicals, but there are indications that traces of alkali inhibit hydroperoxide decomposition [8]. We observed a similar effect. It is possible that at the

TABLE 2

Effects of Alkali and Metal Salts on the Oxidation Rate of Isopropylbenzene (2.5% isopropylbenzene hydroperoxide added in the cold, temperature of experiment 110°, air rate 6 liters/hour)

Expt. No.	Added to isopropylbenzene (%)						Hydroperoxide formed in 6 hours (%)
	in the cold			heated to 110°			
	manganese resinate	cobalt stearate	NaOH	manganese resinate	cobalt stearate	NaOH	
	Isopropylbenzene (Sample 1) treated with H_2SO_4						
1	—	—	—	—	—	—	3.6
2	0.01	—	—	—	—	—	18.6
3	—	—	—	0.01	—	—	12.1
4	—	—	0.1	—	—	—	28.0
5	—	—	—	—	—	0.1	20.1
6	0.01	—	0.1	—	—	—	24.6
7	—	—	0.1	0.01	—	—	44.2
8	—	—	0.1	0.003	—	—	41.0
9	—	—	—	0.003	—	0.1	21.0 *
10	—	—	0.1	0.003	—	—	31.4 **
	Isopropylbenzene (Sample 2) treated with H_2SO_4						
11	0.01	—	0.1	—	—	—	28.0
12	—	—	0.1	0.01	—	—	45.8
13	—	—	—	0.01	—	0.1	25.6 *
14	—	—	—	0.01	—	0.1	50.2 ***
15	—	0.01	—	—	—	—	8.6
16	—	—	—	—	0.01	—	10.0
17	—	0.01	0.1	—	—	—	20.8
18	—	—	0.1	—	0.01	—	35.2
	Isopropylbenzene (Sample 2) not treated with H_2SO_4						
19	0.01	—	0.1	—	—	—	25.7
20	—	—	0.1	0.01	—	—	34.4

*NaOH added 2 minutes after addition of manganese resinate.

**Manganese resinate added 30 minutes after start of experiment.

***NaOH added 2 minutes before addition of manganese resinate.

early stages, when the solution contains only a small amount of added hydroperoxide, the stabilizing action of alkali protects the hydroperoxide from decomposition, and thus preserves it as a source of free radicals for initiation of the oxidation reaction.

SUMMARY

1. The effects of additions of caustic soda, manganese resinate, and cobalt stearate on the oxidation of isopropylbenzene in presence of small amounts of hydroperoxide were studied; it was found that additions of small amounts of caustic soda counteract the inhibiting effects of phenol and thiophene on the oxidation of isopropylbenzene.

2. The oxidation rate of isopropylbenzene in presence of caustic soda and manganese or cobalt salts depends on the sequence in which these substances are added. The oxidation rate is highest if the metal salts are added to isopropylbenzene heated to the temperature of the experiment, after addition of caustic soda.

LITERATURE CITED

[1] B. Kruzhalov and P. Sergeev, Chem. Sci. and Ind. 1, 287 (1956)[USSR].

[2] G. Armstrong, R. Hall, and D. Quin, J. Chem. Soc., 666 (1950).

[3] British Patent 630,286 (1949), Chem. Abs. 43,4489 (1949); British Patent 653,761 (1951), Zbl. 770* (1953); U.S. Patent 2,548,435 (1951), Zbl. 5256 (1953); U.S. Patent 2,632,772 and 2,632,773 (1953), Zbl. 2534 (1955); U. S. Patent 2,663,740 (1953), Chem. Abs. 49,372 (1955).

[4] M. S. Nemtsov, L. L. Radchenko, and S. I. Fisher, Chem. Sci. and Ind. 2, 306 (1957). [USSR].

[5] J. Fortuin and H. Waterman, Chem. Eng. Sci. 2, 182 (1953).

[6]D. Tolopko, Proc. Acad. Sci. USSR 104, 101 (1955).

[7] K. Ivanov and E. Villanskaia, Questions of Chemical Kinetics, Catalysis, and Reactivity [in Russian] Izd. AN SSSR, 1955) p. 270.

[8] E. Lorand, U. S. Patent 2,438,125 (1948), Chem. Abs. 42, 5469 (1948); U. S. Patent 2,527,640 (1950), Zbl. 4358 (1952).

*Chemisches Zentralblatt.

BRIEF COMMUNICATIONS

INVESTIGATION OF THE DECARBURIZATION RATE OF 30 KhMA STEEL PIPES IN A HYDROGEN MEDIUM

V. V. Ipat'ev, O. P. Merkulova, and V. P. Teodorovich

The Leningrad Institute of Petroleum Processing and Production of Synthetic Liquid Fuel

Modern processes of petroleum conversion and production of synthetic liquid fuels are carried out at high temperatures and pressures; the materials used for the reaction equipment must have high strength and chemical resistance in a hydrogen atmosphere. Therefore, a very acute problem at the present time is the choice of steels stable under the conditions used in these processes, and investigations of Russian steels suitable for equipment and pipelines in hydrogenation and other units of the petroleum conversion industry.

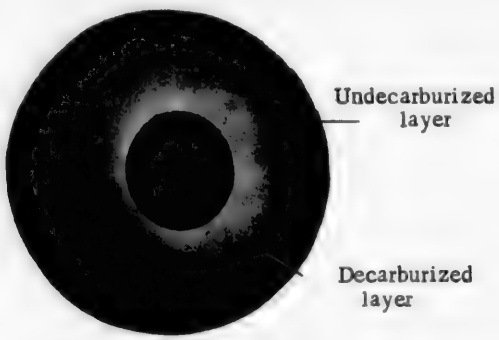

Fig. 1. Polished cross section of a 30 KhMA pipe partially decarburized by hydrogen.

It is known that when hydrogen acts on steel at high temperatures and pressures, it decomposes iron carbide in the steel and converts it into ferrite:

$$Fe_3C + 2H_2 = 3Fe + CH_4.$$

As the result of this reaction the decarburized steel becomes brittle and loses its strength characteristics. Figure 1 is a picture of a polished cross section of a 30 KhMA steel pipe partially decarburized by hydrogen; the inner light layer represents pure ferrite.

There have been many studies of the decarburization of various steels, but as yet there is no clear idea concerning the decarburization rate of steel pipes under the influence of aggressive gases.

The decarburization rates of 30 KhMA steel pipes in hydrogen at temperatures of 400-600° and pressures of 100-700 atmos in hydrogen have been studied at the Leningrad Scientific Research Institute.

The investigation was performed with tubular specimens 24 × 7 mm subjected to the action of hydrogen under pressure in electrical tube furnaces. After the experiments, the tubular specimens were cut and, from their ends, sections were prepared which were investigated metallographically and analyzed chemically layer by

layer. Chemical analysis of the decarburized ferrite layer showed that it always retains 0.03-0.04% carbon (not observed during metallographic examination). Figures 2, 3 and 4 are microphotographs of polished sections of 30 KhMA steel pipes; these give an indication of the nature of the destruction of the carbide structure and the conversion of carbides into brittle and weak ferrite.

Fig. 2. Partial decarburization of 30 KhMA steel at 575° and 400 atmos hydrogen pressure.

Several series of experiments were performed for clarification of the decarburization kinetics of 30 KhMA steel.

The first series of experiments was carried out at 575° and various pressures. The results of these experiments are presented in Fig. 5 as a plot of the decarburization rate against the square root of the time.

The results of these experiments led to the following conclusions: 1) the decarburization of 30 KhMA steel commences some time after the hydrogen has come into contact with the metal, and after that the decarburization rate is proportional to the root of the time, and 2) the initial period of the decarburization process depends on the pressure, and decreases with increase of the latter.

The result casts doubt on the published experimental data on the stability of various steels as determined in brief tests.

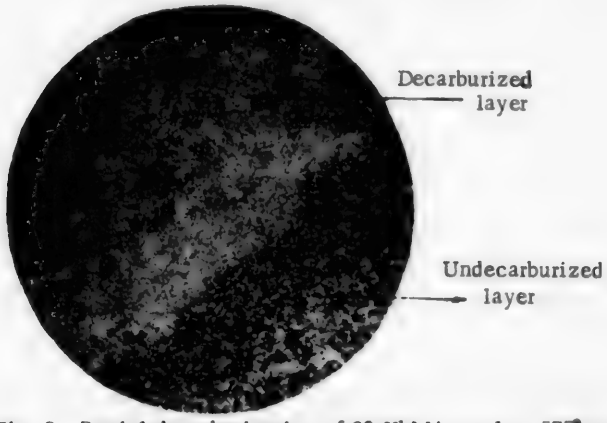

Fig. 3. Partial decarburization of 30 KhMA steel at 575° and 400 atmos hydrogen pressure.

The second, third, and fourth series of experiments on 30 KhMA steel were performed at constant pressures (100, 200, and 400 atmos) and at various temperatures in the 400-600° range.

The results of these experiments were plotted to give a series of curves analogous to that shown in Fig. 5.

Figure 6, represents the results of one series of experiments, performed on tubular specimens of 30 KhMA steel at 450-575° and 400 atmos.

The graph, like Fig. 5, shows that, after the initial period, all the experimental points lie on a straight line passing through the coordinate origin. The degree of decarburization during the initial period is immeasurably less than is indicated by the equations for the straight lines.

From these results we may derive a general equation relating the depth of decarburization and the time,

$$K = \frac{\Delta l}{l\sqrt{\tau}},$$

where K is the decarburization rate constant, Δl is the depth of the decarburized layer (mm), l is the thickness of the tube wall (mm) and τ is the time (hours).

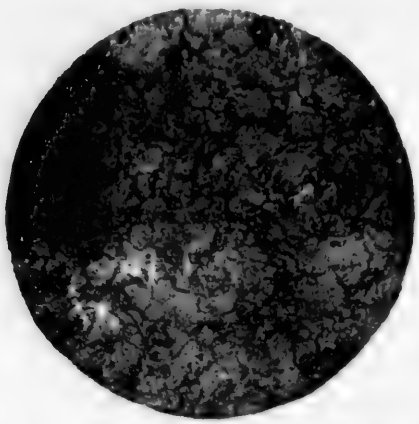

Fig. 4. Complete decarburization of 30KhMA steel at 575° and 400 atmos hydrogen pressure.

If the logarithms of the average values of K are plotted against the reciprocal absolute temperature, linear plots are obtained (Fig. 7).

From these results the apparent activation energy of the decarburization of 30 KhMA steel was calculated to be 15,000 cal, and the following general equation was derived for the dependence of the decarburization rate of 30 KhMA steel pipes on the pressure and temperature:

$$\log K = \frac{-15\,000}{2.3RT} + 0.0034P + 1.13.$$

This equation can be used for determining the extent and rate of decarburization of 24 × 7 mm pipes made from 30 KhMa steel, and for estimating the service life of these pipes under different process conditions.

This equation was derived for the action of pure hydrogen on the steel pipes.

In practice, mixtures of hydrogen (50-80%) with hydrocarbons are present in hydrogenation and other units of the petroleum industry.

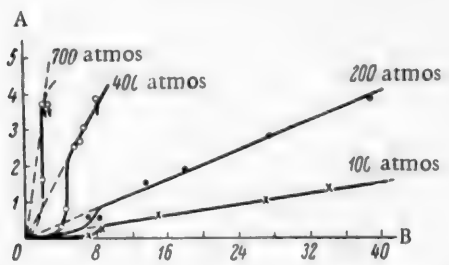

Fig. 5. Variation of the depth of decarburization with pressure and time at 575°: A) depth of decarburization (mm), B) $\sqrt{\tau}$ (hours).

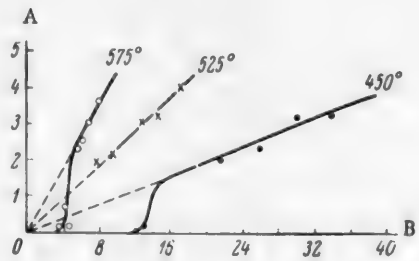

Fig. 6. Variation of the depth of decarburization of 30 KhMA steel with the temperature at 400 atmos hydrogen pressure: A) depth of decarburization (mm), B) $\sqrt{\tau}$ (hours).

It was therefore desired to study the influence of added hydrocarbons on the decarburization rate of steel. A series of experiments was performed at 575° and total pressure 400 atmos. The hydrogen—methane ratio was 1 : 1.

These experiments showed that the decarburization rate of 30 KhMA steel is lowered sharply by addition of methane.

Thus, at a total pressure of 400 atmos, when the hydrogen partial pressure in the mixture is 200 atmos, the depth of decarburization of 30 KhMA steel is 0.4-0.5 times that produced by the action of pure hydrogen at 200 atmos pressure.

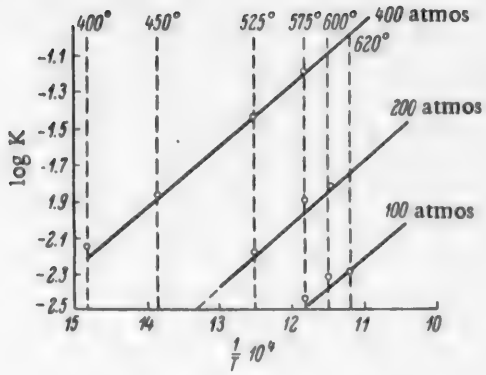

Fig. 7. Log K as a function of $\frac{1}{T}$.

Therefore, if the above formula is used for calculation of the depth of decarburization of 30 KhMa steel in presence of hydrogen–hydrocarbon mixtures (production gases), the results will always be somewhat high, thus providing a certain safety margin in the calculations.

Received May 8, 1957

DECARBURIZATION OF CARBON STEELS BY HYDROGEN AT HIGH TEMPERATURES AND PRESSURES

S. L. Skop, V. P. Teodorovich, and V. V. Ipat'ev

The Leningrad Scientific Research Institute of Petroleum Processing and Production of Synthetic Liquid Fuel

The planning and construction of plants for synthetic fuel production raises a number of problems related to the behavior of metals at high temperatures and pressures and in presence of aggressive media.

One such medium is hydrogen, the destructive action of which was first met in the synthesis of ammonia [1]. When hydrogen comes in contact with heated steel, it can penetrate into the metal, where it combines with carbon in the carbides and decarburizes the steel. The extent of decarburization depends on many factors, including the hydrogen pressure, temperature, time, and metal thickness [2].

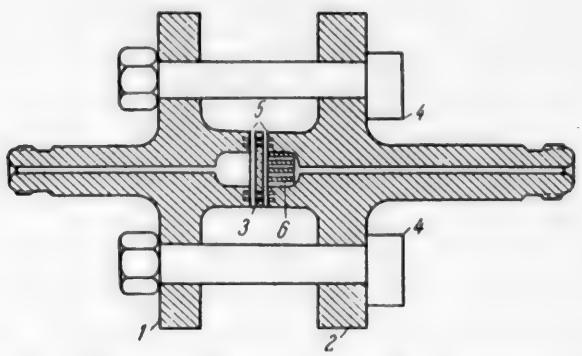

Fig. 1. Diagram of apparatus for studying the decarburization rate of steel plates: 1, 2) flanges, 3) test plate, 4) bolts, 5) packing, 6) perforated plate.

The question of decarburization rate is hardly touched upon in the published investigations, and it is impossible at the present time to calculate the depth of decarburization of steel under particular conditions.

In this investigation a study was made of the effects of temperature, pressure, and time on the depth of decarburization of carbon steel 35.

EXPERIMENTAL

The experimental specimens were prepared in the form of circular plates, and were fixed in a special apparatus consisting of a pair of bolted flanges. The outer parts of the flanges terminated in nipples through which hydrogen could be fed into the apparatus. Usually hydrogen was fed under pressure to one side of the plate, while the other side was open to the atmosphere. A schematic diagram of the assembled apparatus with the test plate is shown in Fig. 1. The assembled apparatus was placed in a furnace and heated. After the required temperature had been reached, hydrogen was fed in at the required pressure to one side of the plate.

The temperature of the specimen was determined by means of thermocouples fixed in the apparatus, and the pressure was measured by means of a manometer attached to the apparatus.

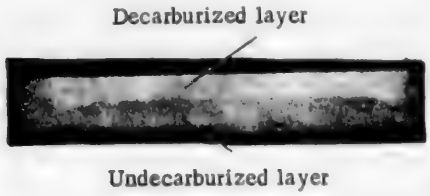

Fig. 2. Cross section of plate after decarburization.

Fig. 3. Structure of steel after incomplete decarburization.

After a fixed time the hydrogen was released from the apparatus, the furnace was cooled, and the test specimen extracted. The specimen was cut along its diameter and a metallographic section was prepared from the cut. The decarburization boundary is clearly seen both with the naked eye (Fig. 2) and under the microscope (Fig. 3).

The decarburization depth was measured under the microscope to an accuracy of 0.1 mm.

The experimental results obtained for different temperatures and pressures are plotted in Figs. 4 and 5. The plates used in the experiments were 6 mm thick.

A common feature of all the graphs is the presence of some sort of induction period during which there is very little or no decarburization.

It follows from Figs. 4 and 5 that the extent of the induction period depends on the temperature and pressure.

The induction period is quite unrelated to saturation of the metal with hydrogen. Special experiments on the permeability of steel to hydrogen showed that the penetration rate of hydrogen becomes constant within 15-30 minutes, whereas the incubation period is measured in hours. In some cases the specimens were more extensively decarburized at the edges. It was found that this was caused by wider copper gaskets (obturators), the edges of which entered the space between the perforated plate and the speci-

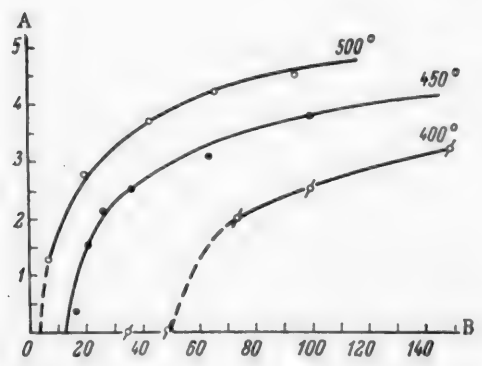

Fig. 4. Variations of decarburization depth with time at 200 atmos hydrogen pressure and temperatures of 400, 450, and 500°: A) decarburization depth (mm), B) time (hours).

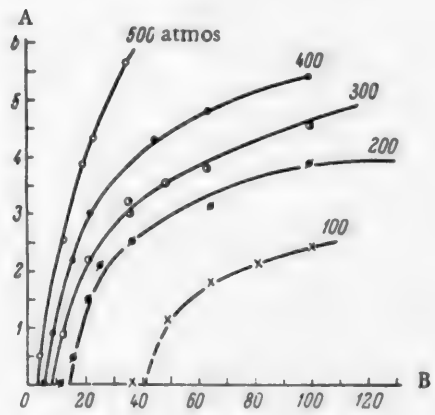

Fig. 5. Variations of decarburization depth with time at 450° and pressure from 100 to 500 atmos: A) decarburization depth (mm), B) time (hours).

men. Two experiments were performed to check this. In the first experiment a copper ring was placed between the test specimen and the grid, and in the second, a copper plate was placed at the center of the specimen.

Photographs of sections after these experiments are shown in Fig. 6.

It is seen that the test plate was completely decarburized in the regions where it was pressed against the copper plate.

The extent of the induction period of decarburization was determined by extrapolation of the curves in Figs. 4 and 5, and checked by an experiment of duration less than the induction period determined graphically. It is clear that the relationship between the induction period and pressure at constant temperature is represented by Equation (1), while the relationship between the induction period and temperature at constant pressure conforms to Equation (2)

$$\tau_0' = \frac{A}{P^{1/2}}, \tag{1}$$

$$\tau_0'' = \frac{e^{\frac{K}{T}}}{B}, \tag{2}$$

where τ_0 is the induction period (hours), P is the hydrogen pressure (atmos), t is the experimental temperature (°C), and A, B, and K are constants.

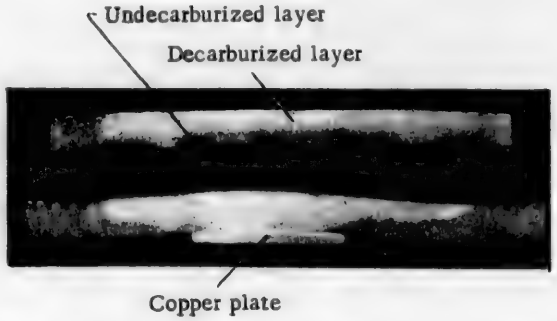

Fig. 6. Cross section of plate after decarburization (with copper interlayer).

TABLE 1

P (atmos)	t (°C)	τ_0 (hrs)	log C
500	450	3	3.48
400	450	5	3.39
300	450	8	3.38
200	450	14	3.39
100	450	42	3.38
200	500	4	3.40
200	400	55	3.39

TABLE 2

P (atmos)	t (°C)	τ_0 (hrs)	log C
Steel containing 0.76% carbon			
80	500	20	3.31
50	600	5	3.40
80	550	5	3.40
130	500	5	3.60
200	465	10	3.40
200	490	5	3.40
300	475	5	3.3[illegible]
Steel containing 0.22% carbon			
260	550	5	2.75
180	550	10	2.68

The general equation for the relationship between the induction period, pressure, and temperature is of the form

$$\tau_0 = \frac{e^{\frac{12320}{t}}}{P^{3/2}C}, \qquad (3)$$

where C is a constant.

The values of log C found from Equation (3) are given in Table 1.

Table 2 gives values of log C calculated from Nauman's data [3] for steel containing 0.22 and 0.76% carbon.

Tables 1 and 2 show that the values of log C for our experiments and for Nauman's experiments are the same.

Lower values are found for the constant calculated from Nauman's data for steel containing 0.22% carbon. Nauman reported that this steel had higher chromium and manganese contents.

The decarburization process begins at the end of the induction period.

The results of these experiments were used to derive an equation for the decarburization depth (Δl) as a function of pressure temperature, and time for plates 6 mm thick:

$$\Delta l = \frac{\tau - \tau_0}{\frac{575 - t}{33} + \frac{600 - P}{1700}(\tau - \tau_0)}.$$

SUMMARY

1. An equation for the induction period as a function of pressure and temperature has been derived. The value of the constant in this equation agrees with the values calculated from Nauman's data.

2. An approximate empirical formula is derived for calculation of the decarburization depth of a steel plate 6 mm thick over the 400-500° temperature range at different hydrogen pressures.

LITERATURE CITED

[1] Nelson, Welding J. No. 1, 125 (1955).

[2] Küntscher, Kilger, and Biegler. Technische Baustähle [1953)

[3] Nauman, Die. Chemische Fabrik, 31 / 32, 365 (1958.

Received April 29,1957

SOLUBLE POLY-p-XYLYLENE

A. A. Vansheidt, E. P. Mel'nikova, L. V. Kukhareva,

and M. G. Krakoviak

Institute of High-Molecular Compounds, Academy of Sciences USSR

Poly-p-xylylene (I), formed in the pyrolysis of p-xylene as the result of polymerization of the intermediate product p-xylylene (II)

appears by its properties to be a weakly cross-linked linear polymer. This is indicated by it behavior in high-boiling solvents, in which it dissolves only after prolonged heating above 300° or after degradation by atmospheric oxygen, by its conversion into an insoluble but strongly-swelling sulfonated cation-exchange resin even under mild sulfonation conditions, and by the difficulties which arise in molding it under pressure [1-4].

It was shown by Farthing [5] that the same hydrocarbon may be made by means of the Wurtz reaction from p-dichloromethylbenzene

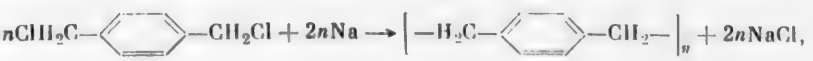

in boiling xylene or dioxane. However, under these conditions,the reaction proceeds very violently with formation of a polymer which is only partially soluble in high-boiling solvents. We therefore attempted to carry out polycondensation of the dichloride under milder conditions, at room temperature, on the assumption that in such conditions the side reaction of cross linking can be completely eliminated. It was found that although sodium dispersed in xylene does not react at all with the dichloride at room temperature, [illegible] dioxane is added to the solution appreciable polycondensation occurs under the same conditions, the reaction rate increasing with the dioxane concentration and reaching a maximum when xylene is completely replaced by dioxane.

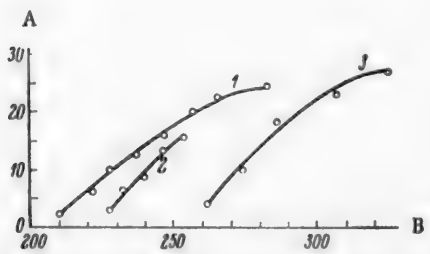

Effects of temperature and nature of the solvent on the concentration of saturated poly-p-xylylene solutions: A) concentration of saturated solutions (%), B) temperature(°C); solvents: 1) α-bromonaphthalene, 2) diphenyl, 3) benzyl benzoate.

To carry out the reaction in pure dioxane at 20-25°, metallic sodium was first dispersed in boiling dioxane in an atmosphere of dry nitrogen with vigorous stirring. The temperature was then lowered to 15°, and a mixture of p-xylylene dichloride in dioxane was added; the temperature rose as the result of polycondensation, and the mixture became black. The temperature of the mixture was maintained at 20-25° by external cooling, and the reaction was continued until heat evolution ceased, which occurred 2-3 hours after the start of the reaction. The mixture was stirred for half an hour, the unchanged sodium (enclosed within

Solubility of Poly-p-Xylylenes Formed Under Different Conditions

Poly-p-xylylene	Melting point (°C)	Solvent									
		diphenyl			α-bromonaphthalene			benzyl benzoate			
		temperature (°C)	heating time (hours)	soluble portion (%)	temperature (°C)	heating time (hours)	soluble portion (%)	temperature (°C)	heating time (hours)	soluble portion (%)
Film, made by pyrolysis	365—375	255 (b.p.)	6	Slight	281 (b.p.)	3	100	325 (b.p.)	—	—
Made in boiling dioxane	365	255 (b.p.)	6	10	281 (b.p.)	6	Slight	325 (b.p.)	6	60
Made in boiling xylene	Does not melt	255 (b.p.	6	Slight	281 (b.p.)	6	Slight	325 (b.p.)	6	30
Made in dioxane at 20-25°	385—395	228	Several minutes	100	210	Several minutes	100	263	Several minutes	100

the polymer granules) was quenched by addition of methanol, and the polymer was filtered off and heated for a long time in boiling water and then in acetone for complete removal of mineral impurities and unchanged dichloride. The polymer yield reached 80-85% of the theoretical. The polymer was a white granular powder, corresponding to poly-p-xylylene in composition (found: C 92.11%, H 7.74%; calculated: C 92.26%, H 8.03%) and containing only 4-5% of low-molecular hydrocarbons, which could be removed by warming with chloroform or by reprecipitation.

When heated in a capillary in a CO_2 atmosphere it became clear at 395-405°, and then melted, without visible decomposition, to a thick liquid, which flowed down to the bottom of the capillary and became turbid when cooled to 385-395°, owing to crystallization. In this respect it differed sharply from the cross-linked polymer made from the dichloride in boiling xylene, which did not become fluid even at 500°.

The poly-p-xylylene made in the cold showed even greater differences from cross-linked polymers when heated in a CO_2 atmosphere in high-boiling solvents — diphenyl, α-bromonaphthalene, and benzyl benzoate (in our experiments 8 g of each solvent was taken per 0.25 g of each condensation polymer and 5 mg of the pyrolytic polymer). It follows from the data in the table that polymers made at high temperatures, in nearly every case, dissolved only slightly or partially even after 6 hours of boiling in the above-named solvents, whereas the poly-p-xylylene, made from the dichloride in the cold, dissolved completely in a few minutes, well before the boiling point was reached, yielding nonviscous solutions. However, even on slight cooling it separated out of the solutions as the result of supersaturation; it was therefore possible to determine the solubility of the polymer in these solvents at various temperatures.

For these determinations weighed quantities of the polymer were added successively to a definite amount of solvent in a CO_2 atmosphere, and the temperature at which the polymer dissolved completely, the temperature at which the polymer was precipitated on cooling, and the temperature at which it redissolved when heated again (the latter two temperatures coincided within 2-3°) being determined for each addition. It must be noted that the melting point and solubility of the polymer precipitated from the solvent on cooling did not change during repeated determinations; this shows that the polymer did not undergo any appreciable degradation when heated in carbon dioxide.

The results of these determinations are plotted in the figure, which shows that the solubility of the polymer in all three solvents increases with temperature, reaching 25% at 280° in α-bromonaphthalene and at 310° in benzyl benzoate; at 260° the solubility was 21% in the first of these solvents, and only 2% in the second. Thus, as was to be expected, the best solvent for this polymer is α-bromonaphthalene, whereas the commonly used benzyl benzoate dissolves large amounts of the polymer only at much higher temperatures.

It is not possible as yet to determine the molecular weight of the polymer, as it is insoluble in low temperatures and does not contain end-group halogen.

SUMMARY

1. Poly-p-xylylene can be prepared from p-xylylene dichloride and metallic sodium, at close to room temperatures, in dioxane and in xylene–dioxane mixtures.

2. In contrast to the polymer made in boiling solvents, poly-p-xylylene made by this method is readily soluble at high temperatures in diphenyl, α-bromonaphthalene, and benzyl benzoate (in a nitrogen atmosphere); this shows the presence of a linear polymer without cross links.

LITERATURE CITED

[1] M. Kaufman, H. Mark, and R. B. Mesrobian, J. Polymer Sci, 13, 68 3 (1954).

[2] R. S. Corly, H. C. Haas, M. W. Kane, and D. L. Livingston, J. Polymer Sci., 13, 68, 137 (1954).

[3] L. Auspos et al., J. Polymer Sci. 15, 79, 9, (1955).

[4] L. Errede and B. Landrum, J. Am. Chem. Soc., 79,4952 (1957).

[5] A. C. Farthing, J. Chem. Soc. 3261 (1953).

Received January 10, 1958

SOME REACTIONS OF ACID DEXTRIN SULFATES•

G. Ia. Liandzberg

It is known that strong H_2SO_4 is most commonly used as a catalyst for acetylation of cellulose. It is an active catalyst and is readily available.

It is believed [1] that H_2SO_4 initially forms acetylsulfuric acid — $CH_3CO \cdot OSO_2OH$, — with acetic anhydride, and this acetylates the cellulose with liberation of H_2SO_4.

$$HOSO_2OH + \begin{matrix} CH_3CO \\ CH_3CO \end{matrix}\!\!>\!O \longrightarrow CH_3CO \cdot OSO_2OH + CH_3COOH, \quad (1)$$

$$CH_3CO \cdot OSO_2OH + HO\cdot \text{cellulose} \longrightarrow \text{cellulose} \cdot OCOCH_3 + H_2SO_4. \quad (2)$$

It has also been stated [2] that the role of H_2SO_4 in acetylation consists of preliminary formation of cellulose sulfate esters, with the sulfate groups displaced by acetyl during the subsequent stages.

It was decided to investigate in greater detail the role of cellulose sulfates in acetylation.

It was shown by Veitsman [3] that cellulose sulfates can react with acetic anhydride with replacement of the sulfate groups by acetyl.

For investigation of the reactivity of cellulose sulfates toward acetic anhydride, we developed a method for synthesis and isolation of acid cellulose sulfates corresponding to the formula cellulose-OSO_2OH.

The isolated acid cellulose sulfates correspond by their degree of polymerization to the sulfodextrins. The latter were prepared by the treatment of cellulose fibers (cotton) with chlorosulfonic acid diluted with anhydrous dichloroethane, whereby it was possible to avoid charring caused by dehydration of the cellulose. The reactions were mainly performed at temperatures below 0°.

It proved possible under certain conditions to isolate the free acid sulfodextrins, consisting mainly of the mono-, di-, and triesters with degrees of polymerization between 6 and 100, in the form of amorphous precipitates. They are weak acids with dissociation constant $K = 10^{-2} - 10^{-3}$, capable of forming various salts.

Acid sulfodextrins are soluble in water, methyl, ethyl, and butyl alcohols, and glacial acetic acid. The solubility in glacial acetic acid at 100° reaches 10%.

Acid sulfodextrins react very vigorously and rapidly with acetic anhydride; when water is added to the reaction products, substances containing about 62% acetyl groups are precipitated.

A very unexpected fact is that when cellulose fiber is impregnated with solutions of acid sulfodextrins in water, alcohols, or glacial acetic acid, the fiber reacts readily with acetic, propionic, and butyric anhydrides or their mixtures. The mechanism of this reaction is not yet clear.

It is suggested that the process occurs as follows. When the fiber is impregnated with solutions of acid sulfodextrins, the latter are absorbed by the cell walls and are contained in capillary cavities between the

•This work was performed under the guidance of N. Ia. Solechnik, Doctor of Technical Sciences, Professor of the S. M. Kirov Academy of Wood Technology.

fibrils and the molecular aggregates, because cellulose is a heterocapillary system.

When the above-named anhydrides acts on the cellulose, the sulfo groups in the sulfodextrins are replaced as described above (by acetyl or other groups), due to the tendency for the formation of less-soluble substances. The molecular rearrangements which ensue within the fiber cell walls break down the aggregates of cellulose macromolecules, with weakening of the hydrogen bonds between them, because of the steric forces which arise in the formation of new compounds.

A fiber in this state, with its molecules pushed apart and accessible to chemical action, has greatly enhanced reactivity, and the cellulose macromolecules react directly with acetic, propionic, or butyric anhydrides. The fibers dissolve in the reaction medium even at low degrees of substitution.

The probable mechanism of the reactions whereby sulfo groups in acid sulfodextrins are replaced by acetyl groups may be represented as follows:

$$C_6H_7O_2(OSO_2OH)_3 + 3\begin{matrix}CH_3CO\\CH_3CO\end{matrix}\!\!>\!O \longrightarrow C_6H_7O_2(OCOCH_3)_3 + 3CH_3CO \cdot OSO_2OH, \quad (3)$$

$$C_6H_7O_2(OH)(OSO_2OH)_2 + 3\begin{matrix}CH_3CO\\CH_3CO\end{matrix}\!\!>\!O \longrightarrow$$

$$\longrightarrow C_6H_7O_2(OCOCH_3)_3 + 2CH_3CO \cdot OSO_2OH + CH_3COOH, \quad (4)$$

$$C_6H_7O_2(OH)_2(OSO_2OH) + 3\begin{matrix}CH_3CO\\CH_3CO\end{matrix}\!\!>\!O \longrightarrow$$

$$\longrightarrow C_6H_7O_2(OCOCH_3)_3 + CH_3CO \cdot OSO_2OH + 2CH_3COOH. \quad (5)$$

Acid sulfodextrins may be used as catalysts for acceleration of cellulose esterification.

EXPERIMENTAL

Preparation of acid sulfodextrins. A weighed sample of 20 g of dry cotton was placed in a 750 ml conical flask and wetted with 200 g of dichloroethane, dehydrated by means of $CaCl_2$ and by redistillation. A mixture of 200 g of dichloroethane and 100 g of redistilled chlorosulfonic acid, cooled to −3°, was also added. The flask was placed for 24 hours in a refrigerator at 0−3°. The fibrous material was washed 4 times with anhydrous dichloroethane, and then 3 times with a cold 1:6 mixture of ethyl alcohol and ethyl ether. The washed fibrous material was extracted twice with ethyl alcohol. The alcoholic solution of acid sulfodextrins was filtered through cotton wool on a suction funnel, cooled to −3°, and cold ethyl ether was added to it. A white, amorphous, curdy precipitate was formed; this was washed several times with ether and kept for a long time under ether; this precipitate is acid sulfodextrin.

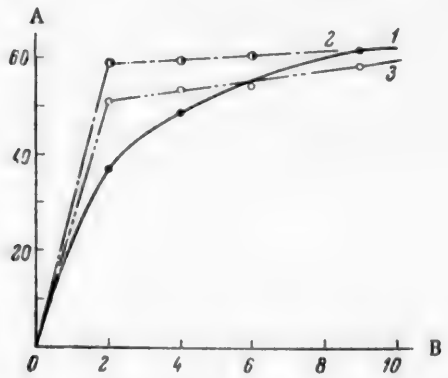

Acetylation rates: A) acetate group content (%), B) time (hours); acetylation of cotton in presence of: 1) H_2SO_4 (10% on the fiber), 2) acid sulfodextrins (2% on the fiber) with 400% of acetic anhydride (without heating), 3) acid sulfodextrins (2% on the fiber) with 250% of acetic anhydride (without heating).

Esterification of cotton in presence of acid sulfodextrins. The precipitated acid sulfodextrin was dissolved to saturation in glacial acetic acid heated to 100°. Under these conditions the solubility of the acid sulfodextrins is about 10%. The cotton samples were pretreated with a solution of the

acid sulfodextrins in glacial acetic acid (this process is known as fiber activation). After activation, acetic, butyric or propionic anhydride was added to the fiber. The acetylation of the fiber proceeded at a high rate, which increased on heating.

It was shown by Bakk [4] that the acetylation rate of cotton, in presence of 10% H_2SO_4 on the weight of the fiber, in a bath containing 500% glacial acetic acid and 400% acetic anhydride increases rather slowly (Figure, Curve 1). Acetylation in presence of acid sulfodextrins proceeds at a higher rate than acetylation with H_2SO_4 (Curves 2 and 3). The acetylation rate increases on heating. Thus, triacetates soluble in methylene chloride and insoluble in acetone were formed by acetylation on a water bath at 40-45° for 2.5-3 hours. Under these conditions the consumption of acetic anhydride could be reduced to 250% on the air-dry cotton. The following amounts were taken for homogeneous acetylation: 10 g of air-dry cotton, 4 ml (4% on the fiber weight) of a solution of acid sulfodextrins in glacial acetic acid, 46 ml of glacial acetic acid, and 25 ml of acetic anhydride.

For heterogenous acetylation, acetic anhydride (25 ml) was added in a mixture with benzene (20 ml).

Cellulose acetate butyrate was prepared by the reaction of 10 g of air-dry cotton with 38 ml of butyric anhydride and 5 ml of acetic anhydride in presence of 2 ml (2% on the fiber) of a solution of acid sulfodextrins, 48 ml of glacial acetic acid, and 10 ml of ligroin. The dry precipitated cellulose acetate butyrate was readily soluble in acetone and methylene chloride.

Cellulose tripropionate was prepared by the reaction of 10 g of air-dry cotton with 40 ml of propionic anhydride in presence of 3 ml (3% on the fiber) of a solution of acid sulfodextrins and 50 ml of glacial acetic acid. The dry precipitated cellulose tripropionate was readily soluble in acetone.

LITERATURE CITED

[1] Z. A. Rogovin and N. N. Shorygina, Chemistry of Cellulose and Associated Substances [in Russian] (GONTI, 1953) p. 428.

[2] N. I. Nikitin, Chemistry of Wood [in Russian] (Izd. AN SSSR, 1951) p. 114.

[3] A. E. Veitsman, Artificial Fibers 1, 7 (1932) [USSR].

[4] A. Bakk, Dissertation Leningrad Tech. Inst. 1953).

Received April 22, 1957

PREPARATION OF FURFURYL ALCOHOL

A. P. Salchinkin and L. B. Lapkova

Chair of Organic, Physical, and Colloid Chemistry of the Kuban' Agricultural Institute

The numerous furan derivatives known at the present time include furfuryl alcohol, the production and applications of which are of considerable interest, as shown by the publication of a number of patents relating to the production of synthetic resins and plastics [1].

In the laboratory preparation of furfuryl alcohol, use is generally made of the Cannizzaro dismutation reaction, or the allied Meerwein–Ponndorf reaction, or catalytic reduction of furfural.

The Cannizzaro reaction is based on the conversion of furfural into pyromucic acid and furfuryl alcohol in an alkaline medium [2]:

$$2C_4H_3O{-}CHO + KOH = C_4H_3O{-}COOH + C_4H_3O{-}CH_2OH.$$

It follows from the reaction equation that it is not possible to obtain more than 50% yield of the alcohol, calculated on the aldehyde taken.

A modification of the Cannizzaro reaction is the "crossed" Cannizzaro reaction, based on disproportionation, which is possible if molecules of two different aldehydes are involved [3]:

$$C_4H_3O{-}CHO + H{-}CHO = C_4H_3O{-}CH_2OH + H{-}COOH.$$

The Meerwein–Ponndorf reaction consists of the reduction of carbonyl compounds by aluminum alcoholate. Aluminum alcoholate, prepared separately and introduced in the pure form, takes part in the slow reaction [4].

The aldehyde and aluminum alcoholate form an addition compound (the first stage of the reaction), which decomposes in the final stage:

$$R{-}CHO + \frac{Al}{3}OC_2H_5 \rightarrow R{-}CH\begin{matrix}O\frac{Al}{3}\\ \\ OC_2H_5\end{matrix} \rightarrow R{-}CH_2O\frac{Al}{3} + CH_3CHO,$$

where R is alkyl or aryl.

The over-all equation for the reaction with furfural may be written as follows:

$$6C_4H_3O{-}CHO + 2(C_2H_5O)_3Al = 3CH_3COOC_2H_5 + 2(C_4H_3O{-}CH_2O)_3Al.$$

The mild and specific reduction of an aldehyde by aluminum alcoholate can be accelerated considerably in the case of furfural, analogously to the reduction of furylacrolein to furylallyl alcohol [5].

The method described in the literature for the catalytic reduction of furfural in presence of copper chromite at 150° and 100 atmos is among the most recent methods [6] but because of the required techniques and specific characteristics of the catalytic reactions it is not suitable for every laboratory.

The present communication describes a method for the preparation of furfuryl alcohol from furfural by reduction of the latter by aluminum ethylate, by the use of the variant of the Meerwein–Ponndorf reaction proposed for furylacrolein by Likhosherstov et al. [5].

EXPERIMENTAL

The first stage of the work was preparation of aluminum ethylate. 10 g of aluminum turnings and 30 ml of xylene distilled over metallic sodium was put into a round-bottomed flask, 150-200 ml in capacity, fitted with a reflux condenser with a calcium chloride tube, and a dropping funnel. The flask was heated on an oil bath until the solvent boiled, and 40 ml of absolute alcohol, containing 0.1 g each of mercuric chloride and crystalline iodine in solution, was added gradually from the dropping funnel.

Hydrogen was soon evolved rapidly and the contents of the flask became viscous. The rate of alcohol addition was varied according to the course of the reaction. The heating was continued for about 3 hours. During this time 30 ml of xylene was added each 1.5 hours.

The hot solution of aluminum ethylate in xylene was decanted into a round-bottomed flask 200 ml in capacity; 50 g of freshly-distilled furfural was then added and the mixture was heated under reflux for 3 hours. Completion of the reaction was confirmed by the aniline acetate test. The mixture was then cooled to room temperature and poured out by portions into a beaker containing 250 ml of 20% sulfuric acid solution cooled to 0° in ice.

The solution in the beaker became turbid and brown. The mixture soon separated into two layers: a lower aqueous layer, pale brown in color,, and an upper layer consisting of furfural alcohol and ethyl acetate dissolved in xylene.

The mixture was transferred from the beaker to a separating funnel of suitable size for settling and subsequent separation. When a clear separation boundary appeared, the aqueous layer was separated off. The xylene layer was dried by means of calcined sodium sulfate. Xylene was distilled off under vacuum on a water bath. The xylene distillate was used for additional extraction of the aqueous layer. It is quite sufficient to extract the aqueous layer with two 20 ml portions of the distilled xylene.

The combined xylene extracts of the aqueous layer were dried by means of sodium sulfate and distilled under vacuum.

After removal of the ethyl acetate and xylene, furyl alcohol came over. Most of the alcohol distilled at 71° (vacuum 12 mm).

The slower the vacuum distillation, the greater are the losses due to formation of dark viscous polymerization products. The distilled furfuryl alcohol was usually colorless, but near the end of the distillation it acquired a pale straw-yellow color. The yield was 35-40 g or 70-80% of the theoretical.

Characteristics of the compound: $d^{23}_4 = 1.1151$, $n^{23}_D = 1.4850$, t = 71° at 12 mm.

Literature data [7]: $d^{23}_4 = 1.1282$, $n^{23}_D = 1.48515$, t = 75—77° at 15 mm.

LITERATURE CITED

[1] Chemistry and Chemical Technology (abstracts and summaries of papers from the foreign periodical literature) 2, 212 (1953); 5, 254 (1955); 4, 106 (1956); Referat. Zhur. Khim. 15, 364 (1955); C. H. Schmidt, Ang. Ch., 12, 317 (1955).

[2] Organic Syntheses, 1 (Moscow, IL, 1949) [Russian translation].

[3] A. M. Berkengeim and T. A. Dankova, J. Gen. Chem. 9, 928 (1939) [USSR].

[4] H. Meerwein and R. Schmidt, Lieb, Ann., 444, 221 (1925); T. Berzin, Progr. Chem. 10, 5, 606 [USSR] (1941); W. Hickinbottom, Reactions of Organic Compounds (GONTI, NKTP, 1939) [Russian translation].

[5] M. V. Likhosherstov et al., J. Gen. Chem. 20, No. 4, 627 (1950). •

[6] R. Elderfield (ed.) Heterocyclic Compounds, 1 (Moscow, IL, 1953) [Russian translation]; Newer Methods of Preparative Organic Chemistry (Moscow, IL, 1950) [Russian translation].

[7] Dictionary of Organic Compounds, 2 (Moscow, IL, 1949) [Russian translation].

Received May 3, 1957

•Original Russian pagination. See C.B. Translation.

MISSING PAGES ARE INDEX PAGES
WHICH HAVE BEEN PHOTOGRAPHED
AT THE BEGINNING OF THE VOLUME(S)

SCIENTIST - TRANSLATORS WANTED

For over a decade, Consultants Bureau, Inc. has provided Western scientists with high quality cover-to-cover translations of Soviet scientific journals. Our unique contracts with the Soviet government are constantly revised to include more extensive coverage of technical activity in the USSR. In order to produce these journals at the high standards set down by both the Soviet and American governments, it is of prime importance to maintain a large staff of scientist-translators who can translate with precision in their specific scientific field. It is our strict policy to assign a translator only that material which is within his scope.

As part of our current and future* expansion programs, we have openings for a limited number of scientist-translators who can translate in the fields covered by the following journals:

Journal of General Chemistry

Antibiotics
Biochemistry
Bulletin of Experimental Biology and Medicine
Entomological Review
Microbiology
Pharmacology and Toxicology
Plant Physiology

Automation and Remote Control
Industrial Laboratory
Instruments and Experimental Techniques
Measurement Techniques

Czechoslovak Journal of Physics
Soviet Journal of Atomic Energy
Soviet Physics - Acoustics
Soviet Physics - Crystallography
Soviet Physics - Technical Physics

Our basic requirements are that the scientist-translator have a native command of English, a minimum degree of B.S. in his specific field, and a thorough knowledge of the contemporary technical terminology of his scientific discipline.

Translation may be done at home on a full or part-time basis.

For further information, please contact:

Translation Editor
CONSULTANTS BUREAU, INC.
227 West 17th Street
New York 11, New York

*We expect, in the near future, to initiate a program of translation from the growing amount of important Chinese scientific literature available. In preparation, we are accepting applications from Chinese to English translators.

the latest Soviet Research on...

- animal biochemistry
- antibiotics
- biophysics
- immunology
- industrial hygiene
- morphology
- oncology
- pathology
- pharmacology
- physiology
- plant biochemistry
- toxicology

NOW AVAILABLE ON SUBSCRIPTION

reports written by leading Soviet authorities...

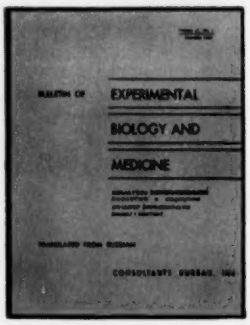

BULLETIN OF EXPERIMENTAL BIOLOGY AND MEDICINE (Byulleten' Eksperimental'noi Biologii i Meditsiny)

Important journal that features research reports, written by leading Soviet authorities, on *physiology, pathology, immunology, biophysics, pharmacology, oncology, morphology* and related fields. Translation is by special arrangement with the National Institutes of Health.

ANNUAL SUBSCRIPTION: 12 issues, $20.00
BACK ISSUES: 1956-1958 (12 issues per year) $20.00 per year

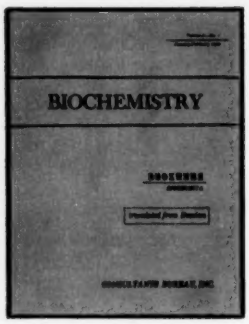

BIOCHEMISTRY (Biokhimiya)

The most comprehensive Soviet journal in this field. Each issue contains more than twenty articles on plant and animal biochemistry. Translation is by special arrangement with the National Institutes of Health.

ANNUAL SUBSCRIPTION: 6 issues, $20.00
BACK ISSUES: 1956-1958 (6 issues per year) $20.00 per year

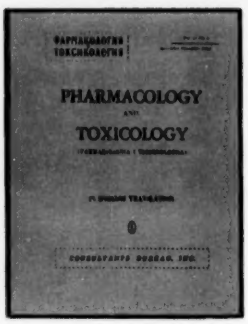

PHARMACOLOGY AND TOXICOLOGY (Farmakologiya i Toksikologiya)

This journal contains reports of the latest Soviet research on physiological effects of drugs, industrial hygiene, and related chemico-pharmacological-toxicological fields. The translation is published by special arrangement with the American pharmaceutical industry.

ANNUAL SUBSCRIPTION: 6 issues, $25.00
BACK ISSUES: 1957-1958 (6 issues per year) $25.00 per year

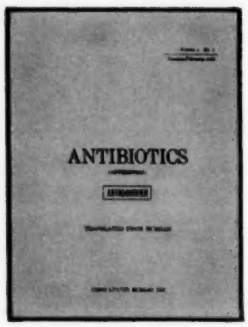

ANTIBIOTICS (Antibiotiki)

This outstanding new publication surveys the entire field with timely research reports by leading Soviet scientists. It is translated and published with the financial assistance of some leading U. S. companies.

ANNUAL SUBSCRIPTION: 6 issues, $25.00

(Add $5.00 for foreign mailings of current subscriptions)

COVER TO COVER TRANSLATIONS

c/b CONSULTANTS BUREAU, INC.
227 WEST 17TH STREET, NEW YORK 11, N. Y.